

INTRODUCTION

James Cook University (JCU) School of Engineering & Physical Sciences developed a comprehensive RF and microwave electronic engineering course that is now available to qualified universities world-wide.

The course material contained on the following pages has been developed by JCU Associate Professor Keith Kikkert and is based upon AWR's Microwave Office® and Visual System Simulator™ (VSS) design software.

CHAPTERS/LECTURES

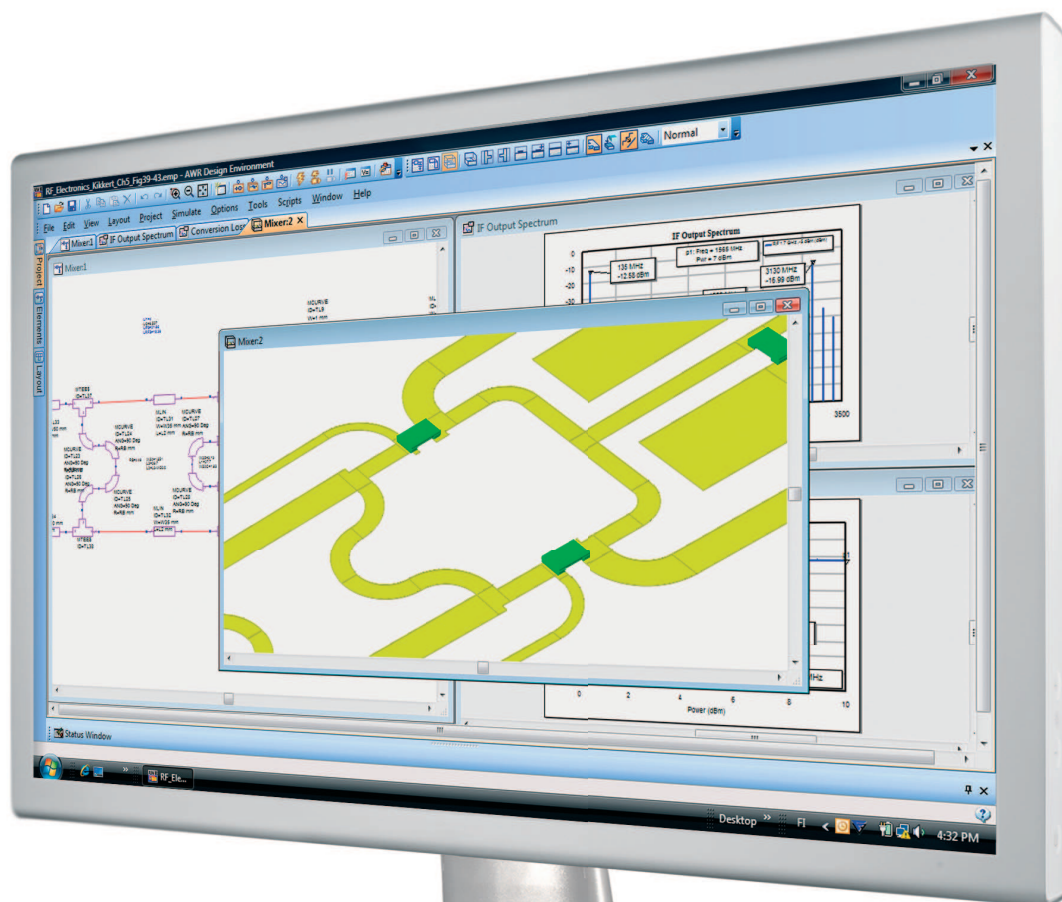
- Introduction
- Computer Simulation
- Transformers and Hybrids
- Transmission Line Transformers and Hybrids
- Mixers
- Local Oscillators
- RF Filters
- Amplifiers, Stability, Noise and Gain Circles

VERSION

Rev1 - March 2009



RF & Microwave
Electronics Design
Course - Final Year
Undergraduate and/or
Masters Students



Index

Lectures	Page
Chapter 1: Introduction	1.1
Computer Simulation	1.3
References	1.3
Chapter2: Computer Simulation	2.1
Introduction	2.1
Example 1: Low Pass Filter	2.1
Equations in MWO	2.5
Example 2: Diplexer	2.6
Optimisation	2.7
Example 3: Amplifier	2.10
Transistor Models	2.12
Determination of Line Parameters	2.14
Summary	2.16
References	2.17
Chapter 3: Transformers and Hybrids	3.1
Introduction	3.1
Wideband Transformers	3.2
Example: RF Transformer Design	3.3
Bifilar and Trifilar Windings	3.4
Transmission line transformers with ferrite cores	3.5
Transformer Hybrids	3.7
Power Combiner / Splitter	3.8
Wilkinson Transformer Hybrid	3.8
Design Example	3.10
Transmission Line Hybrid with Ferrite Cores	3.11
Many Way Hybrids	3.12
References	3.13
Chapter 4: Transmission Line Transformers and Hybrids	4.1
Introduction	4.1
Example: Bandwidth Calculation	4.1
Wilkinson Transmission Line Hybrid	4.3
Compensated Wilkinson Hybrid	4.5
Unequal Split Wilkinson Hybrid	4.6
Wideband Wilkinson Hybrid	4.7
Quarter Wave Hybrid or 1.5λ Rat-race hybrid	4.10
Branchline Coupler	4.12
Backward Travelling Wave Hybrid	4.17
Edge Coupled Lines	4.18
Example: 20 dB Coupler	4.18
Lange Coupler	4.22
Broadside Coupled Lines	4.22
Example: 3 dB Coupler	4.24

	Page
Chapter 5: Mixers	5.1
Introduction	5.1
Conversion Loss	5.2
Isolation	5.2
Compression Point	5.3
Dynamic Range	5.3
Two-tone Third Order Intermodulation Distortion	5.3
Third Order Intercept Point	5.5
LO Level	5.6
Example: Mixer LO Required Level Calculation	5.6
Single Diode Mixer	5.6
Computer Simulation of Mixers	5.8
Balanced Mixer	5.14
Double Balanced Mixer	5.17
Microwave Mixers	5.23
Microwave Mixer using a Branchline Coupler	5.25
Active Single Transistor Mixer	5.28
Gilbert Cell Active Mixer	5.29
Examples of Commercial Active Mixers	5.32
Quadrature Mixers	5.33
Active IQ Mixers	5.34
LTC Mixers	5.34
Other Mixers	5.35
Chapter 6: Oscillators	6.1
Oscillator Principles	6.1
Requirements	6.1
Positive Feedback Oscillators	6.1
Oscillator Design Process	6.2
Q of Frequency Selective Networks	6.3
Oscillator Design Procedure	6.4
Transistor Selection	6.4
Amplifier Design	6.5
Design the Resonator	6.6
Linear Oscillator Analysis	6.7
Non-linear Analysis	6.7
Crystal Oscillators	6.9
Design Example	6.9
RF and Microwave Oscillators	6.12
Design example	6.12
Chapter 7: RF Filters	7.1
Introduction	7.1
Filter Design Revision	7.2
Filter Tables	7.2
Butterworth Filters	7.3
Bessel Filter	7.4
Chebyshev Filter	7.5

	Page
RF Lowpass Filter Design	7.8
Bandpass Filter Design	7.13
LC Bandpass Filters	7.13
Low-Pass to Band-Pass Transformation	7.13
LC Coupled Resonator Filter	7.14
HF Filters	7.19
Cauer-Chebyshev Bandpass Filters	7.21
Parallel Coupled-Line Filter	7.21
Example: Design of 1GHz filter, 70 MHz BW	7.21
Hairpin Filter	7.24
Helical Filters	7.27
Design Example: 100MHz filter, 1 MHz BW	7.28
Interdigital Filters	7.31
Round Rod Interdigital Filters	7.32
PCB Interdigital Filters	7.33
Example: Design of 1GHz filter, 70 MHz BW	7.34
Direct Coupled Resonator Filters	7.39
Filter Design Example	7.40
Fine Tuning the Filter	7.41
Microstrip Filter Comparison	7.43
Coaxial Filters	7.49
Ceramic Filters	7.52
SAW Filters	7.52
References and Bibliography	7.53
Chapter 8: Amplifiers: Stability, Noise and Gain.	8.1
IF Amplifiers	8.1
MMIC	8.1
Stability	8.2
Smith Chart Revision	8.3
Scattering Parameters Revision	8.4
Stability Requirements	8.5
Stability Factors	8.6
Amplifier Noise Figure	8.7
Improving Noise Figure	8.11
Chapter 9: Impedance Matching of Power Amplifiers	9.1
Introduction	9.1
LC Matching	9.2
Pi Network	9.2
Low Pass T Network	9.3
Band Pass L Network	9.4
Band Pass T Network	9.5
Capacitive impedance Transformer	9.6
Design Example	9.7
Transformer Matching	9.11
Transmission Line Matching	9.12
Broadband Matching	9.14

	Page
Broadband Amplifier Design Example	9.17
Chapter 10: Circuit Manufacture	10.1
Introduction	10.1
Conductive Track Removal	10.1
Depositing Tracks and Vias	10.1
Printed Circuit Board Materials	10.1
Conventional PCB Substrates	10.1
FR3	10.1
FR4	10.2
Microwave and RF Printed Circuit Board Materials	10.3
RT/duroid 58X0	10.3
RT/duroid 6000	10.4
RO3000 and RO3200	10.4
RO4000	10.4
Multilayer Boards	10.4
Non-Clad Substrates	10.5
D6	10.5
Alumina Substrates	10.5
D30	10.6
D43	10.6
D88	10.6
Manufacturing	10.6
Manufacturing using a PCB Milling Machine	10.6
Layout Hints	10.6
Thin Film	10.7
Thick Film	10.8
Screens	10.8
Pastes (Inks)	10.9
RF Applications of Thick Film Circuits	10.9
Low Temperature Cofired Ceramic (LTCC)	10.10
Chapter 11: RF Operational Amplifiers	11.1
Voltage Feedback Amplifier	11.1
Current Feedback Amplifier	11.3
Amplifier Comparison	11.4
Low Noise designs using Operational Amplifiers	11.5
References	11.9

Practical Sessions

	Page
RF Simulation Practical Session	P1.1
Aim	P1.1
Requirements	P1.1
Procedure	P1.1
Task 1: Simulation of a Wilkinson Transformer Hybrid	P1.1
Simulation Steps	P1.1
Task 2: Simulation and Layout of a Branchline Coupler	P1.3
Equipment	P1.4
Transformers and Mixers	P2.1
Aim	P2.1
Procedure	P2.1
Equipment Required	P2.1
RF Filter Design Practical Session	P3.1
Aim	P3.1
Task	P3.1
Procedure	P3.1
Equipment	P3.2

Chapter 1

Introduction

RF electronic designs require different techniques than electronic designs at lower frequency since:

- 1 The Resistors, Capacitors and Inductors used do not necessarily behave like ideal components. In particular, leads on resistors and capacitors have an inductance associated with them, which can easily dominate.
- 2 The wavelength of the signals is comparable to the size of components used. This presents some challenges and some opportunities.
- 3 The track lengths may be a significant fraction of a wavelength, allowing microstrip-lines or strip-lines, to be used as elements for filters, couplers, impedance matching circuits etc.
- 4 The tracks on the circuit boards must have a specified characteristic impedance, to ensure that the devices connected to it work correctly at all the required frequencies. Conventional printed circuit boards are lossy at high frequencies. Circuit boards for RF and Microwave frequencies normally use low loss materials and have carefully controlled thicknesses, to provide constant impedances for transmission lines.

At lower frequencies, many of the analogue circuits are being replaced with digital circuits. At RF frequencies, analogue circuit design techniques are the only design techniques that can be used for the design of any transmitter and receiver circuit used in Radio, TV, Microwave, Mobile Phone, Wireless LAN etc.

A typical block diagram of a receiver and a transmitter is shown in Figure 1. The basic building blocks in this diagram are: RF Transformer, Mixer, RF and IF amplifier, Local Oscillator and a demodulator or detector. In this course, we will look at many of these elements in detail.

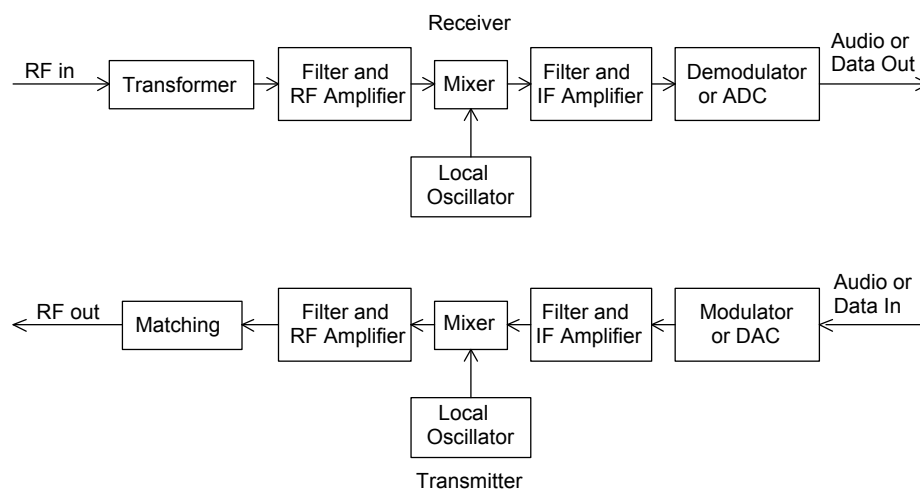


Figure 1. Typical Transmitter and Receiver Block Diagram.

For consumer devices with large production runs, such as mobile phones or USB dongles for Digital TV, Bluetooth or WLAN, many of the blocks in figure 1, are combined in one IC. A typical example of this is a Bluetooth dongle, shown in figure 2. All the RF functions, including the 2.5 GHz transmitter and receiver, all the protocol handling and the USB interface are contained in the two IC's on figure 2. The antenna is included as an element on the PCB.

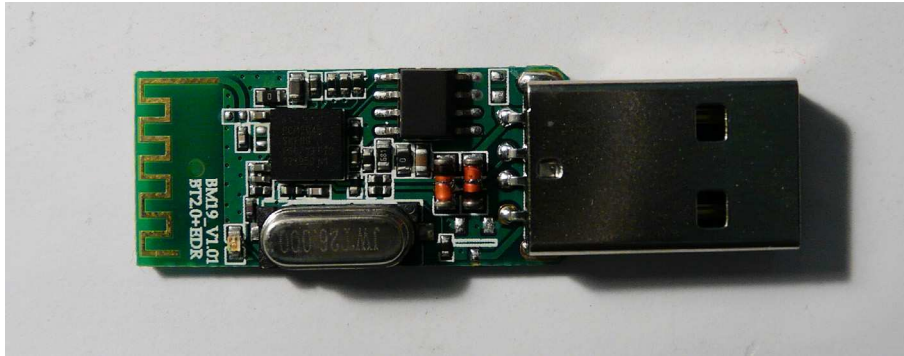


Figure 2. Typical Consumer RF Module. (Unbranded EDR Bluetooth USB Adapter)

For non-consumer applications, such IC's may be too expensive, or the performance that can be obtained from an IC cannot meet the required specifications, such as output power or adjacent carrier rejection. As a result a discrete implementation is often required for precision applications. Figure 3 shows a harmonic multiplier for a Satellite Beacon Receiver built at James Cook University. The input is a 162 MHz signal, the output is the 5th harmonic at 810 MHz. The active device is a Microwave Monolithic IC (MMIC) amplifier.

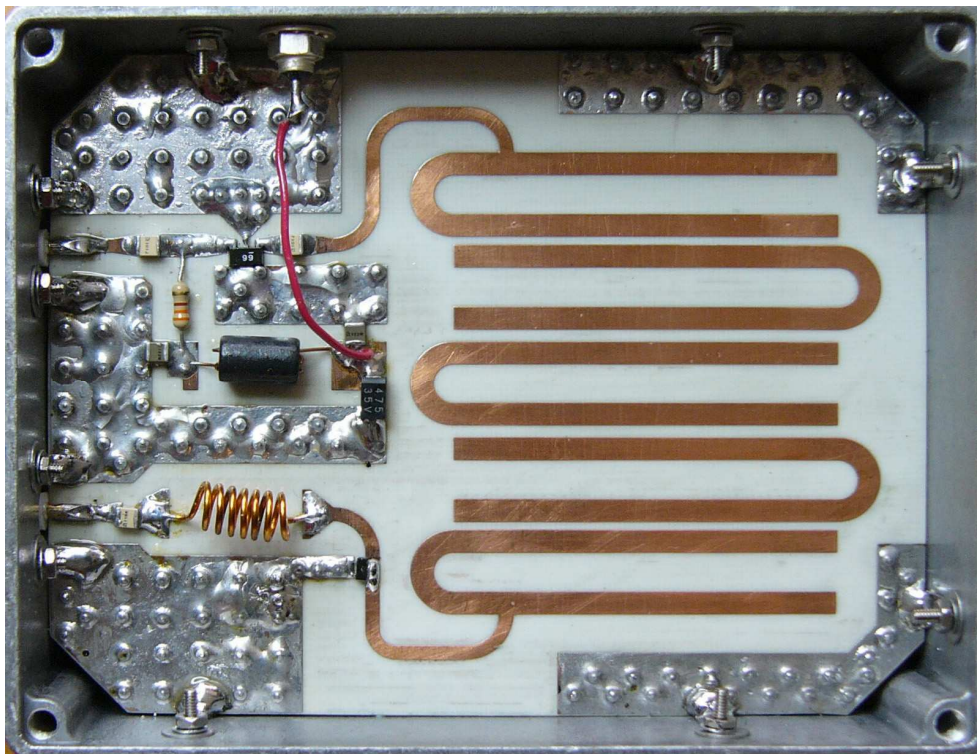


Figure 3. Harmonic Multiplier, to produce 810 MHz from 162 MHz.[1]

Currently wireless services operate at frequencies of 1.8 GHz for mobile phones, 2.5 GHz for Bluetooth and WLAN and 5 GHz for WLAN. In many cases IC's specially designed for these applications can be used at other frequencies. The designer should keep this in mind as can reduce the cost of specialised circuits.

Computer Simulation

For any commercial design, it is important to produce a properly function design as quickly as possible. Ideally there should be just one design iteration, it should be correct and reliable with the first realisation, since any further design iterations will cost more money and will delay the time before product comes to market, thus reducing any competitive advantage.

Computer simulation allows most aspects of the design to be investigated and optimised quickly before any hardware is produced. The modern computer simulation tools are very good and generally allow a correctly functioning design to be produced first time. The main commercial computer simulation systems are 1) EEs of EDA from Agilent [2] comprising Advanced System Design (ADS), GoldenGate RFIC Simulator (EMDS), Eagleware and other packages and 2) AWR software suite [3] comprising Microwave Office (MWO), Visual Systems Simulator (VSS), Analogue Office and other packages. Both perform well, and both allow linear, non-linear and time-domain circuit simulation, as well as the more detailed electromagnetic simulation. The author has used both ADS and MWO for many years and in the author's experience MWO is easier for the students to learn and as a result MWO has been used in the RF electronics course at James Cook University for which these lecture notes were produced by the author.

Both the Agilent and AWR software allow the design and simulation of RF IC's. It is very expensive to actually manufacture an RF IC. The author encourages the RF designs by the students to be manufactured, to allow the students to measure the actual performance of their designs and thus provide better feedback and a better learning experience to the students. As a result these notes concentrate on using commercial PCB substrates for components like couplers, combiners and filters and using commercial transistors and IC's in active RF designs.

References

1. Kikkert, C. J. "The Design of a Ka band Satellite Beacon Receiver", ICICS07, Dec 10-13, Singapore.
2. Agilent EEs of EDA <http://eesof.tm.agilent.com/>
3. AWR Corp: MWO, VSS Design Software <http://web.awrcorp.com/>

Chapter 2

Computer Simulation

Introduction

There are many computer simulation programs available. The most accurate ones use Spice models, which include all relevant parameters. At lower frequencies programmes like the commercial “Multisim” and the free “Microcap” are useful, but for RF circuits computer simulation tools that incorporate transmission lines as elements, and are specially designed to handle high frequency effects are preferred. Typical examples are ADS by Agilent [1] and Microwave Office by AWR [2]. For these notes AWR Design Environment Version 8.03 [3] is used extensively. This is a very powerful computer simulation suite. At James Cook University, students have found this to be easier to become proficient at than ADS, which we used earlier.

Microwave Office is very good for RF simulations, in that many commercial RF transistors and diodes can be simulated using both linear models and non-linear (harmonic balance) models.

The linear models treat any passive and active devices as “linear” devices and use conventional circuit analysis techniques to solve the equations for the circuit to be simulated. As a result the simulation is fast but will not deal with non-linear effects such as those that occur in a mixer, oscillator or amplifier. Applying optimisation techniques to the linear simulation of the circuit allows the best performance to be obtained quickly.

Non-linear simulation uses a full Spice model to analyse the non-linear behaviour of a circuit. As examples, it allows the conversion loss of mixers to be calculated, and allows the variations of gain with signal amplitude in an oscillator to be calculated and it allows all the harmonics produced by the oscillator to be determined. Using the appropriate non-linear amplifier models, it allows the intermodulation distortion of an amplifier to be determined as a function of output power. Because this simulation is much more detailed, it takes significantly longer to complete. As a result, most designs are initially done using linear simulation models and then the final design is optimised using the harmonic balance models.

Computer simulation is a powerful tool for ensuring that a circuit has been designed to perform correctly. Normally one would firstly check the circuit under the ideal design conditions and then one would check that the circuit still performs correctly for all the component tolerances that are possible. Since the production of a PCB containing an RF circuit is quite expensive it is always good practice to fully simulate the circuit first.

The computer simulation process is illustrated by some examples.

Example 1: Low Pass Filter

Design a 4th order low pass filter and a high pass filter to have a cut off frequency of 250 MHz and an impedance level of 75 Ω , and in the second example combine these filters to form a VHF-UHF TV antenna diplexer.

For Butterworth filters the design equations are well known [4] and the components are:

$$C_i = \frac{1}{\pi F_c R} \sin\left(\frac{(2i-1)\pi}{2n}\right) \quad i = 1,3,5\dots \quad \text{Eqn. 1}$$

$$L_i = \frac{R}{\pi F_c} \sin\left(\frac{(2i-1)\pi}{2n}\right) \quad i = 2,4,6\dots \quad \text{Eqn. 2}$$

Where R is the desired load impedance and F_c is the cut off frequency. These equations can easily be entered into a spreadsheet, to give the results for the 250 MHz filter as follows:

Impedance	75		
Freq MHz	250		
Order	4		
Element			
	Normalised	Lowpass	Highpass
	Rs, Rn	R	R
	1 0.765367	75	75
	1 0.765367	C 6.497E-12	L 6.23838E-08
	2 1.847759	L 8.822E-08	C 4.59382E-12
	3 1.847759	C 1.568E-11	L 2.58402E-08
	4 0.765367	L 3.654E-08	C 1.10905E-11

Table 1. Butterworth filter element values

The highpass filter is obtained using the standard lowpass to highpass transformation described in most filter textbooks. We now enter these values into MWO, to do this we must create the required project as follows:

Open Microwave Office. This will then open up a blank project as shown in figure 1.

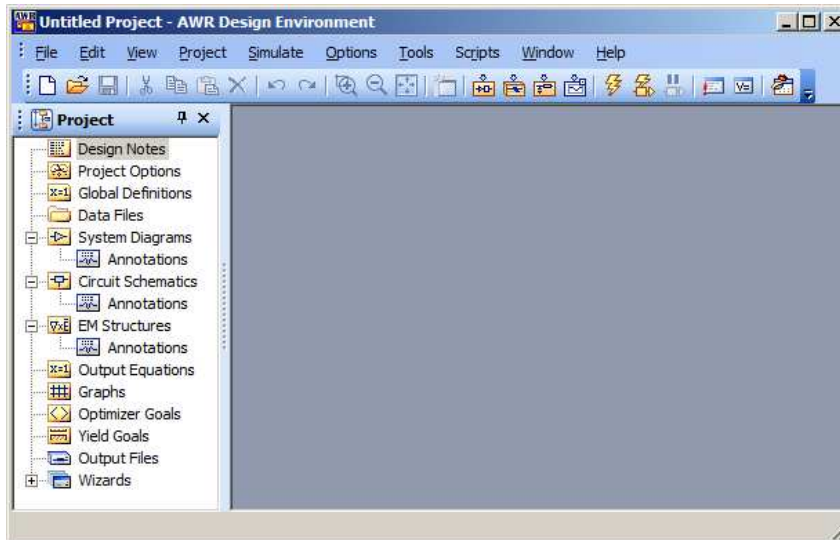


Figure 1. MWO blank project screen.

Select Project ⇒ Add Schematic ⇒ New Schematic and name the Schematic “LowPass”. Then select the Element window at the bottom left of the Design Environment window and select Lumped Elements ⇒ Capacitor and drag the CAP symbol into the circuit schematic as shown in figure 2.

Now place all the other capacitors and inductors in the correct location. When placing the component, a right mouse click rotates the component. Draw \Rightarrow Add Port allows the input and output ports to be added to the circuit. Draw \Rightarrow Add Ground allows a ground connection to be added. Double Left Click on a component allows the required value for that component to be entered. Repeat this for all the other components to give the final circuit as shown in figure 3.

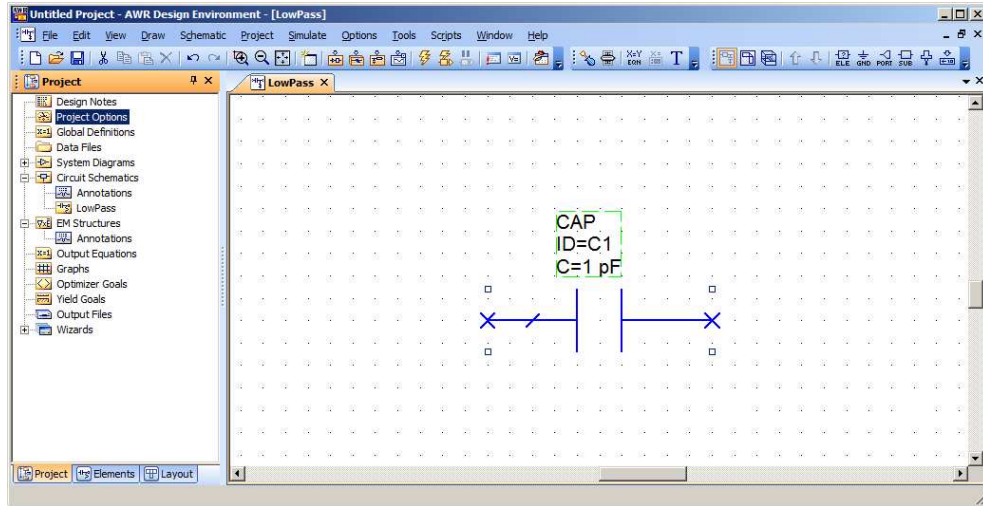


Figure 2, Capacitor placed.

Note that normally filters are designed with the smallest number of inductors, so that odd order filters with the end elements being capacitors are far more common. Since the filters are to be used as part of a diplexer consisting of a high-pass and a low-pass filter in parallel, the high-pass filter must not short out the low-pass filter at low frequencies and the low-pass filter must not short out the high-pass filter at high frequencies, so that an open circuit input impedance is required in the stopband of these filters. This is achieved with the first (series) element being an inductor for the low-pass filter, and the first element being a capacitor for the high-pass filter.

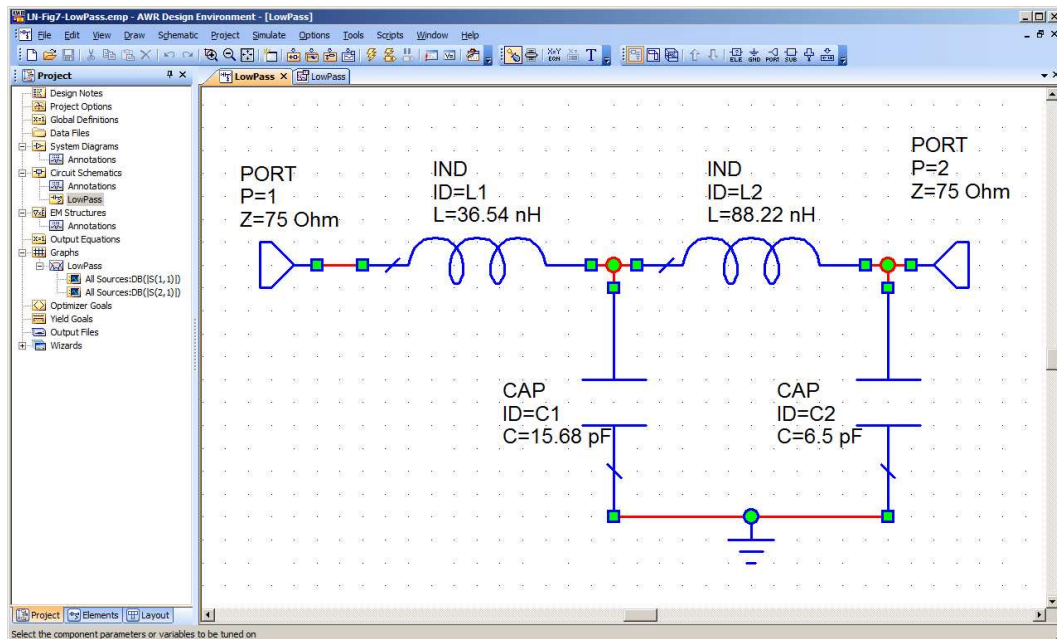


Figure 3. Low-pass filter circuit.

Select the project window again and select Graph and right mouse click and select add measurement. RF devices are normally specified by the Scattering (S) parameters, with S11 and S22 being the input and output return loss, indicating how well the device is matched and S21 and S12 being the forward and reverse gains. Select Linear Measurement type \Rightarrow Port Parameter and S parameter to obtain S parameter measurements of the filter, as shown in figure 4. Save the project as “LowPassFilter” to keep these values. Ensure that the impedance of the ports is changed from the default value of $50\ \Omega$ to $75\ \Omega$.

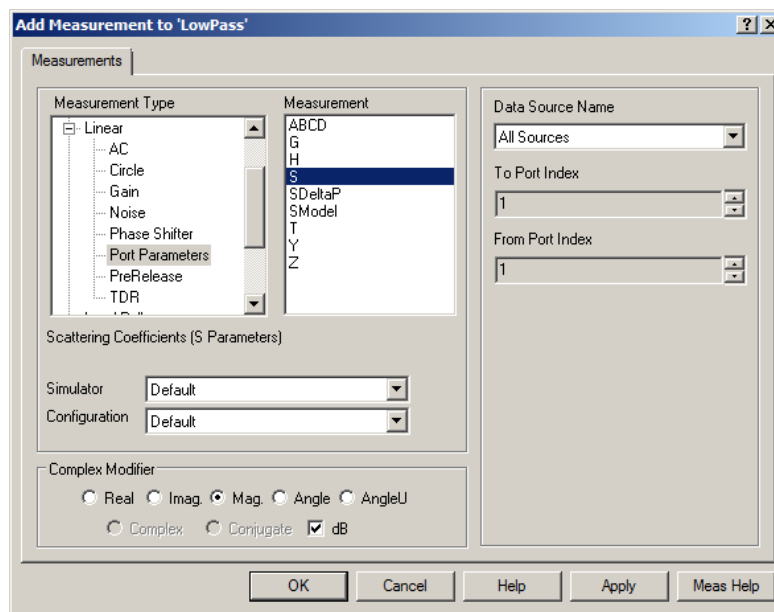


Figure 4. “Add Measurement” window.

Now set the operating frequency range using the Project options entry in the left bar. Set the Global Units frequency to MHz and then set the operating frequency range in the Frequencies window as shown in figure 5.

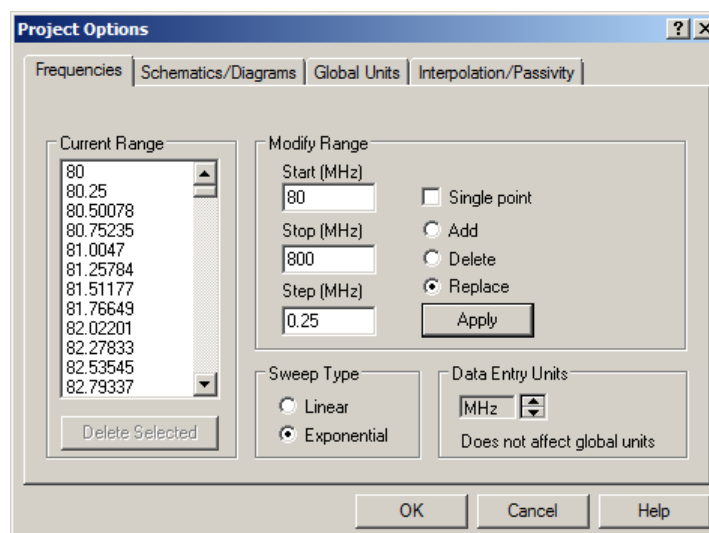


Figure 5. Project frequencies.

Select Simulate \Rightarrow Analyse to give the required frequency response as shown in figure 6. The scales, line thickness and other parameters of the graph can be set from inside the

Graph Property toolbar, (the left element of the right toolbar shown the blue area in figure 6).

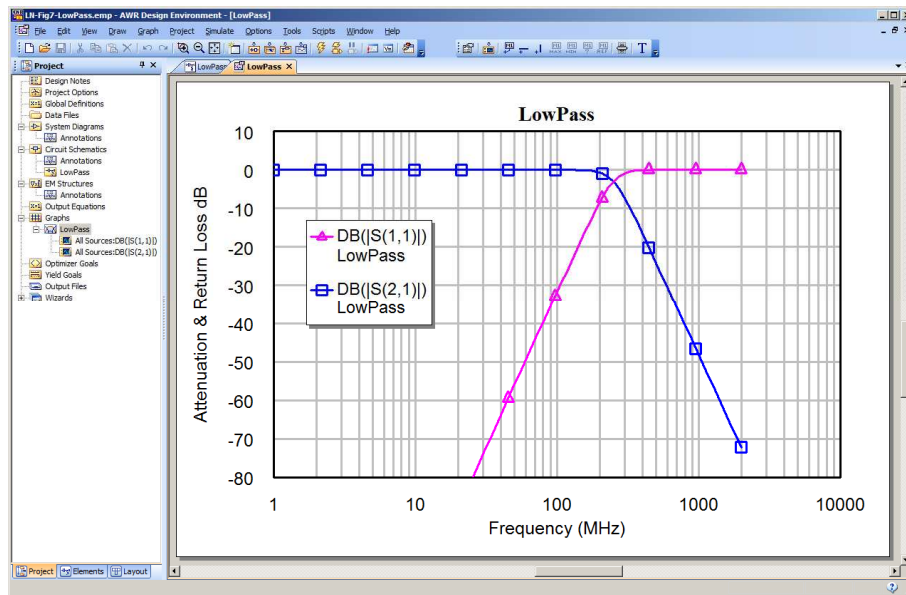


Figure 6. Frequency response of the low-pass filter.

The blue graph is the transfer function S_{21} and the magenta one is the input reflection coefficient S_{11} .

Equations in MWO

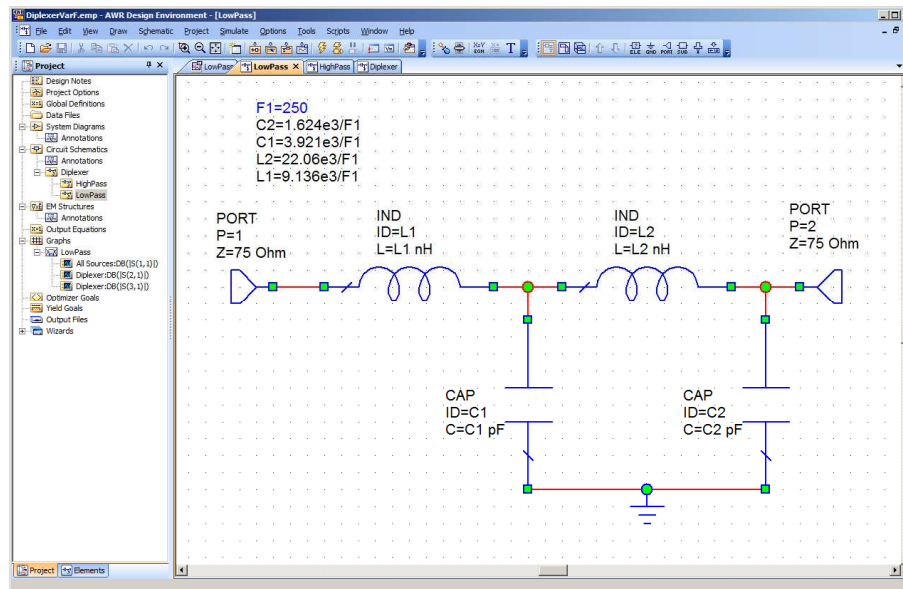


Figure 7. Tuneable filter.

It is possible to use variables and equations as part of the circuit diagram. This allows greater control over the filter parameters. For instance by making the cut off frequency a variable, the filter can easily be tuned to achieve a required cut off frequency. The cut off frequency can be tuned or optimised to meet required specifications. The resulting circuit diagram is shown in figure 7. The variables can be placed in any order, provided that any variable specification is above the variable usage. The frequency variable F1

must thus be on top, since that is used by C1, C2, L1 and L2. C1 must be higher than the capacitor using the variable C1 and so on. Unknown variables are shown in red. Any corrective action may simply be the moving around of a variable to satisfy this top to bottom flow requirements.

Example 2: Diplexer

It is required to design a Diplexer to permit VHF and UHF TV signals to be received by separate antennae and then combined to be fed to a TV. The corner frequency is chosen to be 250 MHz. The same circuit can be used as a splitter, to separate FM radio from UHF TV. A diplexer consists of a low pass filter selecting the low frequency components and a high pass filter selecting the high frequency components.

The low-pass filter can be the Butterworth low-pass filter of figure 7. A Butterworth High pass filter with a 250 MHz cut off frequency can be designed and entered into MWO.

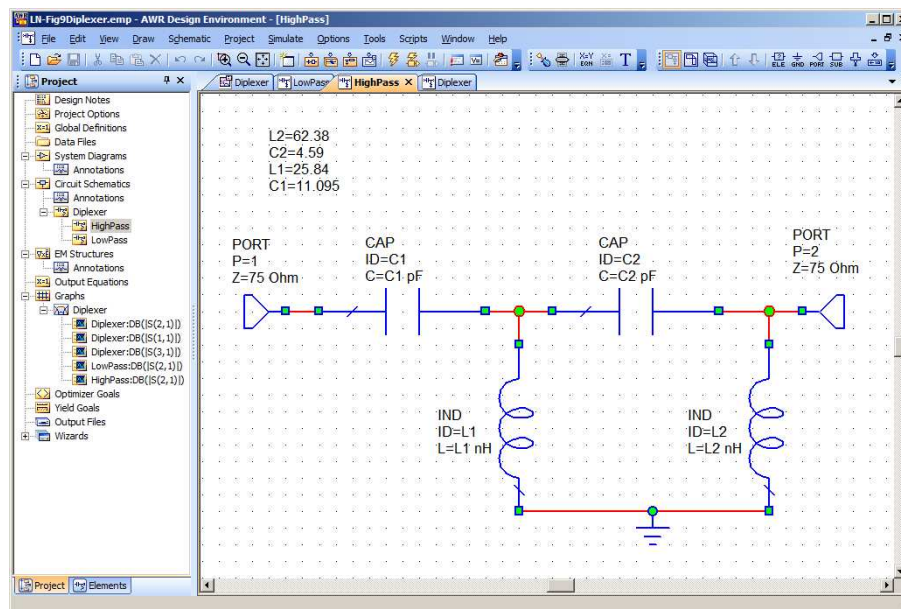


Figure 8. High-pass filter.

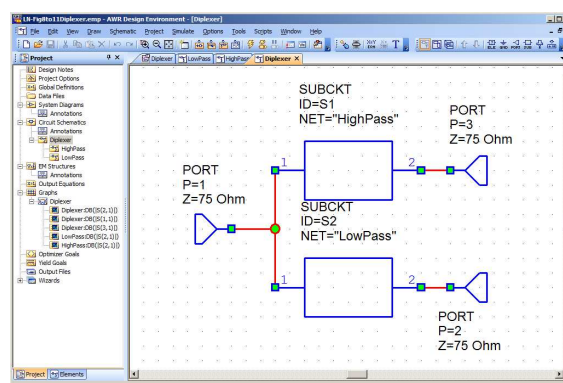


Figure 9. Diplexer using low-pass and high-pass sub-circuits.

The easiest way to produce the diplexer is to produce a separate high pass filter and then use that and the low pass filters as sub-circuits to produce the diplexer. The High pass filter uses the component values from table 1 and is shown in figure 8. The full diplexer

is shown in figure 9, and the resulting S parameters are shown in figure 10. Since the high pass filter and low pass filter are in parallel, the low pass filter must have an open-circuit input impedance at high frequencies and the high pass filter must have an open circuit input impedance at low frequencies. This is achieved by using filters that have the first element as a series element for the input.

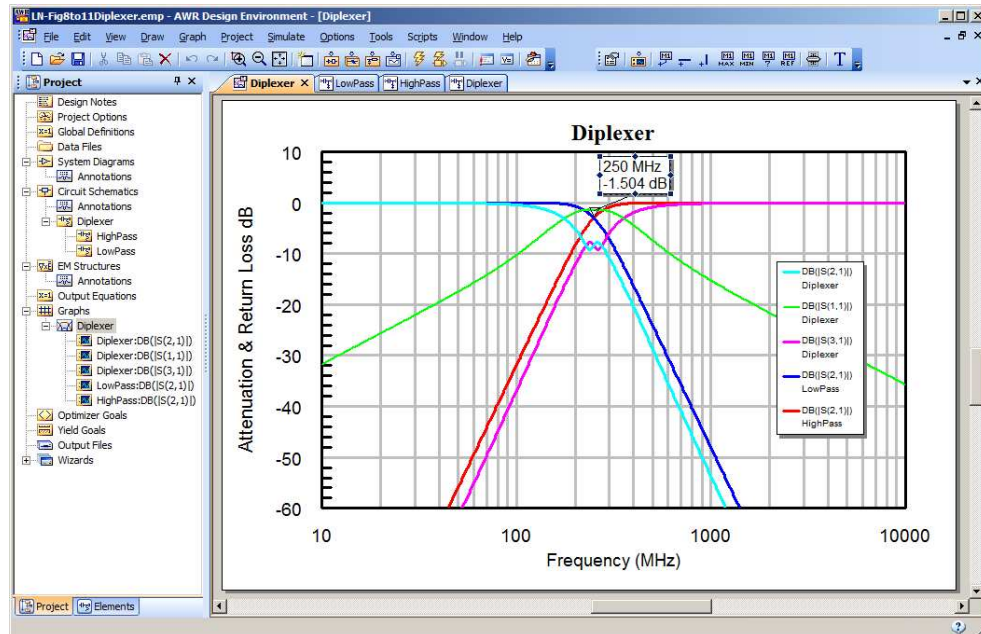


Figure 10. Frequency response of the diplexer.

Optimisation

As can be seen from figure 10, return loss (S_{11}) is only -1.4 dB near the cut off frequency of the filters so that the input is poorly matched. By comparing the blue curve of the low pass filter by itself, with the cyan curve of the low pass filter as part of the diplexer, it can be seen that there is a significant interaction between the lowpass and highpass filters. There is a similar degradation in performance of the highpass filter, as shown by the red and magenta traces. One can use the optimisation capability to improve the performance of the diplexer at the crossover frequency range. The first task is to specify the optimisation goals. For this design the requirements are that S_{11} is less than -20 dB over the entire VHF and UHF TV frequency range. In Australia the VHF TV frequencies range from 46 MHz to 230 MHz and the UHF TV frequencies range from 527 MHz to 820 MHz. Similar frequency ranges are used in other countries. For the example here 250 MHz is used as the boundary between VHF and UHF. As a result S_{21} (low-pass transfer function) is to be greater than -3 dB for frequencies below 250 MHz and S_{31} (high-pass transfer function) is to be greater than -3 dB for frequencies above 250 MHz.

These optimisation goals are entered in the optimisation goal function as shown in figure 11. Double click on the elements to be optimised and selecting the “opt” checkbox in the element options window, for the component or the variable linked to a component as shown in figures 7 and 8, to ensure that the element can be optimised. In addition some attenuation limits at 100 MHz and -40 dB and 625 MHz and -40 dB are added, to ensure a steep rolloff for the diplexer. The weighting of the optimisation limits for S_{21} and S_{31} are made 1000 since we want to ensure that these limits are satisfied.

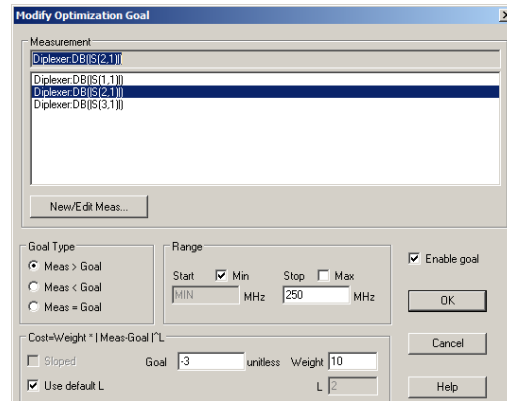


Figure 11. Specification of optimisation goals.

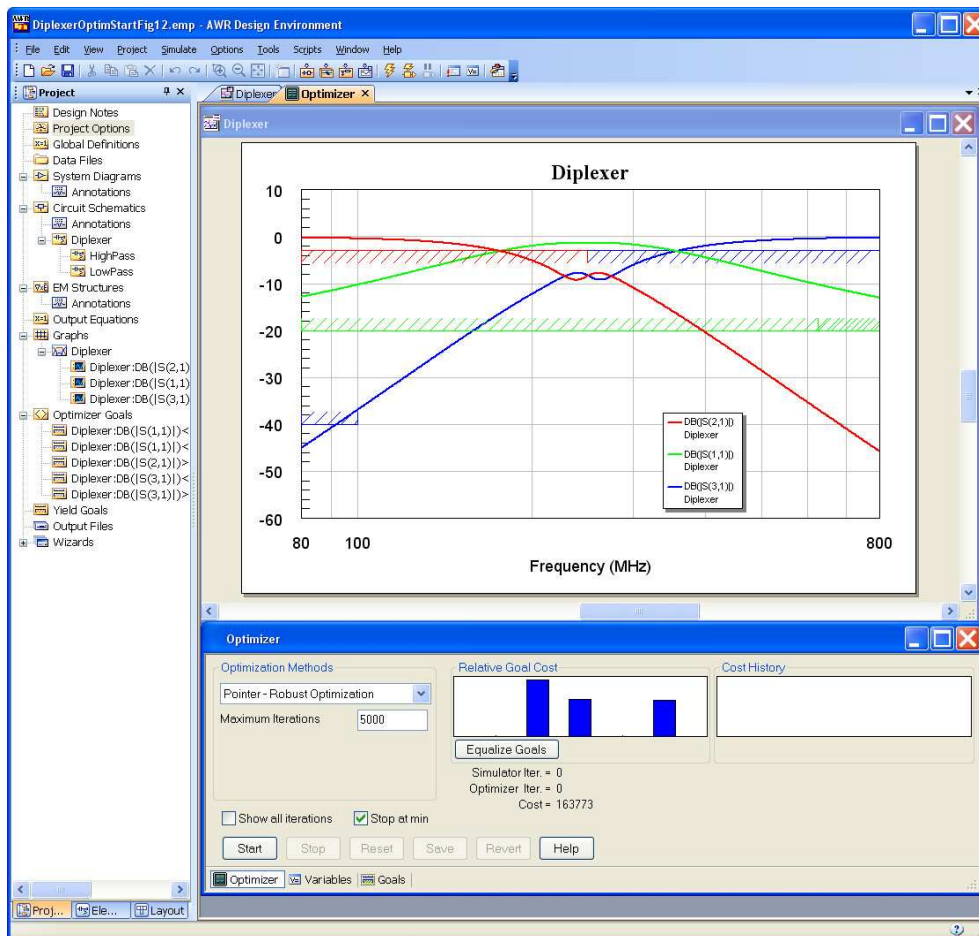


Figure 12. Optimisation criteria and the diplexer performance before optimisation.

Simulate \Rightarrow Optimise is selected to start the optimisation. For the first part of the optimisation Pointer-Robust optimisation is a good optimisation method to use. Once the requirements are met, the S_{11} limit is progressively reduced from -20 dB to -35 dB. Figure 12 shows the optimisation starting performance with the optimisation goals and the Optimizer panel

When the Pointer-Robust optimisation becomes stuck, so that the cost function does not decrease, it is worthwhile to change some conditions since the optimisation may be stuck in a local minimum rather than the global minimum for the cost function. Changing the weight for one or more of the goals or changing the optimisation function

may get the optimisation out of the local minimum. The “random local” optimiser is good for a complex optimisation function that will exist close to the global optimum condition. Figure 13 shows the optimisation criteria and the performance after the optimisation has been completed. It can be seen that the diplexer meets all the required specifications and that it is even possible to meet a -35 dB return loss on S_{11} .

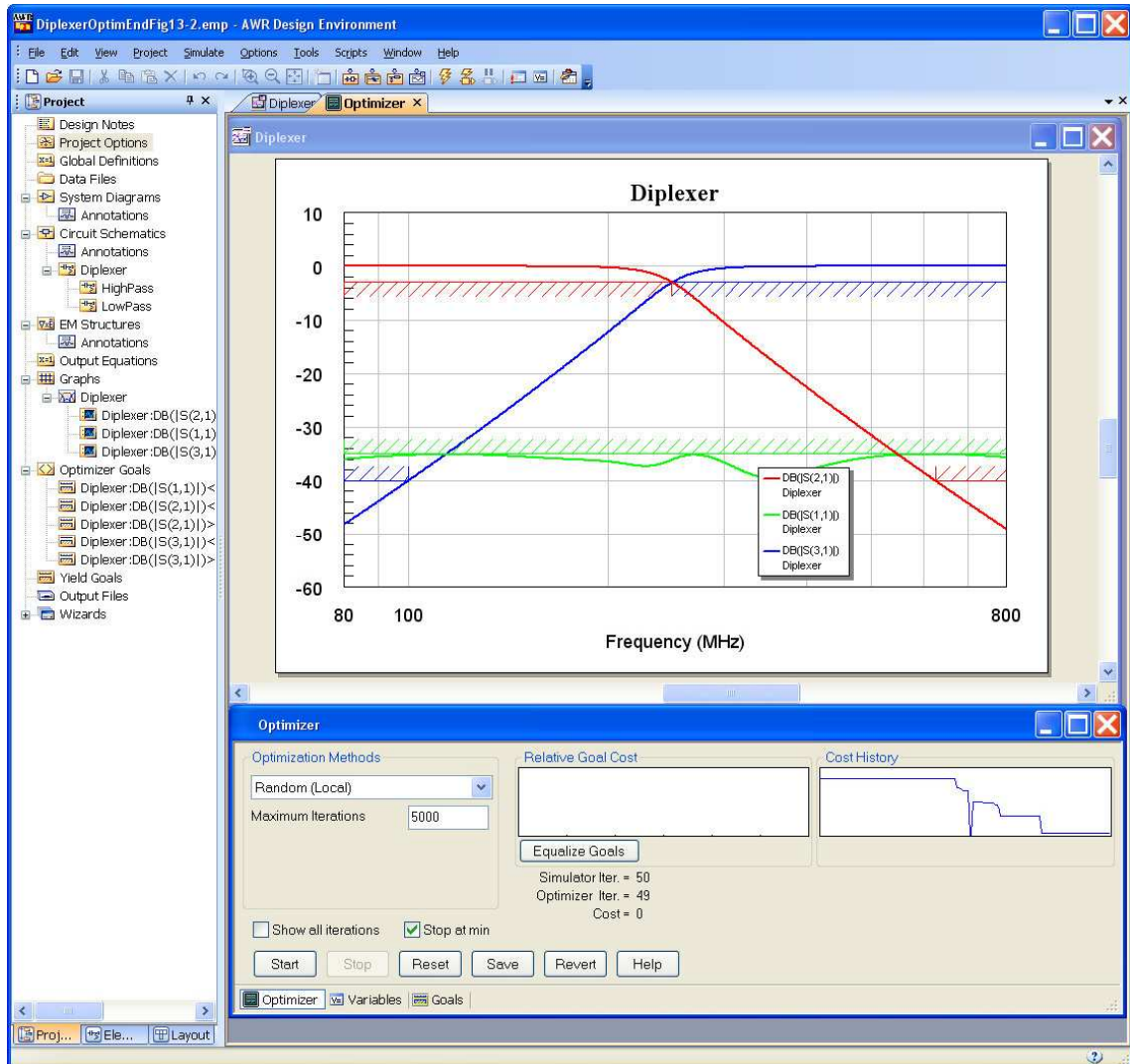


Figure 13. Optimisation criteria and the diplexer performance after optimisation.

The component values of the filter after optimisation for the low-pass sub-circuit are shown in figure 14 and those for the high-pass sub-circuit are shown in figure 15. Note that the component values are significantly different from the starting values using the Butterworth filter table values. The component values are very practical, so that the diplexer can easily be made

It is possible to replace the inductors using microstrip lines as outlined in the lecture notes on RF filters. That allows this diplexer to be made on a low cost FR3 or FR4 PCB using only capacitors and microstrip lines. If this is done then the length and impedances of the microstrip lines must be further optimised to meet the same specifications as this diplexer.

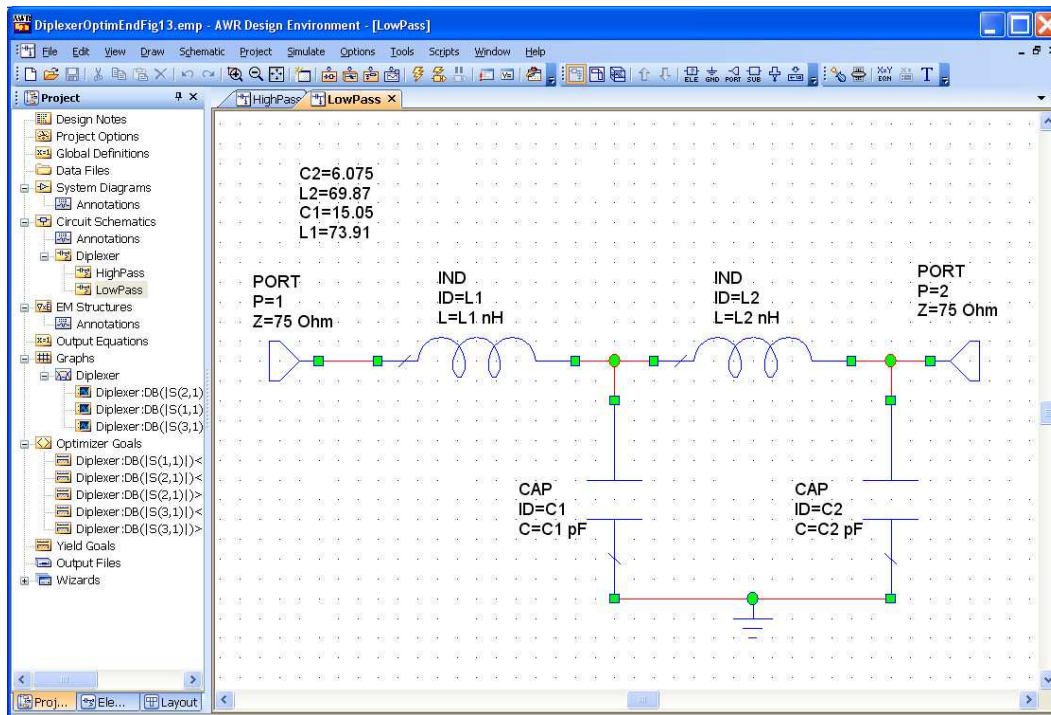


Figure 14. Final low-pass filter for diplexer.

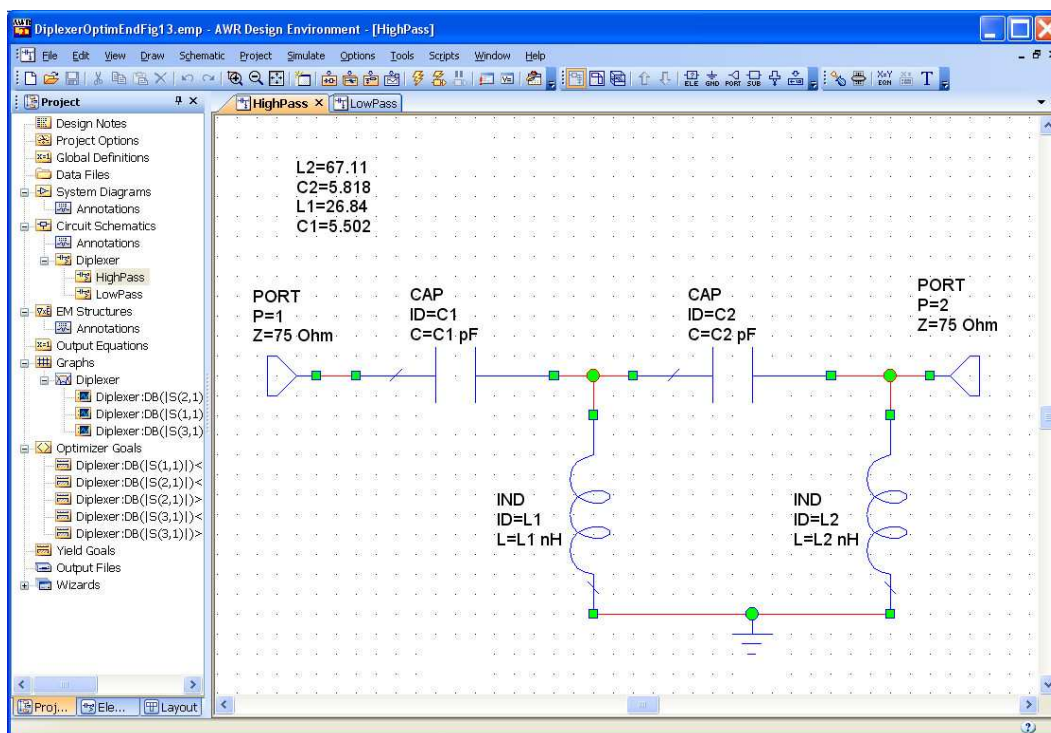


Figure 15. Final high-pass filter for diplexer.

Example 3: Amplifier

For the second example an amplifier is designed and its performance is determined. The design is to use a 2N4124 transistor. The transistor data can be obtained from the manufacturer's (Fairchild) web site. Since the 2N4124 transistor is not included in the standard MWO parts list, the parameters for the transistor model must be entered manually. If the full model is entered, the quiescent voltages can be determined by

MWO using the harmonic balance simulation. This is very useful to ensure that the biasing is correct. Figure 16 shows the circuit of a simple amplifier using the 2N4124 transistor and the manufacturer's data. Many manufacturers of RF transistors now give full transistor models for MWO or ADS from their web site.

The most critical of any transistor design is the biasing. By right clicking on the Transamp circuit schematic and selecting "Add Annotation" and then selecting "DCVA_N" will provide voltages at all the nodes in the circuit, to enable the biasing voltages to be checked and compared with the design values. The node voltage annotation is shown in figure 16. Similarly currents in and out of all the nodes can also be shown. If needed the effect of supply voltage and component variations can be investigated, to ensure that the design works properly for all expected component tolerances.

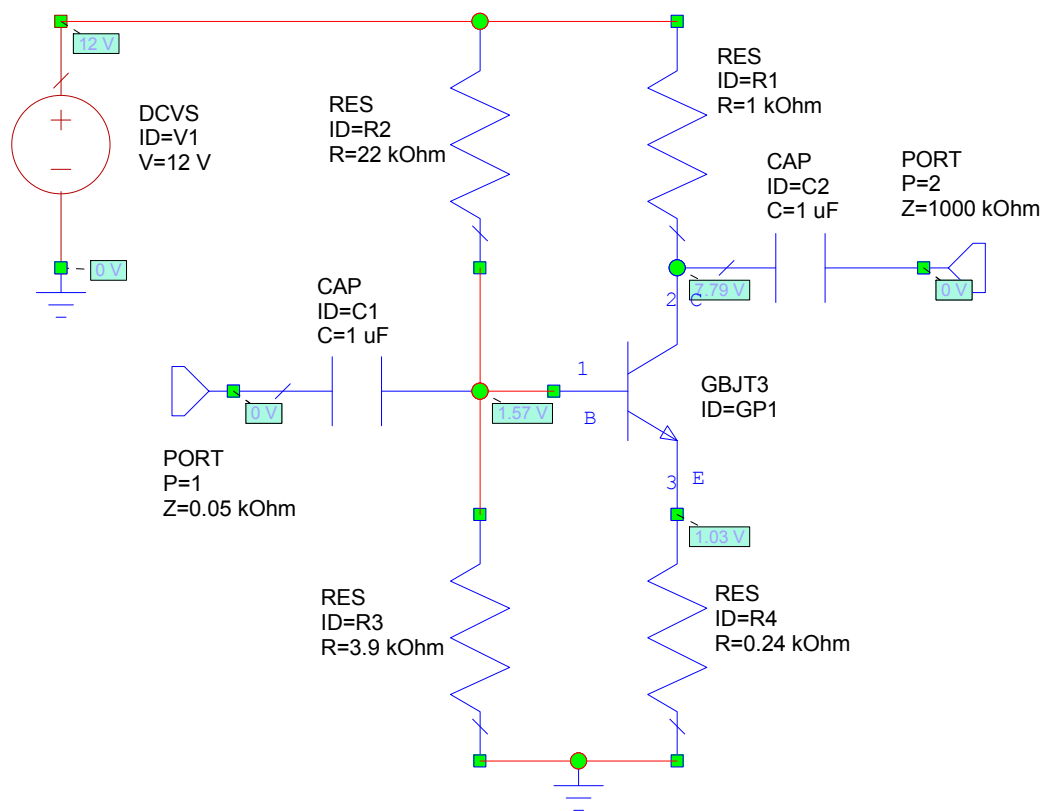


Figure 16. MWO transistor amplifier schematic diagram.

The resulting frequency response of the amplifier is obtained by selecting Graph \Rightarrow New Graph \Rightarrow Rectangular. Then right clicking in on that graph label in the Project Browser and selecting Add Measurement to add the measurement required. In this case VTG (Voltage gain from input to output terminal) with the magnitude response in dB is selected. The frequency range over which the measurements are made are set by double clicking on "Project Options" in the Project Browser and then specifying the frequency range. In this case The data entry units are set to kHz and the start frequency is set to 0.03 kHz and the stop frequency is set to $3e5$ kHz and the exponential step size is set to 0.03 kHz. The resulting frequency response from the amplifier is shown in figure 17. The results from MWO are virtually identical to those from Microcap. Selecting Graph

⇒ Marker ⇒ Add Marker, allows markers to be added to the graph. These markers can search for the maximum value of the voltage, or for specific attenuation values or frequencies. Using these markers, the amplifier has a gain of 11.9 dB and an upper 3dB point of 94.4MHz.

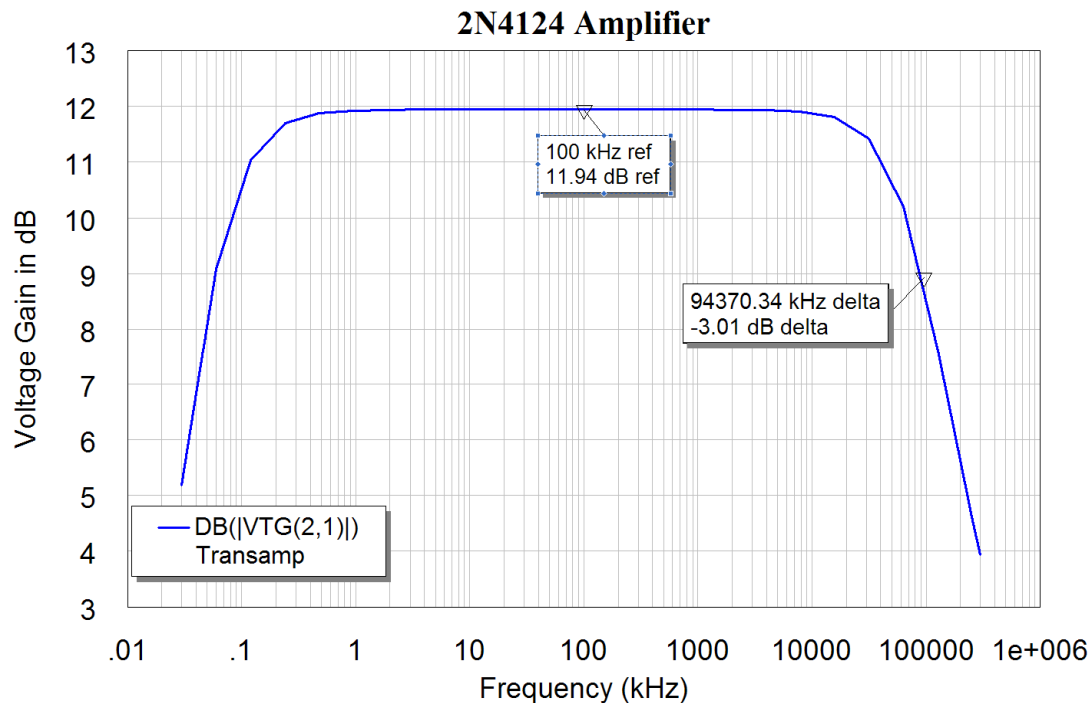


Figure 17. Frequency response from Microwave Office.

Transistor Models

Two types of transistor models can be used, firstly a very simple closed form model, like the Hybrid, Pi or T models used in basic electronic design subjects. For the simple closed form transistor model, MWO treats the transistor as a linear device and only AC analysis can be performed. The model used by MWO is as follows:

Equivalent Circuit

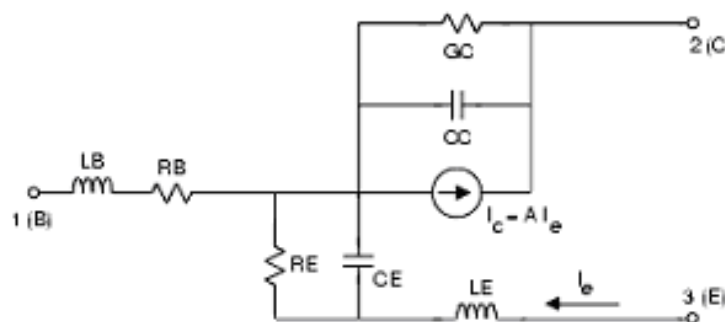


Figure 18. Circuit of the closed form transistor model from Microwave Office [5].

Parameters

Name	Description	Unit Type	Default
ID	Element ID	Text	B1
A	Magnitude of DC current gain (alpha)	None	0.8
T	Current gain time delay	Time	0 ns
F	-3dB frequency for current gain	Frequency	0 GHz
CC	Collector capacitance	Capacitance	0 pF
GC	Collector conductance	Conductance	0 S
RB	Base resistance	Resistance	1 Ohm
LB	Base inductance	Inductance	0 nH
CE	Emitter capacitance	Capacitance	0 pF
RE	Emitter resistance	Resistance	1 Ohm
LE	Emitter inductance	Inductance	0 nH

Figure 19. Parameters of the closed form transistor model from Microwave Office.

Alternately a more sophisticated Spice model can be used. Spice models for a wide variety of transistors can be obtained from Fairchild Semiconductors. The model for the 2N4124 transistor obtained from the Fairchild web site is as follows:

```
.model 2N4124 NPN(Is=6.734f Xti=3 Eg=1.11 Vaf=74.03 Bf=495 Ne=1.28
Ise=6.734f Ikf=69.35m Xtb=1.5 Br=.7214 Nc=2 Isc=0 Ikr=0 Rc=1 Cjc=3.638p
Mjc=.3085 Vjc=.75 Fc=.5 Cje=4.493p Mje=.2593 Vje=.75 Tr=238.3n Tf=301.3p
Itf=.4 Vtf=4 Xtf=2 Rb=10)
* Fairchild pid=23 case=TO92
* 88-09-08 bam creation
```

Circuit simulation software like Multisim, MicroCap and MWO all use the same basic Spice transistor model, with Multisim using exactly the same model as produced by Fairchild. Microcap uses some extra parameters. MWO uses a slightly more sophisticated model, which is better for high frequencies and includes:

- 1 Terminal inductances LB , LC , and LE ,
- 2 Complete collector-to-substrate diode parameters, CJS , VJS , MJS , ISS , NS , and TS ,
- 3 A different (but equivalent) formulation for nonlinear base resistance,

Equivalent Circuit

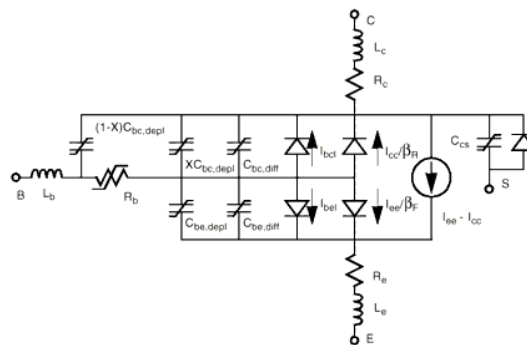


Figure 20. Circuit diagram of the Gummel-Poon Transistor model From Microwave Office.

The Gummel-Poon Transistor model [5] included in Microwave Office has the circuit diagram as shown in figure 20. The model is significantly more complex than the simple closed form model shown two pages previously. This model is however far more accurate. Note the transistor lead inductances, which have significant impedances at higher frequencies.

The parameters for the Gummel-Poon transistor model can be accessed by double clicking the transistor as shown in figure 21 and selecting secondary properties in the parameter window [6]. Using an existing transistor as a starting point, the model for another transistor can be produced by editing the secondary parameters and then saving that with a new part number.

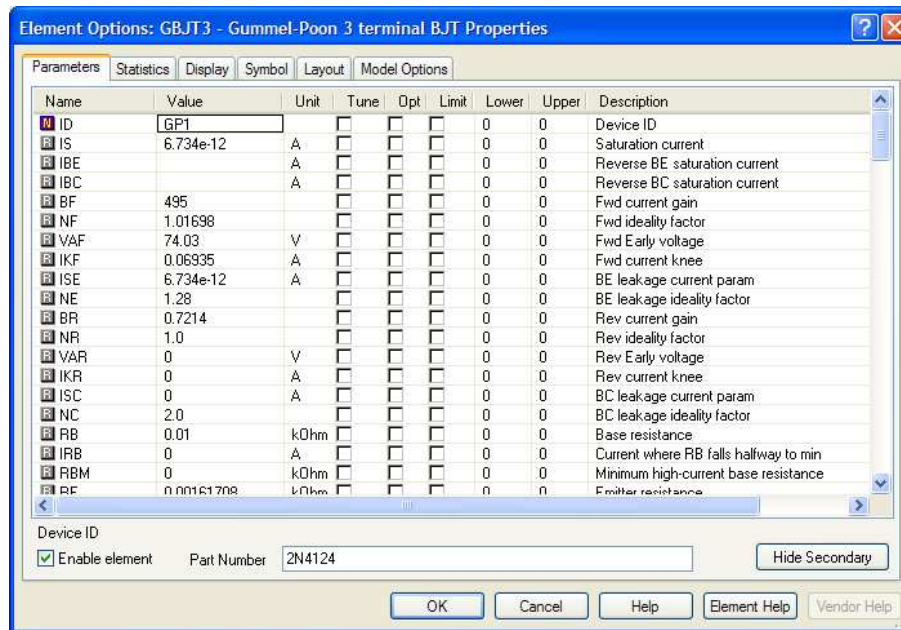


Figure 21. Parameters from the Gummel-Poon Transistor model From Microwave Office.

Determination of Line Parameters

In many applications a printed circuit layout using microwave printed circuit board materials needs to be made. The widths and lengths required can be determined from a program Txline, which is part of Microwave Office. ADS has a similar program called Linecalc. Both these programs do not cover all the different coupled lines or strip lines available. In many cases it is more convenient to use the schematic circuit realisation of the transmission line models to determine the required line parameters, rather than using Txline or Linecalc. This technique is illustrated by the following example of a quarter wavelength microstrip line with a 50Ω impedance at 1 GHz.

The calculations for the width of a 50Ω microstrip line using Txline for a Rogers RO4003 substrate, with a dielectric constant of 3.38, a loss tangent of 0.0027, a substrate thickness of 0.8128 mm and 35 micron (1 oz) copper cladding, is shown in figure 24. This shows that a quarter wavelength microstrip line with a 50Ω impedance at 1 GHz requires a track width of 1.84308 mm and should be 45.9755 mm long.

The same line width determination can be done by making some very simple test circuits and optimising the relevant parameters. Figure 22 shows a schematic for determining the correct line width for a 50Ω track on a RO4003 substrate. When the line is exactly 50Ω , then the return loss (S_{11}) is very small regardless of frequency, as

described in chapter 4 of these notes [7]. The same PCB parameters that are used in Txline are used for the substrate element in the circuit schematic of figure 23. Tuning or optimising the line width to give the lowest return loss S_{11} results in a -60 dB return loss for a 1.851 mm line width. That width is close to the result from Txline.

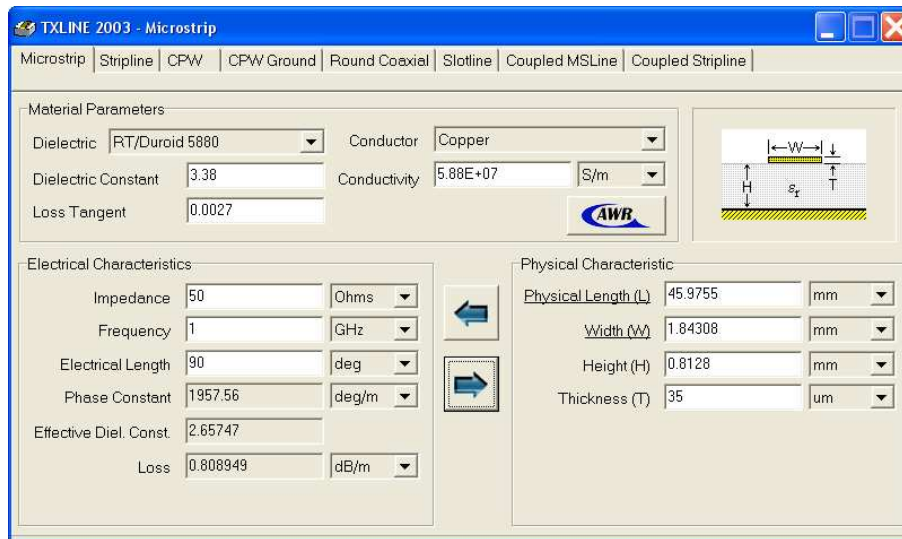


Figure 22. Txline program for calculating line parameters.

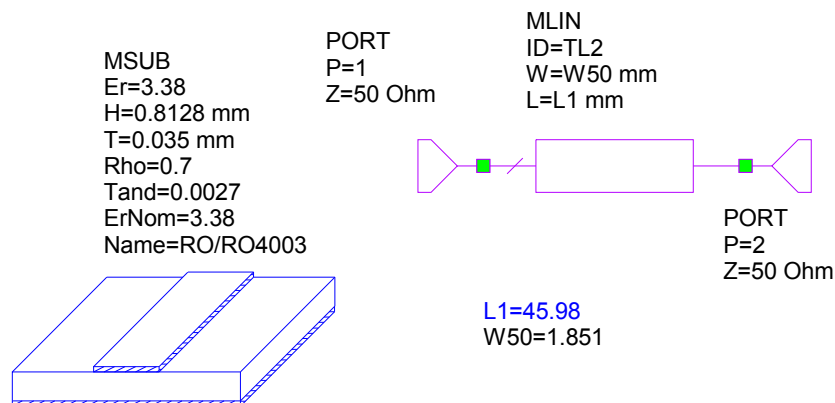


Figure 23. Circuit for determining Microstrip line widths.

When the length of a quarter wavelength long line needs to be determined, then the circuit of figure 24 can be used. The open circuited stub will reflect as a short-circuit when the length of the stub is one quarter wavelength. Using the width as determined in figures 23 or 24, the length is now tuned or optimised to produce a notch at the required frequency, as shown in figure 25. The T junction can be included to ensure that the actual layout, including the required junctions, performs exactly as required. This technique is very useful for obtaining the correct length when the stub has bends in it, as is the case for folded branch-line couplers as used in the first laboratory session for these notes [8].

For many circuits, simple test circuits like those of figures 23 to 25 can be used to determine the basic parameters of stripline or microstrip lines that can then be used as part of a more complex circuit. This technique for determining microstrip, or stripline,

parameters from circuit schematic measurements is used in several places throughout these lecture notes.

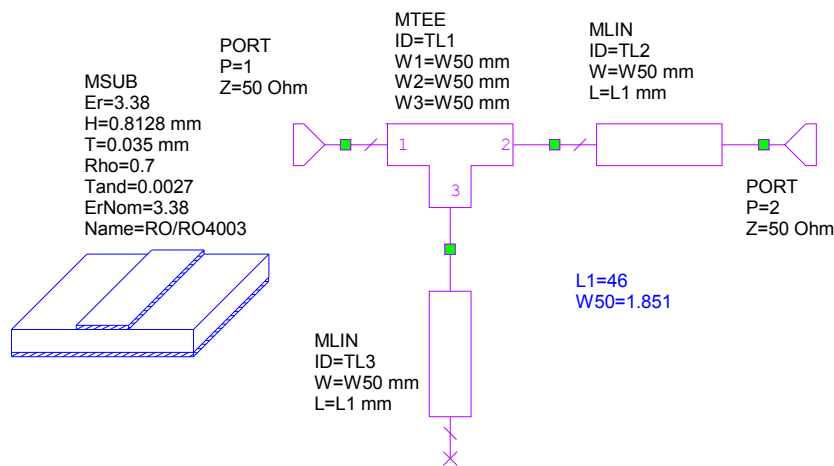


Figure 24. Circuit for determining the length of one quarter wavelength.

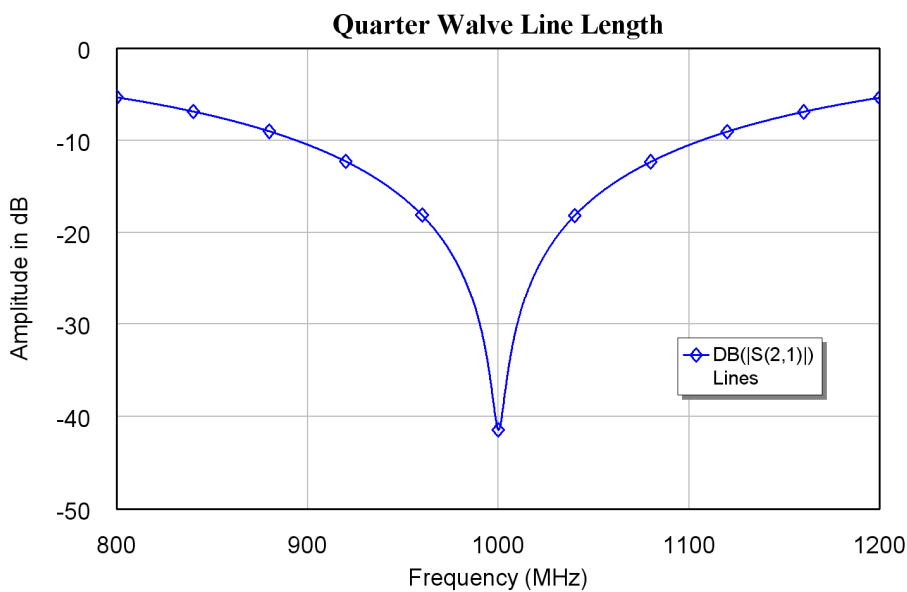


Figure 25. Frequency response of the circuit in figure 24.

Summary

This chapter has introduced some basic aspects of computer simulation using Microwave Office. During the rest of these notes, the computer simulation will be expanded with both linear and non-linear applications and examples.

MWO has a good interactive help capability, with specific information available for every circuit element. The interactive element help can be accessed by right clicking on the element and selecting “Element Help”. In addition the examples included with the AWR software will assist in understanding the operation of RF computer simulation software.

References

1. Agilent EEsof EDA <http://eesof.tm.agilent.com/>
2. AWR Corp: MWO, VSS Design Software <http://web.awrcorp.com/>
3. Microwave Office <http://web.awrcorp.com/Usa/Products/Microwave-Office/>
4. Zverev, A. I. "Handbook of filter Synthesis", Book Publisher John Wiley & sons 1967.
5. H. K. Gummel and R. C. Poon, "An Integral charge control model of bipolar transistors", Bell Syst. Tech. J. Vol 49, pp827-852, May-June 1970.
6. AWR Corp. "MWO Help files: MWO/AO Element Catalog>Nonlinear>Gummel-Poon BJT:GBJT"
7. Kikkert C. J. "RF Electronics : Transmission Line Transformers and Hybrids" Chapter 4, Available through AWR.
8. Kikkert C. J. "RF Simulation using Microwave Office" Practical Session 1, Available through AWR.

Chapter 3

Transformers and Hybrids

Introduction

At RF frequencies Transformers are used to:

- 1 Invert signals by producing a 180 degree phase shift.
- 2 Change Impedances, to ensure that devices are matched correctly, thus ensuring that most of the power is transferred into or out of the devices.
- 3 Change balanced signals from a TV antenna to unbalanced signals for transmission using coaxial cables and connecting to a TV set.
- 4 Change unbalanced signals to balanced ones for use in mixers.
- 5 Provide DC isolation and permit DC and RF signals to be carried on the same coaxial cable for masthead amplifiers and other remote powered applications.

RF Transformers differ from audio and 50 Hz mains transformers in that:

- 1 Ferrites are normally used for the magnetic material.
- 2 The windings may be an appreciable fraction of the wavelength.
- 3 Capacitive coupling between the primary and secondary windings must be taken into account.
- 4 The transformers may need to operate over several decades of frequency.
- 5 At VHF frequencies and above, transmission lines may be used as transformers, without the use of ferrites. Such transformers operate over a relatively small frequency range.

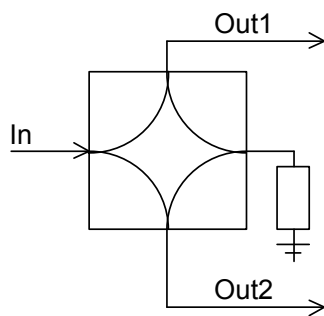


Figure 1. Hybrid symbol.

Hybrids are used to split or combine signals, while providing isolation between those signals.

Figure 1 shows the commonly used symbol for a hybrid. The input signal is divided equally between Out1 and Out2. Out1 and Out2 are isolated from each other. This allows us to drive two amplifiers, thereby improving amplifier stability and increasing the output power handling capability.

The power-handling capability of RF transistors operating up to 1 GHz is typically 100 Watt. Figure 2 shows how two such 100 Watt amplifiers, together with two hybrids can be used to produce a 200 Watt amplifier. This also gives some redundancy against failure of an amplifier. If one amplifier fails, the output will drop by 6 dB, but the system still operates. For higher power output requirements, many of these modules can be combined in a similar manner. As a result, solid state amplifier modules with output powers of several kW can be made.

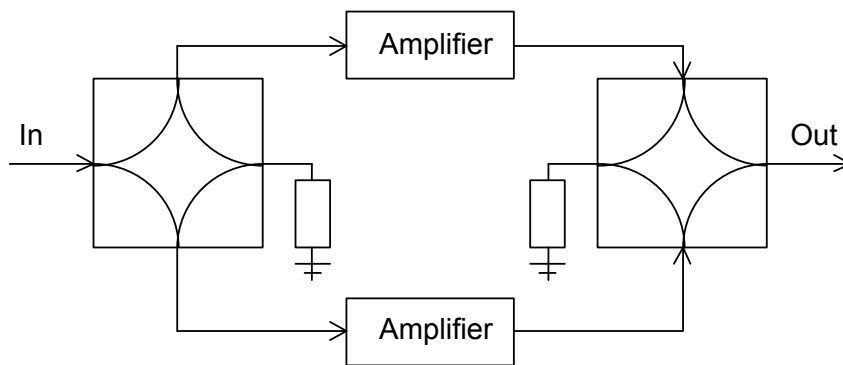


Figure 2. Parallel operation of amplifiers.

At VHF frequencies the hybrids are normally made using transmission lines. At lower frequencies the hybrids can be made using transformers. Most telephone handsets have either a transformer hybrid or an active hybrid using an ASIC (Application Specific IC).

Wideband Transformers

For a conventional ferrite transformer, the upper length of the winding is limited to approximately 10% of the wavelength. At 1 GHz the wavelength is 300 mm and the maximum winding length is thus 30 mm. If the windings are like a transmission line, as used in TV baluns shown in figures 7 and 8, this limit does not apply.

The corresponding lower limit [1] is:
$$l_{\min} = \frac{R_l}{2(1 + \mu_r) f_{\min}} \quad \text{Eqn.1}$$

Where R_l is load impedance in ohm, f_{\min} is the lowest operating frequency of the transformer in MHz and l_{\min} is the length of the winding in metres. For a Neosid F14 material with a μ_r of 220, operating at 1 MHz in a 50Ω system, the minimum winding length is thus 113 mm. This minimum winding length should be allowed for in transformers made using ferrites.

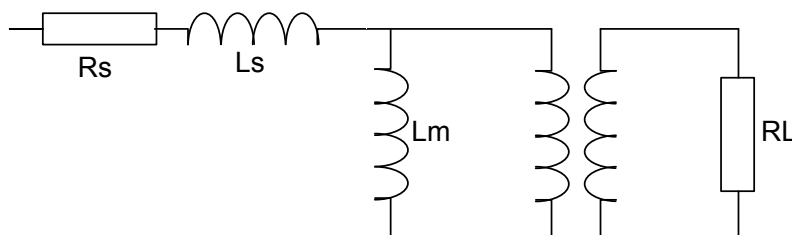


Figure 3. Simplified RF transformer model.

Transformers can be designed using the above equations, however by considering the simple conventional transformer model [2] shown in Figure 3, containing a Leakage inductance L_s and a Magnetising inductance L_m , the optimum number of turns required for RF transformers can be easily determined. To simplify the calculations assume that the transformer has a 1:1 turns ratio, so that the load R_L is also the load reflected into the primary. For other turns ratios, the load impedance reflected into the primary, is the impedance used for calculations.

At low frequency the Magnetising inductance L_m shunts the output load. The lower cut off frequency is thus when $j\omega L_M = R_L$. At high frequencies the Leakage inductance is in series with the output. The upper cut off frequency is thus when $j\omega L_S = R_L$.

The leakage inductance can most easily be measured by short circuiting the secondary winding of the transformer. Under those conditions the input impedance of the transformer is $R_s + j\omega L_S$. When the transformer is open circuited, the input impedance is $R_s + j\omega L_S + j\omega L_M$. Since L_m is typically 1000 times larger than L_s , the leakage inductance can be ignored as part of the lower frequency calculation.

If one normally wants to operate the transformer at a frequency F_c then it is desirable to make this $F_c = \sqrt{F_{low} F_{high}}$ where F_{low} and F_{high} are the upper and lower cut off frequencies of the transformer. As described above, the upper and lower cut off frequencies are determined by the leakage and magnetising inductance respectively.

The input impedance of the transformer at the centre frequency is thus:

$$Z_c = \sqrt{Z_{L_s} Z_{L_m}} = \sqrt{\omega L_s \omega L_m} \quad \text{Eqn. 2}$$

For a 50 Ω system, one wants this Z_c to be 50 Ω . Under those conditions $R_s + j\omega L_S$ is much smaller than R_L and $j\omega L_M$ is much larger than R_L , so that virtually all the input power is transferred to the output.

Since the inductance is proportional to the number of turns squared, the characteristic impedance of the transformer is also proportional to the number of turns squared. The number of turns chosen for the transformer winding is such that the characteristic impedance of the transformer matches the system impedance. Since in many cases the detailed properties of the ferrite may not be known, the characteristic impedance is most easily determined by winding a trial winding on the transformer and using the measured open and short circuited impedances to then calculate the correct number of turns required.

In practice the magnetising inductance has some losses associated with it and the resistive losses of the windings are in series with the leakage inductance. The resistive losses are normally very small. Since the inductance is proportional to the frequency, at the upper and lower frequency limits the inductance dominates, so that in the calculation for the upper and lower frequency limits, the resistive part of the measured input impedance can be ignored.

Example: RF Transformer Design

A ferrite coil has an 11 turn bifilar trial winding on it. At 1 MHz, input impedance with the secondary winding short-circuited is $Z_{L_s} = j0.4 \Omega$, corresponding to a leakage inductance of 64 nH. The input impedance measured with the secondary open-circuited is $Z_{L_m} = j400 \Omega$, corresponding to a magnetising inductance of 64 μ H. From equation 2, the characteristic impedance is thus $Z_c = \sqrt{(400 \times 0.4)} = 12.65 \Omega$.

The inductance is proportional to the square of the number of turns. Thus, for a 50 Ω transformer we need $11 \times \sqrt{(50/12.65)} = 22$ turns. For the 22 turn winding one will thus have a leakage inductance of 256 nH and a magnetising inductance of 256 μ H.

The ratio of the open circuit to the short circuit impedance is 1000:1. The ratio of the upper and lower cut off frequency is thus also 1000:1, with the centre frequency being

at the geometric mean of the upper and lower cut off frequencies. The upper cut off frequency is thus $1 \cdot \sqrt{1000}$ MHz = 32 MHz. The lower cut off is $1/\sqrt{1000}$ MHz = 32 KHz.

The measured performance normally agrees closely with the calculated one. The actual upper corner frequency is often a little lower than the calculated one, since the losses in the ferrite increase non-linearly with frequency and are thus proportionally lower at the centre frequency, where the measurements of the leakage and magnetising inductance are made. RF transformers using bifilar and trifilar windings operate well at frequencies up to several GHz.

Bifilar and Trifilar Windings

For a bifilar winding, two wires are twisted together to form a primary and secondary winding of a transformer, with close capacitive coupling between the windings, which result in a wide frequency response. Bifilar windings are used for inverting transformers. Trifilar windings use three wires twisted together as shown in figures 4 and 5. Trifilar windings are used for Baluns (Balanced-Unbalanced transformers) [3] and for transformers with a 4:1 impedance transformation ratio, as shown in figure 4. For most TV antennae, the output from the antenna is a balanced signal, on two active wires carrying signals of opposite polarity. For low loss transmission without interference, a coaxial cable is normally used to transmit this signal between the antenna and the TV set. A Balun is used to convert the balanced signals from the antenna to the match the unbalanced signal for the coaxial cable.

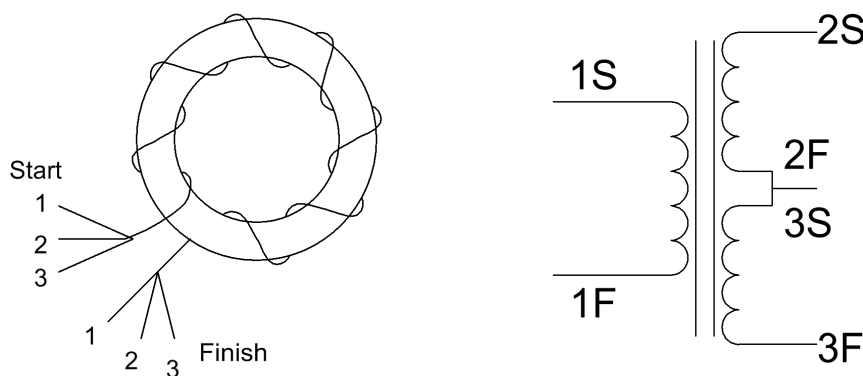


Figure 4. Trifilar winding diagram.



Figure 5. A trifilar wound RF Transformer (left) and a penta-filar transformer (right).

If port 2F-3S is earthed, then the transformer is a balanced to unbalanced transformer, called Balun. For a 75Ω input impedance, a 300Ω output impedance is obtained. Such a Balun is often used in TV antenna systems.

For instrumentation grade double balanced mixers a very good balance in the output signals is required, then an additional core, as shown in figure 6, can be added [3]. This provides winding 1 with a balanced input, thus causing the impedances at 2S to be exactly the same as those at 3F. Often the cost of the additional core is not justified.

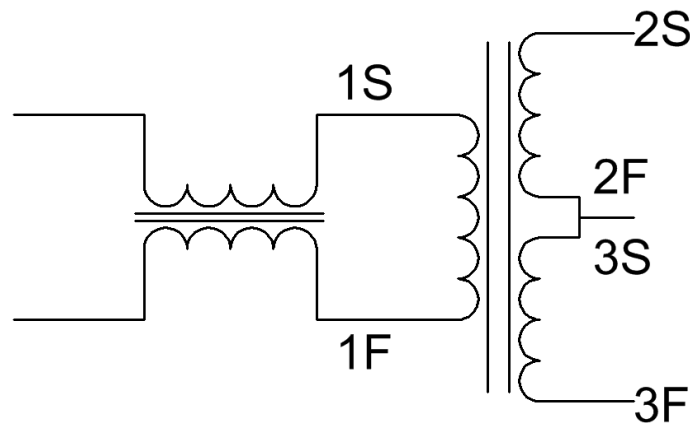


Figure 6. Balun with improved output balance.

Transmission line transformers with ferrite cores

At high frequencies, the primary and secondary windings are sometimes wound using transmission lines, as shown in Figures 7 and 8.

For a 50Ω system, the characteristic impedance for the transmission lines used for the windings are 100Ω . There is thus no reflection, at the junction where the two lines are connected in parallel. The two transmission lines are in series at the right hand side and the balanced output then form a 200Ω system. Since the same propagation delay occurs through both the top and bottom transmission lines, the + and - signals are perfectly balanced at all frequencies.

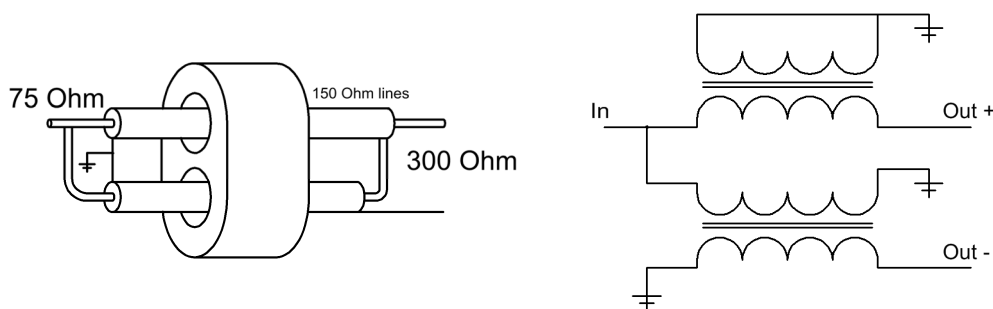


Figure 7. Diagram of transformers with ferrites and transmission lines.

The determination of the number of turns required for this transformer is exactly the same as for the bifilar or trifilar winding outlined above. The lower corner frequency is determined by the magnetising inductance. The upper corner frequency is determined by the losses in the ferrite. For the transmission line transformer the winding length is no longer limited to be less than 10% of the wavelength, as both outputs have the same

propagation delay through the transmission line. Typically these cores are wound on low loss ferrites, giving them very high upper cut-off frequencies.

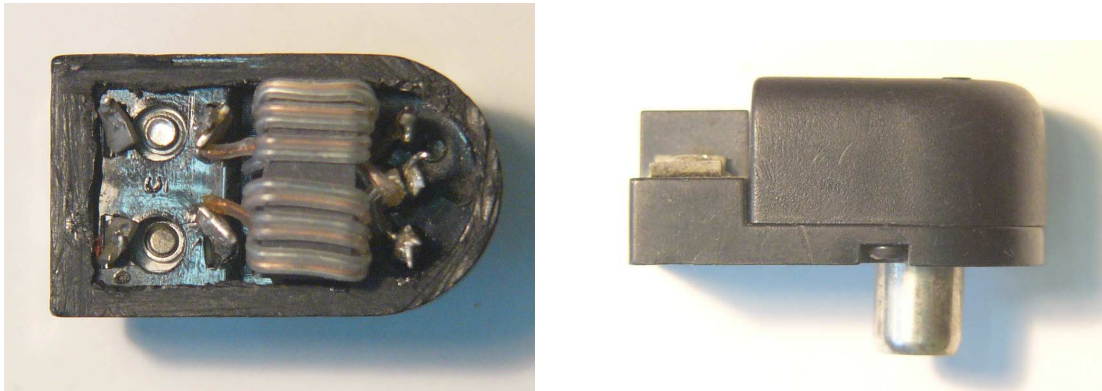


Figure 8. TV Balun using Ferrite RF transformer and transmission line windings.

This arrangement for a Balun is common for $300\ \Omega$ to $75\ \Omega$ baluns used in TV antenna systems. A typical dipole antenna has a $300\ \Omega$ impedance and the signals are balanced. For connecting these received signals to a TV, coaxial cable gives the best results, since it is shielded and does not pick up other radiation. The outer of the coaxial cable is at ground potential and the coaxial cable is $75\ \Omega$ impedance. The transmission line balun is this an ideal match at the high frequencies.

A transformer, using transmission lines for the windings, can be used as an isolating transformer, by connecting opposite sides of the transmission line to ground as indicated in figure 10. The lower frequency of this transformer is determined by the magnetising inductance of the former. This can be increased by simply adding more cores or having the transmission line go through the hole in the core many times.

By simply wrapping a coaxial lead around a ferrite or steel former, a non-inverting transformer, like figure 10, is obtained. This will provide isolation between both ends of the coaxial cable. Such a lead is useful in preventing earth loops with low voltage measurements.

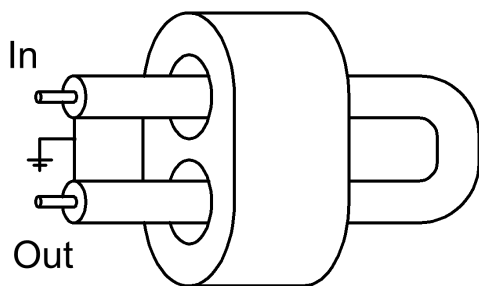


Figure 9. Non-inverting transformer.

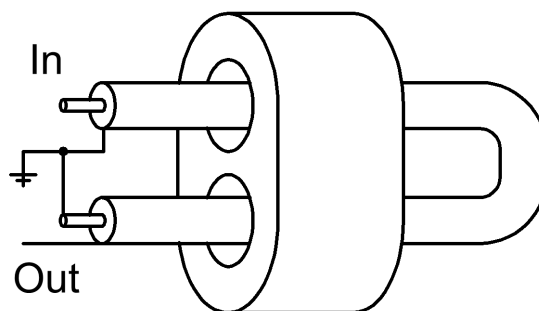


Figure 10. Inverting transformer.

Transformer Hybrids

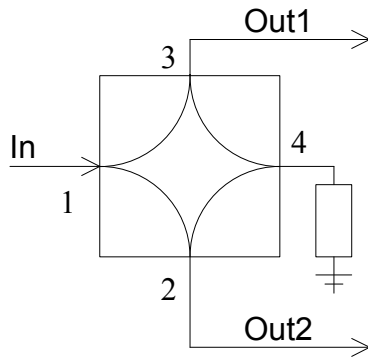


Figure 11. Hybrid.

In a hybrid, the input power at port 1 is split two ways to adjacent ports 2 and 3. Port 4, opposite the input port is isolated from the input port, and should have no energy going to it. A hybrid can thus be used as a power splitter.

Hybrids are normally symmetrical and bi-directional. Port 2 can thus also be used as an input, and under those conditions, half the power appears at port 1 and the other half appears at port 4. Under these conditions port 3 is isolated. If we now apply another input signal at port 3, that will also split two ways with half appearing at port 1 and the other half at port 4. For most hybrids, the phase angle at port 4 is 180 degrees

out of phase for inputs at either port 2 or port 3, so that if equal signals are applied to ports 2 and 3, the sum of the signals will appear at port 1 and the difference will appear at port 4. If the signals applied to port 2 and port 3 are the same, the powers are combined at port 1. A hybrid can thus be used as a power combiner as well.

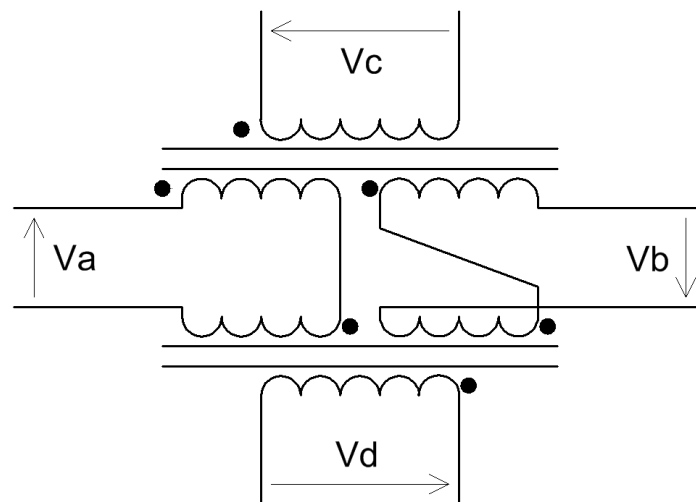


Figure 12. Audio transformer hybrid.

Transformer hybrids like the ones in figure 12 are used in telephony networks, where the signals to and from the normal telephone are sent in both directions on two wires.

Assume that all the windings on the transformers have the same number of turns. For the Audio transformer hybrid in figure 12, the voltages at each of the ports are related as:

$$\begin{aligned}
 V_a &= V_c + V_d \\
 V_b &= V_c - V_d \\
 2V_c &= V_a + V_b \\
 2V_d &= V_a - V_b
 \end{aligned}
 \tag{Eqn. 3}$$

By changing the turns ratio to 0.707, the same equations are obtained for all the ports:

$$\begin{aligned}
 V_a &= 0.707V_c + 0.707V_d \\
 V_b &= 0.707V_c - 0.707V_d \\
 V_c &= 0.707V_a + 0.707V_b \\
 V_d &= 0.707V_a - 0.707V_b
 \end{aligned}
 \tag{Eqn. 4}$$

This ensures that the impedance levels in each port are the same. Note that V_a does not couple into V_b and V_c does not couple into V_d and vice versa. A 40 dB isolation is typical under properly matched conditions.

Figure 13 shows how this audio hybrid can be wired up for use with amplifiers to produce a bi-directional amplifier, to amplify signals travelling in both directions along a wire. If the 2 wire circuit is not terminated properly, then part of the energy travelling out of this amplifier will be reflected and come back as input to the amplifier and be amplified again. If the gain of the amplifier is A dB and the isolation is B dB, then the singing margin is $2(B-A)$. The singing margin is the gain around the amplifier/hybrid loop. If the gain around the loop is more than 0 dB, then oscillations will occur. In practice the singing margin should be better than 6 dB. We should thus have more than 6 dB loss around the loop, even in the worst conditions.

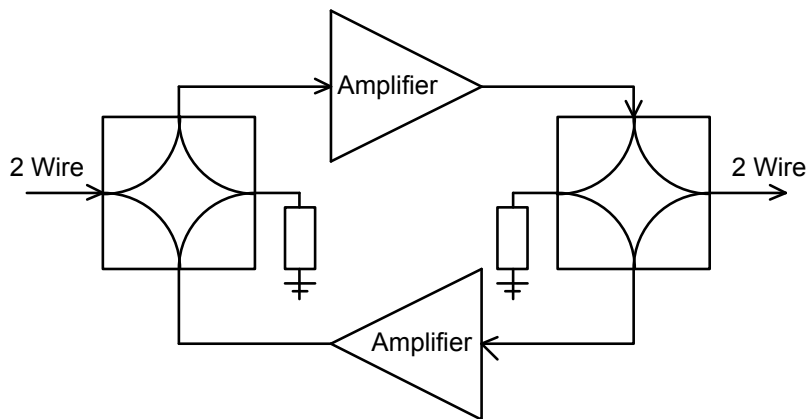


Figure 13. Bi-directional amplifier.

Power Combiner / Splitter

In a power combiner or power splitter, the terminating port is not brought out. The power combiner or power splitter is thus a 3-port device. Since linear passive devices are bi-directional, the same device can be used as both a power splitter and a power combiner. Often these devices are still called a hybrid. A common transformer based power splitter is a Wilkinson Hybrid. The two-way power splitters sold by department stores to permit two TVs to be operated from one antenna are Wilkinson Hybrids.

Wilkinson Transformer Hybrid

Figure 14 shows the circuit diagram of a Wilkinson Transformer Hybrid. If the same voltage input is applied to both ports A and B, then there is no voltage drop across the terminating resistor or transformer and port C is at same voltage as ports A and B. If the impedance levels for ports A and B are Z_0 , then for power conservation, the impedance level at port C must be $\frac{1}{2} Z_0$. For those situations where the output impedance should be Z_0 then a 3:2 turns ratio transformer will change the impedance level by 2.25, which is close enough to 2:1.

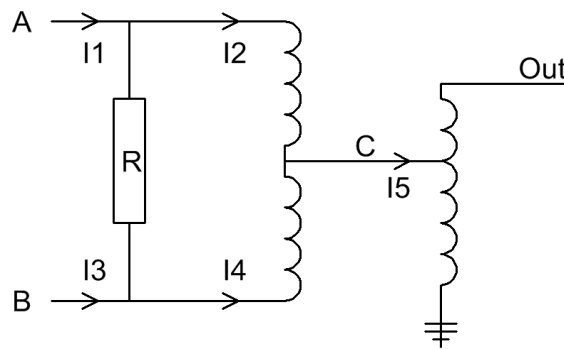


Figure 14. Wilkinson Transformer Hybrid.

If a voltage is applied to port A and 0 Volt is applied to port B, then the voltage at port C is $\frac{1}{2}$ of that at port A. If the input current at port A entering the transformer is I_2 then through transformer action an equal and opposite current is flowing through the bottom part of the transformer, so that $I_2 = I_4$, under all conditions. If the load impedance at port C is $\frac{1}{2} Z_0$ as before then the input impedance seen at port A at the input of the transformer is $2 Z_0$ since the transformer has a 2:1 turns ratio and a 4:1 impedance transformation ratio, since at port C one has half the voltage and twice the current.

Consider figure 14. For complete isolation between ports A and B, if a signal is applied at port A then the voltage at port B is zero, so that $I_3 = 0$. The current I_4 must thus flow through the resistor. The value of R required to ensure complete isolation between ports A and B can now be calculated. The voltage across the resistor is:

$$V_a = \frac{I_4}{R} = \frac{I_2}{2Z_0} \quad \text{Eqn. 5}$$

Since $I_2 = I_4$, we must have $R = 2Z_0$ to achieve isolation between both input ports. Under those conditions the impedance seen at the input port A is Z_0 , being the transformer input impedance of $2Z_0$ in parallel with the terminating resistor of $2Z_0$.

If this hybrid is used as a power splitter and the loads on ports A and B are matched, then no current will flow through the terminating resistor. Under those conditions that can be removed, at the expense of a poor isolation if unequal loads are present. For a power combiner in an antenna systems, where the output from two identical antenna elements are combined, a hybrid can be used that does not contain any isolating resistor, since the signals arriving at each of the antennae is identical and as a result no power is dissipated in the isolating resistor.

The Wilkinson transformer hybrids are commercially available as wideband power-splitters and power-combiners manufactured by companies such as Minicircuits.

The conventional TV splitter is a cut down version of the Wilkinson hybrid. Since the cable losses will mask any unequal loads, the terminating resistor is not normally present and since impedance variations can be tolerated, no output transformer is used. The omission of those components reduces the cost for this consumer-oriented circuit.

If a Wilkinson Transformer hybrid is used to combine the output from two transmitters, any unbalance will be dissipated in the resistor R. For two 100 watt transmitters, 50 watt will be dissipated in the resistor and 50 watt will be radiated if one of the amplifiers fails. The resistor must thus be selected with this power requirement in mind.

Design Example

Use the same transformer as in the example for the construction of a Wilkinson hybrid and design the hybrid to operate at 1 MHz as before. If the basic hybrid is unbalanced (an input is applied to port 2 but no input is applied to port 3), it behaves like a 25 Ω to 100 Ω transformer. The transformer of the previous example had an 11 turn winding with a characteristic impedance of 12.65 Ω. For the 25 Ω side $11\sqrt{(25/12.65)}$ turns = 15.5 turns is required. Since this has to be an integer number, 16 turns are used. The leakage inductance will then be $64(16/11)^2 = 135$ nH and the magnetising inductance will be 135 μH. The 25 Ω to 50 Ω impedance transformation transformer will have a 2:3 turns ratio auto-transformer, with an 8 turns trifilar winding, so that the 25 Ω winding will consist of two 8 turn windings in series, resulting in the required 16 turns. The 50 Ω port 1 will thus see 24 turns, corresponding to a leakage inductance of 270 nH and the magnetising inductance will be 270 μH.

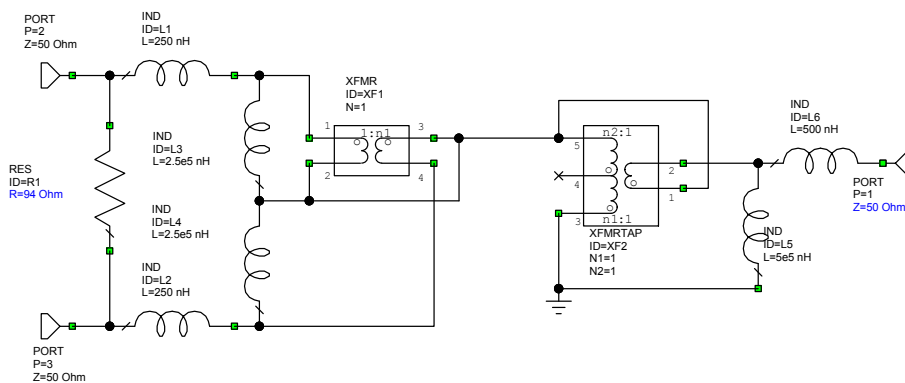


Figure 15. Wilkinson Hybrid model for computer simulation.

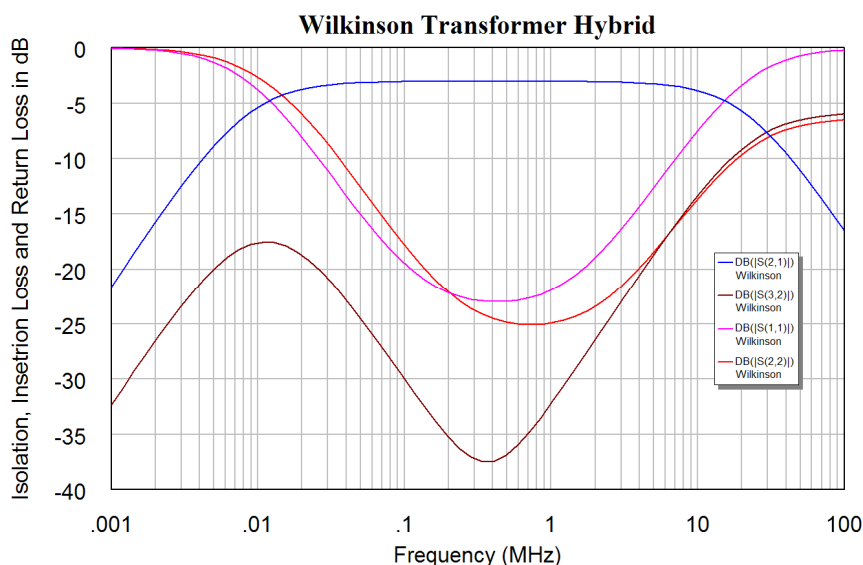


Figure 16. Simulated performance of Wilkinson Hybrid.

The performance of the Wilkinson Hybrid can be determined from computer simulation using Microwave Office as shown in figures 15 and 16. It can be seen that a good

isolation and return loss on all ports is obtained at the design frequency of 1 MHz. Constructing this hybrid normally results in a close agreement with the simulation.

Transmission Line Hybrid with Ferrite Cores

A simple hybrid made using standard 50 ohm transmission line hybrid and ferrite cores is shown in figure 17. If the impedance at A and B is Z_0 then at C the impedance is $\frac{1}{2}Z_0$. The impedance seen when B=0 is $2 \times (\frac{1}{2}Z_0) = Z_0$. The power dissipated in the load resistor is the power associated with the difference in the input signals. For high power operation, the rating of that resistor must be carefully considered. If the input at A and B are the same then no power will be dissipated in the load resistor.

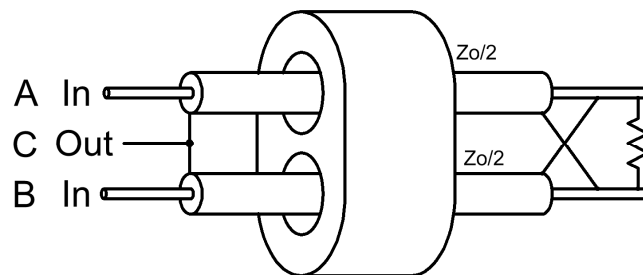


Figure 17. Hybrid with ferrite cores.

The realisation of the hybrid is shown in figure 18 and the circuit can be analysed using the circuit representation in figure 19. In figure 18, the 25 Ω transmission lines are obtained by having two 50 Ω transmission lines in parallel.



Figure 18. Circuit of hybrid in figure 17

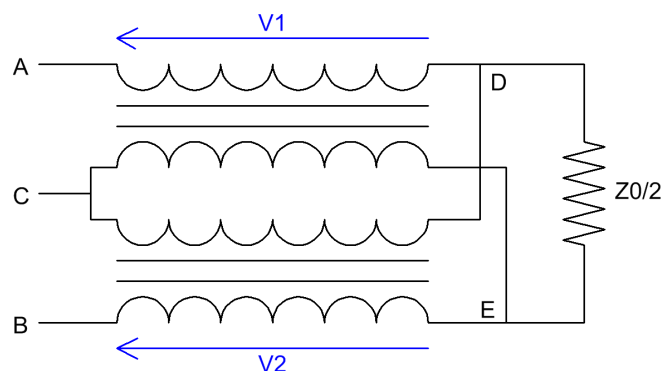


Figure 19. Circuit of hybrid in figure 17.

The equations for this hybrid are:

$$\begin{aligned} V_a - V_d &= V_1 \\ V_c - V_e &= V_1 \\ V_c - V_d &= V_2 \\ V_b - V_e &= V_2 \end{aligned} \tag{Eqn. 6}$$

Subtracting the first two equations and the last two equations and adding the resulting equations gives:

$$V_c = \frac{V_a + V_b}{2} \tag{Eqn. 7}$$

Now consider the conditions required for isolation. If $V_b=0$. For isolation between ports A and B, the current through the bottom transformer is zero, since with a load connected to B the voltage must be zero. That means $V_2=0$ and thus $V_e=0$ and $V_d=1/2V_a$.

For the input impedance at A to be Z_0 then the load resistor must be $1/2Z_0$. Under those conditions the current into A goes through the load and out of C. The voltages are thus:

At input A $V_a = Z_0 \cdot I$ Eqn. 8

Across the Load $1/2V_a = 1/2Z_0 \cdot I$ Eqn. 9

At the output C $1/2V_a = 1/2Z_0 \cdot I$ Eqn. 10

The equations are thus consistent and the assumption that $V_b=0$ is justified and we have full isolation when $R=1/2Z_0$. The circuit works thus as a proper hybrid.

Note: Like the Wilkinson transformer, the impedance at the summing port C has an impedance of $1/2Z_0$ and a transformer needs to be used to change that to Z_0 if required, similar to that for the Wilkinson transformer of figure 14.

Many way hybrids

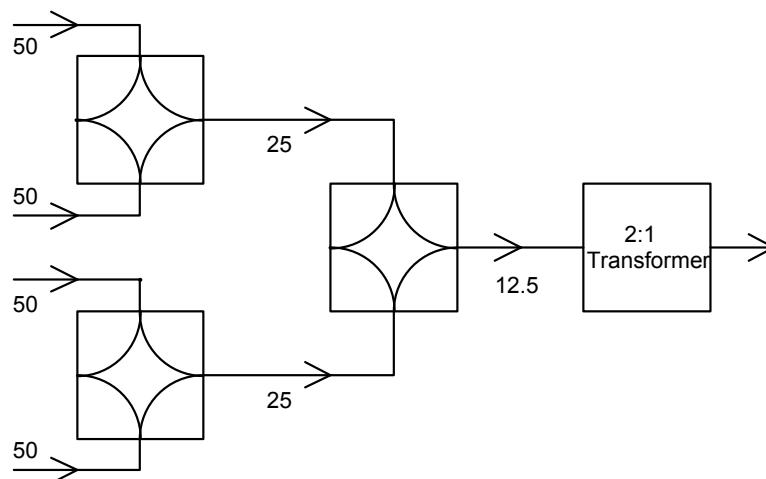


Figure 20. A four-way combiner.

In some instances many signals need to be combined or a signal needs to be split many ways. The hybrids described above can be cascaded to provide a many way splitter/combiner. However each of those hybrids will include a 25 Ω to 50 Ω impedance transformation transformer. Some savings can be made by using a 4 way

hybrid as shown in figure 20, where three of two way hybrids are used together to combine 4 input signals and then have a 12.5 ohm output, which can be transformed to 50 ohm by using a 2:1 transformer, as shown in figure 20. This saves two transformers, each of which will have some losses associated with it. In addition the 4:1 impedance transformation is exact, while the 2:1 impedance transformation is actually a 2.25:1 impedance transformation with the 3:2 turns ratio of the transformer. Two of the hybrids below operate at a 50 Ω impedance and one operates at a 25 Ω impedance. The number of turns on the transformer coils needs to be adjusted to allow for this.

References

1. H. Granberg, "Broadband transformers and power combining techniques for RF", Motorola Application note AN749, Motorola RF Circuits Engineering, 1993.
2. Minicircuits.Application note AN20-001 "How RF Transformers work"
<http://www.minicircuits.com/pages/pdfs/howxfmerwork.pdf>.
3. Minicircuits.Application note AN20-002 "Balun Transformers"
<http://www.minicircuits.com/pages/BalunApplicationNote.htm>.

Chapter 4

Transmission Line Transformers and Hybrids

Introduction

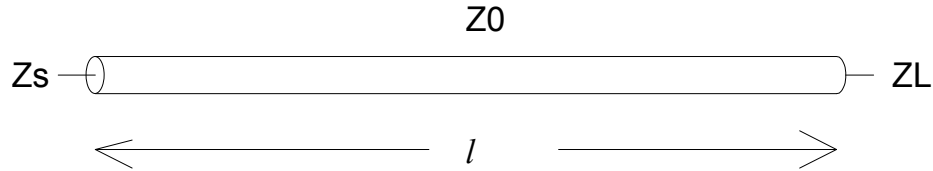


Figure 1. Transmission line parameters.

For a transmission line of characteristic impedance Z_0 and length l , the sending end impedance is given by:

$$Z_s = Z_0 \frac{Z_L + jZ_0 \tan(\beta l)}{Z_0 + jZ_L \tan(\beta l)} \quad \text{Eqn. 1}$$

If the transmission line is close to one quarter wavelength long then $\tan(\beta l) \gg 1$ so that:

$$Z_s = Z_0 \frac{jZ_0 \tan(\beta l)}{jZ_L \tan(\beta l)} = \frac{Z_0^2}{Z_L} \quad \text{Eqn. 2}$$

so that: $Z_s Z_L = Z_0^2$ or $Z_s = Z_0^2 / Z_L$ Eqn. 3

The impedance transformation ratio R is given by:

$$R = \frac{Z_0}{Z_s} = \frac{Z_L}{Z_0} \quad \text{or} \quad Z_s = \frac{Z_0}{R} \quad \text{and} \quad Z_L = RZ_0 \quad \text{Eqn. 4}$$

If the allowable Voltage Standing Wave Ratio (VSWR) is W , so that the limiting value of the sending end impedance is WZ_s , substituting equation 4 into equation 1 gives:

$$WZ_s = W \frac{Z_0}{R} = Z_0 \left| \frac{RZ_0 + jZ_0 \tan(\beta l)}{Z_0 + jRZ_0 \tan(\beta l)} \right| \quad \text{Eqn. 5}$$

Solving for $\tan(\beta l)$ and using the fact that normally $W^2 \ll R^4$ gives:

$$\tan \beta l = \sqrt{\frac{R^4 - W^2}{R^2(W^2 - 1)}} \cong R \sqrt{\frac{1}{W^2 - 1}} \quad \text{Eqn. 6}$$

The higher R , the higher $\tan(\beta l)$ must be and thus the narrower the bandwidth for a given VSWR. This can easily be illustrated with an example.

Example:

If the allowable VSWR is 1.2, that is for a 50 Ω system the impedance should be between 60 Ω and 41.6 Ω , and if $R = 2$ (i.e. a 4:1 impedance transformation) then $\beta l = 70.8^\circ$ i.e. $l = 0.197\lambda$. The bandwidth is thus $2(90-70.8)/90 = 43\%$

If R is changed to $R = \sqrt{2}$ (i.e. a 2:1 impedance transformation) then the same total impedance transformation can be achieved by having two transmission line sections in cascade. If the load impedance is Z_L then the impedance at the end of the first section is $2Z_L$ and the impedance at the end of the second section is $4Z_L$. The total length of the transformer is thus half a wavelength.

Solving for βl gives $\beta l = 59.6^\circ$ i.e. $l = 0.166\lambda$. The bandwidth is thus $2(90-59.6)/90 = 67.5\%$

For very high frequencies, many sections can be cascaded and the line will have an exponential change of impedance for each of the quarter wavelength sections. This can readily be produced using RF PCB technology.



Figure 2. Plot of impedance variation versus frequency.

Figure 2 shows a plot of the input impedance variation of a transmission line transformer, transforming a 12.5Ω load into a 50Ω load. For the one line transformation, the impedance transformation is done in one transmission line section with a characteristic impedance of 25Ω . The Magenta curve is for a 2-line transformation, with the impedance transformation ratio $R = \sqrt{2}$ for each line.

If the impedance transformation ratio of the two lines in a two line impedance transformer is changed from the $R = \sqrt{2}$ for each of the lines, such that the total impedance transformation is still a 4:1 impedance transformation, but that each line has a slightly different transformation ratio, then a very good match is obtained over a 40% bandwidth. In figure 2, the red curve corresponds to the impedance transformation ratio being optimised to obtain close to a 50 ohm match over as wide frequency range possible. The first line has $R_1 = 0.6883$, corresponding to a characteristic impedance of 34.4Ω and the second line has $R_2 = 0.7264$ corresponding to a characteristic impedance of 17.2Ω . Applying similar principles to a 3-line section gives an even wider bandwidth, as shown by the brown curve in figure 2.

Wilkinson Transmission Line Hybrid

The Wilkinson transmission line hybrid consists of two quarter-wavelength long transmission lines forming a combiner, together with a load resistor to provide isolation. The circuit is shown in figure 3 and the performance is shown in figure 4.

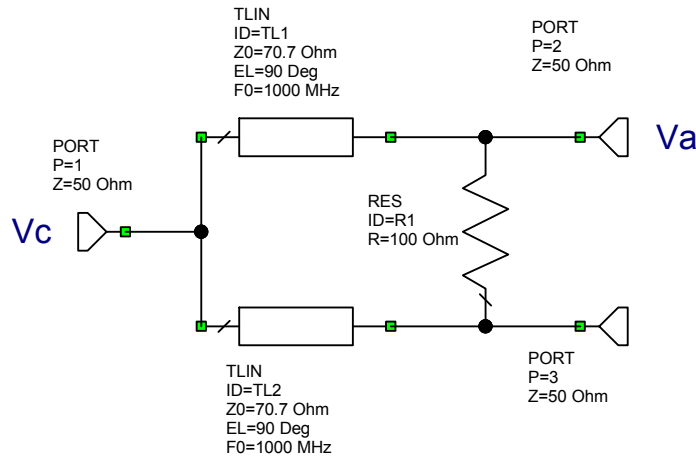


Figure 3. Ideal Wilkinson Hybrid

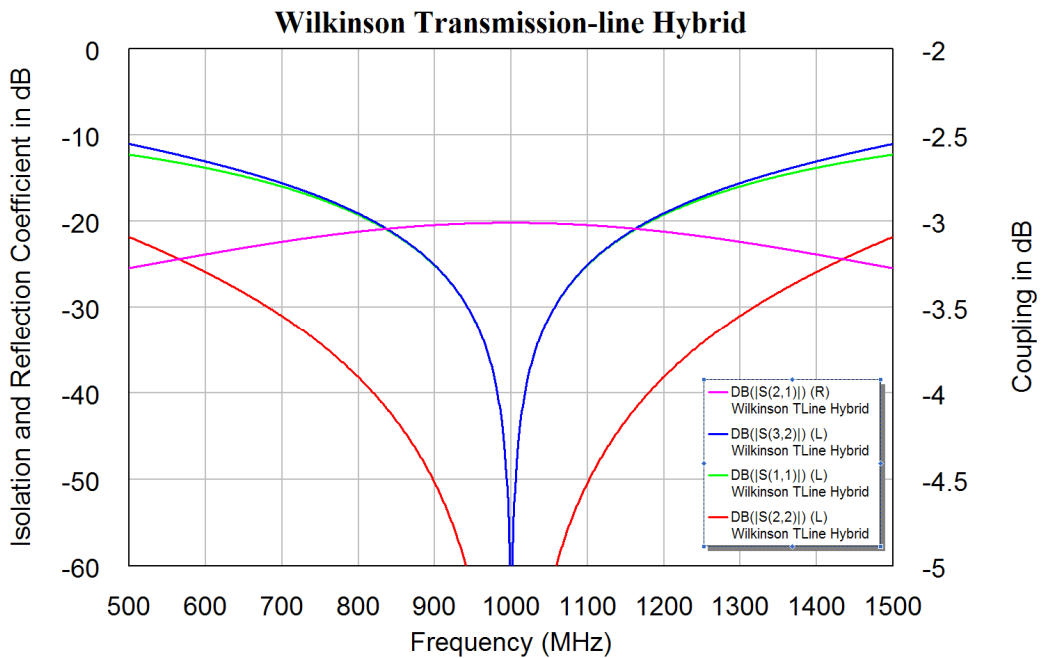


Figure 4. Ideal Wilkinson Hybrid

For the analysis, an input is applied to port 2. For proper hybrid operation, no voltage should appear at Port 3. Transmission line TL2 has a standing wave on it with 0 Volt at the Port 3 side. Since the line is one-quarter wave long, there will be no current flowing into the line at the Port 1 side, as shown in figure 5. For the analysis of the voltage on port 1, we can thus remove TL2, since it is an open circuit at the port 1 end. The voltage at port 1 will thus simply be what we would have if one had the transmission line only, as shown in figure 6.

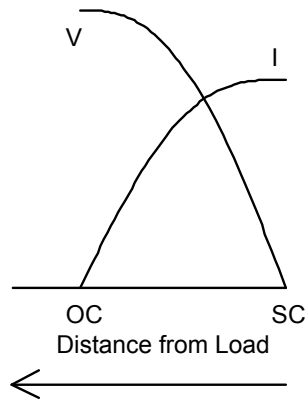


Figure 5. Standing wave along TL2.

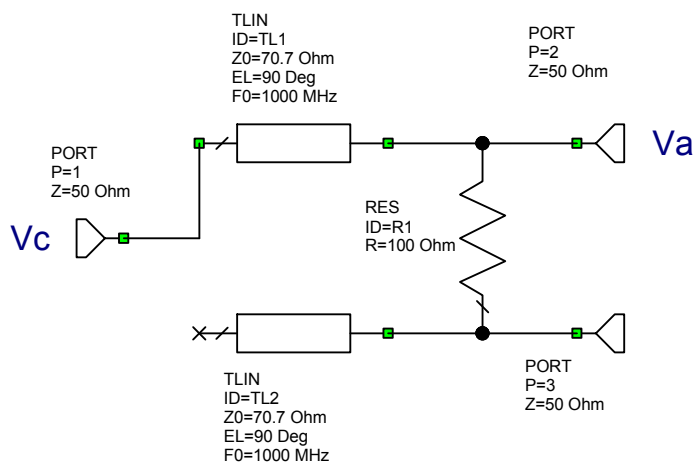


Figure 6. Circuit for analysis purposes.

Since the input power is the same as the output power, the voltage V_c at port 1 and the voltage V_a at port 2 relate as $V_a = \sqrt{2} V_c$.

The maximum current and maximum voltage on a transmission line relate as:

$$V_{\max} = Z_0 I_{\max} \tag{Eqn. 7}$$

In figure 3, the current at the port 3 side of TL2 will thus be:

$$I_{\max} = \frac{V_c}{\sqrt{2Z_0}} = \frac{V_a}{\sqrt{2}\sqrt{2Z_0}} = \frac{V_a}{2Z_0} \tag{Eqn. 8}$$

Since this current must come through the load resistor R then

$$I_{\max} = \frac{V_a}{R} = \frac{V_a}{2Z_0} \tag{Eqn. 9}$$

So that $R = 2Z_0$ for best isolation.

The circuit can be realised using a microstrip PCB layout. Figure 7 shows a typical realisation. A surface mount resistor is used. To ensure that there is no coupling between each of the arms of the hybrid, the spacing cannot be made too small and small

transmission lines are required to connect the resistor into the circuit. The characteristic impedance of those lines must be such that the resistor can be soldered to it. These short lines will have some effect on the performance as shown in figure 8, where the notch of S_{11} is shifted in frequency as a result. The performance is however still satisfactory, since a 20 dB isolation or return loss is normally sufficient.

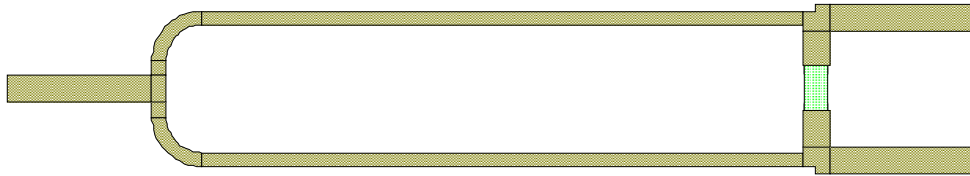


Figure 7. PCB layout of a Wilkinson Hybrid.

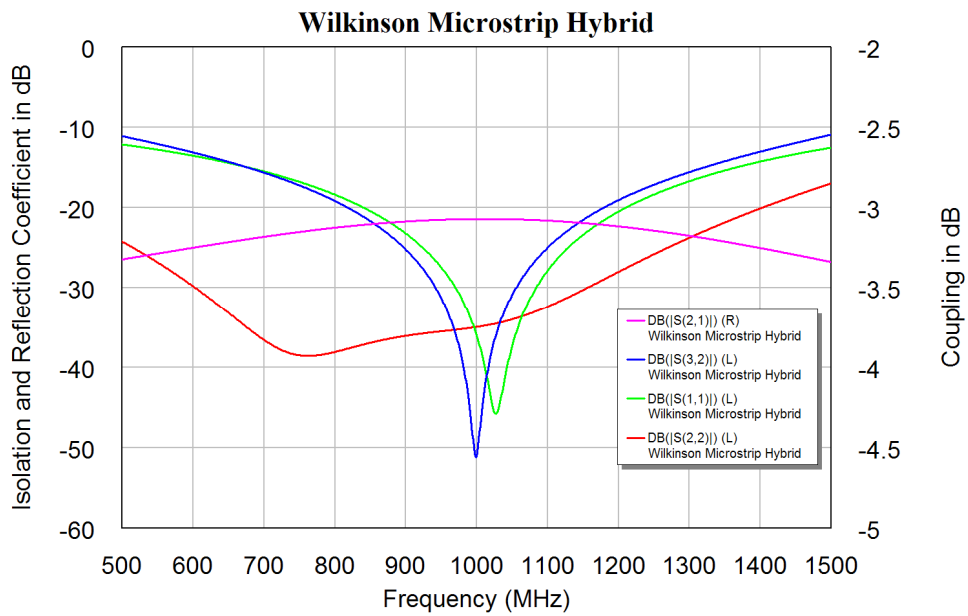


Figure 8. Performance of stripline Wilkinson Hybrid of figure 7.

Compensated Wilkinson Hybrid

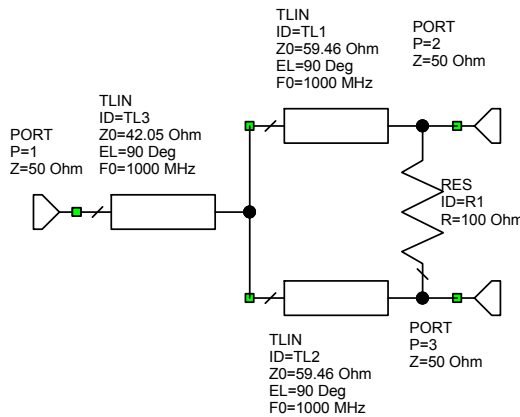


Figure 9. Compensated Wilkinson Hybrid.

In a Compensated Wilkinson Hybrid, a two step impedance transformation is used, like the two line impedance transformation of figures 1 and 2. The resulting circuit is shown in figure 9. The impedance transformation from line TL3 is from 50Ω at port 1 to 35.35Ω at the right of TL3. Lines TL1 and TL2 do an impedance transformation from 50Ω at port 2 and port 3 to 70.7Ω at the left hand side of transmission lines TL1 and TL2. Those in parallel give a 35.35Ω , which matches that at the right hand side of line TL3. Each of the three transmission lines will thus have the same impedance transformation ratio of $\sqrt{2}$.

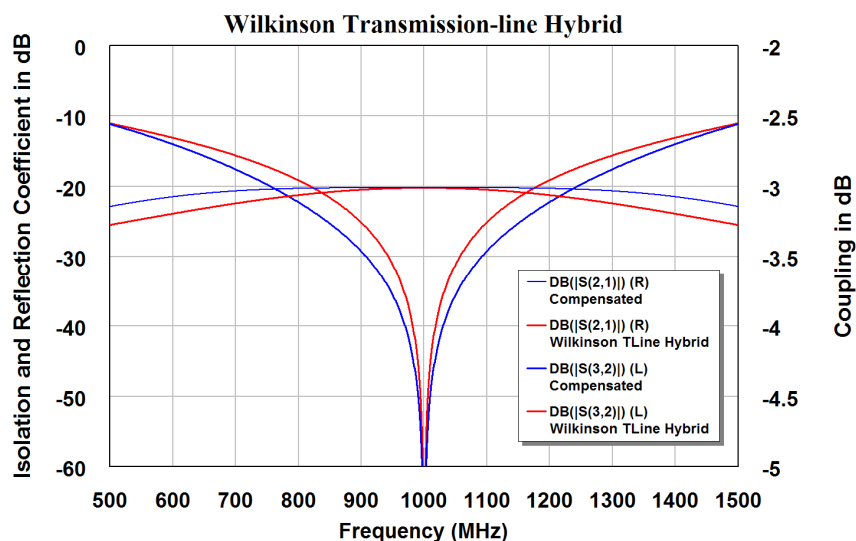


Figure 10. Compensated Wilkinson Hybrid performance.

Figure 10 shows a comparison between the conventional, shown in red, and the compensated (blue) Wilkinson Hybrid. The Compensated Wilkinson Hybrid shown in blue has a wider frequency response for both the isolation and coupling. In addition the compensated Wilkinson Hybrid uses lower impedance transmission lines, resulting in wider track widths for the microstrip layout, thus lowering the resistive losses in the circuit.

Unequal Split Wilkinson Hybrid

Sometimes an unequal power split is required. If a power ratio of $P:1$ is required, then the impedances seen at the source end of each of the transmission lines must also have a ratio of $P:1$. Since the total impedance must be $Z_0 = 50 \Omega$, then the impedances are:

$$\frac{1}{Z_0} = \frac{1}{Z_1} + \frac{1}{Z_2} = \frac{1}{Z_1} + \frac{1}{P * Z_1} = \frac{P+1}{P * Z_1} \quad \text{Eqn. 10.}$$

The line impedances are thus:

$$Z_1 = \sqrt{\frac{P+1}{P}} Z_0 \quad \text{Eqn. 11}$$

$$Z_2 = \sqrt{P+1} * Z_0 \quad \text{Eqn. 12}$$

where Z_1 and Z_2 are the transmission line impedances of the hybrid. As a check when an equal split is used, $P=1$, so that $Z_1 = Z_2 = \sqrt{2}Z_0$.

Thus for a 10:1 power split in a $50\ \Omega$ system, the transmission line impedances are:

$Z_1 = \sqrt{1.1} Z_0$ and $Z_2 = \sqrt{11} Z_0$. For a $50\ \Omega$ system, $Z_2 = 165\ \Omega$. For an RF circuit board substrate, RO4003, which is 0.818 mm thick, at 1 GHz a $50\ \Omega$ track is 1.855 mm wide and a $165\ \Omega$ track is 0.063 mm wide. The $165\ \Omega$ track is too thin to make accurately. The track width limits the ratio of the power split. Lowering the impedances of the split lines by reducing the impedance at the junction point just like the compensated Wilkinson hybrid, will reduce the bandwidth of the hybrid but will permit it to be constructed. Increasing the substrate thickness will also increase the track width.

Wideband Wilkinson Hybrid

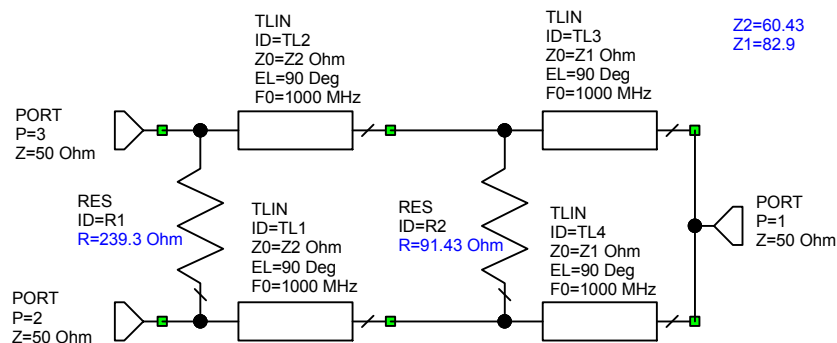


Figure 11. Two-stage wideband Wilkinson Hybrid.

The bandwidth of the Wilkinson hybrid can be increased by cascading two resistor linked transmission lines as shown in figure 11. The Characteristic impedances of the transmission lines and the resistor values can be optimised to give the required isolation over the specified bandwidth. There is a compromise between bandwidth and isolation. A wide bandwidth will result in a low isolation and a smaller bandwidth can result in a better isolation. For the hybrid shown in figure 11 the isolation was specified as -30 dB.

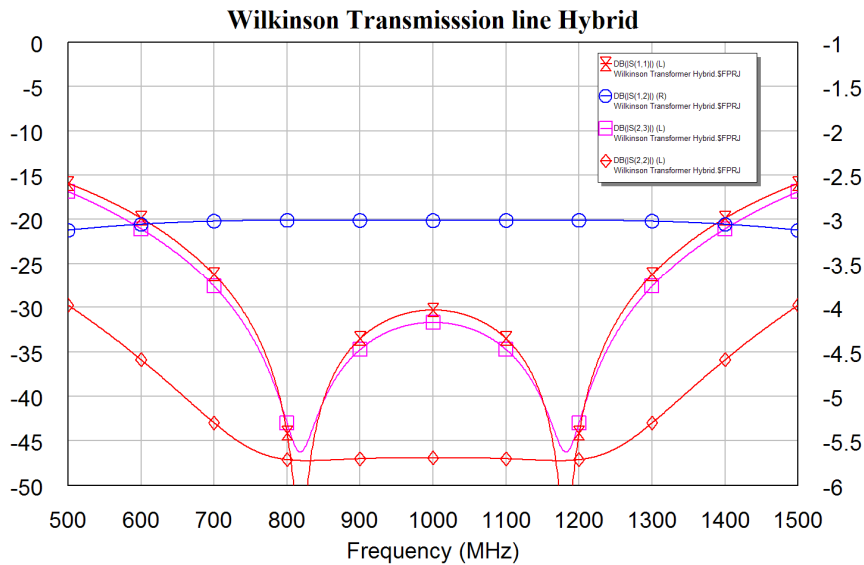


Figure 12. Performance of a 2 stage wideband Wilkinson Hybrid.

From figure 12, it can be seen that a wide bandwidth hybrid results. The impedance for the first section has increased to 83Ω compared with 70.7Ω for the conventional hybrid. The higher impedance will result in an increased insertion loss of the hybrid, due to thinner PCB tracks being required. A compensated hybrid configuration will reduce the impedance values and thus reduce the insertion loss of the hybrid as well as having a wider bandwidth still.

This process can be extended to produce Wilkinson hybrids with good isolation and return loss on all ports over a 2:1 or even 3:1 frequency range. Figure 13 shows the schematic of a 3:1 Wilkinson Hybrid covering the frequency range from 90 MHz to 270 MHz. The values or transmission line impedances and resistor values are those obtained after optimisation. The target specification is a better than 30 dB isolation and better than 30 dB return loss for all the ports. This circuit achieves those specifications.

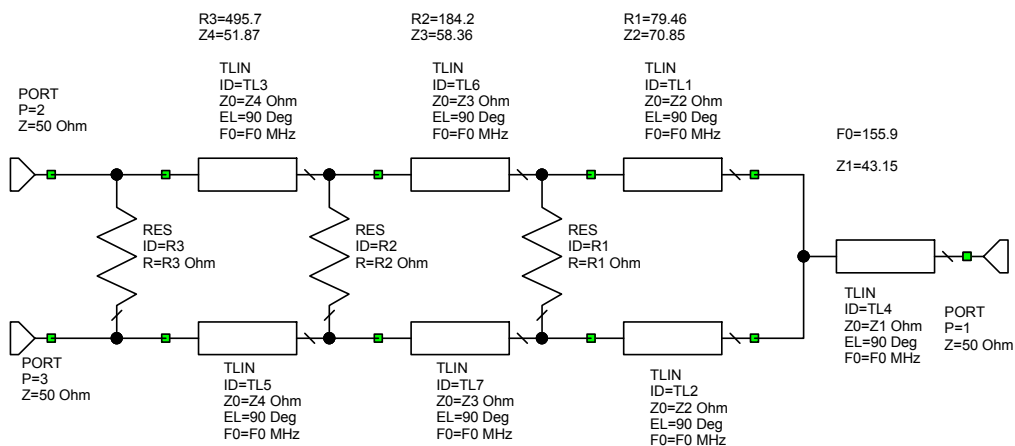


Figure 13. Circuit for a 90 MHz to 270 MHz Wilkinson Hybrid.

The design process requires two steps. Firstly the circuit is designed and optimised using ideal transmission lines for the hybrid, as shown in figure 13. Once the

specifications are achieved for this ideal circuit, then the ideal transmission lines are replaced with microstrip lines, with the same electrical line length and impedance.

Often it is necessary to bend the microstrip lines to fit the circuit in the available space, as shown in figure 14. Each of the transmission lines are a quarter wavelength long. If in figure 13 lines TL2 and TL5 are disabled, resistors R1 and R3 are disabled and resistor R2 is made a short circuit (0Ω), then the circuit becomes a transmission line of various impedances connecting port 1 to port 2 with an open circuited quarter wavelength stub consisting of TL7 connected to it. This line will thus present itself as a short circuit at R2 at the centre frequency. The transfer function from ports 1 to 2 will thus have a notch exactly at the centre frequency of the hybrid, where TL7 is a quarter wavelength. The length of the folded sections making up TL7 in figure 13, can be adjusted to be exactly a quarter wavelength by changing the lengths of the sections to ensure that the notch in the transfer function from ports 1 to 2 occurs exactly at the centre frequency of the hybrid. This process is repeated for the other three different transmission lines in the hybrid. Variables are used to ensure that the folded transmission lines corresponding to the sets of lines TL1 and TL2, lines TL3 and TL5 and lines TL6 and TL7 are exactly the same length and impedances. The accompanying MWO example file can be used to further illustrate this process.

Finally the line lengths and widths are optimised to provide the fine tuning required for the final layout to again meet the specifications. Figure 14 shows the hardware for this layout and figure 15 shows the simulated frequency response for the hybrid. The measured performance agrees closely with the calculated one and the hardware has an isolation that is better than 28 dB over the entire 90 to 270 MHz frequency range and a similar return loss on all ports. The slight degradation in performance is due to slight imperfections in the hardware compared with the simulation.

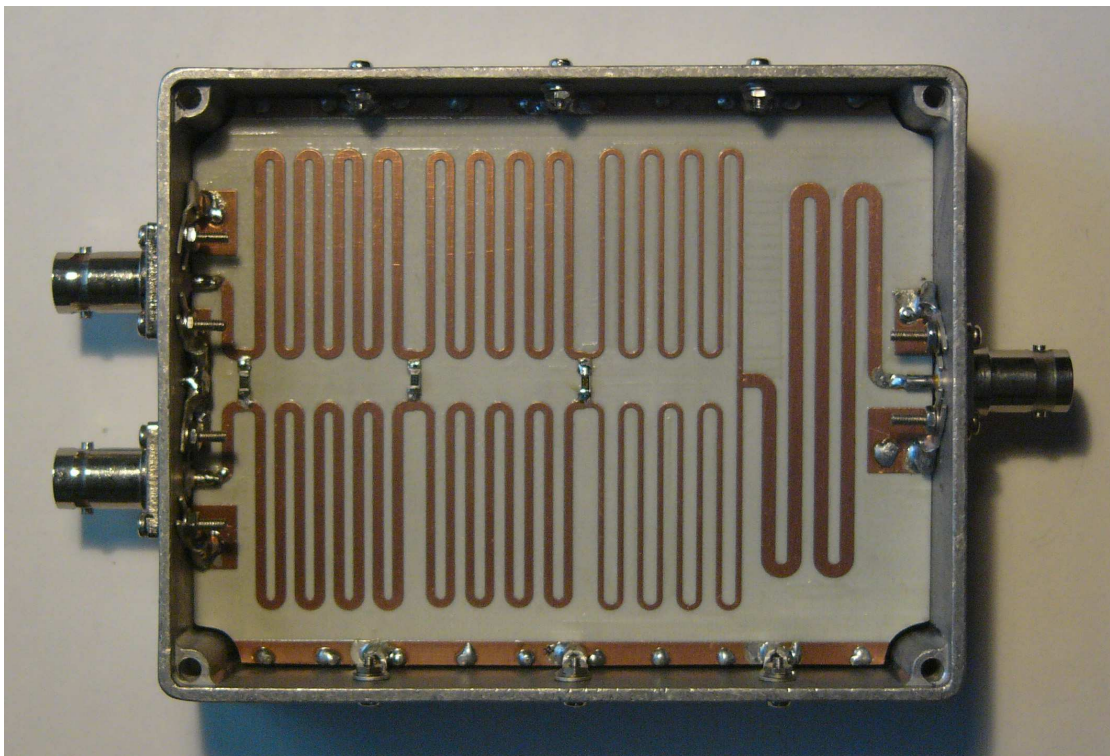


Figure 14. Hardware for 90 MHz to 270 MHz Wilkinson Transmission-line Hybrid.

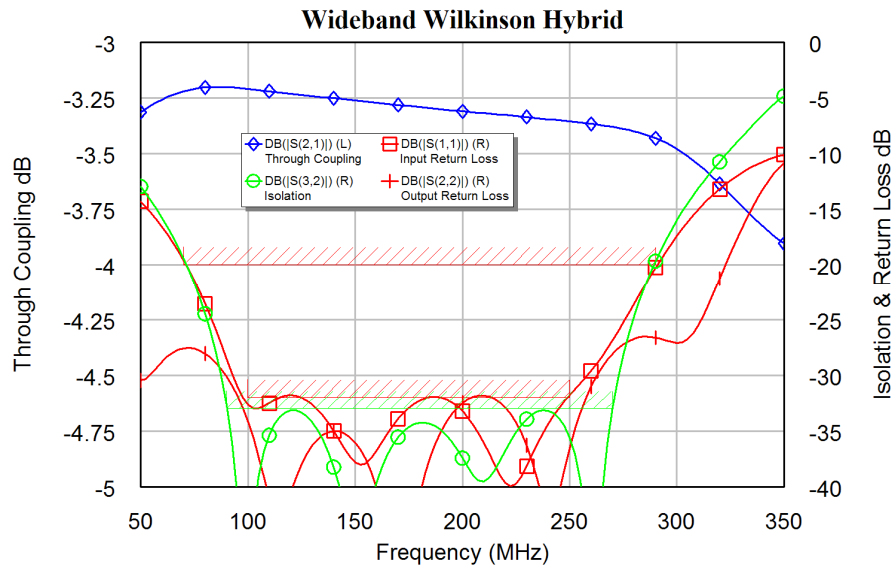


Figure 15. Simulated performance of the Hybrid of figure 14.

The losses in the circuit due to the resistance of the tracks, dielectric losses of the substrate and radiation losses of the microstrip lines, varies with frequency, as can be seen in figure 15. However since the difference is only 0.25 dB over a 3:1 frequency range and can be ignored in practice. Due to this frequency dependence of the losses, it is better to optimise for input reflection coefficient rather than transfer function since a low input reflection coefficient ensures all the energy passes through the hybrid, thus giving the highest S_{21} possible. Optimising for a value of S_{21} may result in a poor return loss at lower frequencies.

Quarter Wave Hybrid or 1.5λ Rat-race Hybrid

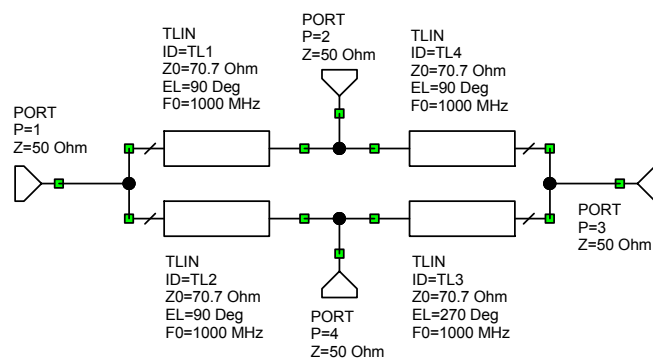


Figure 16. 1.5λ Rat-Race Hybrid

The circuit diagram of this hybrid is shown in figure 16 and its performance is shown in figure 17. For the analysis consider the function of the hybrid. If an input is applied to port 1, then no signal should appear at port 3, resulting at 0 Volt at port 3. Under these conditions, the circuit is similar the Wilkinson hybrid of figures 5 and 6, and no current flows into TL3 of figure 16 at port 2 and into TL4 at port 4. The transmission line TL3 can thus be disconnected at port 4 and line TL4 can be disconnected at port 2, without any effect, as shown in figure 18.

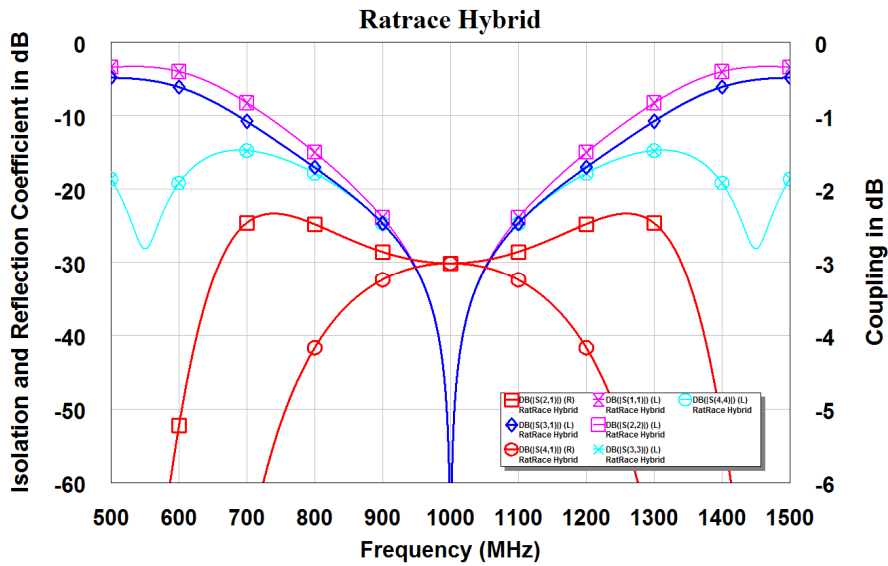


Figure 17. Performance of 1.5 λ Rat-Race Hybrid

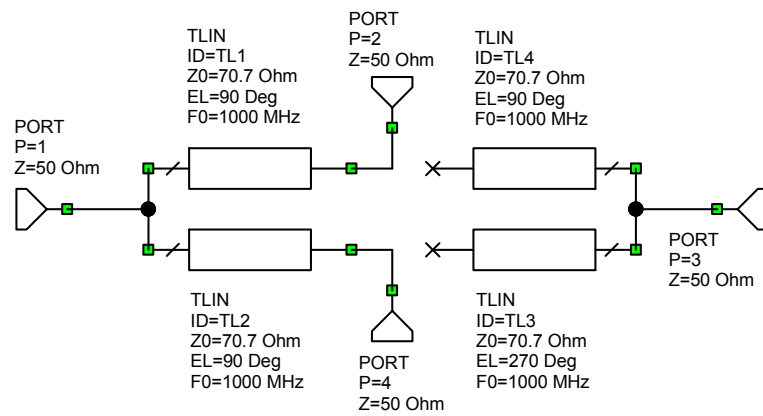


Figure 18. 1.5 λ Rat-Race Hybrid for analysis.

The resulting circuit is thus just like a Wilkinson Hybrid, without the terminating resistor. The line impedances should thus be $70.7 \text{ } \Omega$, just like the Wilkinson Hybrid. The same analysis can be repeated by looking into each port in turn. A three-quarter wavelength transmission line has exactly the same impedance transformation ratio as a quarter wavelength line. All the line impedances will thus be $\sqrt{2}Z_0$.

The 1.5λ Rat-Race Hybrid is commonly used in high power transmitters, and has an advantage over the Wilkinson Hybrid that for a $50 \text{ } \Omega$ system, a $50 \text{ } \Omega$ load resistor to ground is required for the termination rather than a $100 \text{ } \Omega$ load resistor between two active inputs. High power $50 \text{ } \Omega$ loads are readily available from manufacturers such as Bird Electronic Corporation. $100 \text{ } \Omega$ floating loads are however more difficult to obtain.

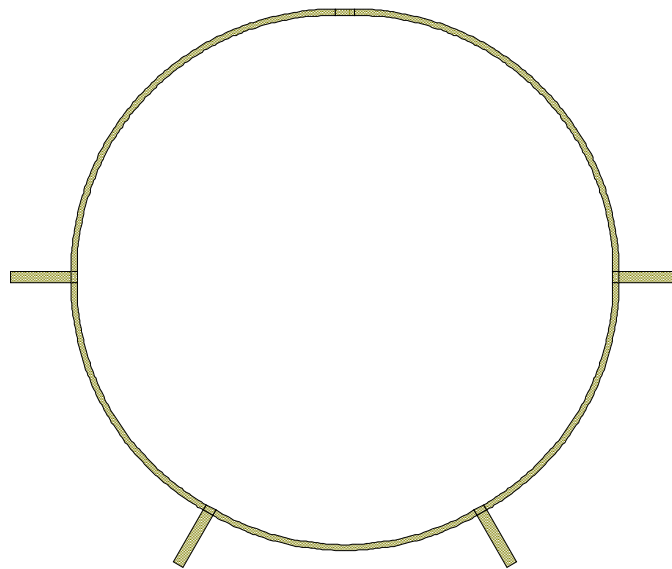


Figure 19. PCB layout of a 1.5λ Rat-race Hybrid

Figure 19 shows an RF PCB realisation of a 1.5λ Rat-race Hybrid. Apart from a slight (0.25 dB typically) increase in insertion loss due to the resistive losses in the microstrip tracks, the performance of the PCB layout of the 1.5λ Rat-race Hybrid is the same as shown in figure 17.

Lower line impedances can be obtained with a compensated 1.5λ Rat-race Hybrid, by having 44.5Ω quarter wavelength transmission lines at the 4 inputs to the hybrid, for a 50Ω system. The line impedances of the hybrid then become 56.119Ω instead of 70.7Ω . Computer simulation shows that this does not increase the bandwidth of the isolation and it does not reduce the losses for a typical PCB layout, so that compensated 1.5λ Rat-race Hybrid are not used in practice.

Branchline Coupler

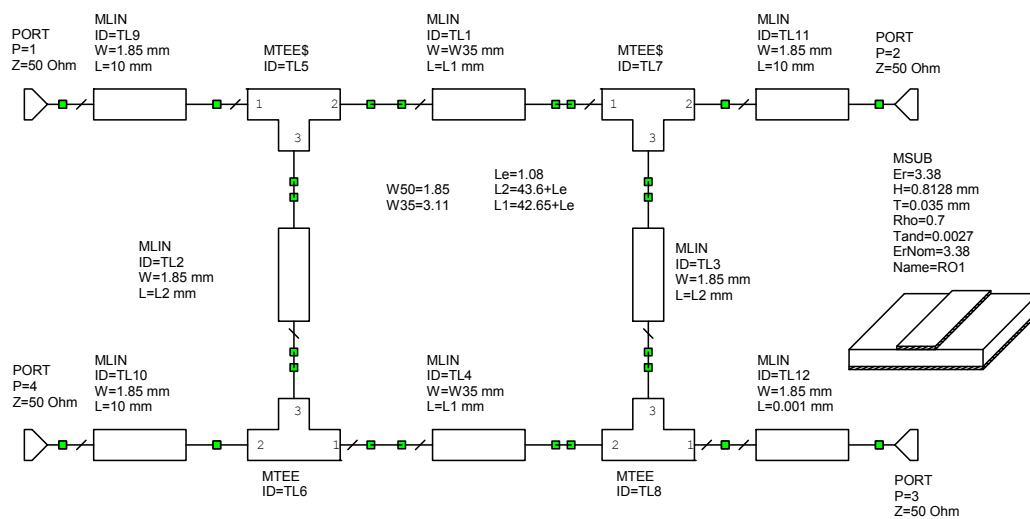


Figure 20. Branchline coupler circuit

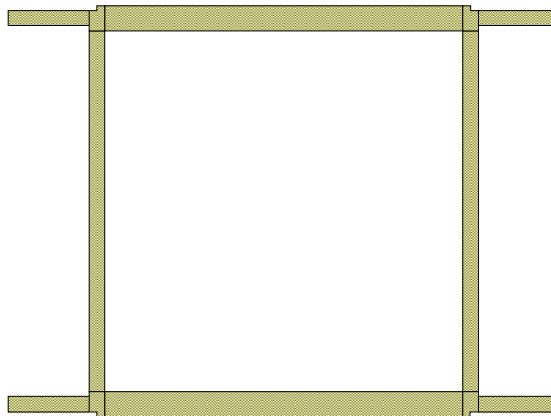


Figure 21. Branchline coupler PCB layout.

The Branchline coupler consists of 4 transmission lines in a ring, as shown in figures 20 and 21. If an input is applied at the top left port 1, then part of the output appears at the coupled port, the bottom right port 3. The remainder appears at the main output port 2 and no power appears at the isolated port 4. For a 3 dB coupler in a 50 Ω system, lines TL1 and TL4 have an impedance of $50/\sqrt{2}$ Ω and lines TL2 and TL3 have an impedance of 50 Ω . A Microstrip PCB layout is shown in figure 21. The resistive losses of a Branchlike coupler are less than that of a 1.5λ Rat-race Hybrid.

For the analysis, consider figures 20 and 22. When an input is applied at port 1, port 4 is isolated and has no voltage at that port. Since lines TL3 and TL4 are quarter wavelength long, no current flows in line TL4 at port 3, so that TL4 can be disconnected from the circuit without any effect. Similarly, no current flows in TL3 at port 1, so that TL3 can also be disconnected, resulting in figure 22.

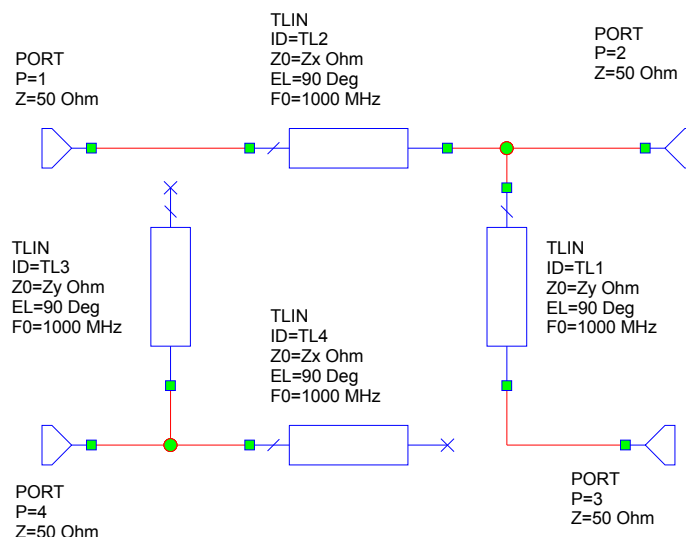


Figure 22. Branchline Coupler analysis.

If a normalised input power of I is applied at port 1 and we want an output power of P to occur at port 3, then a power of $(I-P)$ will be available at port 2.

At port 2, the load impedance is Z_0 , which typically is 50Ω . If the voltage at port 2 is V_2 , then the power split at port 2 is given by:

$$V_2^2 = PZ_p = (1-P)Z_0 \quad \text{so that:} \quad Z_p = \frac{(1-P)Z_0}{P} \quad \text{Eqn. 13.}$$

Where Z_p is the impedance of port 3 transformed through TL1 and seen at port 2 looking into TL1. Since this is obtained by impedance transformation through the quarter wave long transmission line TL1, the impedance required for TL1 is given by:

$$Z_Y = \sqrt{Z_p Z_0} = Z_0 \sqrt{\frac{(1-P)}{P}} \quad \text{Eqn. 14}$$

The impedance Z_2 seen at the end of TL2 is Z_0 in parallel with Z_p and is thus:

$$\frac{1}{Z_2} = \frac{1}{Z_p} + \frac{1}{Z_0} = \frac{P}{(1-P)Z_0} + \frac{1}{Z_0} = \frac{1}{(1-P)Z_0} \quad \text{Eqn. 15}$$

The line impedance Z_X to transform this to Z_0 is thus:

$$Z_X = Z_0 \sqrt{(1-P)} \quad \text{Eqn. 16}$$

In many cases an equal power split is required, so that $P=0.5$. Typically $Z_0 = 50 \Omega$. Substituting this in equations 14 and 16 results in $Z_Y = Z_0 = 50 \Omega$ and $Z_X = 0.707 * Z_0 = 35.35 \Omega$. For a 10 dB coupler $P = 0.1$, so that $Z_Y = 3Z_0 = 150 \Omega$ and $Z_X = 0.949 * Z_0 = 47.43 \Omega$. These can just be made using microstrip circuits, however any lower amount of coupling is extremely difficult to make.

Figure 23 shows the performance of the Branchline coupler. This coupler is a convenient structure with low impedance values (50Ω and 35.35Ω) thus allowing low loss hybrids to be made using microstrip circuits.

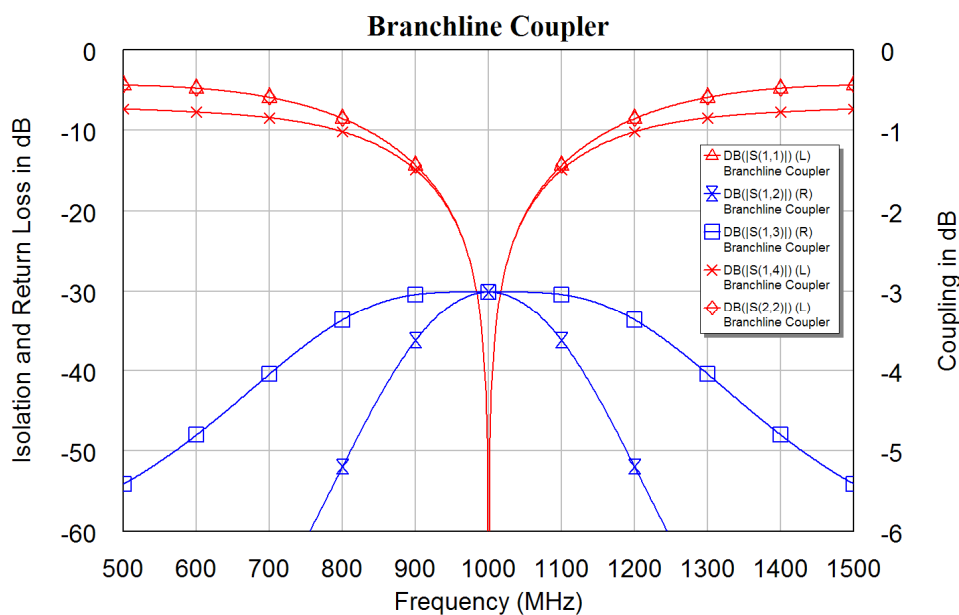


Figure 23. Branchline coupler performance.

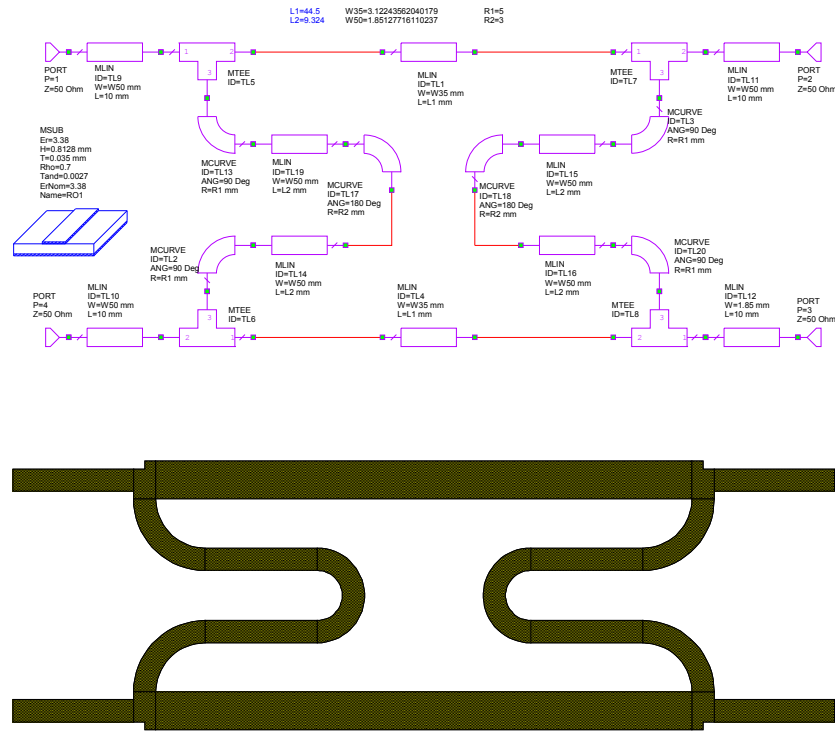


Figure 24. Branchline coupler Schematic and corresponding PCB layout.

In many cases the transmission lines are folded in order to reduce the printed circuit board area, as shown in figure 24. The losses in the microstrip circuit causes a reduced isolation at port 4 and results in a slightly asymmetrical coupling as shown in figure 25. The performance is however very similar to that of figure 23.

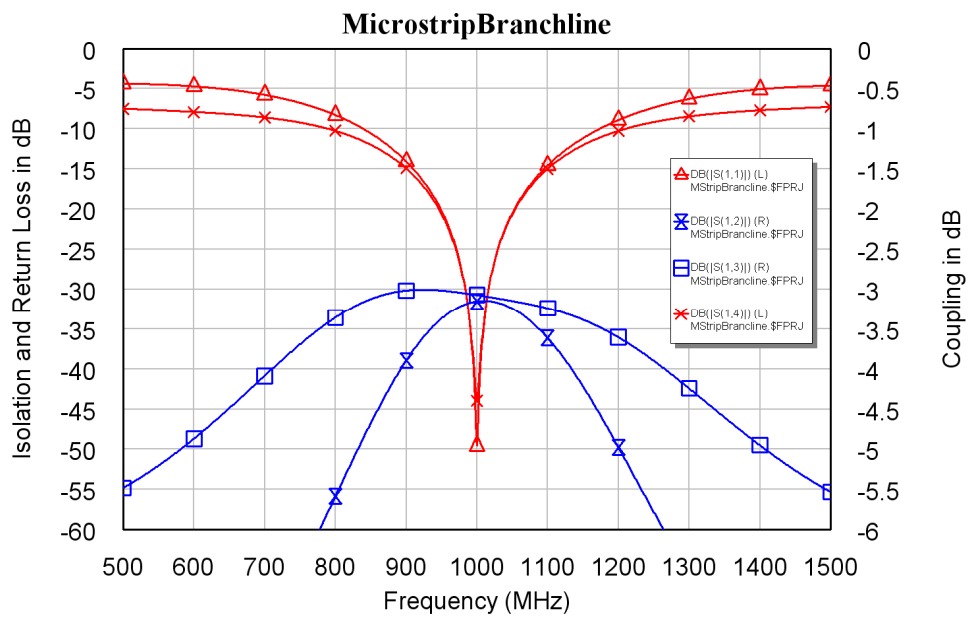


Figure 25. Microstrip Branchline coupler performance.

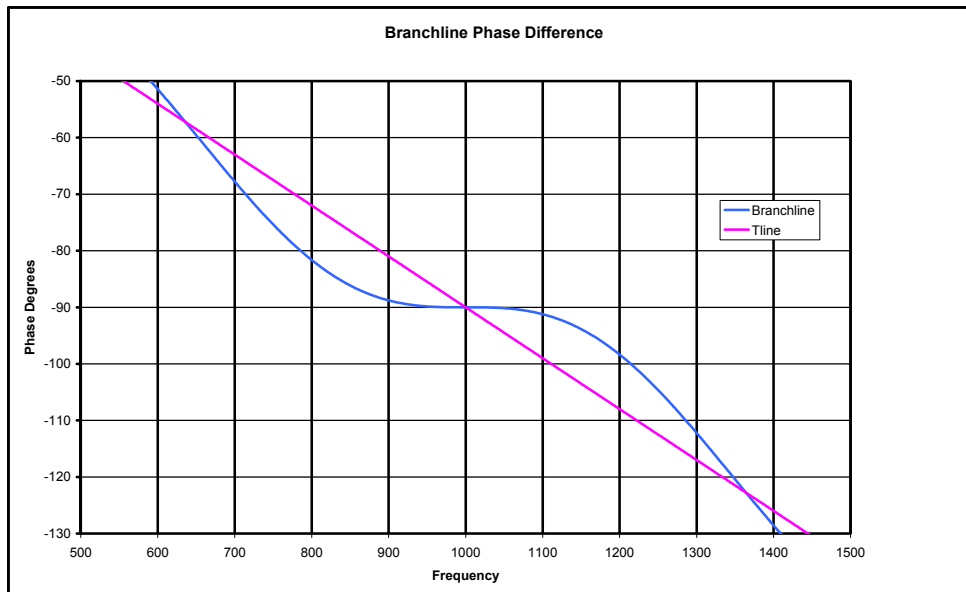


Figure 26. Branchline coupler phase difference between output ports.

The output at the coupled port has a 90° phase shift compared with the direct port and that is useful for many applications. Figure 26 compares the phase difference of signals at port 2 and 3 due to an input at port 1 and compares this with the phase shift in a simple transmission line. It can be seen that at the centre frequency of the hybrid there is only $\pm 1.22^\circ$ variation in phase for a $\pm 10\%$ variation in frequency, while it is $\pm 9^\circ$ for single transmission line. The Branchline coupler can thus be used to provide the I and Q signals, required for image suppressing mixers, with good phase and amplitude accuracy over a 20% bandwidth.

It is possible to produce a wider bandwidth Branchline coupler, by having two loops together as shown in figure 27. For a 3 dB coupler the characteristic impedances of the lines can be shown to be 120.7Ω for the outer vertical lines, 60.35Ω for the centre line and 46.2Ω , for the horizontal lines. Figure 27 also shows the corresponding PCB layout of the circuit. For a RO4003 RF PCB substrate with a 0.818 mm thickness at 1 GHz, the 120.7Ω transmission lines require 0.2387 mm wide tracks, which is close to the smallest track width that can be realised. These tracks are thus very difficult to achieve in practice. It is possible to increase the bandwidth further by using three loops for the coupler. The outer track impedances are then 175Ω . For this RO4003 substrate this corresponds to a 0.04 mm wide track, which is not possible to realise. Doubling the substrate thickness doubles the track width for the same impedance. Using thicker substrates may make some of these configurations realisable.

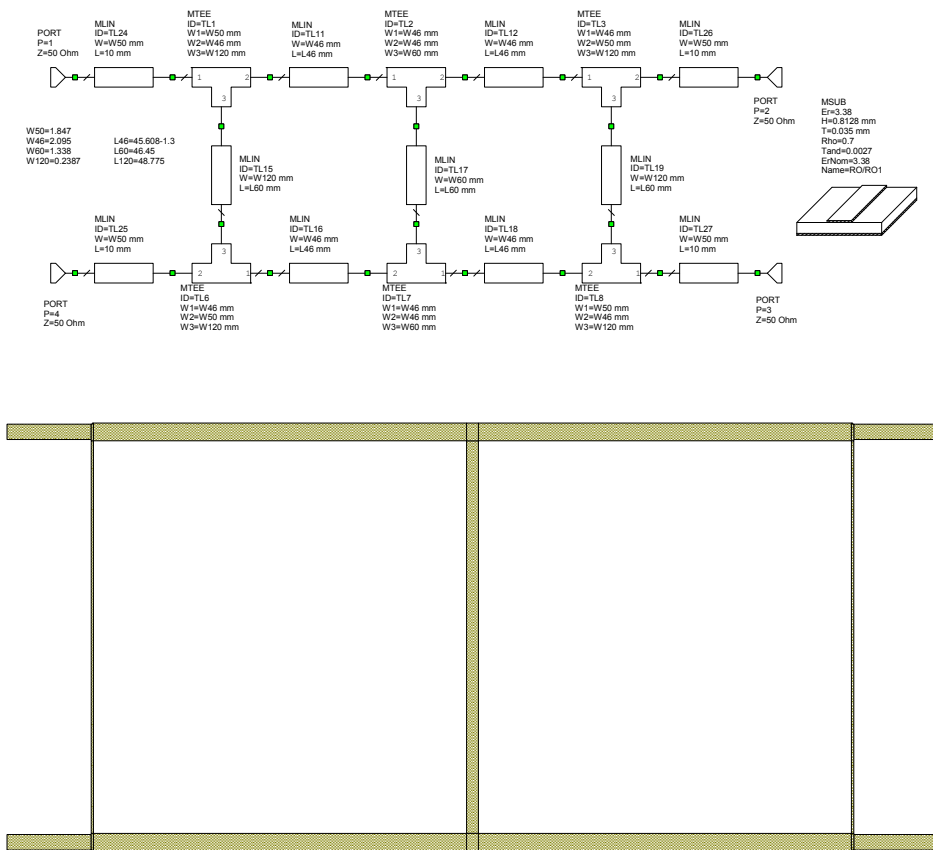


Figure 27. Wideband Quadrature Hybrid Schematic and the corresponding PCB layout.

Figure 28 shows a comparison of the single, double and triple loop Branchline coupler. The green curves are the single line coupler, the blue curves are the double line coupler and the red curves are the triple line coupler. The most significant difference is the isolation (between port 1 and 4). The bandwidth over which a good isolation is obtained is increased significantly by using multiple loops.

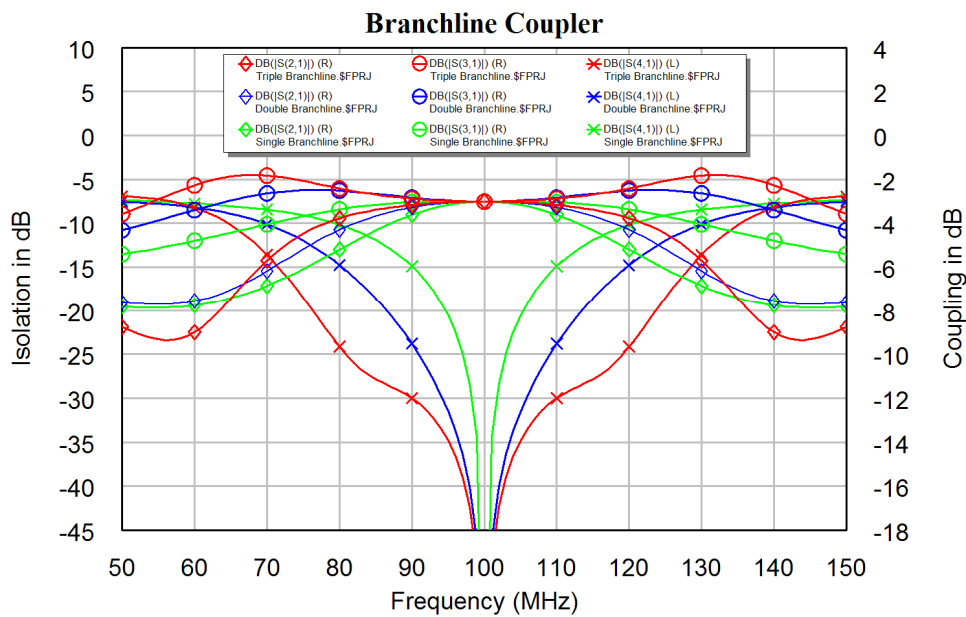


Figure 28. Multi-loop Quadrature Hybrid performance.

Backward Travelling Wave Hybrid

If two lines are in close proximity, then there is coupling between the lines. The amount of coupling depends on the spacing between the lines. TxLine in Microwave Office can be used to calculate the coupling between lines of a given spacing, as shown in figure 29.

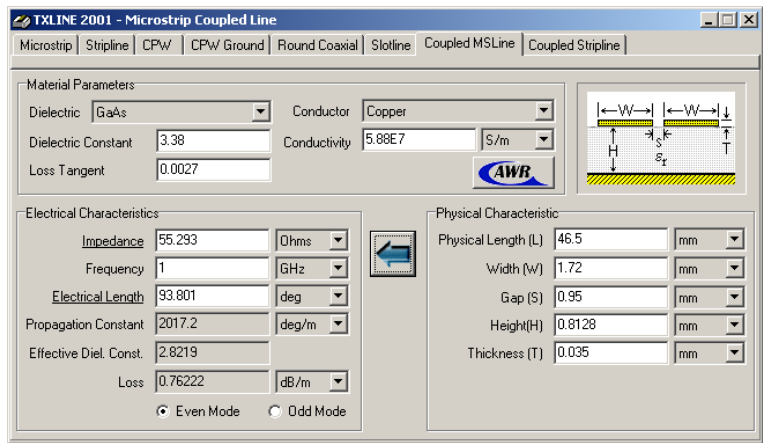


Figure 29. Calculated geometry for a λ/4 20 dB coupler.

Consider the two microstrip coupled lines as shown in figures 29 and 30. The maximum coupling will occur when the coupled lines are a quarter wavelength long. The resulting coupling is related to the even and odd mode impedances by:

$$Z_{OE} = Z_0 \sqrt{\frac{1+C}{1-C}} \quad \text{Even mode impedance.} \quad \text{Eqn. 13}$$

$$Z_{OO} = Z_0 \sqrt{\frac{1-C}{1+C}} \quad \text{Odd mode impedance.} \quad \text{Eqn. 14}$$

Where C is the voltage at the coupled output relative to the input, Z_{OO} is the odd mode impedance, where the two lines of the transmission line are of opposite polarity, so that most of the field is between the conductors. Z_{OE} is the even mode impedance, where both the lines are at the same potential, so that most of the field is between the conductors and the ground-plane.

Edge Coupled Lines

Edge coupled lines correspond to the geometry shown in the top right hand side of figure 29. The coupled lines are made using conventional microstrip lines using double sided PCB with the bottom side a ground-plane. This is easy to manufacture, but places restrictions on the amount of coupling that can be obtained. Typically the spacing between the lines is very small and this spacing must be accurately controlled to obtain the correct amount of coupling. Edge coupled lines are very suitable for sampling the forward and reverse power from transmitters and for filters. The design process of a backward coupled hybrid using edge coupled lines is illustrated with the following example.

Example: A 20 dB coupler for a transmitter at 900 MHz is required. The coupled output is thus 20 dB below the input. The coupled voltage is one tenth of the input voltage, i.e. $C = 0.1$. From the above equations one obtains $Z_{OO} = 45.23 \Omega$ and $Z_{OE} = 55.28 \Omega$. The required physical spacing can now be determined iteratively using the Txline program. The final results from the Txline calculations are shown in figure 29. Note that for the same line length, the electrical length is different for the even and odd mode, since the velocity of propagation of these modes is different. The length chosen is such that the average is correct, but it is likely that the length needs to be fine-tuned to obtain the desired performance.

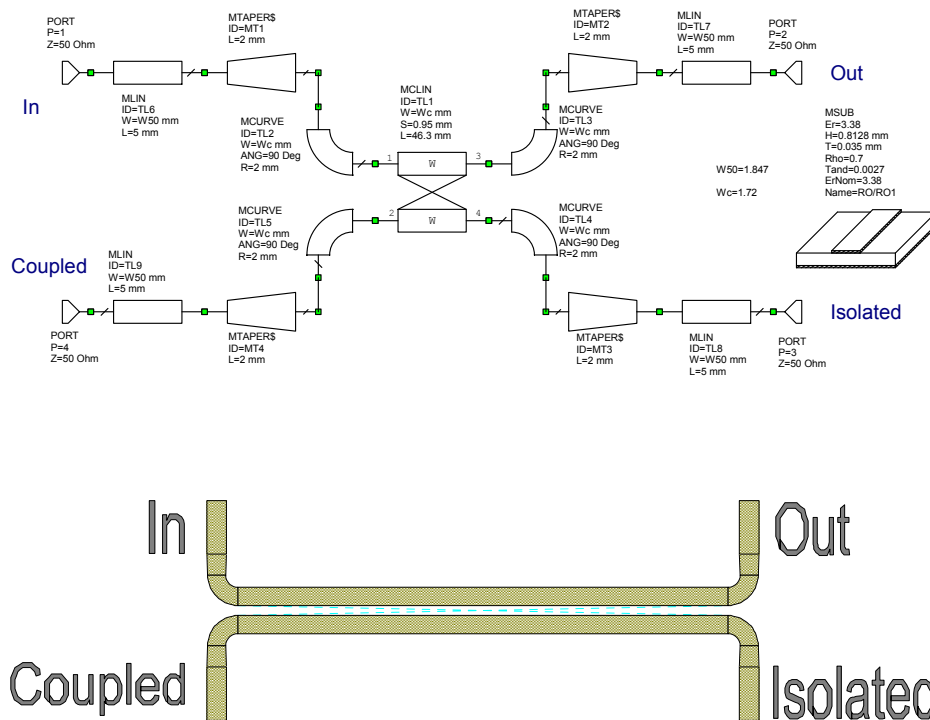


Figure 30. $\lambda/4$ 20 dB coupler Schematic and Corresponding Microstrip Layout.

These calculated values are substituted in the coupled line circuit diagram shown in figure 30. Figure 30 also shows the corresponding PCB layout including $50\ \Omega$ lines needed to connect the input and output ports to the coupler. Figure 31 shows the corresponding performance. The coupling is 20 dB as expected. Note that the coupled port is in a different location compared with the Branchline coupler.

The coupler was designed for a centre frequency of 1 GHz. Coupled lines have a null in coupling at multiples of a half wavelength length. This was used to tune the length of the coupled line to give a null at 2 GHz, thereby giving maximum coupling at the required 1 GHz. Note that the bandwidth of the coupling and the isolation is very wide compared with the other hybrids described before in these notes. At 1 GHz, the isolation (S_{31}) is only 5 dB less than the coupled output (S_{41}), so that this coupler cannot be used as a directional coupler, without further design changes.

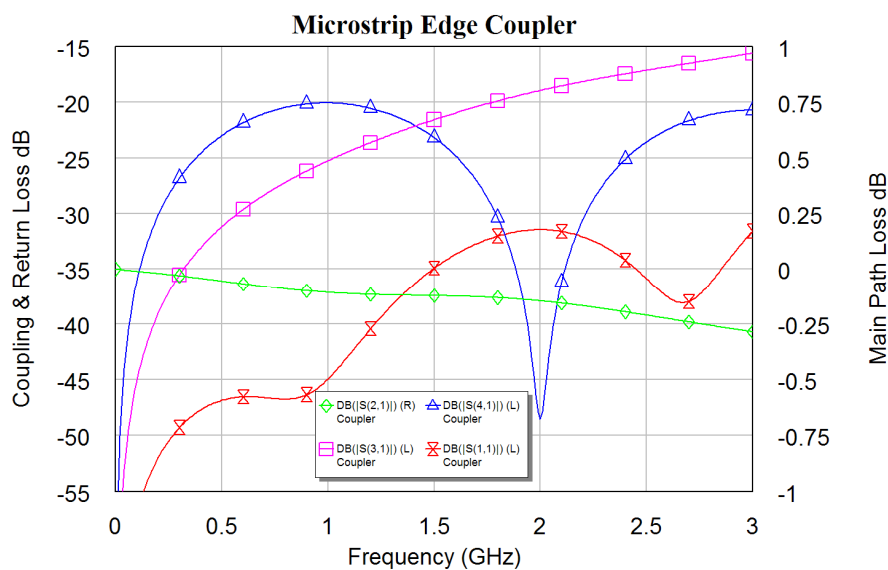


Figure 31. $\lambda/4$ Microstrip 20 dB coupler performance.

Alternately, the coupling can be obtained directly from figure 30. Changing the length of the coupled lines, such that a coupling null is obtained at twice the frequency for maximum coupling, (2 GHz for figure 31) and the spacing of the coupled lines is changed to obtain the correct coupling factor and the coupled line with is changed to obtain a low return loss (S_{11}), allows the same coupler to be designed, without using the Txline program. These values can easily be determined using the optimisation routines included in MWO.

By including some very small, sub-pf, capacitors across the terminals 1 and 4 and terminals 2 and 3 the phase velocity is more equalised over a wide frequency range and a lower input return loss (S_{11}) and flatter isolation (S_{31}) is obtained.

One application of the backward travelling wave coupler is in the measurement of power at the output of a device, such as a signal generator or a transmitter. Typically a coupled signal -20 dB below the forward or reverse power is required. The forward power is the transmitter output power and the reverse power is the reflected signal that occurs if the load for the transmitter is mismatched. To accurately differentiate between forward and reflected power at least a 20 dB front to back isolation is required. The hybrid will thus require a coupled output of -20 dB and an isolated signal < -40 dB.

As can be seen from figure 31, the signal at the isolated port (S_{31}) is too large when a quarter wavelength long coupler is used. A suitable coupler with a good forward to reverse ratio can be obtained by making the length of the coupler smaller than a quarter wavelength and using capacitors shunting the forward and reverse coupled outputs to produce a constant frequency response over the required frequency band.

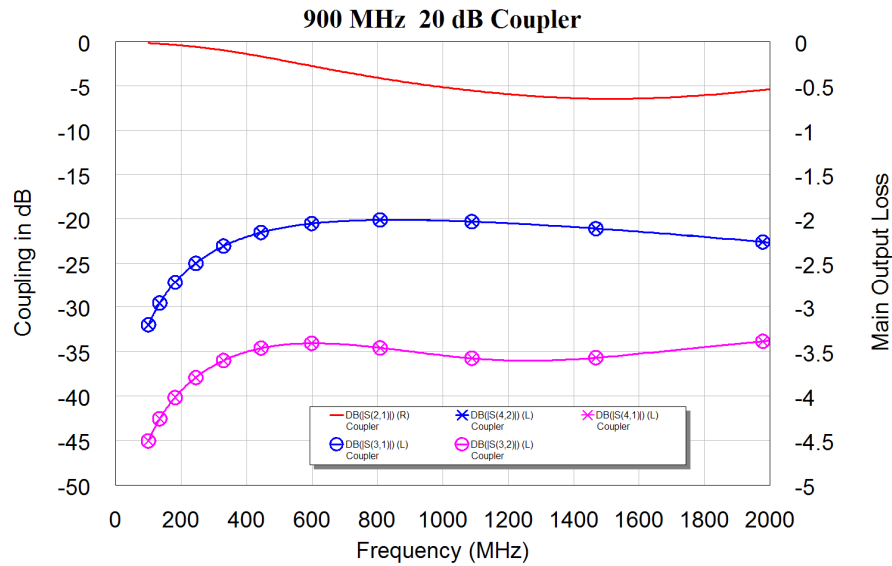


Figure 32. Simulated performance of stripline coupler.

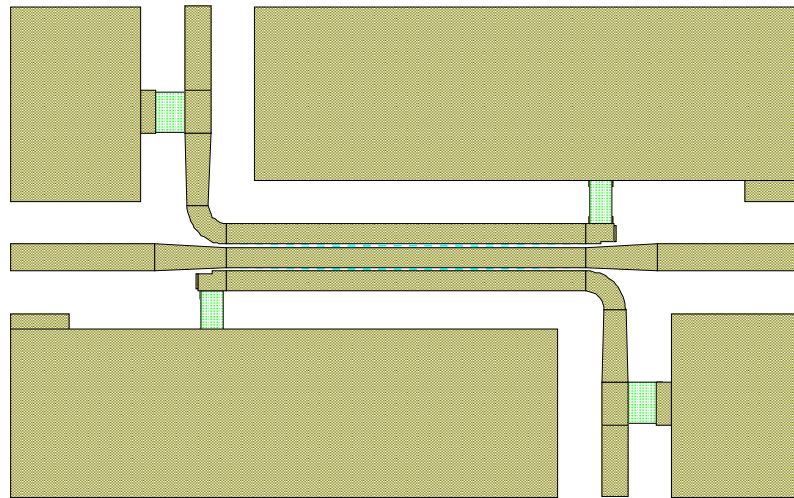


Figure 33. Layout of Microstrip-line coupler.

Figure 32 shows the simulated performance of such a 20 dB coupler. Comparing this with figure 31 shows that the isolated port has a much better isolation and the coupled port has a flatter and wider frequency response. This performance is obtained by using the optimiser in Microwave Office to vary the coupling gap, line widths, lengths and capacitance values until a suitable performance is obtained. The resulting PCB layout is shown in figure 33. For a $\lambda/4$ long coupler and -20 dB coupling, a 0.95 mm gap is required. For the shorter length coupler of Figure 33, the coupling gap is 0.2 mm, which is easy to achieve using current technology. Figure 34 shows a photograph of the

stripline coupler. The measured performance closely matches the simulated performance. Figure 35 shows the corresponding circuit diagram. The blue variables for widths, length, coupling gap and capacitor values are the parameters that are optimised to obtain the specified performance.

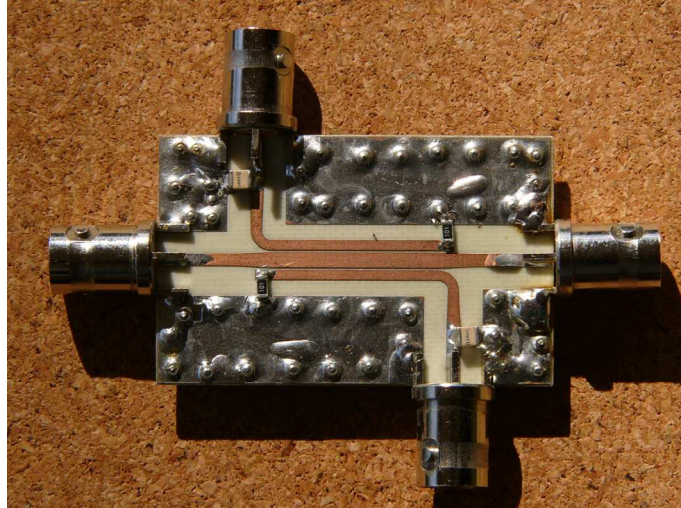


Figure 34. Photograph of the Microstrip-line coupler.

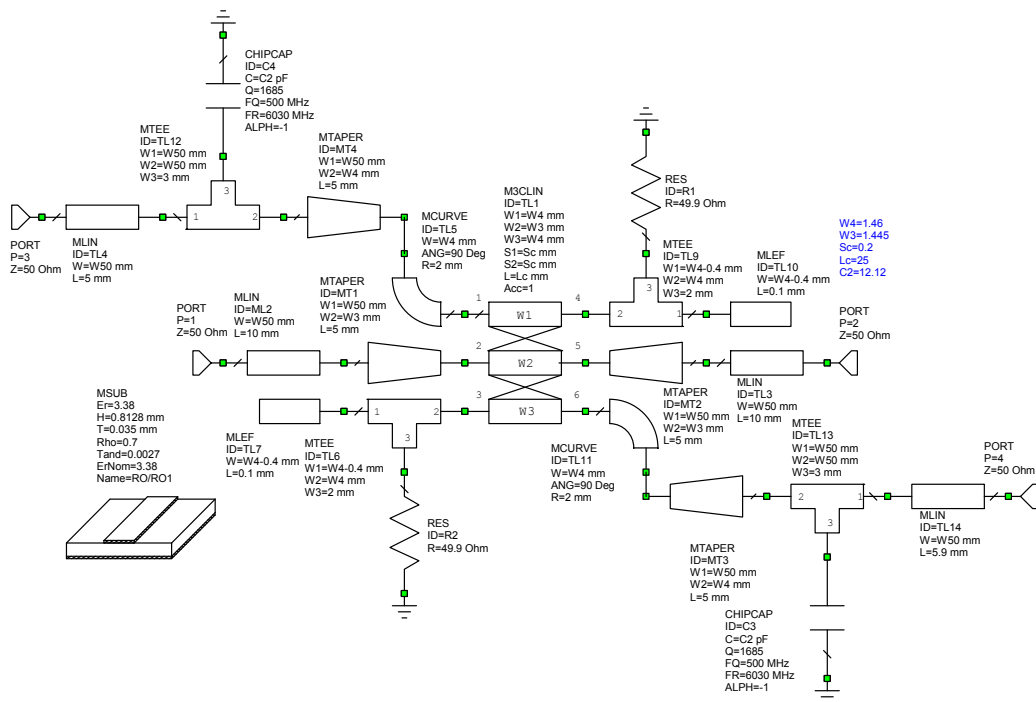


Figure 35. Circuit diagram of Microstrip-line coupler.

For this application Edge coupled Backward travelling wave hybrids are the best choice since a wide bandwidth and low coupled outputs (-20 dB) are required.

Lange Coupler

For a 3 dB coupler, $C=0.707$ and $Z_{OE}=120.7 \Omega$ and $Z_{OO}= 20.7 \Omega$. For edge coupled microstrip lines, this requires a coupling gap far smaller than 0.1 mm, which is impossible to make. To increase the coupling, many lines can be used in parallel. This is called a Lange Coupler. Figure 36 shows a layout of a Lange coupler. At the middle a bonding wire is used to connect the upper track end to the middle track and the lower other track end, thus keeping those transmission lines in parallel. Similarly the track ends at the edges of the coupler are connected to the other appropriate lines. One will thus have the top left port connected by a set of parallel lines to the bottom right port. The top right port is connected by a set of parallel lines to the bottom left port. Typically the spacing between the tracks and the track widths are of the order of 0.25 mm, which is the smallest widths that can conveniently be made using conventional processes.

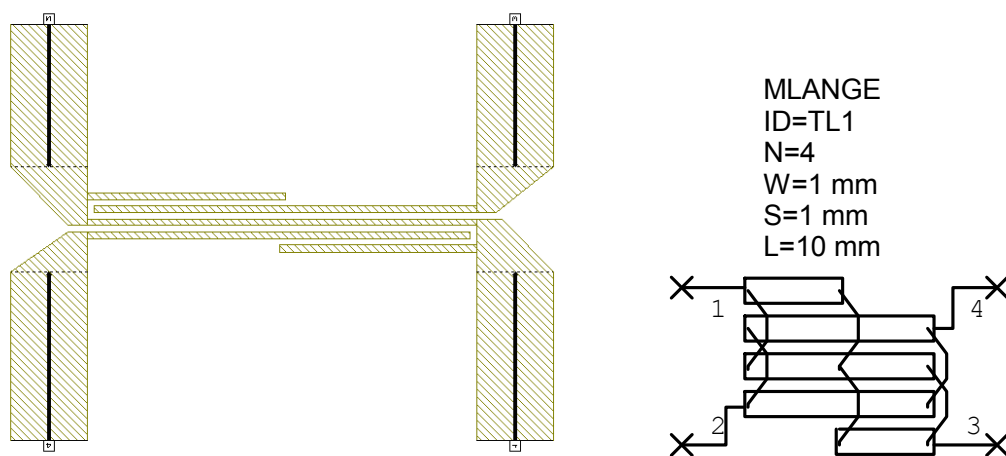


Figure 36. Lange coupler layout (the bond wires are not shown) and schematic.

Even having these parallel lines result in very fine track widths and coupling gaps, making the Lange Coupler expensive to make. The Lange coupler is however the only planar hybrid that offers better than an octave (2:1) of useable bandwidth. With the high cost of manufacturing the Lange Coupler, due to the small track and gap widths and the high cost of attaching the bond wires, Lange Couplers are not often used. The required coupling can be obtained at a lower cost and can be better controlled using broadside coupled lines and multilayer RF printed Circuit Boards. They can also be implemented with Low Temperature Co-fired Ceramic (LTCC) substrates which are discussed in chapter 10.

Broadside coupled lines

It is possible to have multilayer printed circuit boards with RF substrates. These can be used to design coupling structures with higher coupling and 3 dB couplers are quite practical. The typical configuration is shown in figure 37.

The advantages of this structure are firstly that bigger coupling between the transmission lines can be obtained with a good control over impedance values. Secondly the stripline structure has no radiation losses. The disadvantage is that a non-planar structure is required.

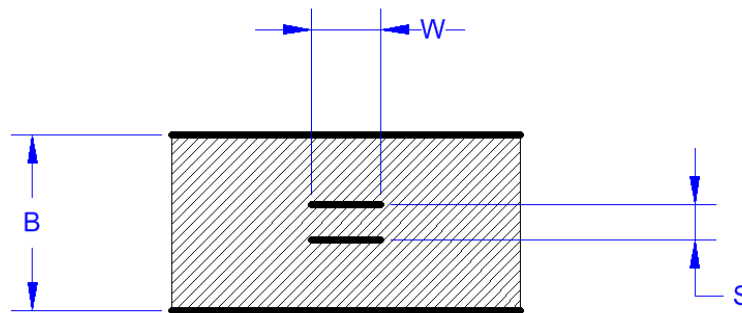
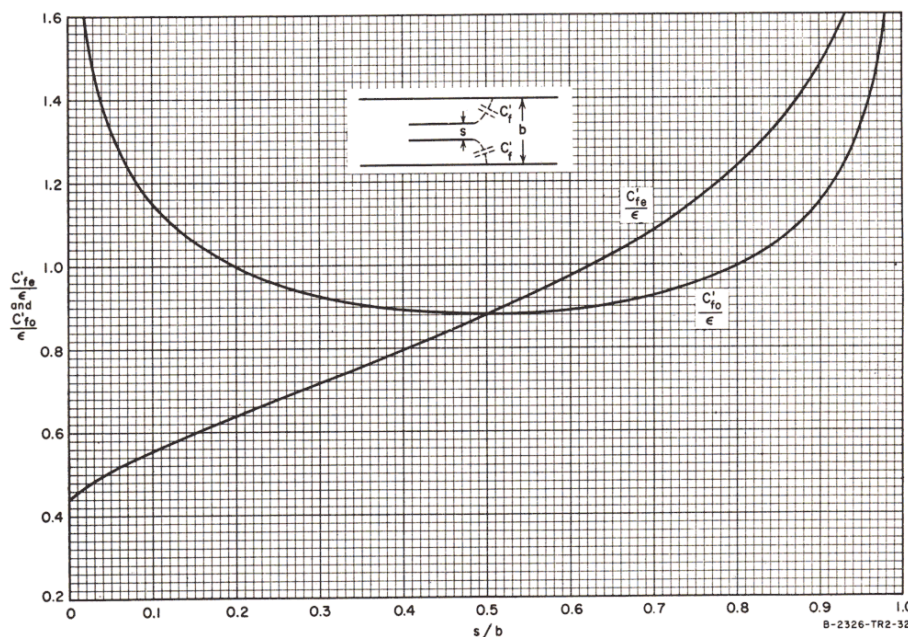


Figure 37. Stripline broadside coupled lines

Txline is not capable of calculation the broadside coupled transmission line coupling gap (s) and line width (W), shown in figure 37. The Agilent’s Linecalc program does allow this. In addition books like Matthei, Young and Jones. Microwave Filters, Impedance Matching Networks and Coupling Structures. Artech House 1980. (McGraw Hill 1964) pages 180 and 181 give empirical equations for Z_{oo} and Z_{oe} are given in equations 15 and 16. The capacitance C_{fe} and C_{fo} are fringing capacitances between the coupled lines and the ground plane and these can be determined from figure 38.

$$Z_{OE} = \frac{188.3/\sqrt{\epsilon_r}}{\frac{w/b}{1-s/b} + \frac{C_{fe}}{\epsilon}} \tag{Eqn. 15}$$

$$Z_{OO} = \frac{188.3/\sqrt{\epsilon_r}}{\frac{w/b}{1-s/b} + \frac{w}{s} + \frac{C_{fo}}{\epsilon}} \tag{Eqn. 16}$$



SOURCE: Final Report, Contract DA-36-039 SC-74862, SRI; reprinted in *IRE Trans., PGMTT* (see Ref. 5, by S. B. Cohn).

Figure 38. Table for C_{fe} and C_{fo} from Matthei, Young and Jones, pp181.

Using the two-line broadside coupled line element, SBCPL, and the schematic circuit simulation, allows an easier and more accurate determination of the broadside coupler parameters, than using equations 15, 16 and figure 38. The SBCPL element is a two-line broadside coupled line element. The cross-section is similar to that of Figure 37.

In addition the width of each of the lines can be specified independently, the lines can be offset and the dielectric constants between the lines can be different from that above and below the line. None of these advanced features can be determined using the alternative techniques. The use of the SBCPL element to determine the required coupling gap and line width for a coupler is illustrated in the following example.

Example

A 3 dB coupler was required to operate at a power level of about 100 Watt at a frequency of 100 MHz. At the time of the design, MWO did not yet exist and the Equations 15 and 16 and Figure 38 were required to complete the design.

Two 12.6 mm thick pieces of Polyethylene, which has a dielectric constant of $\epsilon_r = 2.26$, were used for the top and bottom dielectric sheets for this coupler. Polyethylene sheets of this thickness can conveniently be purchased as a cutting board for bread from most local supermarkets. For a 3dB coupler, $C = 0.707$ and $Z_{OE} = 120.7 \Omega$ and $Z_{OO} = 20.7 \Omega$. Since these impedances must be evaluated iteratively, it is the easiest to enter the above equations for Z_{OE} and Z_{OO} into an Excel or other spreadsheet. Using the values $B = 29$

mm, $s = 2.9$ mm, $w = 12.7$ mm, gives $\frac{s}{B} = 0.1$ and thus from the table gives $\frac{C_{fe}}{\epsilon} = 0.56$

and $\frac{C_{fo}}{\epsilon} = 1.15$. This then results in $Z_{OE} = 119.7 \Omega$ and $Z_{OO} = 20.8 \Omega$, which is close enough. At 100 MHz the length of a quarter wavelength line is given by: $\frac{\lambda}{4} = \frac{c}{\sqrt{\epsilon}F} = 50cm$. As shown in figure 39, the width of 50 Ω terminating lines can be

calculated using Txline or equivalent programmes as 23.2 mm. A 2.9 mm thickness of Polyethylene is not readily available, however a 3.17 mm thickness of Perspex, with a dielectric constant of approximately 3.42 is available and was used. The effect of this substitution cannot readily be calculated using the above techniques. This coupler was constructed and performed as expected, even though the line spacing was not ideal.

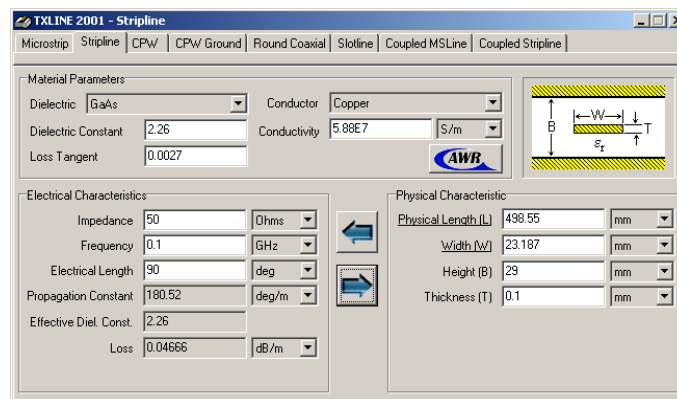


Figure 39. Terminating line-width calculation.

The use of SBCPL in Microwave Office gives much more flexibility and allows a more accurate determination of the performance. The actual cutting boards used are 12.6 mm

(0.5 inch) thick, pieces of Polyethylene. They are to be used for the top and bottom dielectric and a 3.17 mm (0.125 inch) thick Perspex sheet is available to separate the tracks. Entering these values in the SBCPL element and then fine-tuning the track width, track length and offset, allows the required performance to be obtained. Polyethylene has a dielectric constant of $\epsilon_r = 2.26$ and Perspex has a dielectric constant of 3.42 ± 0.3 .

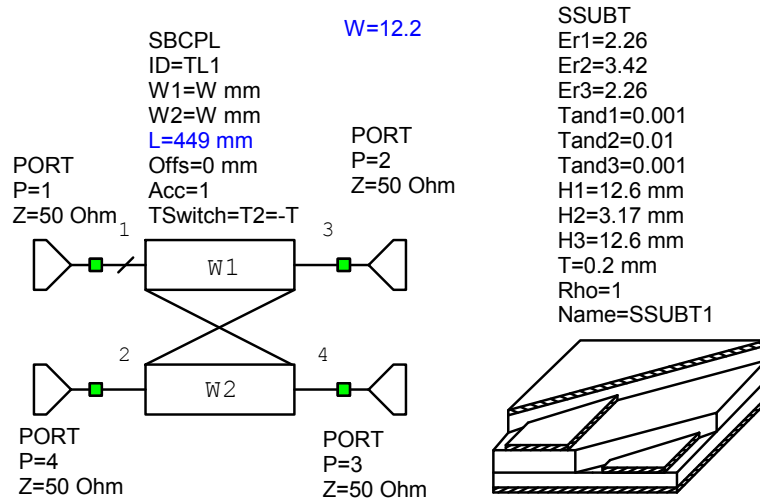


Figure 40. MWO broadside coupled-line circuit using SBCPL.

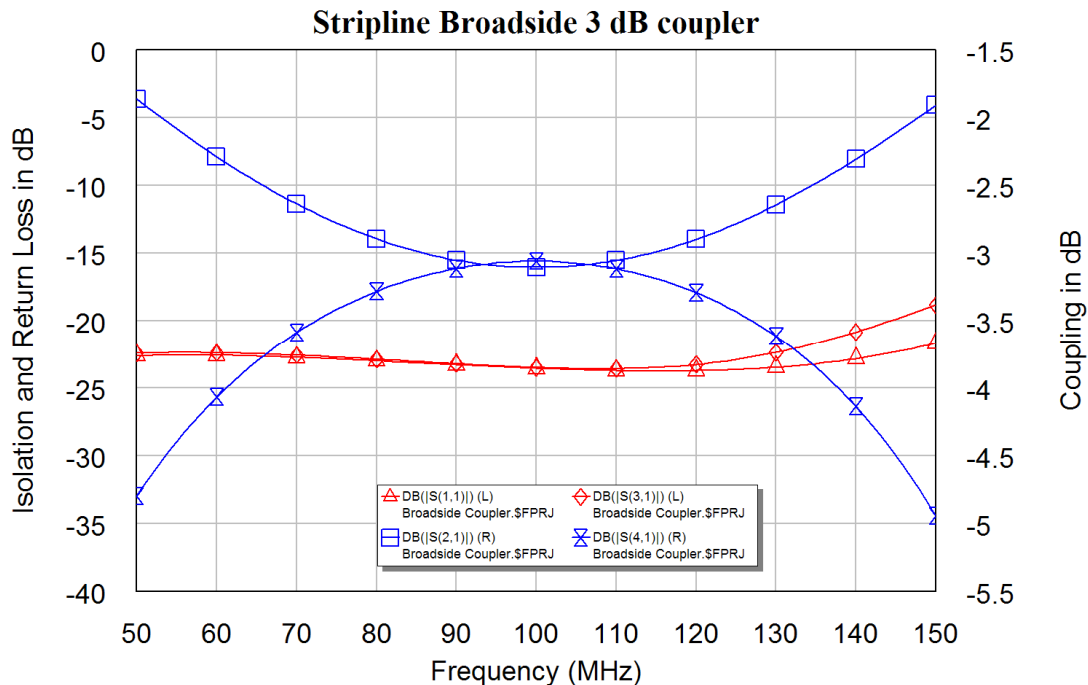


Figure 41. Performance of broadside coupled-line circuit using SBCPL element.

Tuning the coupler length ($L = 449$) sets the centre frequency of the coupler to 100 MHz and tuning the line width ($W = 12.2$) adjusts the coupling to have close to 3 dB coupling over the 85 MHz to 115 MHz frequency range and achieve a return loss on the

ports of less than -20 dB. The resulting MWO circuit diagram is shown in figure 40 and the corresponding performance is shown in figure 41. The track width of 12.2 mm and length of 440 mm obtained from MWO agrees closely with the 12.7 mm and 500 mm obtained for the earlier design using the equations 16 and 17 and figure 38 and used for the construction of the coupler. The MWO design is far more accurate since it allows for losses in the dielectric and the Perspex sheet for separating the tracks, having a different dielectric constant and loss tangents compared with the Polyethylene.

Prepreg sheets are available, which can be used to convert single layer PCB's to multilayer PCB's, so that broadside couplers can be constructed. The Roger's RO4403 prepreg sheets have a dielectric constant of 3.17 and are 0.1 mm thick and can be used to bond two single layer PCB's to form a multilayer PCB. The sandwich is pressed together with a pressure of 2.8 MPa (400 psi) and a temperature controlled profile up to 180 °C (350 °F) for a cycle time of 2 hours to form the correct bond. For further details see the RO4403/4450 data sheet. Other manufacturers have similar materials.

Mixers

Introduction

Figure 1 shows the typical block diagram of a Transmitter and a Receiver. It can be seen that in both cases frequency translation is achieved by the use of a Mixer. The mixers can be either passive mixers using diodes or they can be active mixers using transistors or FETs. In many receivers and transmitters, a succession of mixing and filtering stages are used, to ensure that the filtering requirements can be satisfied.

A mixer is used as an up-converter when the output frequency is higher than the input frequency. This is typical in a transmitter. A mixer is used as a down-converter when the output frequency is lower than the input frequency. This is typical for a receiver.

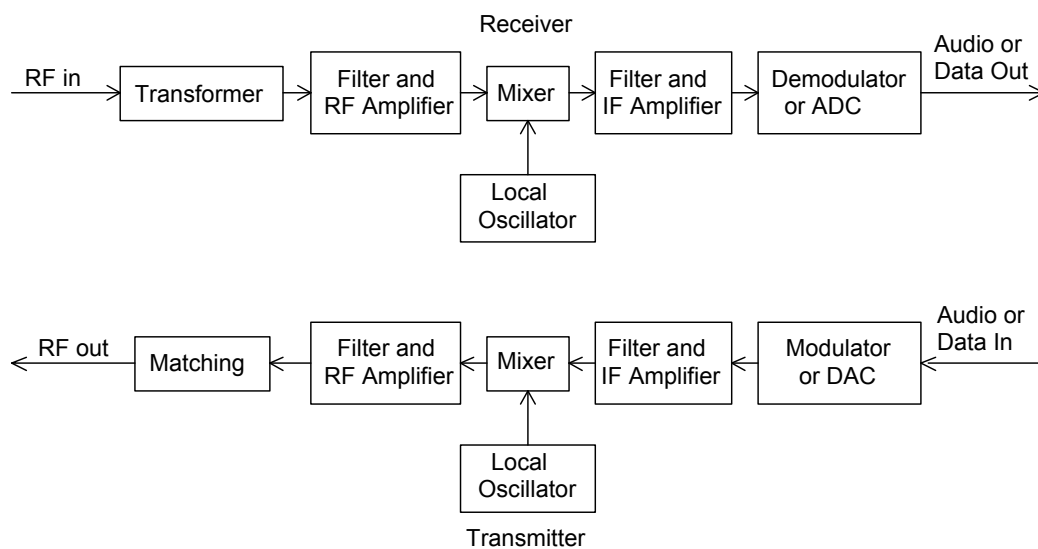


Figure 1. Typical transmitter and receiver block diagram.

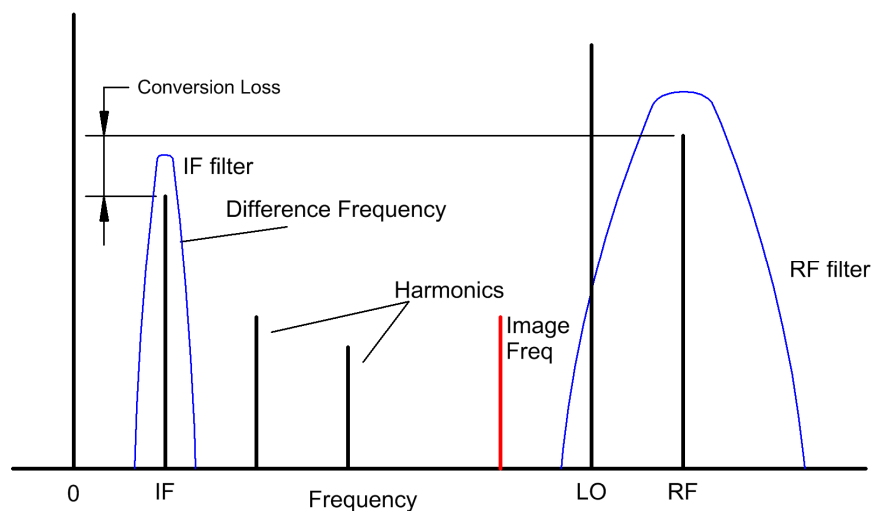


Figure 2. Frequencies of a mixer.

Figure 2 shows the frequencies that need to be considered when using a mixer. For a down-converter the Radio Frequency (RF) signal is mixed with a Local Oscillator (LO)

signal to produce sum and difference frequencies. The sum frequency is outside the operating frequency range of the system and the difference frequency is the required Intermediate Frequency (IF) signal, which is filtered and amplified using an IF filter and its associated amplifiers.

The RF filter should be sufficiently narrow so that the image frequency is not passed through the RF filter, since the difference frequency of the image frequency and the local oscillator is at exactly the same frequency as the required IF signal.

An ideal multiplier is a perfect mixer since when the LO signal is multiplied by an RF signal then sum and difference frequencies are generated, the difference frequency being the required IF signal and the sum signal being an unwanted high frequency component, which is normally filtered out. For an up-converter, the LO signal is multiplied by an IF signal and a double sideband suppressed carrier RF signal results. The aim in mixer design is thus to make the mixer behave as close to an ideal multiplier as possible.

There are two types of mixers: 1) Passive mixers, using diodes, where the LO power provides the power for the mixer. 2) Active mixers, where transistors or FETs supplied with DC power provide the mixing action.

Definition of Terms

Conversion Loss

For a down-converter, the conversion loss is the ratio of the wanted IF output signal to the RF input signal. Most mixers are used in receivers, for which this definition is applicable. For up-conversion, the conversion loss is the ratio of one of the wanted RF output signal spectral components to the IF input signal. For an ideal mixer, half the input power is frequency shifted to the difference frequency and half the power is shifted to the sum frequency. The conversion loss is the ratio of either the sum or the difference component to the input signal. An ideal passive mixer will thus have a conversion loss of 3 dB. Practical balanced or double balanced mixers typically have a conversion loss of less than 6 dB. The conversion loss does depend on the amount of LO signal power applied to the LO port as can be seen in figures 11, 20 and 28. The mixer is normally operated at a LO power close to that giving the lowest conversion loss. Active mixers can have a conversion gain.

The conversion loss must be taken into account in noise figure calculations of a receiver. A mixer with a 6 dB conversion loss typically has a 6.5 dB noise figure. For high quality receivers, an amplifier with a gain much greater than the conversion loss is normally used before the mixer, to ensure that the mixer does not dominate the noise performance of the receiver.

Isolation

In practice it is desirable to have isolation between the LO, RF and IF ports of the mixer. Typical double balanced mixers have more than 30 dB isolation between all ports. Single diode mixers have virtually no isolation between ports. Since single diode mixers are used in TV receivers, the LO signal is coupled to the antenna, which radiates the LO signal. In countries where TV licences are required, the “detector vans” look for the LO radiation and match the radiation coming from a house with any licence fee

payment. One can also do a good survey to find out what TV channel people are watching by simply driving around a street with a spectrum analyser and noting the LO frequencies. For a balanced mixer, the isolation is directly related to the match between the diodes used. As a result many manufacturers sell matched sets of diodes, specially for use in mixers. In many cases two or 4 diodes come as one package.

Compression Point

For an ideal down-conversion mixer the IF output produced should be directly proportional to the RF input signal. However as the RF input approaches about 10 dB below the LO power. The IF output starts to saturate and the conversion loss starts to decrease, as is shown in figure 3. Most manufacturers of mixers specify the 1 dB compression point for their mixers. The 1 dB compression point is typically 6 dB below the LO level for mixers up to +23 dBm LO power.

Since the 1 dB compression point is related to the LO drive, a higher LO level results in a higher 1 dB compression point and as a result a bigger dynamic range of the mixer.

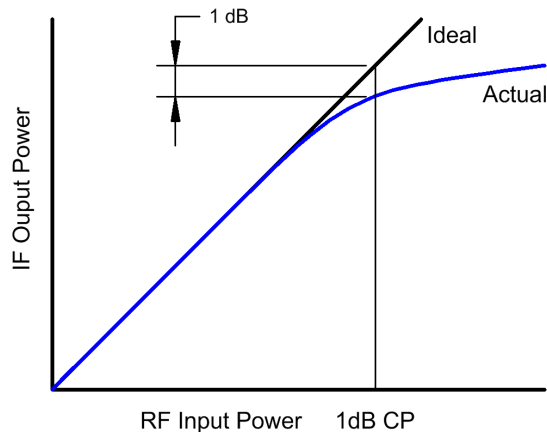


Figure 3. 1 dB Compression Point of a mixer.

Dynamic Range

Dynamic range is the range over which a mixer provides useful operation. The upper limit of the dynamic range is determined by the 1 dB compression point. The lower limit of the dynamic range is limited by the noise figure of the mixer. Since the mixer noise figure is only about 0.5 dB higher than its conversion loss, the lowest conversion loss is desirable to obtain the largest dynamic range. High and Extra High level mixers have a higher 1 dB compression point and thus a bigger dynamic range. Higher level mixers are significantly more expensive and require more LO power, so that a compromise between cost, power consumption and dynamic range exists.

Two-tone Third Order Intermodulation Distortion

In this section one considers the mixer as a “linear” device, since for a down-converter, the IF mixer output amplitude is directly related to the RF input amplitude. The output $Y(t)$ of a mixer or amplifier will depend on the input $X(t)$. The gain of the device, relating the output to the input is a_1 . In addition a DC component and harmonics of the input may be created due to the distortion of the device. The output is thus:

$$Y(t) = a_0 + a_1X(t) + a_2X(t)^2 + a_3X(t)^3 + a_4X(t)^4 + a_5X(t)^5 + \dots \quad \text{Eqn. 1}$$

For the devices we are considering, the terms above the 5th harmonic are so small they can be ignored.

When two signals X_1 and X_2 are used as input. The output will then be:

$$Y(t) = a_0 + a_1[X_1(t) + X_2(t)] + a_2[X_1(t) + X_2(t)]^2 + a_3[X_1(t) + X_2(t)]^3 + a_4[X_1(t) + X_2(t)]^4 + a_5[X_1(t) + X_2(t)]^5 + \dots \quad \text{Eqn. 2}$$

When $X_1(t)$ is a sinewave of frequency F_1 and $X_2(t)$ is a sinewave of frequency F_2 , ($F_2 > F_1$) the frequency components at the fundamental and different intermodulation frequencies can be collected as follows:

The fundamental frequency component, i.e. at F_1 due to $X_1(t)$ and at F_2 due to $X_2(t)$ is:

$$Y_F = a_1 + \left(\frac{3}{4} + 3\frac{1}{2}\right)a_3 + \left(\frac{5}{8} + 10\frac{3}{8} + 5\frac{3}{8}\right)a_5 = a_1 + \frac{9}{4}a_3 + \frac{25}{4}a_5 \quad \text{Eqn. 3}$$

The Third Order Intermodulation (3IM) frequencies are 3IM(upper) due to $\pm F_1 \pm 2F_2$ and 3IM(lower) due to $\pm 2F_1 \pm F_2$, and are given by:

$$Y_{3IM} = \frac{3}{4}a_3 + \frac{1}{2}\left(5\frac{1}{2} + 10\frac{3}{8}\right)a_5 = \frac{3}{4}a_3 + \frac{25}{8}a_5 \quad \text{Eqn. 4}$$

The Fifth Order Intermodulation (5 IM) frequencies are 5IM(upper) due to $\pm 2F_1 \pm 3F_2$ and 5IM(lower) due to $\pm 3F_1 \pm 2F_2$, and are given by:

$$Y_{5IM} = \frac{1}{2}10\frac{1}{8}a_5 = \frac{5}{8}a_5 \quad \text{Eqn. 5}$$

The frequencies of these spectral components are shown in figure 4.

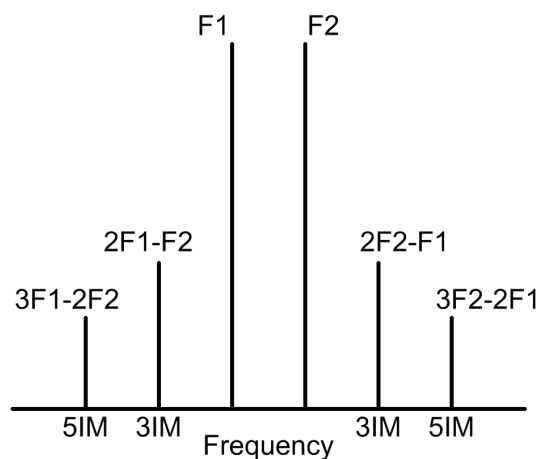


Figure 4. IM distortion of an amplifier or mixer.

The second order intermodulation (2IM) and the fourth order intermodulation (4IM) distortion produced by the amplifier or mixer does not create any components near the desired frequency components as a result the 2IM and 4IM performance is less important for an amplifier. The second order intermodulation produces the required mixing action in a mixer and is thus of utmost importance.

The third order IM (3IM) and fifth order IM performance is very important in linear amplifiers since when two tones are used as an input to the amplifier, the 3IM and 5IM distortion results in additional frequency components, which again can not be filtered out, as can be seen in figure 4. The 5IM components are often too small to be observed in a spectrum like figure 4. For mobile phone base-stations, these IM signals are likely to create interference in adjacent mobile phone channels, as a result the IM performance of amplifiers and mixers are a critical part of their specification.

Third Order Intercept Point

In practice $a_1 \gg a_3 \gg a_5$, so that the fundamental frequency components are proportional to a_1 , the 3IM components are proportional to a_3 and the 5IM components are proportional to a_5 . If the input signals are increased by 1 dB, then the 3IM components will increase by 3 dB since they are caused by $a_3 [X_1(t) + X_2(t)]^3$ in equation 2 and the 5IM components will increase by 5 dB since they are caused by $a_5 [X_1(t) + X_2(t)]^5$ in equation 2.

A popular method of determining the “linearity” of a mixer is the "third-order intercept" approach. The Third-Order Intercept Point is a theoretical point on the RF input versus IF output curve where the desired input signal and third-order products become equal in amplitude as RF input is raised.

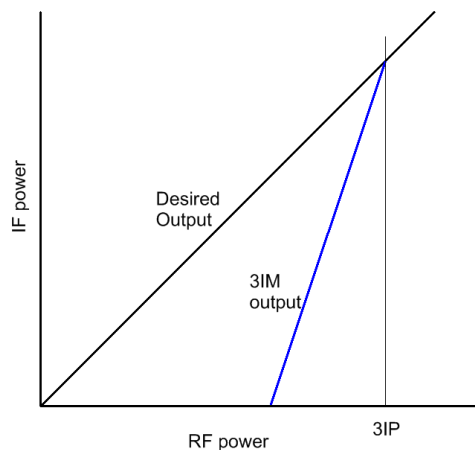


Figure 5. Third order intercept point.

As the RF signal increases by 1 dB, the 3IM distortion component increases 3 dB. The Third Order Intercept Point is determined by increasing the RF level and noting both the desired and the 3IM levels. The third order intercept point is the point where the extension of the plotted desired output and 3IM output level versus RF input meet, as shown in figure 5. It is not possible to drive the mixer to those RF levels. As a rule of thumb the third order intercept point is about 8 to 10 dB above the LO level for a typical diode based double balanced mixer and up to 15 dB above the LO level for passive FET mixers. Passive FET mixers however have a much narrower bandwidth.

The third order intercept point is useful in determining the RF level required for a specified 3IM distortion performance. If for example, the 3IM signal is to be 40 dB below the required signal, then the RF level must be 20 dB below the Third Order Intercept Point, since then the desired signal will be 20 dB below the intercept point and the 3IM signals will be $3 \times 20 = 60$ dB below the intercept point.

LO Level

Mixer manufacturers make mixers to operate at different LO power levels. For standard level mixers, the LO power required is +7 dBm. Other mixer power levels are +10, +13, +17, +23, +27 dBm. Minicircuits denote their mixer according to the LO power required, so a Level 7 mixer requires a LO power of +7 dBm. For a good Double Balanced Mixer, the third order intercept point (IP3) is 10 dB above the LO level. By having a higher power level available, the manufacturers are able to control the diode I-V characteristics more to ensure that the a_2 coefficient in the binomial expansion of the diode I-V characteristic shown as Equation 1, 2, 6 and 7 is maximized in relation to the other terms, thus minimizing the unwanted components.

Example

A maximum RF input signal of -10 dBm and a level of third order intermodulation products (3IM) of 60 dB below the desired signals is required for a specific application. For a typical 7 level mixer, the IP3 point is +17 dBm. The RF signal at -10 dBm is thus 27 dB below the IP3 point. This will result in the 3IM signals being $(3-1)*27 = 54$ dB below the wanted signal.

Similarly, a level 10 mixer will result in the 3IM signals being $(3-1)*30 = 60$ dB below the wanted signals, a level 13 mixer will result in the 3IM signals being $(3-1)*33 = 66$ dB below the wanted signals. A level 17 mixer will result in the 3IM signals being $(3-1)*37 = 74$ dB below the wanted signals. A level 23 mixer will result in the 3IM signals being $(3-1)*43 = 86$ dB below the wanted signals and a level 27 mixer will result in the 3IM signals being $(3-1)*47 = 94$ dB below the wanted signals. The higher the LO level, the higher the cost of the mixer. A level 10 mixer will thus be the lowest cost device, which will satisfy the specifications.

Single Diode Mixer

Single diode mixers use a single diode to produce the required frequency components.

Single diode mixers are often used in cost critical applications, such as Radio or TV receivers, where the low cost is more important than good performance. With the advent of low cost active mixer IC's, single diode mixers are progressively being used less. Single diode mixers are very suitable for microwave applications like speed guns and shopping centre door openers, where the transmitted signal is used as the LO for the received signal, and the receiver diode is simply mounted in the antenna horn. The resulting IF signal is the difference frequency, which is due to the speed of the car being detected or the speed of the person moving towards the door.

A single diode mixer requires a diplexer to separate the high frequency RF and LO signal from the low frequency IF signal. Since the single diode mixer is normally a lower cost consumer type application, the diplexer is normally kept simple with either a first or second order high pass and low pass filters.

Figure 6 shows a simple diplexer consisting of second order high pass and low pass filters. The crossover frequency is chosen to be 20 MHz, allowing baseband signals up to 15 MHz to be used. To obtain the best impedance looking into port 1, series elements are required to connect to port 1. A Butterworth high pass and low pass filter design is a good starting point and optimisation can be used to improve the impedance matches resulting in the diplexer performance as shown in figure 7.

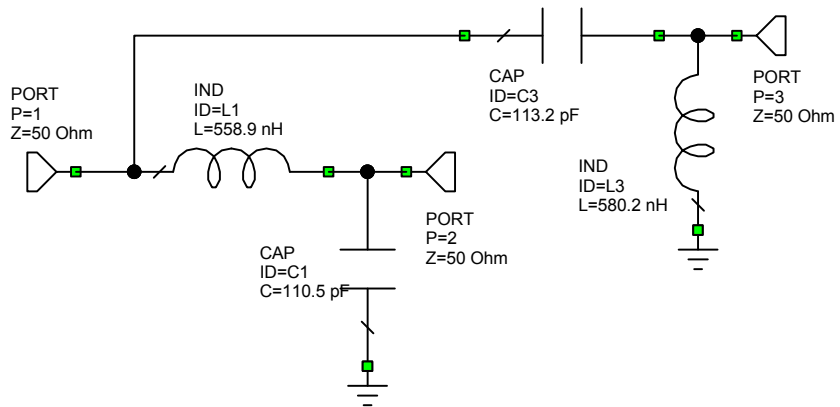


Figure 6. Diplexer circuit.

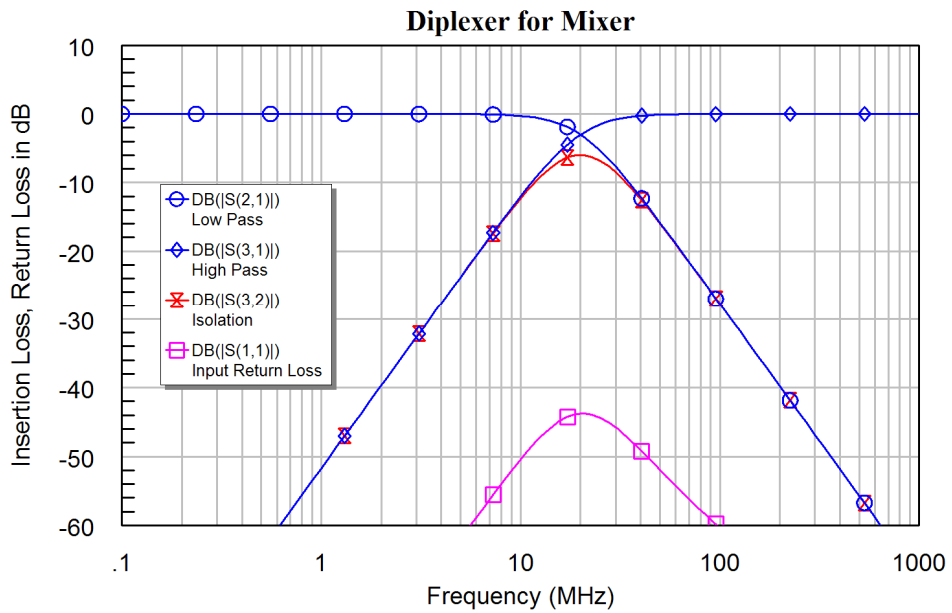


Figure 7. Frequency response of diplexer after optimisation.

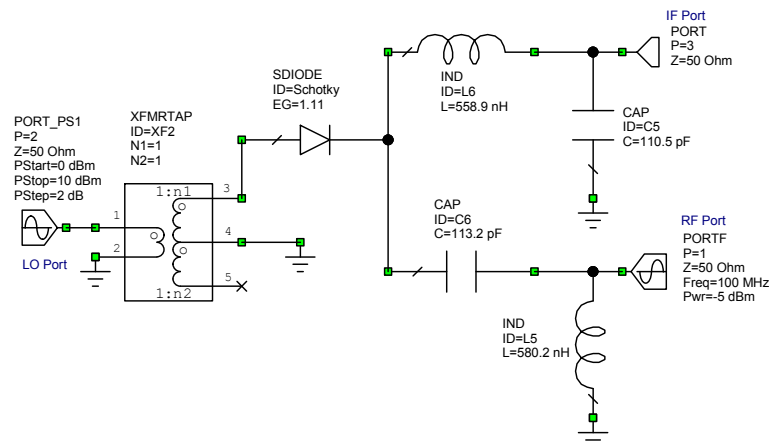


Figure 8. Circuit diagram of a single diode mixer as a down-converter.

Figure 8 shows the circuit diagram of a single diode mixer. The transformer is normally not included in the circuit, since in this case it is simply a non-inverting transformer. It is included here to illustrate the differences between the single diode mixer of figure 8 and the balanced mixer of figure 19.

The mixing behaviour of a single diode mixer can be demonstrated by considering the current flowing through the diode of figure 8. The current can be expressed as:

$$I_a = a_0 + a_1V_a + a_2V_a^2 + a_3V_a^3 + a_4V_a^4 + a_5V_a^5 + \dots \quad \text{Eqn. 6}$$

If two voltages V_a and V_b are now applied to the diode, due to the LO and the RF signals, then the current will be

$$I_a = a_0 + a_1(V_a + V_b) + a_2(V_a + V_b)^2 + a_3(V_a + V_b)^3 + a_4(V_a + V_b)^4 + a_5(V_a + V_b)^5 + \dots \quad \text{Eqn. 7}$$

The term $a_2(V_a + V_b)^2 = a_2(V_a^2 + 2V_aV_b + V_b^2)$ contains the required $2a_2V_aV_b$, which results in the sum and difference frequencies. All the other terms cause unwanted frequency components. It is thus desirable to use diodes with an I-V characteristic where a_2 is large in comparison with the other terms in the binomial expansion of the I-V characteristic. Some of the additional frequency components due to the a_3 , a_4 and higher order diode nonlinearities, can fall close to the desired frequency thus causing an interference.

Computer simulation of Mixers

The advanced RF Computer simulation programs like MWO and ADS allow mixers to be simulated accurately. A mixer requires two inputs, both at different frequencies and the output is normally at a frequency that is different from both the inputs to the mixer. The simulation is thus very different from that of a linear device, like a transformer, hybrid or filter.

The frequencies used for the simulation are set by the Project Options menu. For the single diode mixer of figure 8, these frequencies are used by the PORT_PS1 port element, which is applied to the LO port (Port 2). The PORT_PS1 element allows the signal power to be varied as specified by the parameters for the PORT_PS1 element.

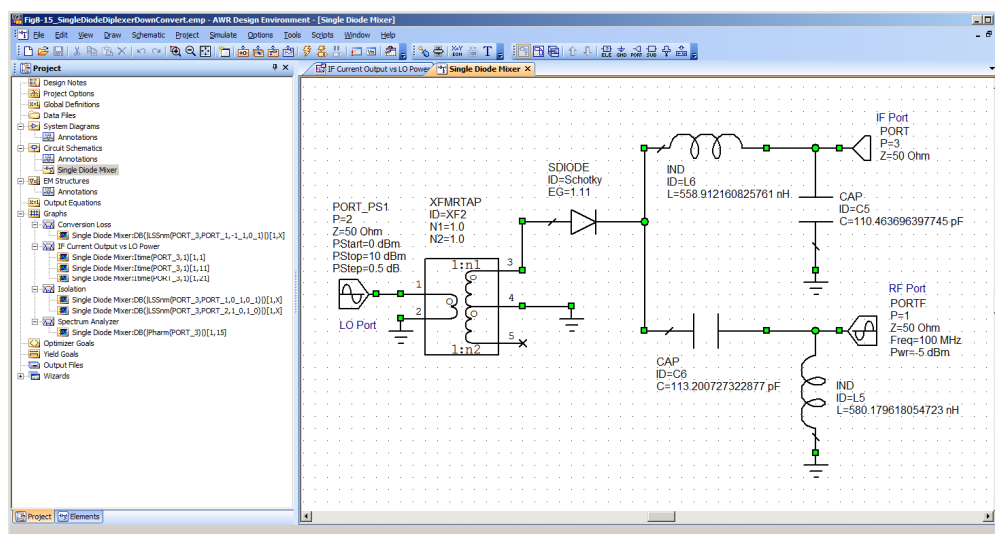


Figure 9. Typical Measurements for a mixer.

A PORTF element produces a single tone signal with frequency and power level set by the parameters for that element. For a down-conversion mixer, the PORTF element is applied to the RF port. The RF simulation will then use these frequency and power levels to determine the time waveforms at the IF port, using a Spice modelling of the diode and the circuit. Figure 9 shows the typical measurements that can be made on a mixer. The first one is the conversion loss.

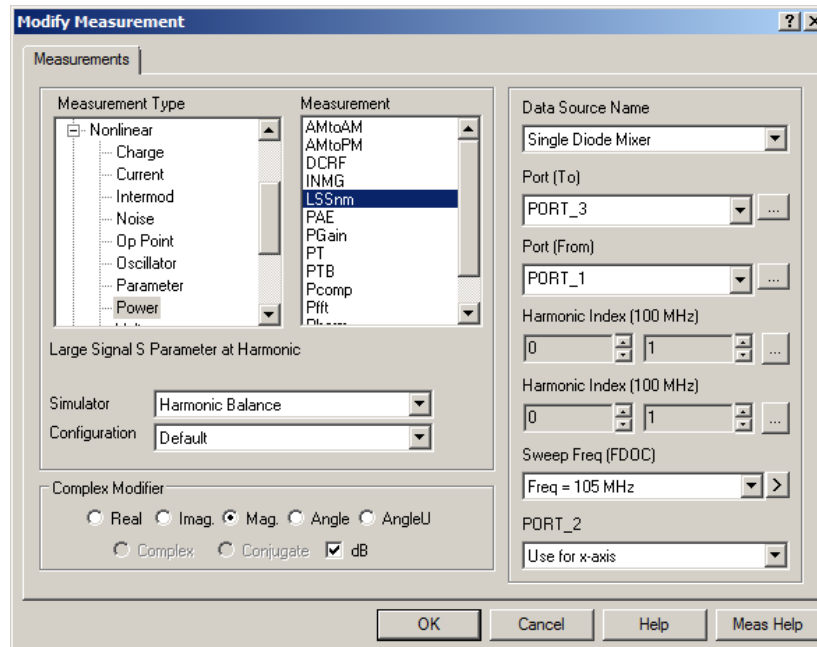


Figure 10. Parameters for conversion loss measurements.

The conversion loss of the mixer can be determined as the LO power level is varied, by setting the relevant parameters of the PORT_PS1 element to provide a power level sweep at the LO port. The sum or difference frequency that is analysed for determining the conversion loss is set by the parameters for the Large Signal S parameter (LSSnm) measurement shown in figure 10. The conversion loss is determined as the ratio of the power levels at the specified frequencies of port 1 as input and port 3 as output.

For a realistic determination of performance of the mixer, a LO frequency of 105 MHz and an RF frequency of 100 MHz with a level of -5 dBm is chosen. The project frequency is set as a single frequency at 105 MHz. If a range of frequencies are specified, then one or all of these can be used for the conversion loss. It is thus possible to determine the conversion loss for a range of LO frequencies as well. For a LO input at 105 MHz and an RF input at 100 MHz, the desired IF output is at 5 MHz. The appropriate harmonic index combinations are selected such that the input is at 100 MHz and the output is at 5 MHz, as indicated in figure 10. MWO automatically calculates the relevant frequency as the harmonic indices are changed.

Figure 11 shows the resulting conversion loss as a function of LO power level for the single diode mixer of figure 8. Note that the conversion loss decreases with an increasing LO drive level. A higher LO power level increases the power consumption of the mixer, requires a higher power LO source and dissipates more heat. By comparing figures 11 and 20, it can be seen that the conversion loss of the single diode mixer is very poor.

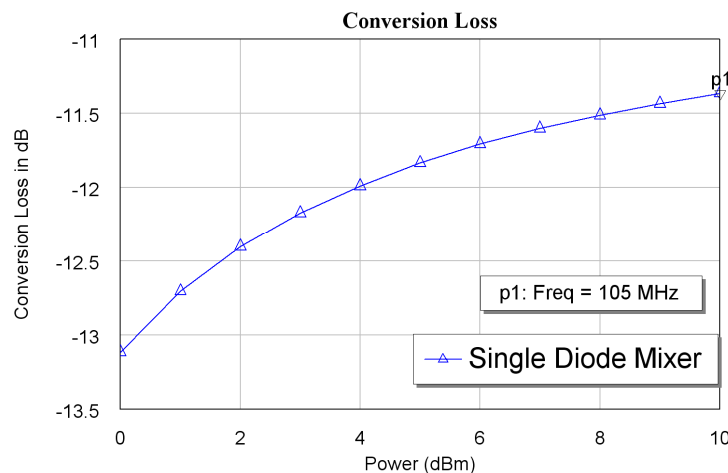


Figure 11. Conversion loss of a single diode mixer.

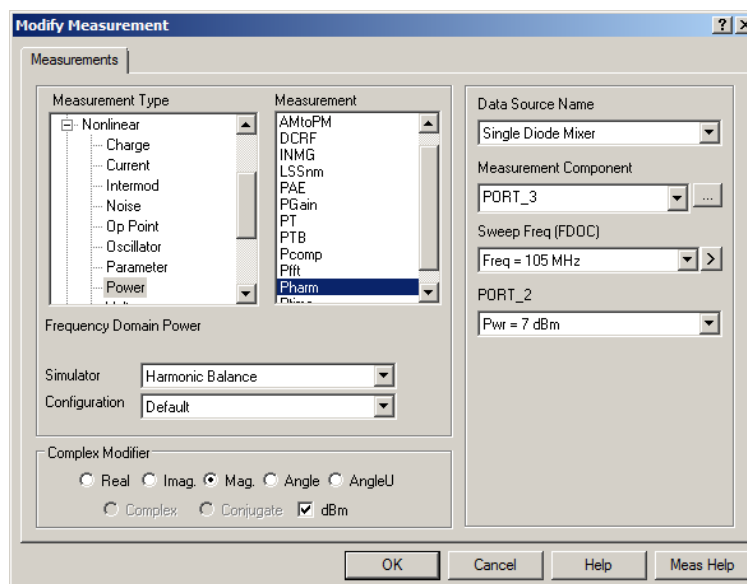


Figure 12. Frequency domain power measurement.

The IF spectrum can be determined using the Frequency Domain Power Measurement shown in figure 12. The waveform at the IF port is determined using the harmonic balance simulator. The spectral components are determined from that waveform. Figure 13 shows the resulting IF spectrum for an input power at the LO port of +6 dBm. It is possible to select other values or to plot the spectra for a sweep of power values. Comparing this with the corresponding figure 21 for the balanced mixer, and figure 29 for the double balanced mixer, it can be seen that the harmonics produced by the single diode mixer are much higher than those of balanced mixers.

The resulting IF spectrum is shown in figure 13. The desired 5 MHz component is -16.6 dBm. Since the RF signal is -5 dBm, the conversion loss is 11.6 dB. The LO signal at 105 MHz is 7 dBm and the LO signal at the IF port is -30.261 dB. The LO to IF isolation is thus 37.26 dB. The RF signal at 100 MHz signal is -5 dBm and the RF signal appearing at the IF port is -28.66 dBm. The RF to IF isolation is thus 23.661 dB. By comparing the conversion loss, the levels of the harmonics and the isolation with the corresponding figure 21 for the balanced mixer, it can be seen that the performance of a single diode mixer is significantly worse.

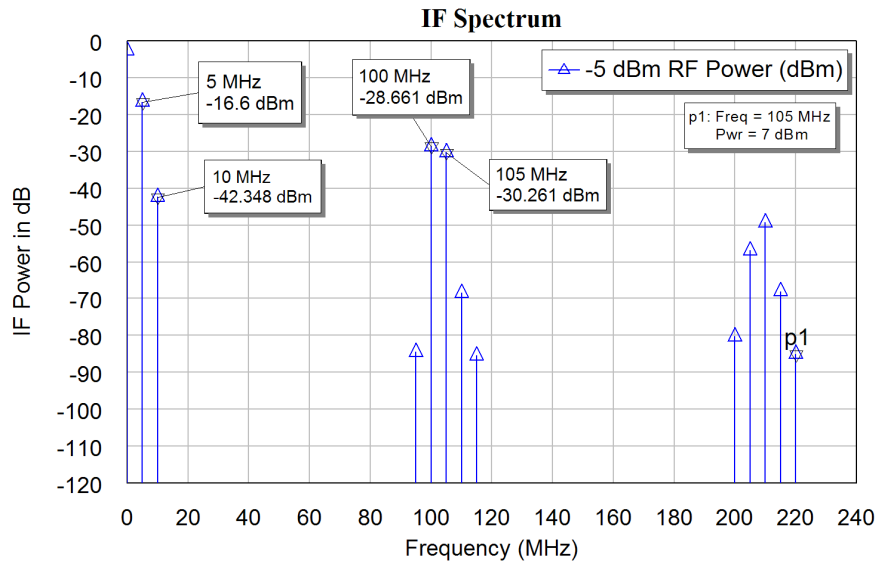


Figure 13. IF spectrum of a single diode mixer as a down-converter.

If a two-tone RF input signal is used, the single diode mixer has a high level of IM components. As a result, the single diode mixer requires more stringent RF filtering to avoid those IM signals being generated by the mixer and appearing in the IF output. The single diode mixer also requires more stringent IF filtering to remove those unwanted IF components from the IF signal, to prevent the unwanted signals from effecting the demodulated output from the receiver. Most AM radios use single diode mixers and this is one reason why their performance is poor compared to FM radios.

The voltage and current time waveforms can also be determined, using the Vtime and Itime measurements. The measurements can be done at a single LO power level or at a range of levels as is done by selecting plot all traces instead of the 0 dBm level in the Port_2 entry of the Itime measurement window shown in figure 14. Alternately, as has been done in this project, a limited power sweep can be obtained by performing multiple single level measurements as shown in figure 9.

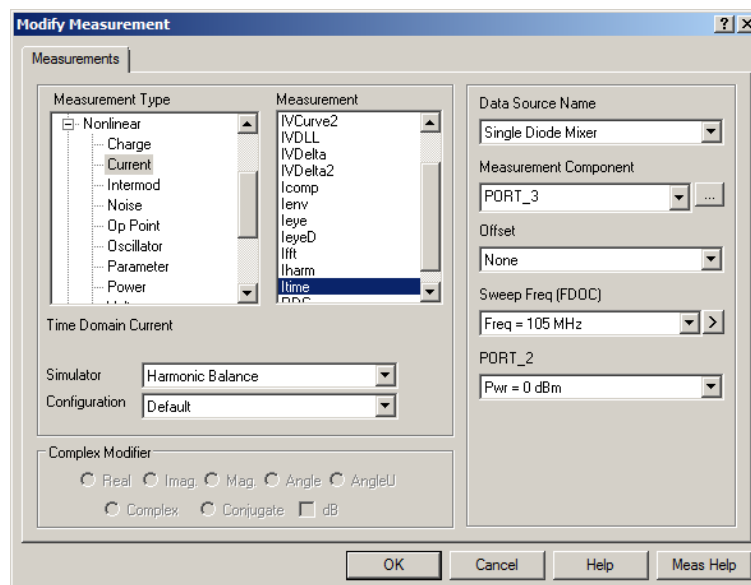


Figure 14. Itime measurement setting.

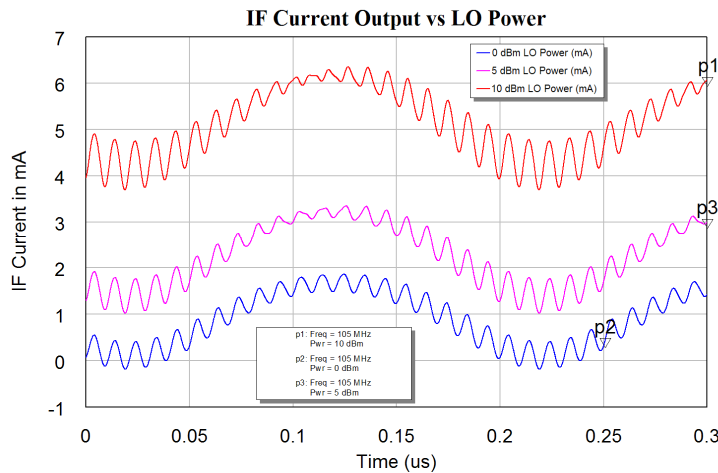


Figure 15. IF currents for a single diode mixer as a down-converter.

Figure 15 shows the resulting IF currents of a single diode mixer, notice with the 2nd order filters used in the diplexer, there is still significant RF current components present in the IF signal. A higher order filter will improve the isolation, but will not improve the performance sufficiently to justify the additional cost. For the frequencies used, the output spectra and conversion loss will be the same if higher order diplexer filters are used. As can be seen from figure 15, the single diode mixer has a significant DC current component, which changes with LO drive level.

To operate the mixer as an up-converter, the PORTF element is applied to the IF port and the signal generated by that port is set to 5 MHz and a power of -5 dBm. The mixer output is then at the RF port. The resulting circuit diagram for the single diode mixer as an up-converter is shown in figure 16. The same measurements can be performed as for the down-converter.

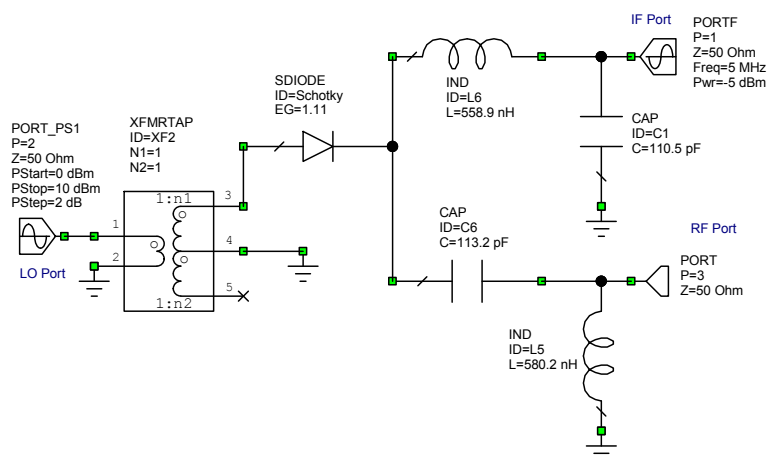


Figure 16. Circuit diagram of a single diode mixer as an up-converter.

The RF output spectrum is shown in figure 17. From this spectrum it can be seen that the conversion loss, being the amplitude of the 100 MHz RF component due to the 5 MHz IF signal is the same as for the down-converter. The components around 100 MHz show a large 105 MHz LO component in the RF output, indicating only a 8.6 dB LO-RF isolation. The LO spectral component at the RF port is larger than any of the wanted

components. The second harmonic components at 90 MHz and 110 MHz are slightly asymmetrical. There are significant components at harmonics of the LO frequency, which must be filtered out in most practical applications.

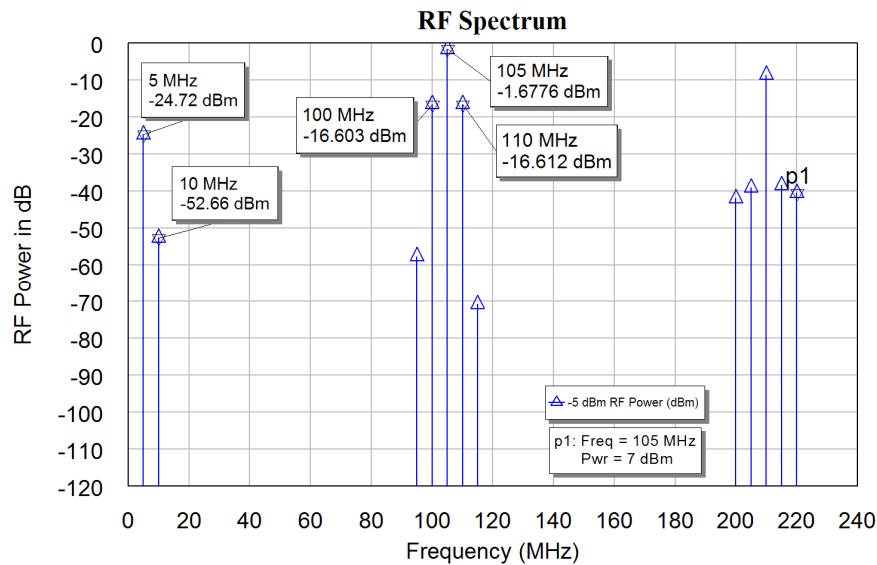


Figure 17. RF spectrum of a single diode mixer as an up-converter.

The RF current waveforms can be determined using the Itime measurement in a similar manner as for the down-converter shown in figure 15. The results for the up-converter are shown in figure 18 and are highly asymmetrical. The waveform is rich in harmonics as can be seen from the spectrum of figure 17.

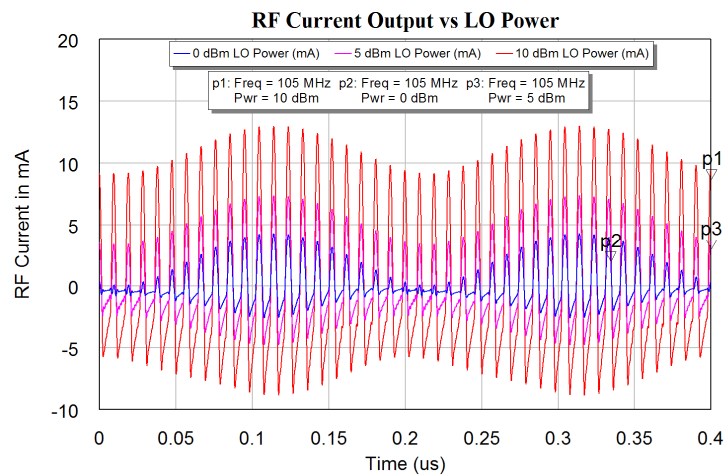


Figure 18. RF currents for a single diode mixer as an up-converter.

Advantages of single diode mixers:

1. Can be used at very high (microwave) frequencies.
2. Low cost, one diode.

Disadvantages of single diode mixers:

3. High Conversion loss.
4. High level of unwanted components.
5. No RF to LO isolation, IF to LO and IF to RF isolation only due to diplexer.

Balanced Mixer

Adding a second diode to the circuit shown in figure 19 results in a balanced mixer. The first diode has V_a+V_b across it and the second diode has V_a-V_b where voltage V_a is the LO and V_b is the RF voltage. The currents through the diodes are thus:

$$I_{D1} = a_0 + a_1(V_a + V_b) + a_2(V_a + V_b)^2 + a_3(V_a + V_b)^3 + a_4(V_a + V_b)^4 + a_5(V_a + V_b)^5 + \dots \quad \text{Eqn. 8}$$

$$I_{D2} = a_0 + a_1(V_a - V_b) + a_2(V_a - V_b)^2 - a_3(V_a - V_b)^3 + a_4(V_a - V_b)^4 + a_5(V_a - V_b)^5 + \dots \quad \text{Eqn. 9}$$

The difference between the diode currents flows into the IF port and RF port, so that the current flowing through the IF and RF port is:

$$I_{IF-RF} = I_{D1} - I_{D2} = +2a_1V_b + 4a_2V_aV_b + 6a_3V_a^2V_b + 2V_b^3 + 8a_4(V_a^3V_b + V_aV_b^3) + 10a_5V_a^4V_b + 20a_5V_a^2V_b^3 + 2a_5V_b^5 + \dots \quad \text{Eqn. 10}$$

For a single diode mixer the current through the IF and RF port is the same as is shown in equation 8. Comparing equation 10 with equation 8, it can be seen that most of the unwanted components cancel. The only components that are in the IF band are:

$$I_{IF} = 4a_2V_aV_b + 8a_4(V_a^3V_b + V_aV_b^3) + \dots \quad \text{Eqn. 11}$$

Which is close to ideal multiplication as the a_4 term is normally very small.

Since the LO voltage, $V_a \gg$ the RF voltage, V_b , the V_aV_b and the $V_a^3V_b$ terms dominate. The V_b and the $V_a^2V_b$ terms do not produce any frequency components in the region of interest. For an ideal mixer one wants the a, c, d and e components to be as small as possible, the manufacturers of mixers ensure their diodes satisfy this as much as possible. The balanced mixer will thus have a much better performance than the single diode mixer.

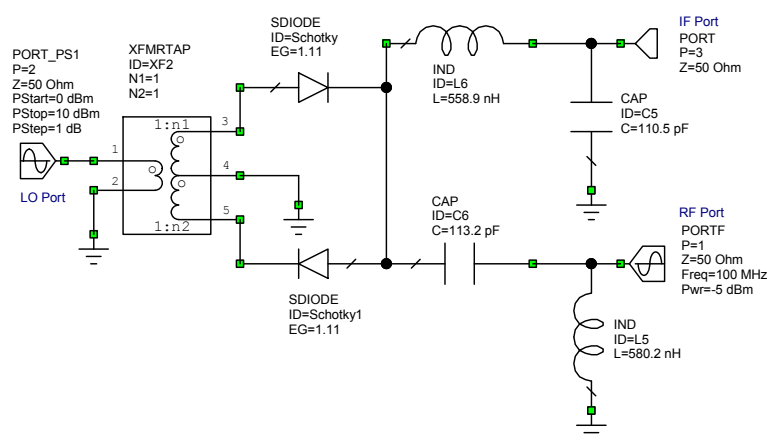


Figure 19. Circuit diagram of a balanced mixer.

The circuit diagram of the balanced mixer is shown in figure 19. The only difference between that and the circuit for the single diode mixer of figure 8 is the use of the second diode, but having the second diode results in a significant performance improvement.

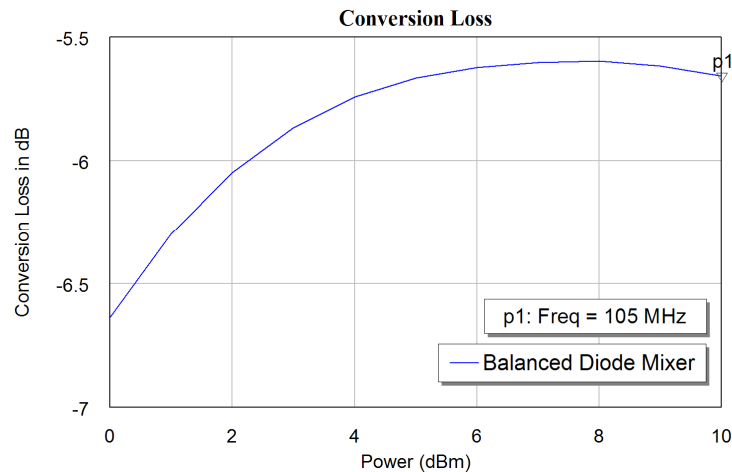


Figure 20. Conversion loss of a balanced diode mixer.

The conversion loss of the mixer is shown in figure 20. The conversion loss is far less than that of a single diode mixer. For LO levels of around 7 dBm, any variation in LO power does not cause any change in conversion loss, so that the mixer is then very insensitive to AM noise of the LO. This is an important advantage of the balanced mixer over the single diode mixer.

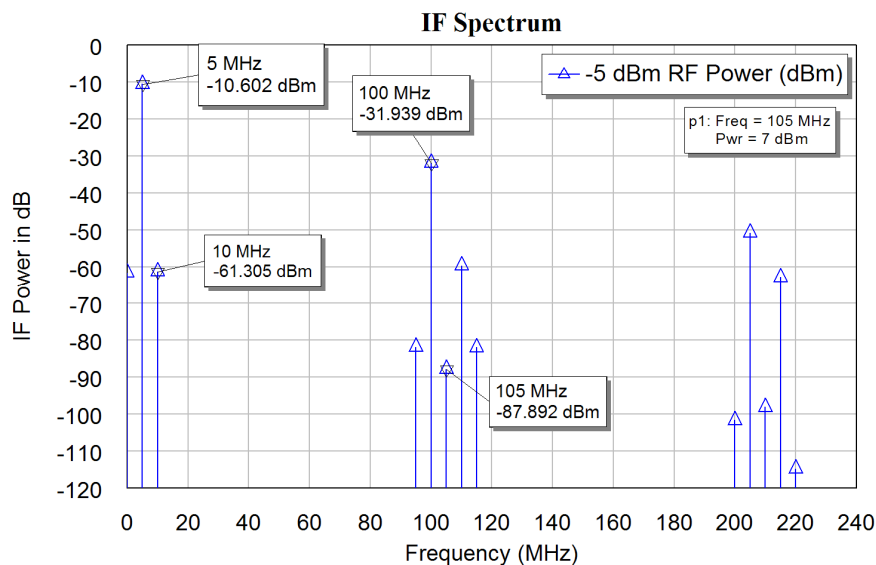


Figure 21. IF spectrum of a balanced diode mixer as a down-converter.

Figure 21 shows the IF spectrum of the balanced mixer. As expected from the equation 10, many of the unwanted spectral components have significantly reduced amplitudes compared with the single diode mixer. The second harmonic of the desired IF signal, at 10 MHz and caused by the mixing process, is more than 40 dB below the desired 5 MHz signal. The LO signal appearing in the IF spectrum is -87.9 dBm, since the LO signal is 7 dBm, the LO to IF isolation is 94.9 dB.

The RF signal appearing at the IF port is -31.939 dBm. Since the RF signal is -5 dBm, The RF to IF is isolation is 26.9 dB. This can only be improved by using a higher order diplexer as part of the mixer, or by using another mixer configuration like the double balanced mixer.

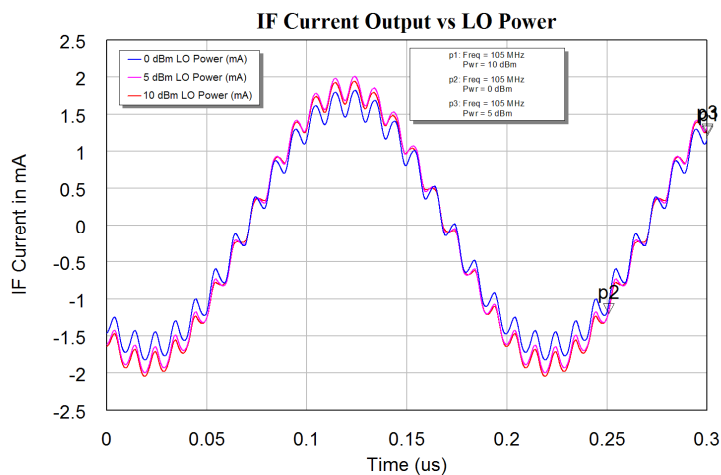


Figure 22. IF currents for a balanced diode mixer as a down-converter.

Figure 22 shows the IF currents for the balanced mixer and it can be seen that the waveforms are much more like a pure sine wave than the corresponding waveforms for the single diode mixer. With the second order filters used in the diplexer, there are still some RF signals present at the IF output but they are small enough not to cause any problems. As expected from equation 10, the balanced diodes mixer has is no DC component produced at the IF port, in contrast to the single diode mixer.

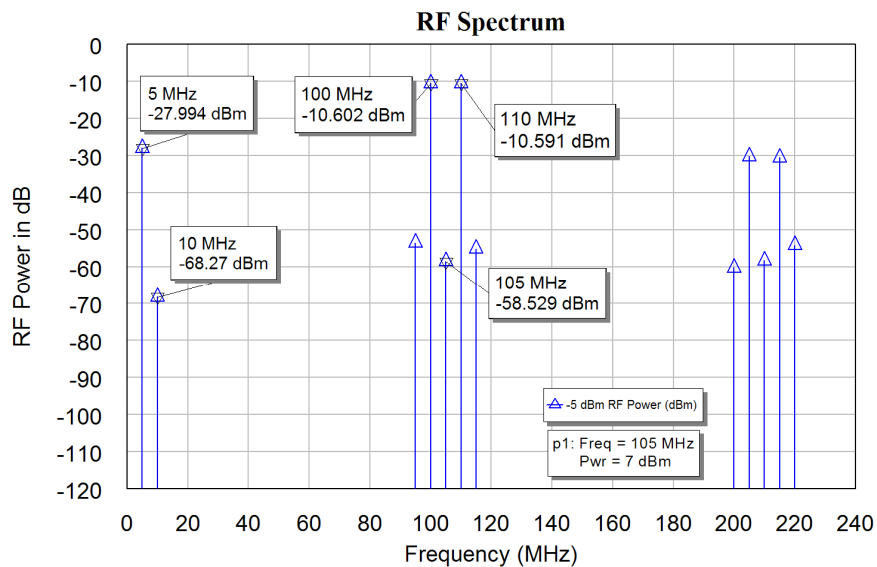


Figure 23. RF spectrum of a balanced diode mixer as an up-converter.

Figure 23 shows the performance of the balanced mixer as an up-converter. It can be seen that a near ideal mixer performance is obtained, with all the unwanted components more than 40 dB below the wanted components. This is good enough for practical applications. The 3IM components increase 3 dB for every 1 dB increase in the RF and IF levels. The RF level can thus be varied to obtain the specified 3IM performance, thereby maximising IF signal and the dynamic range. The LO feedthrough at the RF port can be minimised by adding a very small DC signal to the IF port and adjusting that DC signal to cancel the LO signal at the RF port. This cancellation is temperature dependent, since the diode characteristics change slightly with temperature.

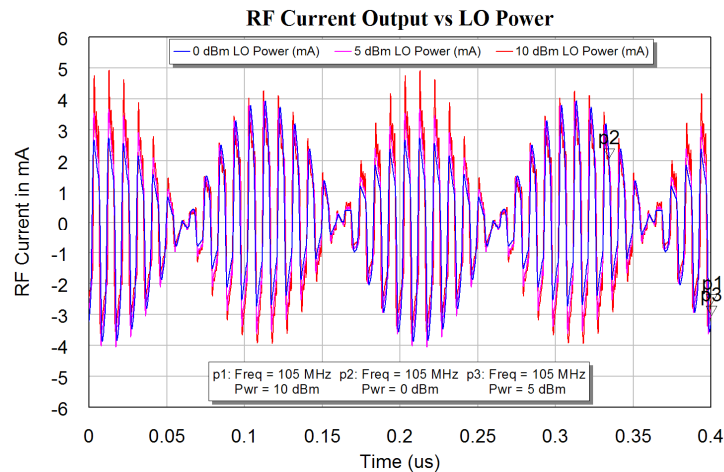


Figure 24. RF currents for a balanced diode mixer as an up-converter.

Figure 24 shows the RF currents for the balanced mixer, note that the waveforms closely resemble the ideal double balanced waveforms obtained from:

The results from the simulation closely agree with those obtained in practice.

There are however still some IF components present, which are due to the limited RF-IF isolation caused by the diplexer. The Double Balanced mixer overcomes those limitations.

Double Balanced Mixer

Mini-Circuits ... we're redefining what VALUE is all about!

RF/IF & Microwave Components [View Shopping Cart](#) [Home](#)

SITE MAP | [About Us](#) | [Application Notes](#) | [Designer Kits](#) | [Tape & Reel](#) | [S-Parameters](#) | [Contact Us](#)

Mixers, Frequency Model SEARCH

Frequency Mixers • Plug-In & Flatpack • Level 7 • 500 Hz to 4.3 GHz

Model Number	Frequency Range (MHz)		Conversion Loss (dB)			LO-RF Isolation (dB)	LO-IF Isolation (dB)	Case Style / Outline Drawing	Price(\$) 1-9 Buy 10!		
	LO/RF	IF	Typ.	σ	Max.	Typ.	Typ.				
(+) Symbol indicates this Model is available as RoHS Compliant/Pb Free .											
<< SORT >>	<<	<<	<<	<<	<<	<<	<<	<<	<<		
ASK-1-KK81 (+)	1	600	DC	600	5.58	0.06	8.5	35	30	KK81	5.95
ASK-1 (+)	1	600	DC	600	5.58	0.06	8.5	35	30	W38	6.95
ASK-1-X65 (+)	1	600	DC	600	5.58	0.06	8.5	35	30	X65	6.95
SAM-1 (+)	1	600	DC	600	5.67	0.05	8.5	45	40	A03	21.20
SBL-1 (+)	1	500	DC	500	5.60	0.09	8.0	45	40	A06	8.0
SBL-1X (+)	10	1000	5	500	5.88	0.10	8.0	40	40	A06	9.70
SBL-1-1 (+)	0.1	400	DC	400	4.84	0.04	8.0	45	40	A06	10.70
SBL-3 (+)	0.025	200	DC	200	4.81	0.05	8.5	45	40	A06	10.70
SBL-11 (+)	5	2000	10	600	7.08	0.11	9.0	35	30	A06	24.20
SRA-1 (+)	0.5	500	DC	500	5.11	0.09	8.5	45	40	A01	16.70
SRA-1W (+)	1	750	DC	750	5.80	0.04	8.5	45	40	A01	20.20
SRA-1-1 (+)	0.1	500	DC	500	4.81	0.11	8.5	45	40	A01	18.20
SRA-2 (+)	1	1000	0.5	500	5.66	0.07	8.5	35	30	A01	20.20
SRA-2CM (+)	5	1000	DC	1000	5.27	0.04	8.5	35	30	A01	18.20
SRA-3 (+)	0.025	200	DC	200	4.61	0.06	8.5	45	40	A01	20.20
SRA-5 (+)	5	1500	10	600	6.69	0.07	8.5	35	30	A06	29.20
SRA-6 (+)	0.003	100	DC	100	4.58	0.05	8.5	45	40	A01	29.20
SRA-8 (+)	0.0005	10	DC	10	5.69	0.11	8.5	50	50	A01	34.20

Model Number	LO Level (dBm)	RF in @ 1dBm Comp. Typ. (dBm)	Frequency Range (MHz)		Conversion Loss (dB)			LO-RF Isolation (dB)		LO-IF Isolation (dB)		IP3@ center band Typ. (dBm)	Case Style/ Outline Drawing	PCB Layout PL	Price(\$) 10-24 Buy It!
			LO/RF	IF	Typ.	σ	Max.	Typ.	Typ.						
(+) Symbol indicates this Model is available as RoHS Compliant/Pb Free .															
<< SORT >>	<<	<<	<<	<<	<<	<<	<<	<<	<<	<<	<<	<<	<<	<<	<<
ADE-1 (+)	7.0	1.0	0.5	500	DC	500	5.0	0.10	7.8	55	40	15	CD636	052	1.99
ADE-1ASK (+)	7.0	1.0	2.0	600	DC	600	5.3	0.10	7.5	50	45	16	CD542	052	3.95
ADE-2ASK (+)	7.0	1.0	1.0	1000	DC	1000	5.4	0.10	9.5	45	32	12	ED542	052	4.25
ADE-2 (+)	7.0	1.0	5.0	1000	DC	1000	6.67	0.26	9.5	47	45	20	ED542	052	1.99
ADE-3G (+)	7.0	1.0	2300	2700	DC	400	5.6	0.10	7.0	36	26	13	ED542	052	3.45
ADE-3GL (+)	7.0	1.0	2100	2600	DC	600	6.0	0.25	8.8	34	20	17	ED541	051	4.95
ADE-4 (+)	7.0	1.0	200	1000	DC	800	6.8	0.10	8.5	53	40	15	ED542	052	4.25
ADE-5 (+)	7.0	1.2	5.0	1500	DC	1000	6.6	0.10	9.3	40	30	15	ED542	052	3.45
ADE-6 (+)	7.0	1.0	0.05	250	DC	200	4.6	0.05	8.4	40	45	10	CD637	052	4.95
ADE-11X (+)	7.0	1.0	10	2000	5	1000	7.1	0.10	9.8	36	37	9	ED542	052	1.99
ADE-12 (+)	7.0	1.0	50	1000	DC	1000	7.0	0.15	9.0	33	37	17	ED541	051	2.95
ADE-13 (+)	7.0	1.0	50	1600	50	1000	8.1	0.10	9.8	40	35	11	ED541	051	3.10
ADE-14 (+)	7.0	1.0	800	1000	DC	200	7.4	0.20	8.9	32	34	17	ED541	051	3.25
ADE-18W (+)	7.0	1.0	1750	3500	DC	700	5.4	0.30	8.9	33	12	11	ED542	051	3.95
ADE-20 (+)	7.0	1.0	1500	2000	DC	300	5.4	0.10	7.8	31	28	14	ED542	051	4.95
ADE-30 (+)	7.0	1.0	200	3000	DC	1000	4.5	0.20	9.8	35	20	14	ED542	052	6.95
ADE-30W (+)	7.0	1.0	300	4000	DC	950	6.8	0.20	9.8	35	16	12	ED542	052	8.95
ADE-35 (+)	7.0	1.0	1600	3500	DC	1500	6.3	0.50	9.8	25	22	11	ED542	051	4.95

Figure 25. Minicircuit mixer catalogue.

Double balanced mixers, together with the active mixers are the dominant mixers used in non-consumer oriented transmitters and receivers. There are several companies making double balanced mixers, Minicircuits is one of the largest of these. A part of a web page of their mixer catalogue is shown in figure 25. There are many different packages available and as can be seen from Figure 25 surface mount packages are a lot cheaper and thus more popular. It is interesting to see the change in price for the SRA-1. For many years this was \$1.95 (US). In recent years the price has risen significantly, reflecting cost increases for that style of packaging, while the cost of surface mount packages is decreasing.

The circuit diagram of a Double Balanced Mixer is shown in figure 26. The two transformers provide isolation for all ports. Four diodes are now required.

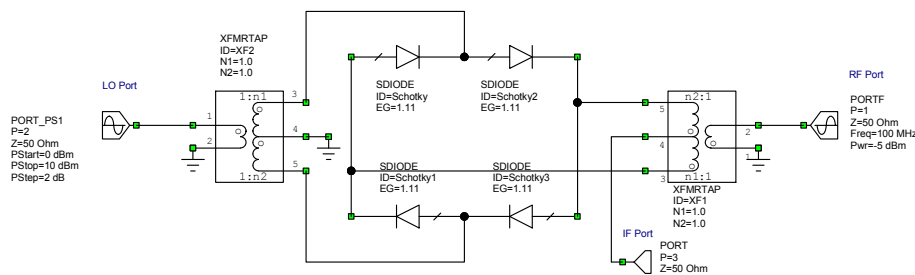


Figure 26. Circuit diagram of a double balanced mixer.

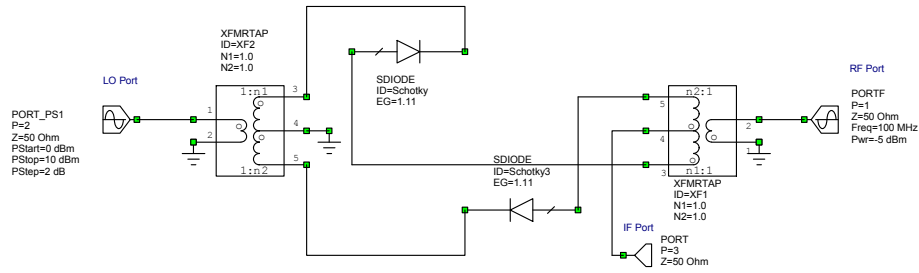


Figure 27a Mixer with +ve voltage applied at the IF port.

For the analysis of the mixer consists of considering what happens if a +ve input signal is applied to the IF port. Under those conditions the diodes shown in figure 27a conduct and the others are an open circuit. As a result a positive signal applied to the LO port, then a positive signal is obtained at the RF port.

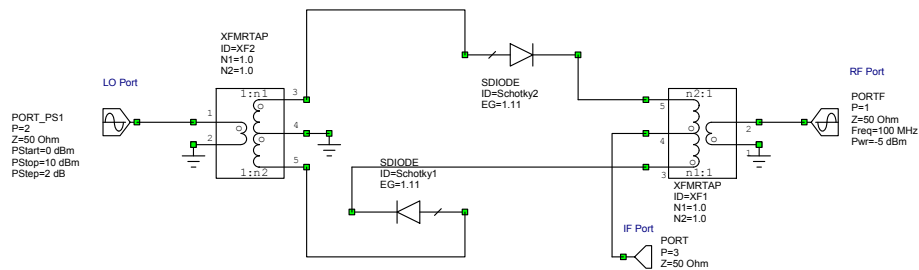


Figure 27 b. Mixer with -ve voltage applied at the IF port.

If a -ve input signal is applied to the IF port, the diodes shown in figure 27b conduct and the others are an open circuit. As a result if a positive signal is applied to the LO port, then a positive signal is obtained at the RF port. If a zero voltage signal is applied at the IF port all the diodes are equal resistances and the LO signal is cancelled at the RF port. In practice having a smaller IF voltage results in a smaller RF voltage. The RF signal is thus the LO signal multiplied by the IF signal, resulting in a proper mixing action.

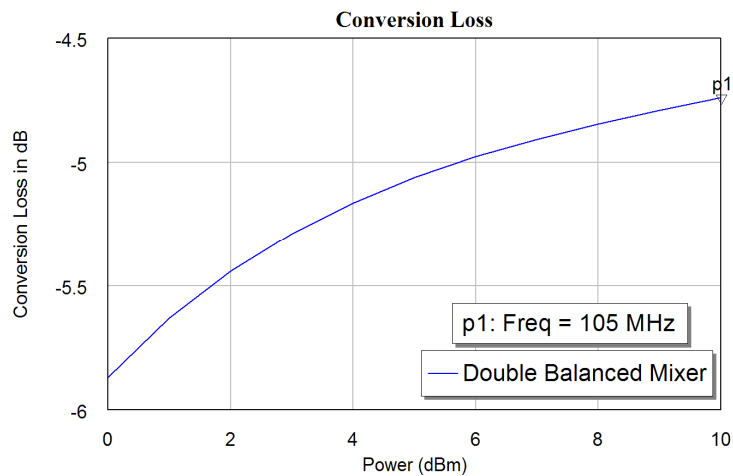


Figure 28. Conversion loss of a double balanced diode mixer.

Figure 28 shows that the conversion loss of a Double Balanced Mixer is approximately 0.5 dB less than that of a balanced mixer and more than 6 dB less than that of a single diode mixer. Comparing the IF spectrum of a down-converting Double Balanced Mixer as shown in figure 29 this with the corresponding figures 13 and 21 for single and balanced diode mixers, it can be seen that there are no spectral components in the 80 to 120 MHz frequency range. The difference signal at 5 MHz and the sum signal at 205 MHz are the same amplitude. The signal at 215 MHz is due to the third harmonic of the input signal mixing with the local oscillator. In a receiver, these harmonic signals must be evaluated, to ensure that they do not cause signals in the IF frequency band.

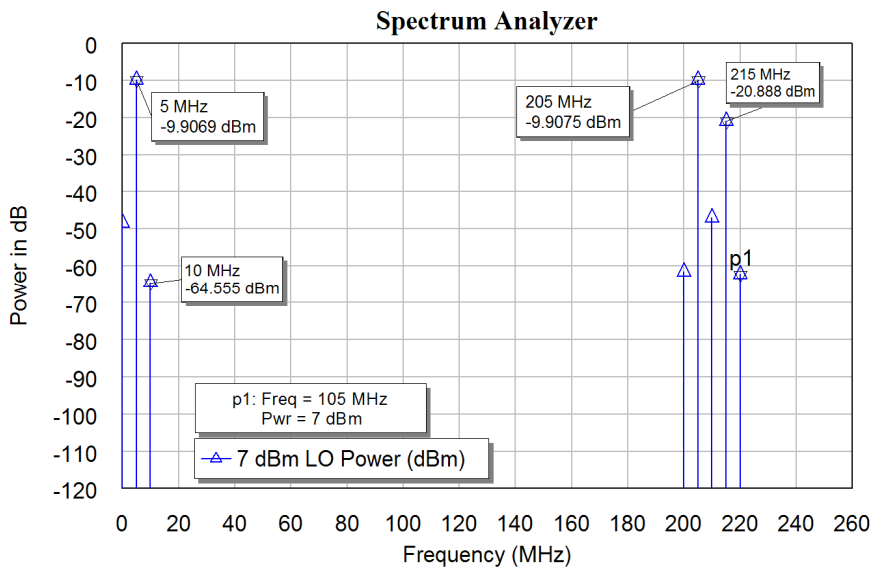


Figure 29. IF spectrum of a double balanced diode mixer as a down-converter.

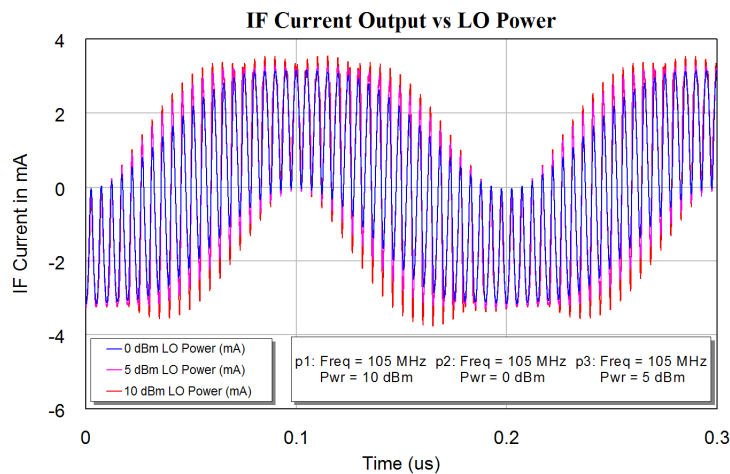


Figure 30. IF currents for a balanced diode mixer as a down-converter.

Figure 30 shows the IF currents. There is a significant high frequency content. Figure 31 shows the same IF currents with the IF signal passed through a 25 MHz low pass filter to remove the high frequency components. The waveform looks like an ideal Sine wave and there is little change in the output as the LO power is changes between 0 dBm and 10 dBm. The LO AM noise will thus have little effect on the IF output.

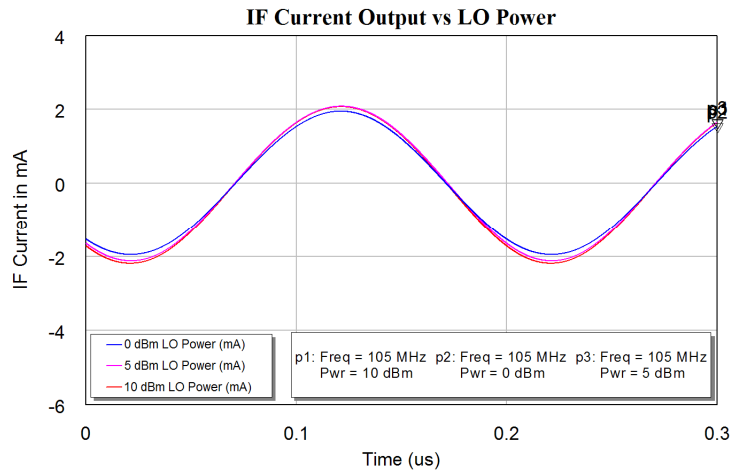


Figure 31. IF currents of figure 29 with frequency components >25 MHz removed.

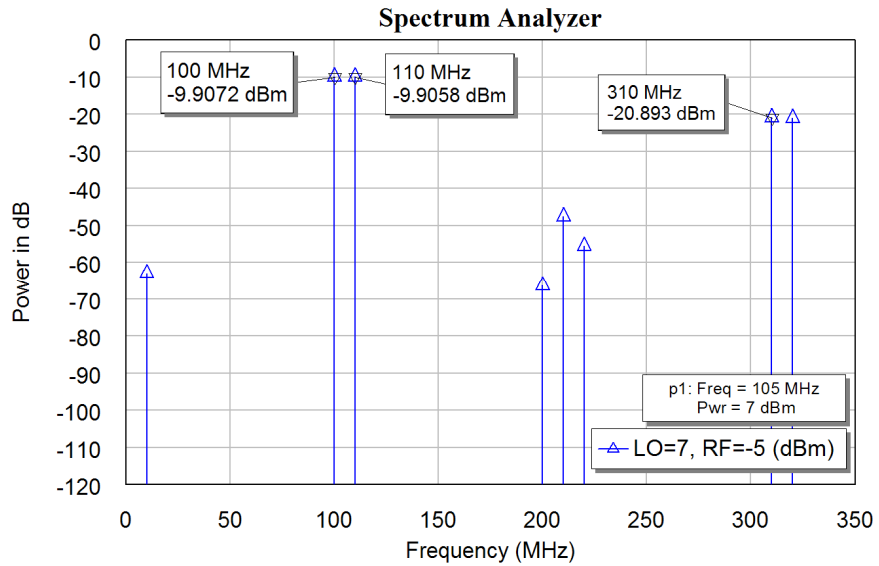


Figure 32. RF spectrum of a double balanced diode mixer as an up-converter.

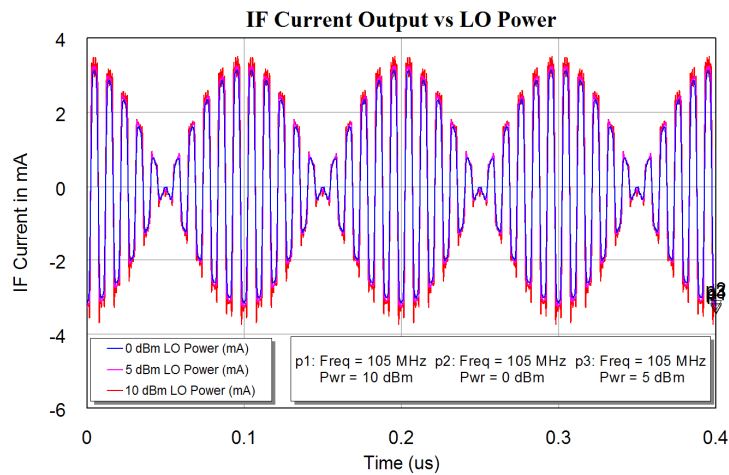


Figure 33. RF currents for a double Balanced Diode Mixer as an up-converter.

Figure 32 shows the RF spectrum of a double balanced mixer as an up-converter. The desired spectrum around the 105 MHz LO is ideal, with no unwanted spectral components. Figure 33 shows the corresponding RF currents. The spectrum and the waveform is very similar to that for an ideal multiplier. Double balanced mixers can be used as analogue multipliers in applications like a phase detector or a true RMS power meter.

Figure 34 shows the construction of a simple home made double balanced mixer, the transformers are held in-place with Silastic (Silicone Sealant). The diodes are conventional Schottky-Barrier diodes that have been matched for their V-I characteristic in order to obtain the best LO \Rightarrow RF isolation.

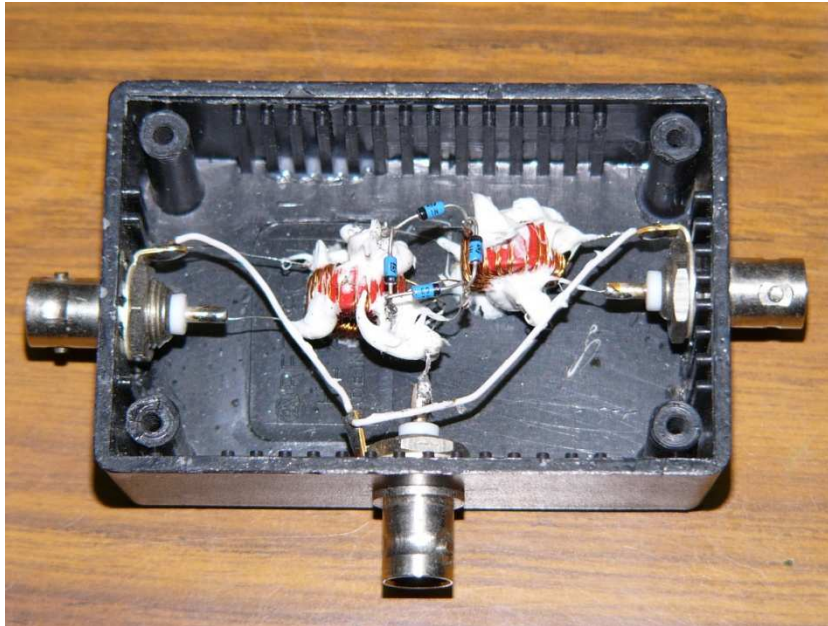


Figure 34. Construction of a Double Balanced Mixer for use in Practical Sessions.

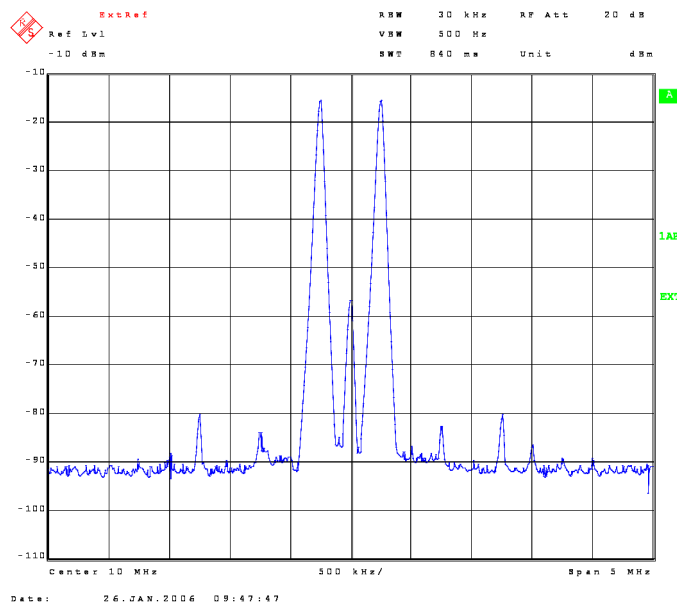


Figure 35. Measured performance of the mixer of figure 34.

The measured performance of the mixer is shown in Figure 35. The transformers for this mixer were designed for operation at 1 MHz, as a result an IF frequency of 250 kHz and an LO of 10 MHz was used for the spectrum in figure 35. For the measurement of figure 35, the LO signal was at a frequency of 10 MHz and a level of +7 dBm. The IF signal was at a frequency of 300 Hz and a level of -10 dBm. The measured conversion loss is 6 dB and the LO \Rightarrow RF isolation is -60 dB. This mixer performs well for RF and LO signals in the range of 30 kHz to 30 MHz and IF signals up to 30 MHz.

Comparing the spectrum around the LO in figure 35 with the corresponding spectrum around the LO in figure 32, shows that in practice there will be some LO \Rightarrow RF carrier feed-through due to a slight mismatch of the diodes. Figure 35 shows that the 5IM distortion components, 1.250 MHz from the LO frequency at the centre of the plot, are bigger than the 3IM components, 750 kHz from the LO frequency.

Microwave Mixers

At microwave frequencies (>1 GHz) transformers become difficult to make. In addition the capacitance associated with the diodes used in the mixer cause the diodes to become less efficient as a mixer. As a result, mixers at microwave frequencies have higher conversion losses than mixers used at lower frequencies. Conversion losses of 6 to 10 dB are typical. Transformer based mixers are available for frequencies up to 12 GHz.

At microwave frequencies, transmission lines are often used to produce the two outputs with a 180° phase shift, to provide a replacement for the transformer in the balanced mixer shown the figure 19. The circuit for the corresponding microwave mixer is shown in figure 36. In this design, the mixer is used for a down-converter for a weather satellite receiver and uses a 1565 MHz Local Oscillator to shift a 1700 MHz RF signal to a 135 MHz IF frequency.

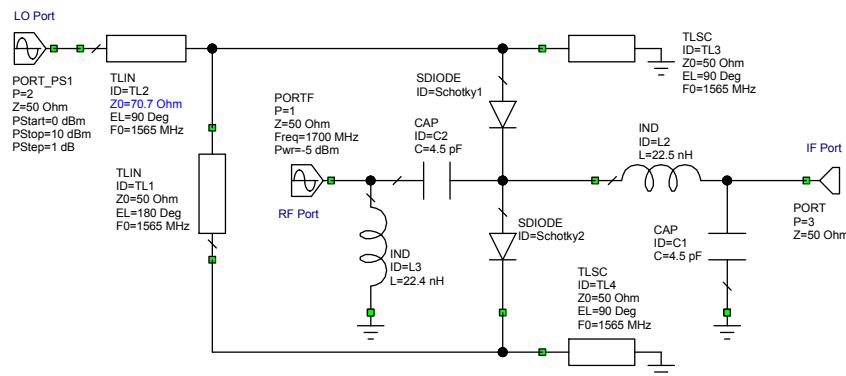


Figure 36. Circuit diagram of a Microwave Balanced mixer.

The conversion loss for this mixer is shown in figure 37, and is 0.3 dB less than the conversion loss for corresponding transformer based mixer, shown in figure 20. Figure 38 shows the spectrum for the mixer as a down converter. The mixer performs well and the spectrum is similar to that of the transformer based mixer in figure 21.

Changing the transformer to a transmission line will thus not change the performance of the mixer very much apart from a reduction of the bandwidth, since the transmission line only produces a 180° phase shift at a single frequency. However in many

microwave applications the resulting bandwidth is sufficient. The mixer can also be used as an up-converter.

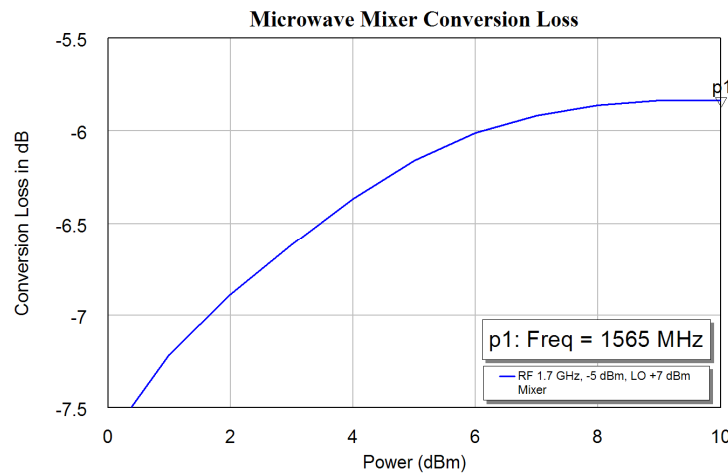


Figure 37. Conversion loss of a Microwave Balanced Diode mixer.

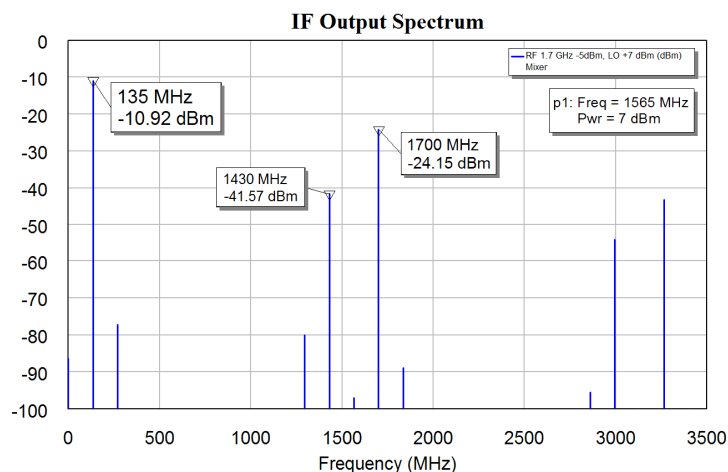


Figure 38. IF Spectrum of a Microwave Balanced Diode mixer as a down-converter.

A transmission line, used to produce the 180° phase shift in figure 36 produces a linear phase shift with frequency. As shown in the lecture notes on Branchline couplers, the Branchline coupler has a nearly constant 90° phase shift over a 10% bandwidth.

The Branchline coupler can be used to produce the required phase shifts for efficient mixing. If the LO signal is applied at port 1 of the Branchline coupler in figure 40 and the RF signal is applied to port 2. The frequency of the Branchline coupler is chosen such that full isolation is obtained at the RF port for the LO signal, since the LO signal is much bigger in power than the RF signal. For a practical down-converting mixer, the LO and RF signals are within 10% of each other, so that reasonable isolation will be obtained for the RF signal at the LO port. The signal at Port 3 will then be $LO \angle 90^\circ + RF \angle 180^\circ$ and the signal at Port 4 will be $LO \angle 180^\circ + RF \angle 90^\circ$. The phase angle between the LO and RF signals is $+\angle 90^\circ$ at Port 3 and $-\angle 90^\circ$ at Port 4. These are the correct conditions for obtaining balanced mixing in a down-converter.

Figure 41 shows the layout of the PCB layout corresponding to the circuit diagram of figure 39 and 40. The vertical transmission lines of the Branchline coupler are folded using bends, to reduce the size of the PCB. The green pads are the locations for the diodes and the capacitor. The short circuited quarter wave stubs are thin, corresponding to a high characteristic impedance to ensure as high an impedance over as wide a bandwidth around the LO and RF frequencies. The open circuited quarter wavelength stubs are wide transmission lines, providing a low shunt impedance for as wide a bandwidth as possible corresponding to as wide a bandwidth around the LO and RF frequencies, so that as much of the RF energy is converted to IF signals as possible. The distance between the capacitor and each of the diodes is half a wavelength at the LO frequency, to ensure that the low impedance of the capacitor reflects as a low impedance at the diodes. The length of the transmission line between the diodes is a half wavelength at the LO frequency to ensure each open-circuited stubs reflect as a short circuit at both diodes, thus enhancing the efficiency of the frequency conversion.

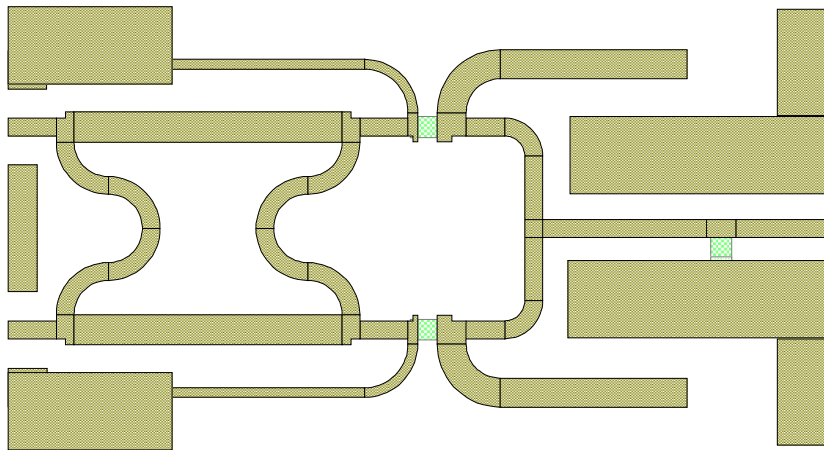


Figure 41. Branchline mixer layout.

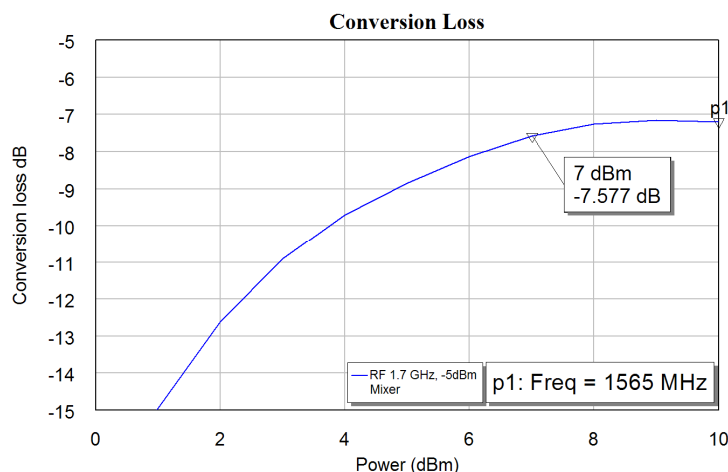


Figure 42. Conversion loss of a balanced mixer with a Branchline coupler.

Figure 42 shows the conversion loss of the microwave mixer of figure 41. The conversion loss is 1.5 dB worse than that of the ideal microwave mixer of figure 36.

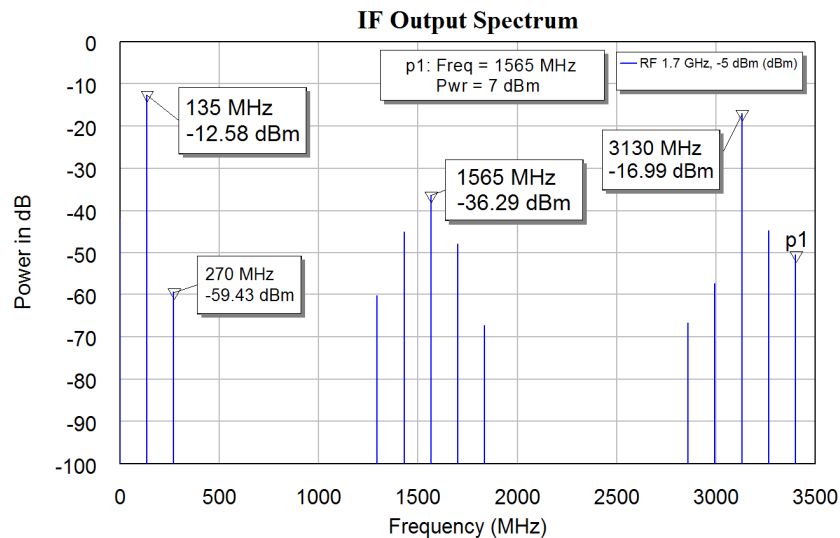


Figure 43. IF spectrum of a balanced mixer with a Branchline coupler.

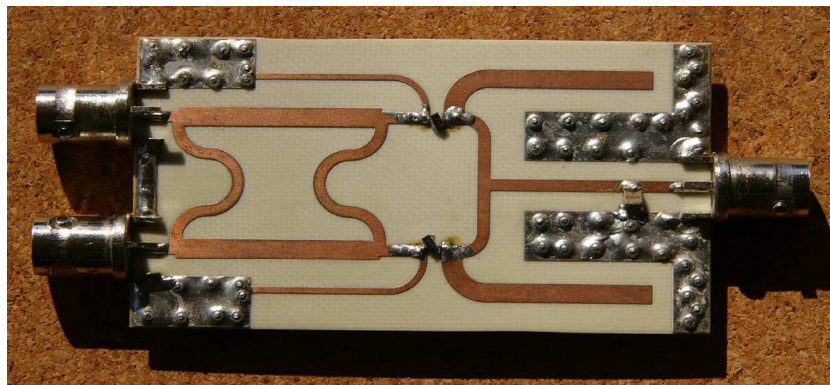


Figure 44. Hardware realisation of the balanced mixer using a Branchline coupler.

The conversion loss includes approximately 0.5 dB losses in the PCB tracks. Figure 43 shows the IF spectrum of the mixer and it can be seen that the mixer performs well. The components above 1 GHz can easily be filtered out using a simple low pass filter at the IF output. Figure 43 shows the hardware for the PCB layout of figure 42.

Figure 45 shows the measured performance of the hardware of figure 44. The IF spectrum closely resembles the results obtained from simulation and shown in figure 43. The measured conversion loss for a LO level of 5 dBm at 1.565 GHz and an RF signal of -5 dBm at 1.7 GHz was 7.25 dB, being within 0.4 dB of the performance shown in figure 35. The second harmonic distortion at 270 MHz, at -55 dBm, is 5 dB larger than in the computer simulation. The LO feedthrough is 10 dB larger, but two microwave diodes were selected for the mixer, without being matched. A third harmonic distortion is not present in figure 43, but it is present in figure 45. The signal components in the region 88 to 108 MHz at -80 dBm are the local FM transmitters, located less than 5 km from JCU.

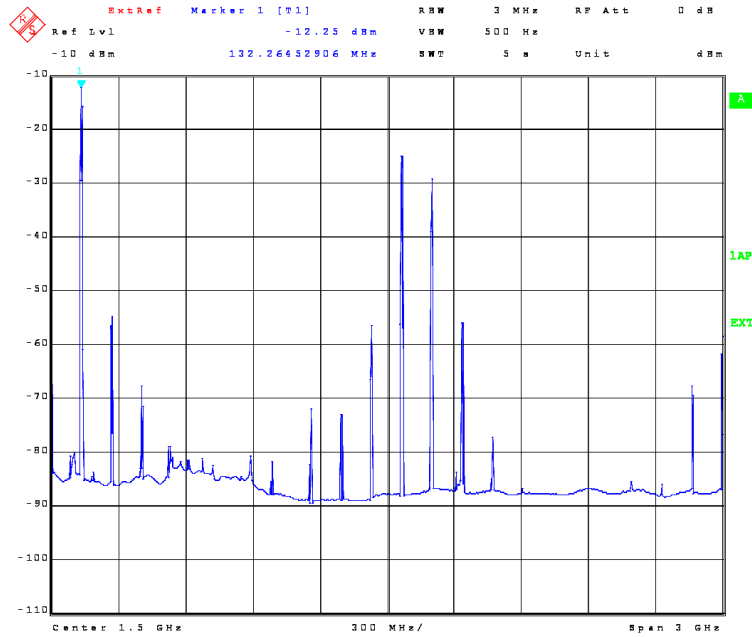


Figure 45, Measured spectrum of Branchline coupler mixer of figure 44.

Active Single transistor mixer

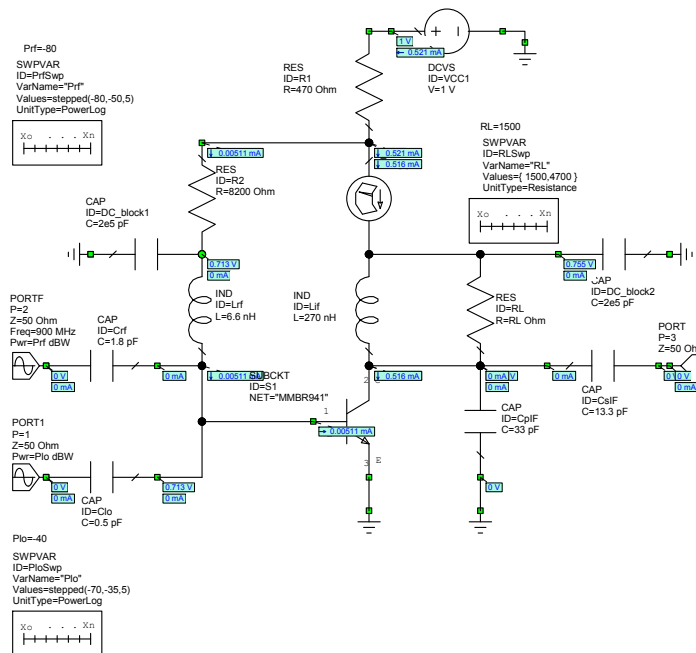


Figure 46. Active single diode mixer (AWR example, Low_Power_Mixer).

Figure 46 shows the *Low_Power_Mixer* active single diode mixer from the Microwave office mixer examples. An active single transistor mixer has a similar spectral performance to a passive single diode mixer, but has a conversion gain. The mixer of figure 46 has a conversion gain of more than 10 dB. Active single transistor mixers are used in many consumer devices like radio and TV.

Gilbert Cell Active Mixer:

It is possible to use two transistors in a push-push amplifier configuration and thus produce an active balanced mixer. However, the Gilbert Cell or long tail multiplier is much more commonly used as an active mixer, as it provides close to ideal multiplier performance. The Gilbert cell mixer is used in many IC's. There is a *Gilbert-Cell* mixer in the examples provided by MWO. That Gilbert cell example has been simplified to illustrate it's principle of operation as shown in figure 45. Gilbert Cell mixers with very good IM performances and a frequency range from DC to 5 GHz are available.

Figure 47 shows the basic circuit diagram of a Gilbert Cell mixer. Normally all these components would be included in an IC. Figure 48 shows the corresponding conversion gain. The LO and RF frequencies are chosen to be the same as that for the microwave mixer of figure 36 and 39. The circuit consists of 3 parts, the left part consisting of transistors TR1 to TR7 is the Gilbert Cell multiplier. Transistor TR1 is a constant current source for the long tail pair amplifiers making up the Gilbert Cell. The resistor chain R1 to R4 is a biasing chain, providing the biasing voltages. Transistors TR8 to TR11 form the output buffer amplifier, with transistors TR9 and TR11 being constant current sources and TR8 and TR10 being voltage followers.

A fully differential output circuit is required to obtain the best LO isolation, without having to tune the RL13 and RL24 for best LO \Rightarrow IF isolation. The differential IF output also minimises the IF harmonic output at 270 MHz.

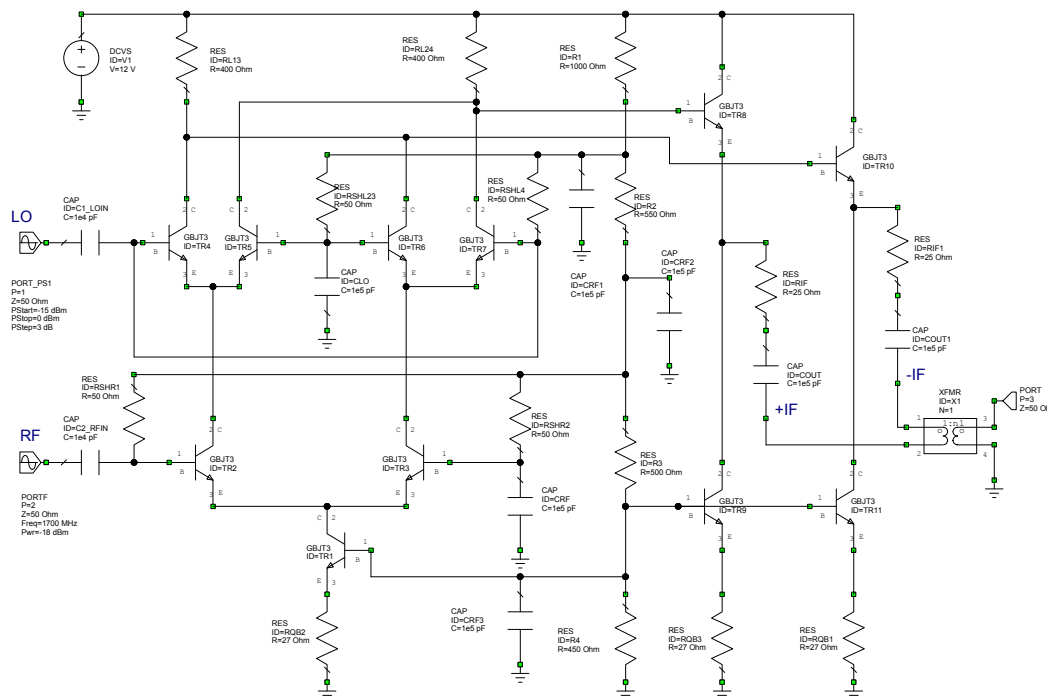


Figure 47. Basic Gilbert Cell active multiplier.

The Gilbert Cell mixer is different from the diode mixers in that the best performance is obtained when the LO signal does not cause saturation in the transistors of the Gilbert Cell. Figure 48 shows that the largest signal that can be used without the mixer saturating too much is -6 dBm and that level of LO power has been used for the

subsequent measurements. Using a lower LO power gives more ideal mixer action but reduces the conversion gain. The RF level of -18 dBm corresponds to a 1 dB reduction of the conversion gain of the mixer and thus corresponds to the 1 dB compression point.

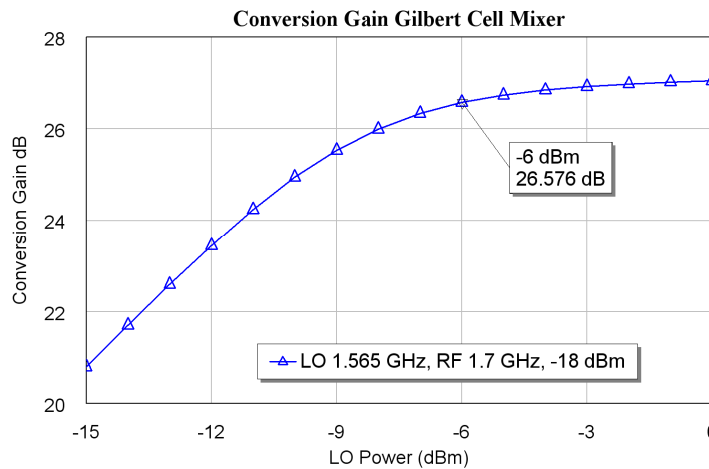


Figure 48. Conversion gain of the Gilbert Cell mixer of figure 45.

Figure 49 shows the IF spectrum of the Gilbert Cell Mixer. The LO power is -6 dBm and the RF level is -18 dBm corresponding to the maximum levels for each of these. Using a lower RF power level gives a better performance with a better LO and RF isolation at the IF output. The RF signal is at 1.7 GHz and the LO signal is at 1.585 GHz resulting in a difference signal at 135 MHz and a sum signal at 3.265 GHz. Figure 49 shows that these are of equal power level and are the largest signals. The Gilbert cell acts thus as a near ideal mixer.

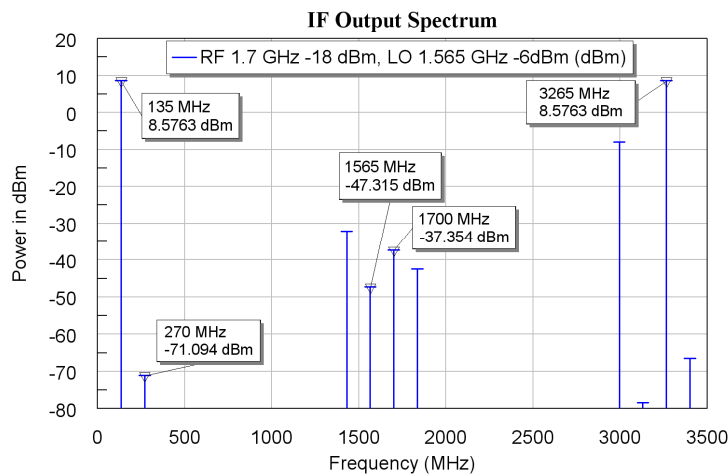


Figure 49. IF spectrum of the Gilbert Cell mixer of figure 45 as a down-converter.

Figure 50 shows the RF spectra of the Gilbert Cell mixer used as an up-converter, when the IF signal level is varied. The LO signal is -6 dBm and IF signal level is -18 dBm, -23 dBm and -28 dBm. For an IF signal of -28 dBm, the unwanted components are more than 55 dB below the wanted components, so that the Gilbert Cell is near ideal mixer. Changing the IF level by 5 dB, from -28 dBm to -23 dBm, causes a 4.9 dB change in level of the 1.7 GHz and 1.43GHz components and a 15.5 dB change in the 3IM component at 1.16 GHz. The mixer is thus operating in a linear range and the expected

third order intercept point is at $(0.5 \cdot (56.628 - 0.48462) - 0.48462) = 27.587$ dBm at the output and $27.587 - 27.515 = 0.072$ dBm at the IF input. Changing the IF level by 5 dB, from -23 dBm to -18 dBm causes a 4.157 dB change in the level of the 1.7 GHz and 1.43 GHz components, so that the -18 dBm IF input power corresponds closely to the 1 dB compression point. The computer simulations or similar measurements on the actual devices can thus easily be used to determine the critical mixer parameters. Passive Double Balanced mixers, can operate at higher input levels, but produce lower output levels.

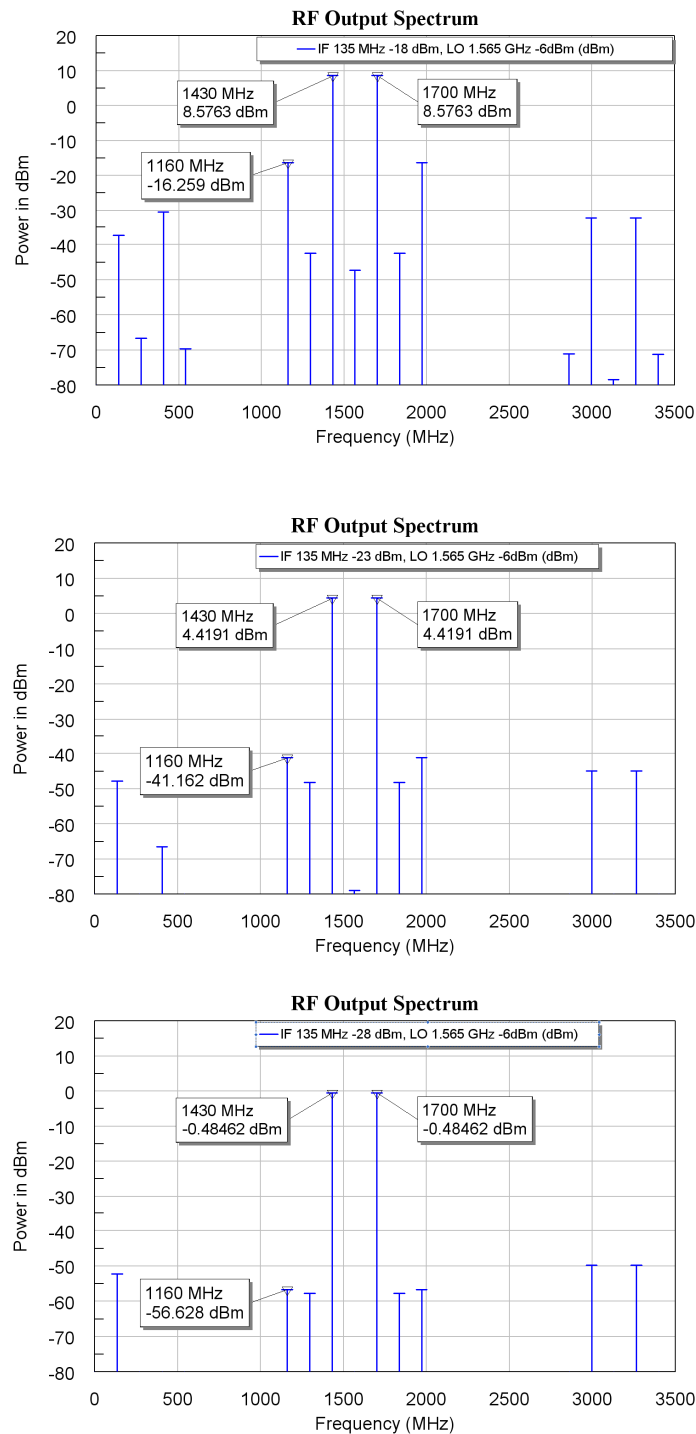


Figure 50. RF spectra of the Gilbert Cell mixer of figure 47 as an up-converter, RF levels of -18dBm (top), -23 dBm (middle) -28 dBm (bottom).

Figure 51 shows the corresponding RF waveform. The waveform corresponds to an ideal Double Sideband Suppressed Carrier waveform and any unwanted signals cannot be observed in the time waveform, but can be detected in the spectrum of figure 50.

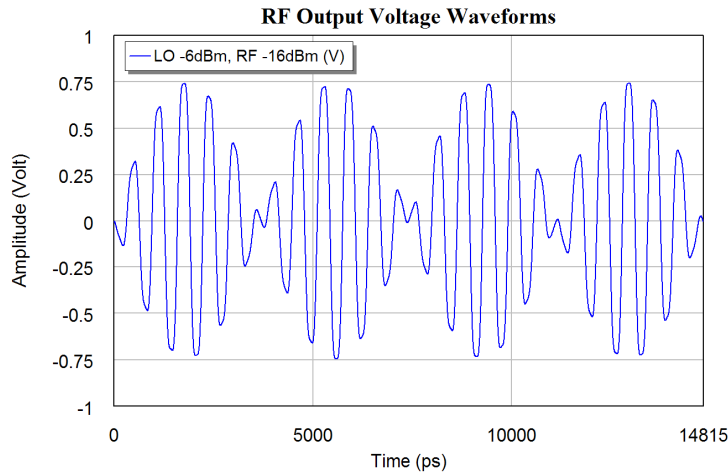


Figure 51. RF Waveform corresponding to figure 47.

Examples of Commercial Active Mixers

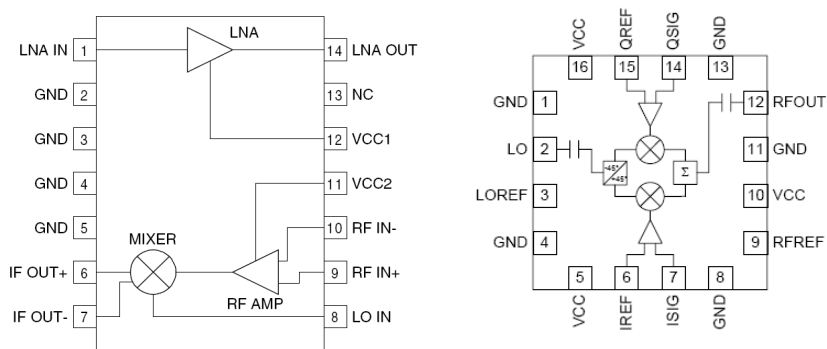


Fig 52. RF MicroDevices RF2411 LNA and Mixer and RF2850, IQ active mixer

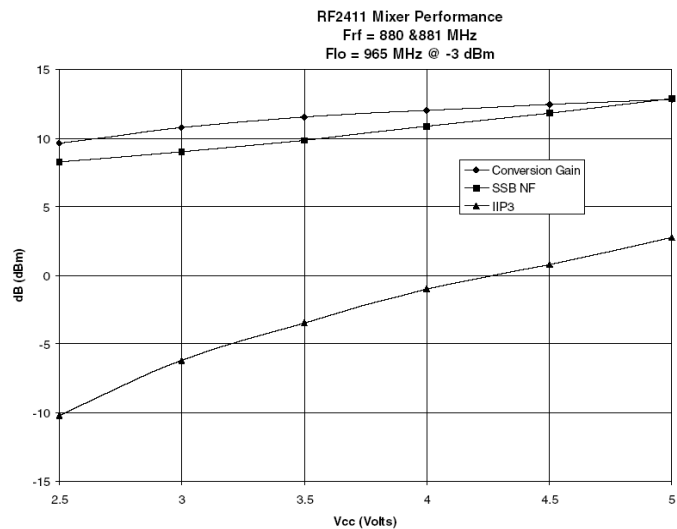


Figure 53. RF MicroDevices RF2411 LNA and mixer performance.

Many manufacturers produce active mixers for use in commercial equipment. In particular mixers for use in mobile and cordless phones, wireless LANs and similar consumer devices are readily available. The RF2411 Receiver front end and the RF2850 IQ active mixer, produced by RF MicroDevices are some examples of commercial active mixers. Figure 52 shows the pin connections of two commercial mixer IC's.

As shown in figure 53, the LNA used in the RF2411 IC, has a noise figure which varies from 1.7 dB at 500 MHz to 2.5 dB at 1500 MHz. The gain of the LNA is 17 dB at 1 MHz and slopes to 11 dB at 1500 MHz. The RF2411 can thus be used in many commercial applications.

Quadrature Mixers

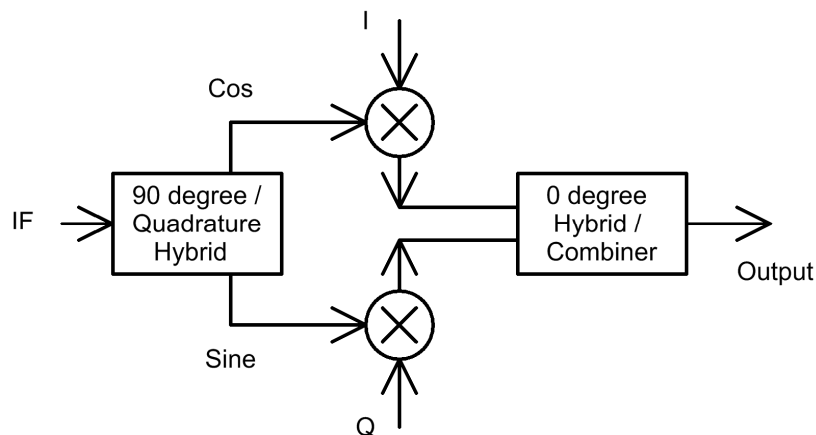


Figure 54. Block diagram of a quadrature mixer.

In quadrature mixers a 90 degree hybrid, like a Branchline coupler is used to produce two LO signals, corresponding to Sine and Cosine of the LO frequency. The Cosine signal is then multiplied with the In-Phase (I) component of the baseband signal, and the Sine signal is multiplied with the Quadrature (Q) component of the baseband signal, as shown in figure 54. The resulting signals are then added using a combiner like a Wilkinson hybrid to produce the RF signal. When the I and Q signals are the Hilbert transform of each other, then a Single Sideband RF signal results. When the I and Q signals are an RF signal that is passed through a 90° hybrid then the image frequency components are suppressed. When the I and Q signals are individually controlled baseband signals a vector modulated RF signal results. In most cases the I and Q signals are produced using Digital Signal Processing techniques. Quadrature mixers are thus required for the vector modulation used in many modern communication systems.

The 90 Degree hybrids required for quadrature mixers can also be produced using LC networks, so that quadrature hybrids at frequencies below 500 MHz are possible. As an example, Minicircuits make quadrature mixers at a wide range of frequencies as shown in figure 55.

Local oscillators produced using phase locked loops or using Direct Digital Synthesis, can have two outputs which have an exact 90 degree phase difference over a wide range of frequencies, as is required for the quadrature mixers.



JCIR-4MH (+15 dBm LO)
JCIR-25 (+13 dBm LO)

MODEL NO.	FREQUENCY MHz			CONVERSION LOSS dB			IMAGE REJECTION dBc		LO-RF ISOLATION dB		LO-IF ISOLATION dB		RF-IF ISOLATION dB		IP3@ center band (dBm)	CASE STYLE	CONNECTION	PRICE \$		
	RF f_c-f_u	LO f_c-f_l	IF	\bar{x}	σ	Max.	RF>LO	LO>RF	Typ.	Min.	Typ.	Min.	Typ.	Min.					Typ.	
◆ JCIR-4MH	430-930	500-1000	65-75	7.9	0.15	9.0	●		28	18	55	40	25	20	25	15	20	BG291	kj	54.95
◆ JCIR-25	2490-2550	2420-2480	57-83	7.0	—	8.5		●	27	17	35	25	26	18	25		16	BG291	kk	44.95

L = low range [f_l to $10f_l$] M = mid range [$10f_l$ to $f_u/2$] U = upper range [$f_u/2$ to f_u]
m = mid band [$2f_l$ to $f_u/2$]

features

- excellent image rejection, 28 dB typ. (JCIR-4MH)
- low conversion loss, 7.9 dB typ. (JCIR-4MH) 7.0 dB typ. (JCIR-25)
- solder plated J-leads for excellent solderability & strain relief

applications

- cellular
- ISM

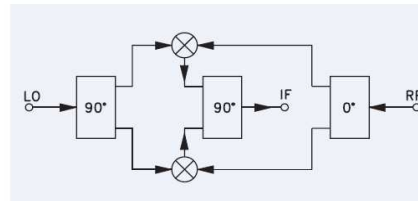


Fig 55. Minicircuit IQ mixers. (From their catalogue)

Active IQ Mixers

The RF2850 IQ mixer shown in figure 52, is used as an up-converter for mobile radio applications. This mixer used Gilbert cells for the mixers. Using an IQ mixer allows the required RF output signal to be produced, without the need to filter out unwanted sidebands. In addition a zero IF frequency can be used, so that the LO is at the centre of the RF band, again avoiding the need for filters. Such RF filters are large and heavy. It is desirable to have a small and light mobile phone. An I and Q signal, up to 250 MHz can be used, together with a LO signal in the range 1.7 GHz to 2.5 GHz, to produce a quadrature modulated RF signal in the range 1.7 GHz to 2.5 GHz. A typical carrier suppression of 25 dB unadjusted and 55 dB adjusted is obtained. The mixer has a typical (unadjusted) unwanted sideband suppression of 45 dB. The mixer performance satisfies all the mobile radio standards. These are low cost devices aimed for a consumer market.

For modern signal generators, IQ modulation is used to produce the complex modulated waveforms used in modern communication systems. The mixers used in such signal generators are often active (Gilbert cell) IQ mixers. Computer controlled DC bias (control and calibration) signals are used to ensure that the carrier feed-through, Quadrature phase shifts and I and Q gains are correct. The design of such IC's can cost more than one million dollars. The resulting devices have a better performance than those of figure 55 or 56, but each mixer will also be more expensive.

LTC Mixers

At higher frequencies, it becomes more difficult to wind the transformers required for the mixers. Low Temperature Cofired (LTC) thick film technology allows a circuit to be made up from multiple layers of ceramic materials. By depositing conductive or magnetic inks, a set of layers can form a strip-line transmission line, a ferrite loaded hybrid or it can contain semiconductor elements like diodes. Because high dielectric constant materials are used, the resulting package can be made small. Since the process can be automated, lower production costs result. Minicircuits use this technology for

producing high frequency mixers. A typical example is their IQBG-2000 I&Q modulator. The block diagram is the same as the IQ mixer in figure 54. This device is designed for the 1.8 GHz to 2 GHz mobile phone market. The Package is shown in figure 56. This LTC IQ mixer has an image rejection of better than 30 dB, which is comparable to the transformer based mixers shown in figure 53, but this isolation could not be obtained using conventional transformer based technology. More details on LTC circuits are given in the lectures on Circuit Manufacture.

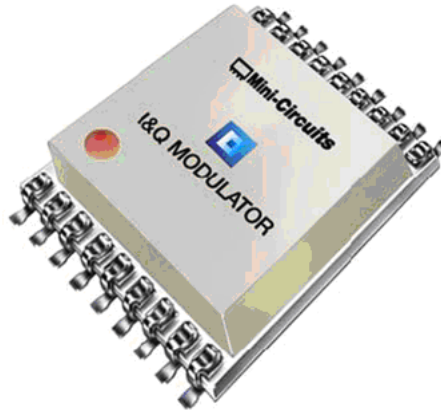


Fig 56. Minicircuits LTC IQ mixer, IQBG-2000. (From www.minicircuits.com)

Other Mixers

Mixer manufacturers make other types of mixers, such as triple balanced mixers, which result in a better input impedance and double balanced mixers using FETs in a passive mode (no DC supplied to the FET) in order to obtain an improved IP3 performance. The description of such devices are beyond the scope of these notes, but some further details can be found at the Minicircuits web site (www.minicircuits.com).

Oscillators

Principles of Oscillators

Requirements

- 1 The LO must be able to supply sufficient power to drive the mixer at the required level.
- 2 The LO must have a sufficient low Phase and amplitude noise for the application. For example FM 75 kHz deviation, for 60 dB SNR need an LO with < 75 Hz phase noise when measured in the 50Hz to 15 KHz band.
- 3 The harmonics of the LO must be sufficiently small not to cause interference to other users or other parts of the receiver. In particular harmonic mixing products must be very small and not cause any spuri.

Oscillator Types

There are two basic oscillator types:

Oscillator using positive feedback: This is the common lower frequency oscillator design technique used in EE3300, and can be used at any frequency.

Oscillator using negative Resistance: This relies on S_{11} of an amplifier in a circuit being >1 at some frequencies, resulting in oscillation. The amplifier is unstable at those frequencies where $S_{11} >1$, causing the amplifier to oscillate. This design technique is predominantly used for microwave operating frequencies. The design of oscillators using negative resistance is beyond the scope of this course.

Positive Feedback Oscillators

The oscillator consists of an amplifier and a Frequency Selective Network. The amplifier output is applied to the frequency selective network, the output of which is applied to the amplifier input. For the analysis a switch can be imagined to open the closed loop signal path. If V_2 is exactly the same as V_1 , both in amplitude and phase then steady state oscillations result. If the magnitude of $V_2 > V_1$ and the phase is the same then the oscillations will grow. If $V_2 < V_1$, then the oscillations will decay.

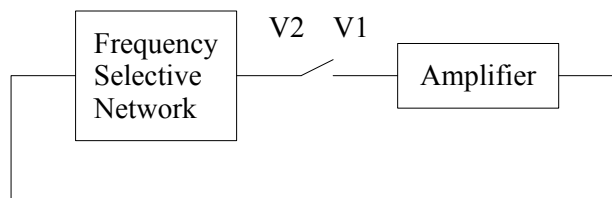


Figure. 1. Feedback Oscillator Block Diagram

Oscillator design process:

- 1: Design the Feedback network to have the correct frequency selective behaviour at the required operating frequency. A high Q network will have a rapid change of phase with frequency resulting in a lower phase noise of the resulting oscillator.
- 2: Select or design the amplifier to have the required gain at the operating frequency. The input and output impedances should also match the expected loads to be seen by the frequency selective network.
- 3: Simulate the amplifier and ensure the biasing is correct to provide the required gain and phase shift at the operating frequency.
- 4: Connect the frequency selective network and amplifier and do a linear analysis to ensure that the required gain (>1) and phase (V_2 in-phase with V_1) conditions are satisfied. In MWO the OSCTEST element is specially designed to perform this function and is used in place of the switch shown in the above diagram.

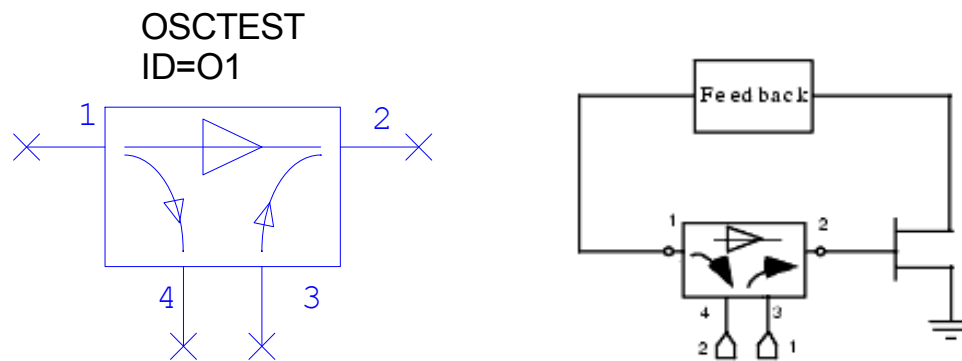


Figure 2. The use of Oscptest for linear analysis of oscillators.

- 5: Once the circuit has been adjusted to have the correct gain and phase for oscillation, modify the linear circuit by replacing the Oscptest probe with the Oscaprobe. The Oscaprobe is connected to ground at the point where the switch was, as shown below.

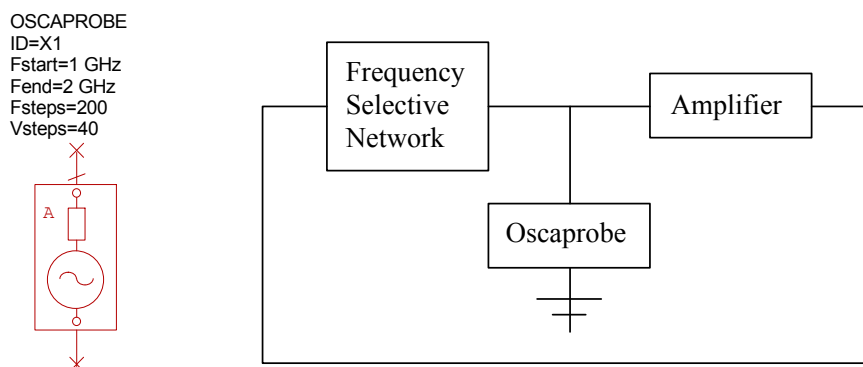


Figure 3. The use of Oscaprobe for nonlinear analysis of oscillators.

The Oscaprobe is a network that is a short circuit at the specified frequency of oscillation and an open circuit at all other frequencies, the voltage amplitude and phase is adjusted until no current flows through the probe, under which conditions the correct oscillating amplitude is determined. This amplitude is then used in a non-linear (spice) simulation of the oscillator circuit. This then allows output waveforms, harmonics and

the phase noise of the oscillator to be determined. The MWO oscillator example which is located in the MWO directory: Examples/Circuit Design Types/Oscillators/BJT Oscillator, and the Colpitts oscillator design example in these lecture notes are design examples which follow this process.

Frequency Selective Networks

For typical RF and Microwave oscillators, the following oscillator types are commonly used:

Wien Bridge Oscillator, using an RC network with a $Q=1/3$. This is a low Q resulting in a high phase noise for the oscillator. The oscillator is however easy to construct and time and as a result this oscillator is often used for audio frequencies, where the inductors required by other configurations would be too large to be used in oscillators.

Colpitts Oscillator, using a tapped capacitor LC network.

Hartley Oscillator, using a tapped Inductor LC network. Both the Colpitts and Hartley oscillators are similar, in their frequency range of operation, output voltage and phase noise. The LC resonators used in both the Colpitts and Hartley oscillators will have a typical maximum Q of 250. In practice unloaded Q values of 100 are more common.

Voltage Controlled Oscillator. One of the capacitors in the LC network for a Colpitts or Hartley oscillator is replaced with a varactor diode, allowing the capacitance of the LC network to be varied by applying a DC bias. Voltage controlled oscillators are used in many applications.

Crystal Oscillator. A quartz crystal is used as part of the frequency selective network, resulting in a very high Q resonator. Fundamental mode crystal oscillators are available for frequencies between 32 kHz and 100MHz. Crystal oscillators have very low phase noise. Quartz Crystal resonators will be discussed in more details later.

Stripline or microstrip transmission line resonator. At VHF and microwave frequencies such resonators are a reasonable size and have unloaded Q values of the order of 200.

Coaxial cavity oscillator. The resonators can be made from Coaxial resonators with a centre length of one quarter wavelength. These resonators can have unloaded Q values of several thousand. The resonators are large, restricting the applications.

Dielectric resonator oscillator. By filling the coaxial resonator with a material with a high dielectric constant, the linear dimension is reduced by the square root of the dielectric constant. Having a dielectric constant of 25 will thus reduce the volume of the resonator to 1/25 of the air filled resonator volume. Dielectric resonators are used frequently at microwave frequencies. The resonators can be based on the coaxial resonator and have a centre conductive resonator and conductive walls, or they can simply be a high dielectric material, relying on the dielectric-air interface to keep the electric fields inside the resonator.

A plot of the Q values of different resonators and the corresponding volume, is shown in figure 1.

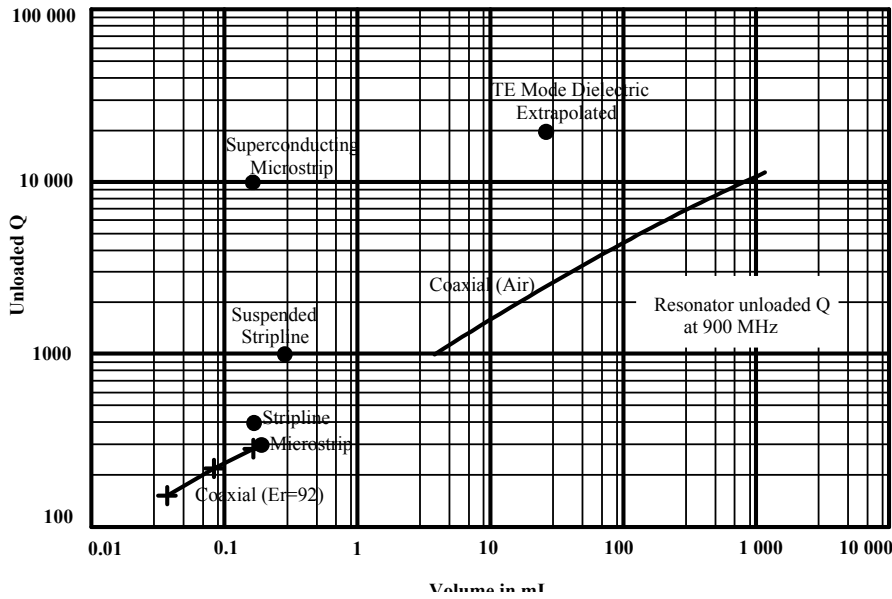


Figure 4. Q values and Volume of different resonators at 900 MHz.

The phase noise of an oscillator is primarily determined by the Q of the resonator used in the oscillator, and the way that the amplifier loads the resonator. The higher the Q of the resonator, the lower the phase noise and in general, the lower the frequency variation that can be obtained by tuning the resonator. The choice of the resonator and its Q is thus the primary factor affecting the oscillator properties.

Oscillator design procedure

Step 1: Select a transistor, FET or amplifier

The active device used in an oscillator is very important, factors for consideration are: Output power, oscillating frequency, supply voltage and cost. The low frequency phase noise of the oscillator does depend on the flicker noise of the amplifier, so that the noise figure of the amplifier is important for low noise oscillators.

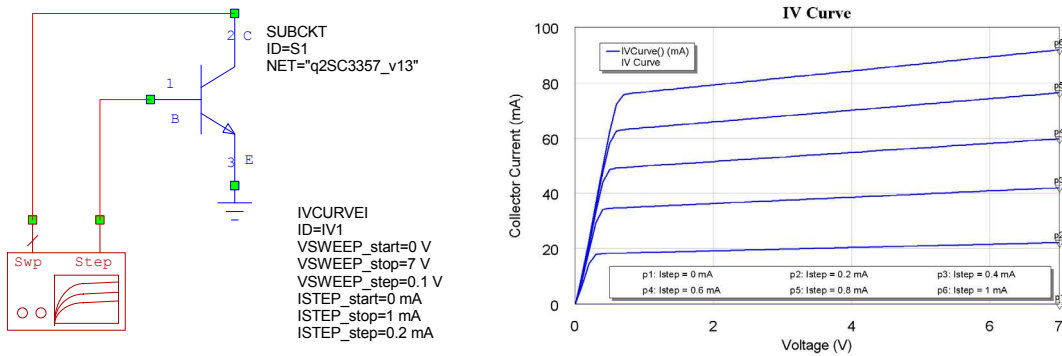


Figure 5. Circuit for determining the I-V characteristic of a transistor.

The most important design parameter is the Biasing of the transistor. In EE2300 and EE3300 it was shown that the IV curve is very useful in determining the correct biasing

conditions. It should be realised that some of the critical transistor parameters like β can vary over a 5:1 ratio between transistors. The transistor parameters used in the models of the computer simulation software, include typical values. The design must be such that the oscillator will work under all permissible variations of transistor parameters. The I-V curve can easily be obtained in MWO as shown in figure 5:

For linear biasing, a 7V supply and quiescent collector current of between 40 and 5 mA is required. 15 mA is a good compromise to minimise the power dissipation in the transistor and still have sufficient output power.

Step 2: Design an amplifier

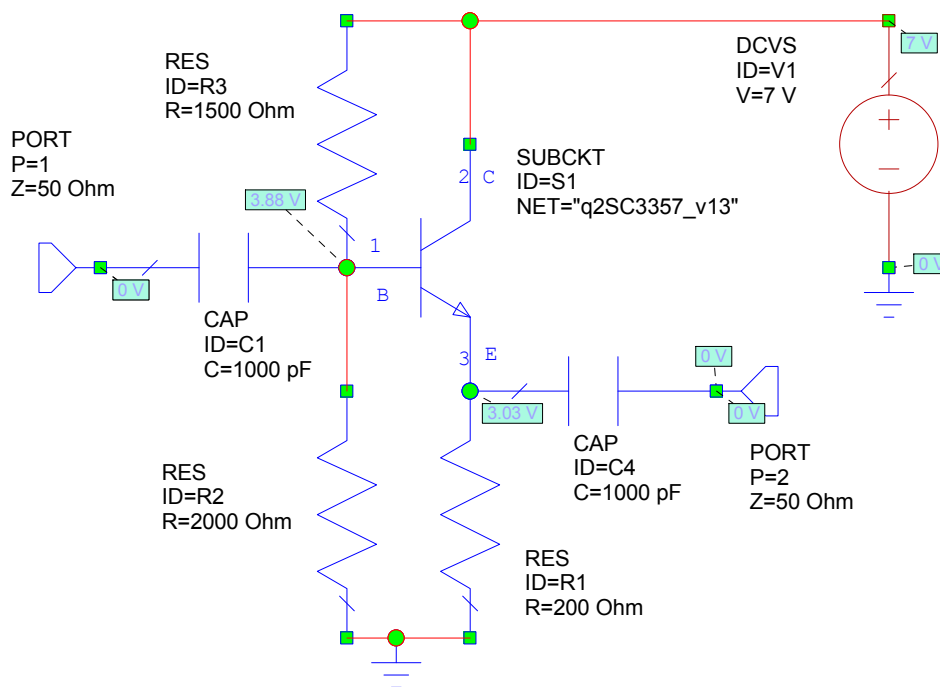


Figure 6. Amplifier for the Colpitts oscillator

A typical amplifier configuration and one that is used for this design is shown in figure 2. The first step is to select the bias voltages. For a 7 Volt supply, and having an emitter follower configuration for the amplifier, the emitter voltage should be close to half of the supply voltage, minus one volt. This results in a large swing without the transistor saturating. For a quiescent current of 15 mA, the current through the biasing chain should be of the order of 1.5 mA to 3 mA, for good quiescent current stability with temperature. For an emitter voltage of 3 Volt, a base voltage of 3.5 Volt is desired, so that a biasing resistor, between 2.4 k Ω and 1.2 k Ω is required for R3, when the values are rounded to the nearest available resistor values. Since a relatively high input impedance is required, a 2 k Ω resistor is used. A 1.5 k Ω resistor is required to then obtain the 3.5 V at the base of the transistor using a 7 V supply. The annotation setting allows the circuit voltages to be indicated on the circuit diagram in Microwave Office and allow the biasing and voltages to be checked.

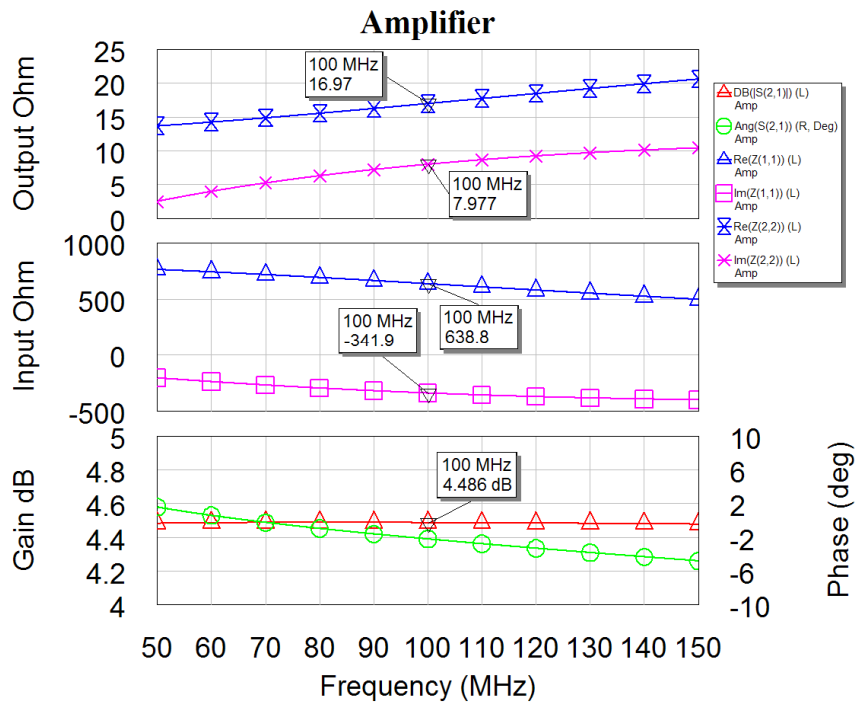


Figure 7. Amplifier Performance.

Note The gain of 4dB is the power gain taking the different input and output impedances into account. Input Impedance 638 Ω and the output impedance is 17 Ω, with a significant reactive component that will effect the resonance of the Collpits oscillator if it is not allowed for in the design process.

Step 3: Design a resonator

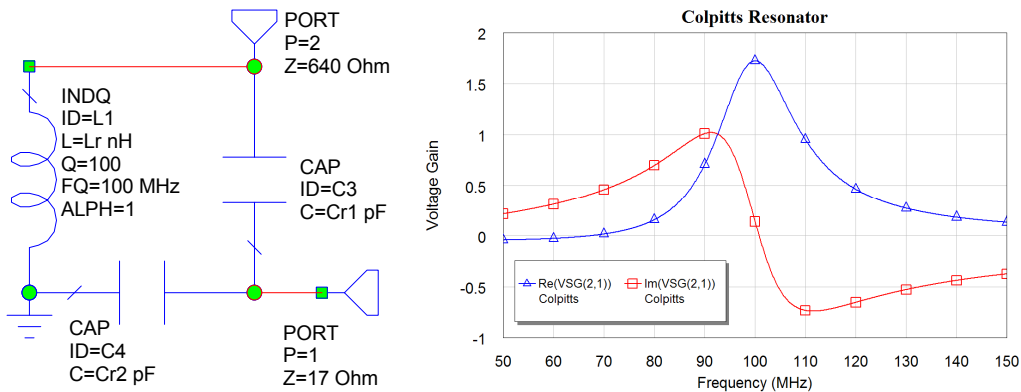


Figure 8. Colpitts resonator network

The resonator must be a frequency selective network, to ensure that the conditions for oscillation only apply at one frequency. In addition the network must be matched to the input impedance and output impedance of the amplifier and have a high Q. The components can be tuned to ensure a zero (or 180 degree if needed) phase shift at the required operating frequency. In figure 8, the imaginary part of the transfer function is not exactly zero, since the network shown is corresponds to the one actually used in the oscillator and allows for phase changes produced by the amplifier.

Step 4: Linear Oscillator Analysis

The resonator and amplifier are now combined into the once circuit. The element OSCTEST is used to determine the loop gain and phase shift. The resonator network is now tuned to give a phase shift of zero degrees between port 1 and 2, at the required operating frequency. If needed, the loop gain is changed to ensure that it is just slightly above one at the operating frequency. That then corresponds to the correct conditions for oscillations.

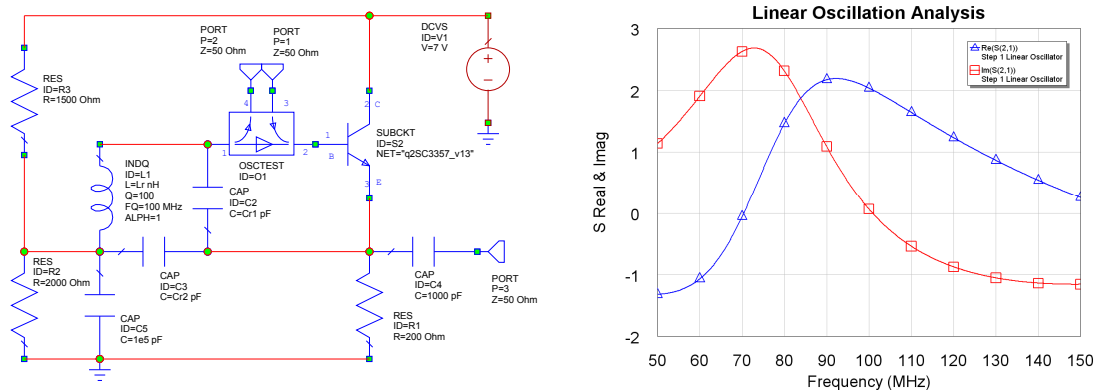


Figure 9. Linear analysis using OCSTEST

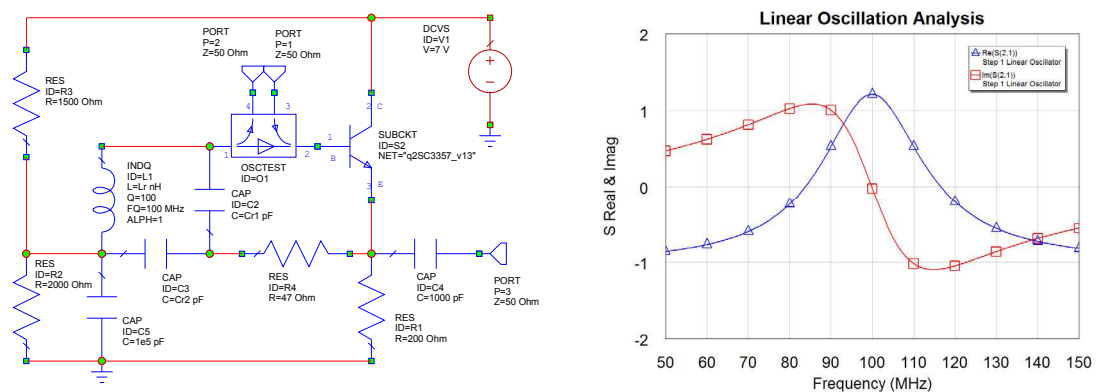


Figure 10. Linear analysis using OCSTEST Resistor added to increase Q and reduce gain.

The gain in figure 9 is too large and the 17 Ω output impedance of the amplifier, causes a severe reduction of the Q of the resonator network, resulting in a high phase noise. The gain can be reduced by inserting a 47 Ω resistor in series with the output of the amplifier. That also increases the Q if the resonator and reduces the phase noise of the oscillator, since the output impedance dominates the load to the network.

Step 5: Nonlinear Analysis

Replace OSCTEST with OSCPROBE as shown in figure 11, to do a harmonic balance analysis. This will allow the oscillation frequency, output power and output waveforms, including the amplitude of each of the harmonics to be determined. The output spectrum obtained using the harmonic balance is shown in figure 11, the tuning frequency range can be investigated by plotting the Inductance required versus oscillating frequency, and the output waveform can be determined as shown in figure 12.

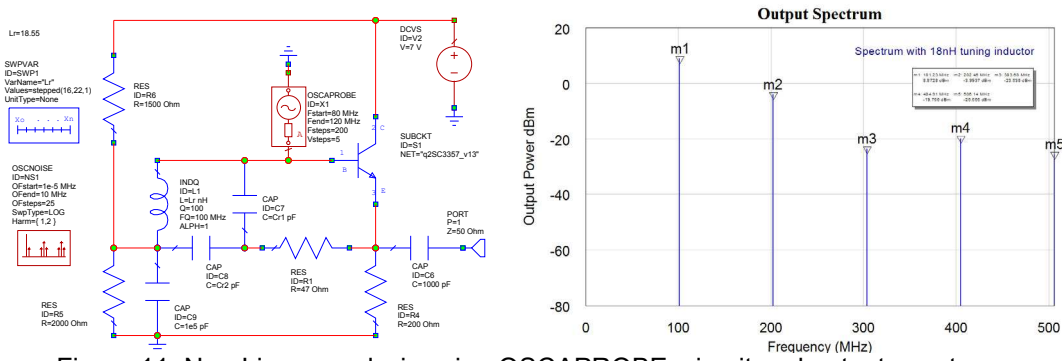


Figure 11. Non-Linear analysis using OSCAPROBE, circuit and output spectrum.

The SWPVAR simulation control (Element ⇒ Simulation Control ⇒ SWPVAR) shown in the schematic of figure 11 allows the plotting of the sweep of inductor values and their corresponding frequency. Note that the output waveform is smaller than expected, since the amplifier should have a linear output swing of at least ±2 Volt. The waveform can then be used to investigate the suitability of the biasing.

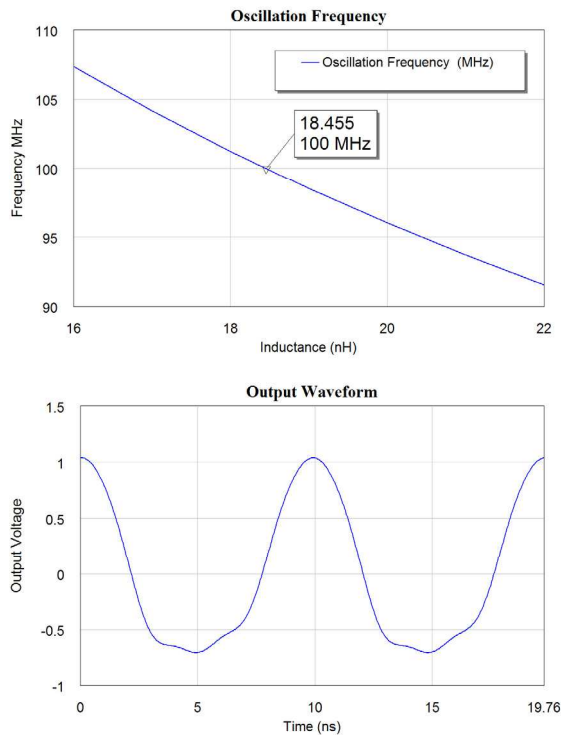


Figure 12. Non-Linear analysis using OSCAPROBE, Tuning range and output waveform.

The non-linear analysis can also be used to determine the Phase Noise of the oscillator. The OSCNOISE measurement (Element ⇒ MeasDevice ⇒ Controls ⇒ OSCNOISE) allows the phase noise of the oscillator to be measured as shown in figure 13. The phase noise will depend on the Q of the resonant network as well as other parameters, such as the noise figure of the amplifier and the amplifier power level and the loading that the amplifier places on the resonant network. In general the higher the oscillating frequency, the higher the phase noise.

Microwave Office allows the performance of an oscillator to be determined prior to the hardware being produced. This greatly reduced the cost of designing oscillators. The non-linear analysis can only be produced when a full Spice model of the active device is available. Many transistor manufacturers provide the required models for their transistors. Unfortunately the Spice models are not available for many MMIC's.

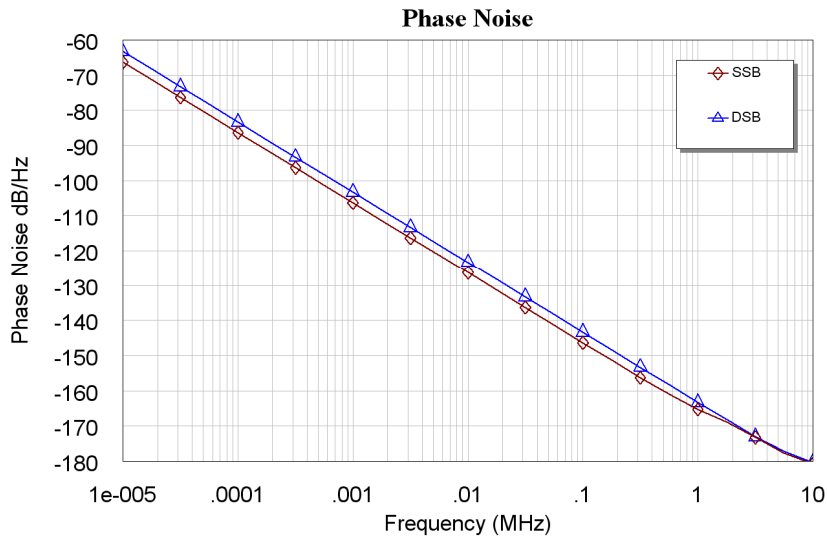


Figure 13. Phase noise of the oscillator using non-linear (harmonic balance) analysis.

Crystal Oscillators

Quartz Crystals

For details of Quartz Crystals see "Quartz Crystal Resonators and Oscillators for Frequency Control and Timing Applications - A Tutorial" by the 2009 IEEE president John Vig. He has graciously given permission for those PowerPoint slides to be available as a resource for this course. As a result they are included in the "Resources"

Crystal Oscillator Design Example

The design of a crystal oscillator is similar to that of any other oscillator. For most fundamental mode crystal oscillators, the crystal is inductive at the operating frequency and the inductor in any LC oscillator is replaced with the crystal. In figure 14, the inductance of a phase shift oscillator is replaced with a quartz crystal.

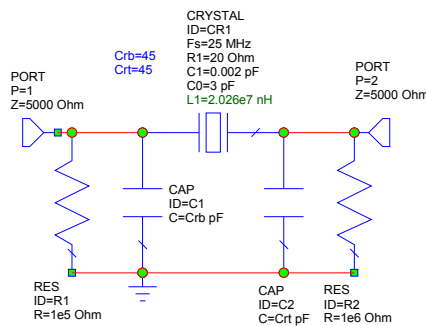


Figure 14. Phase shift network using a Quartz Crystal

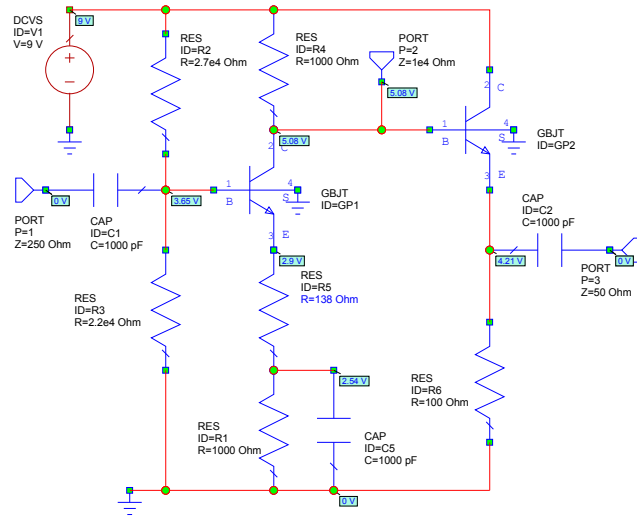


Figure 15. Resonator Network and Amplifier for Crystal Oscillator

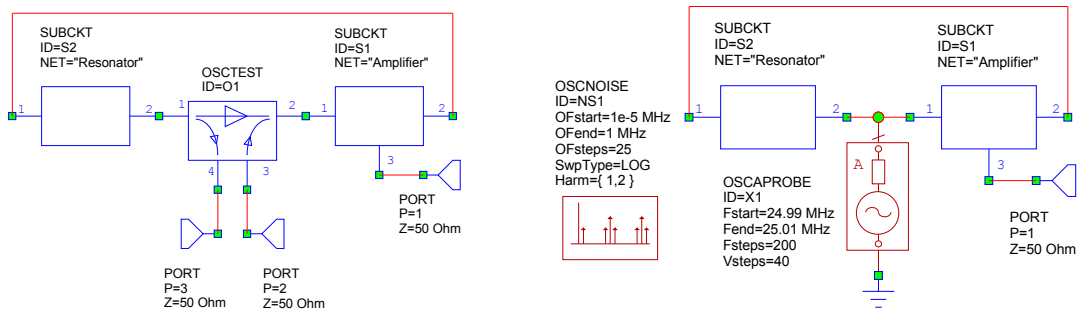


Figure 16. Linear and Non-linear Oscillator Circuits

The amplifier shown in figure 15 has a gain of 21.5 dB from the input port 1 to the output port 3. The gain from the input to port 2 is enough to cause oscillations. The gain of the amplifier can be controlled by changing R4, the resistor connected to the emitter, without affecting many other parameters. The resonant network and the amplifier are connected together to form a Crystal oscillator as shown in figure 16.

Using OSCTEST, the gain around the amplifier and resonator loop is now determined using a linear oscillator analysis as shown in figures 17 and 18.

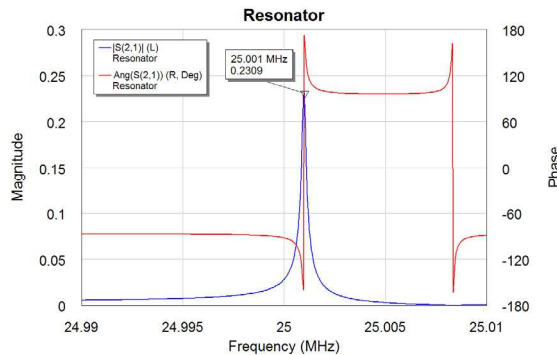


Figure 17. Frequency response of the resonator of figure 14.

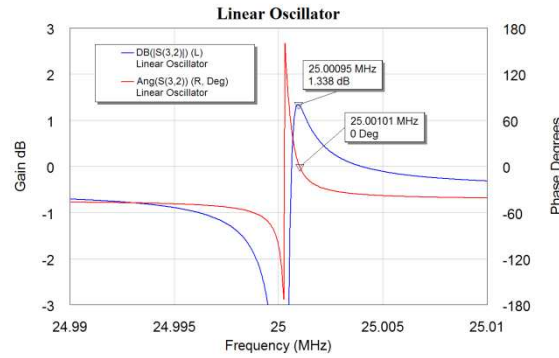


Figure 18. Frequency response for the oscillator using linear oscillator analysis (OSCTEST).

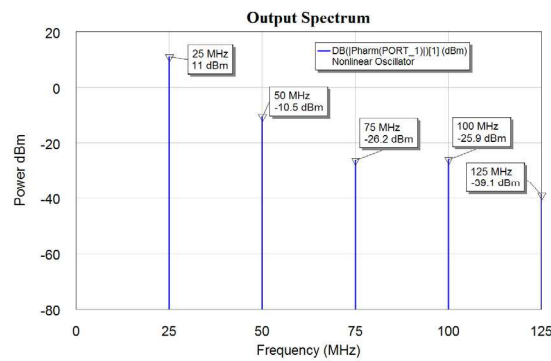


Figure 19. Output spectrum obtained using harmonic balance analysis. (OSCAPROBE)

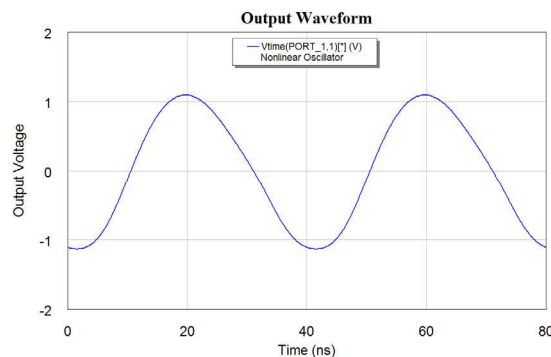


Figure 20. Output waveform obtained using nonlinear (harmonic balance) analysis.

Replacing the OSCTEST element with the OSCAPROBE element as shown in figure 16, allows a harmonic balance analysis to be done, so that the output spectrum can be determined as shown in figure 19, the output waveform can be determined as shown in figure 20 and the phase noise can be determined as shown in figure 21.

By comparing figure 13 and figure 21, it can be seen that the crystal oscillator has a much lower phase noise, due to the Q of the resonator being much higher. Using a varactor diode permits the electronic control of the frequency of the oscillator of figure 6 to 13. A 2:1 frequency range is possible. The frequency of crystal oscillators can however only be varied by several parts per million. For low noise crystal oscillators, the amplifier should impose a negligible load

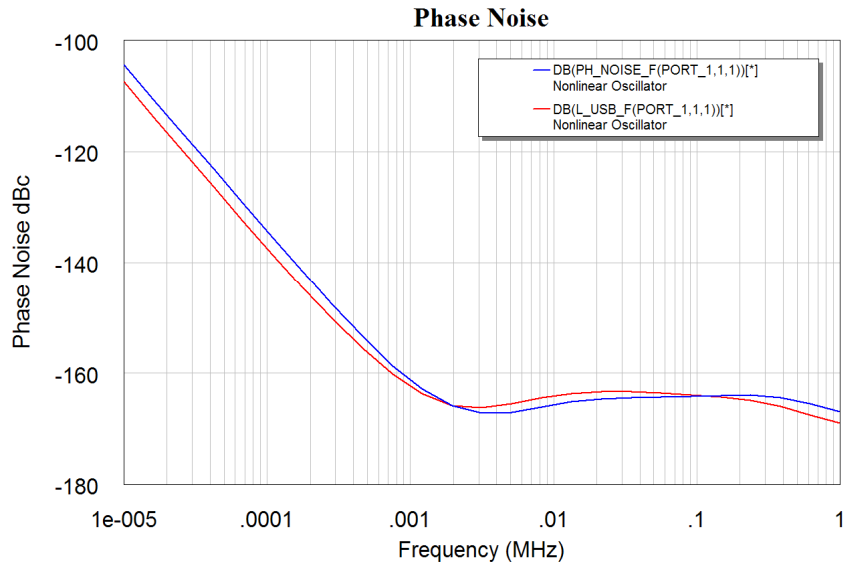


Figure 21. Phase noise of the oscillator.

RF and Microwave Oscillators

At RF and Microwave frequencies (above 1GHz), transmission lines are often used as circuit elements. The MAR6 amplifier, used here, is a typical MMIC (Microwave Monolithic IC) costing less than \$10. These devices are very simple to use and are convenient and can be used as low power amplifier blocks in many applications. The S parameters for these devices can be obtained from the Minicircuits web site as follows:

```

!MAR-6 (TA = 25°C, Id = 16mA)
!FREQ. S11 S21 S12 S22
!MHz dB Ang dB Ang dB Ang dB Ang
# MHZ S DB R 50
100 -27.96 171 20.1 171 -22.50 5 -27.96 -30
500 -26.02 -105 18.7 138 -21.30 21 -20.00 -104
1000 -17.72 -118 16.4 107 -18.80 28 -17.08 -150
1500 -13.56 -140 14.1 84 -17.10 28 -16.48 180
2000 -10.75 -163 12.0 65 -15.80 26 -15.92 157
2500 -9.37 -176 10.3 55 -15.20 28 -15.92 150
3000 -7.74 169 8.7 42 -14.80 25 -16.48 143
3500 -6.74 157 7.2 30 -14.20 22 -17.72 144
4000 -6.20 146 6.1 18 -13.80 20 -20.00 156
    
```

Table 1. S parameter file from Minicircuits with added line in blue.

This file can be imported into Microwave Office so that those S parameters for the device can be used in a simulation. The import the s parameter file, it needs to be in the "Touchstone" file format. (Touchstone was the name of an early RF simulation software, which was later taken over by EESOF, which in turn was taken over by

HP/Agilent and is now called ADS. The only change that needs to be made to the S parameter file as obtained from Minicircuits, is the addition of the line shown in blue:

```
# MHZ S DB R 50
```

That line indicates to Microwave Office that the file has frequencies in MHz, contains S parameters, which must be in the order S11(Real, Imag), S21(Real, Imag), S12(Real, Imag) and S22(Real, Imag). The real part is in DB and the reference impedance is 50 ohm. Any line beginning with ! is a comment line and is ignored in the data file import.

For other formats for data files see the Microwave Office help files on “Adding Data Files to a project”, which includes details on the Touchstone Import files format. That data file is then used as a sub-circuit in the circuit diagram.

This data file is now used to design a 1 GHz oscillator using this MAR6 amplifier and using microstrip circuits on a Rogers RO4003 substrate. The oscillator consists of three parts: The MAR6 amplifier, A microstrip resonator (TL1) with tap coupling in order to obtain the correct impedance levels for the coupling into and out of the resonator and thirdly transmission lines TL2 to TL11, which are required to connect the output back to the input and thus provide feedback. The path length around the loop must have the appropriate phase shift to ensure that oscillations will result. In addition, two coupling capacitors are used to provide the correct DC levels at the input to the MAR6 and prevent the output from being shorted at DC.

The impedance of the resonator should be as low as possible to provide a reasonable Q, with low radiation losses and a good frequency stability. This is achieved by making the width of the resonator 5mm, which corresponds to a characteristic impedance of 24.8 Ω . A program TxLine, which is part of microwave Office is used for the calculations of the required length of the resonator. A screenshot of the resulting line parameters is shown in figure 22.

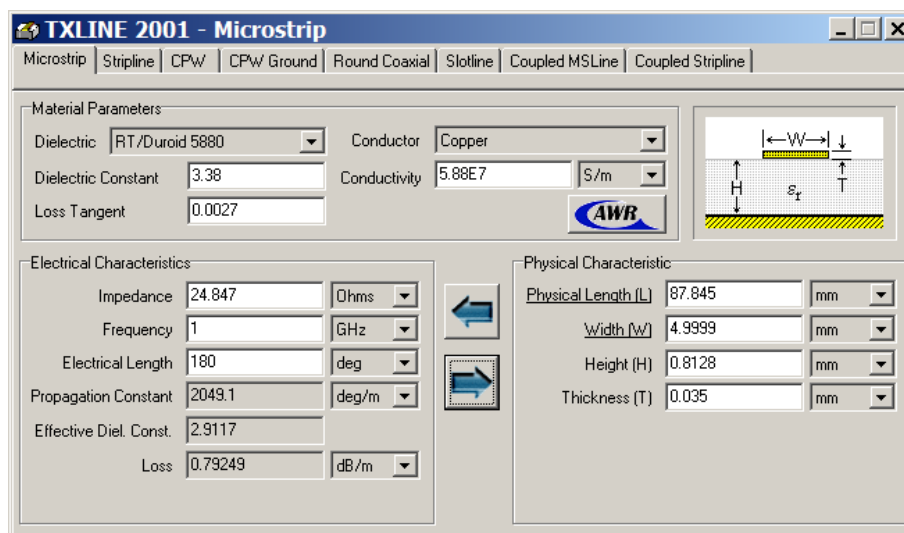


Figure 22. Resonator Width and Length Calculation

Since a full Spice model is not available for the MAR6, only a linear analysis of the oscillator can be carried out. The circuit schematic for the oscillator is shown in figure 23. Figure 24 shows the circuit diagram of the resonator. A capacitor is incorporated. That capacitor can be replaced with a variable capacitor in the hardware, to allow the

oscillator to be fine tuned to the correct frequency. With a minor modification, this can be replaced with a varactor diode, to enable the oscillator to be frequency modulated.

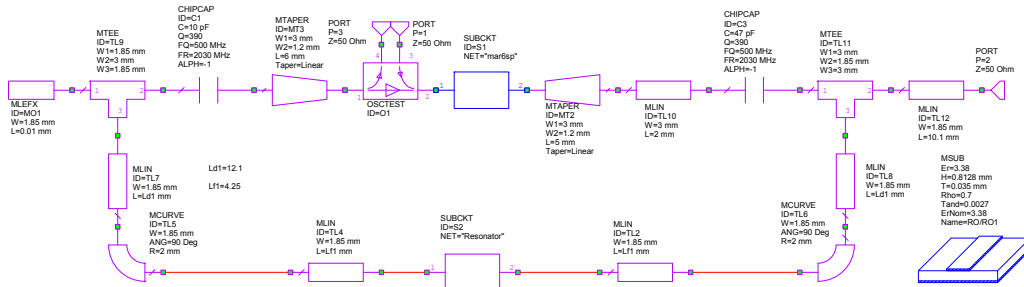


Figure 23. Circuit Schematic for 1GHz oscillator.

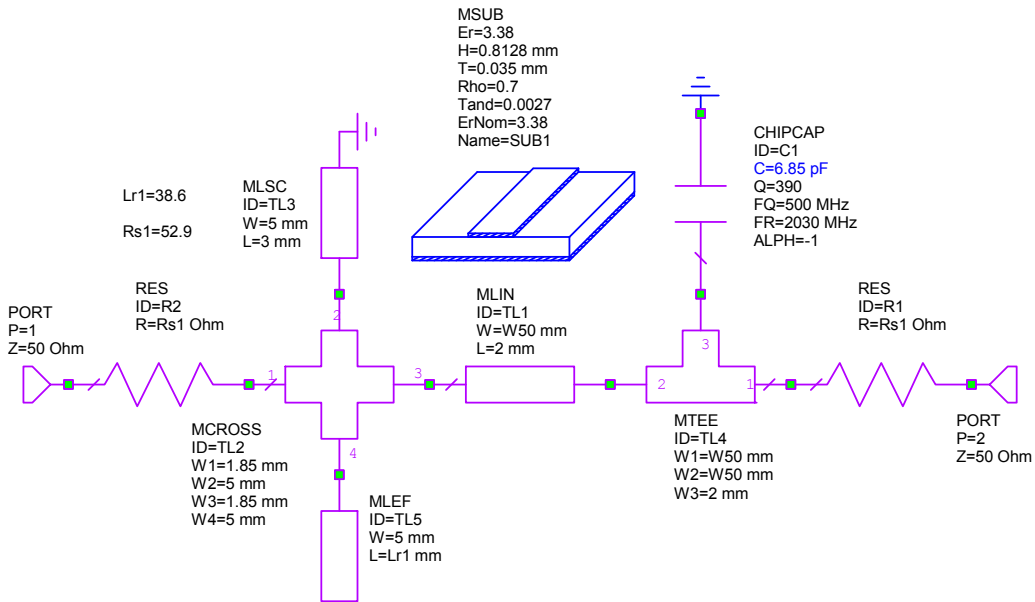


Figure 24. Circuit Schematic for 1GHz microstrip resonator.

Figure 25 shows the layout for the resonator and the coupling capacitors. The left end of the circuit is grounded.



Figure 25. Layout for 1GHz microstrip resonator.

Figure 26 shows the amplitude and phase of the resonator of figure 24, as a function of frequency. The resonator has a well behaved response at 1 GHz, but is the amplifier gain is too high, there is a possibility of oscillation at 1.34 GHz. The loop gain of the amplifier and resonator must thus be carefully controlled to ensure that only oscillation at 1 GHz is possible.

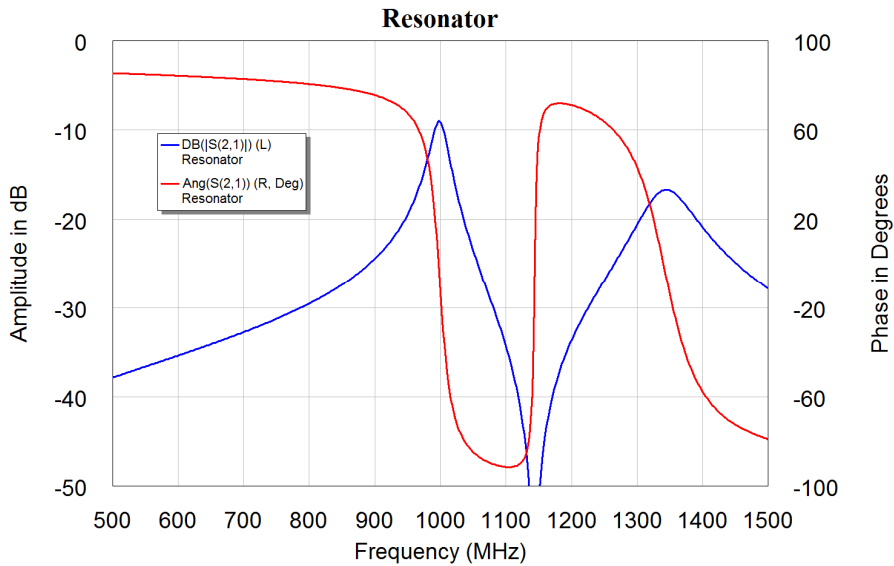


Figure 26. Resonator Transfer function, Amplitude and Phase

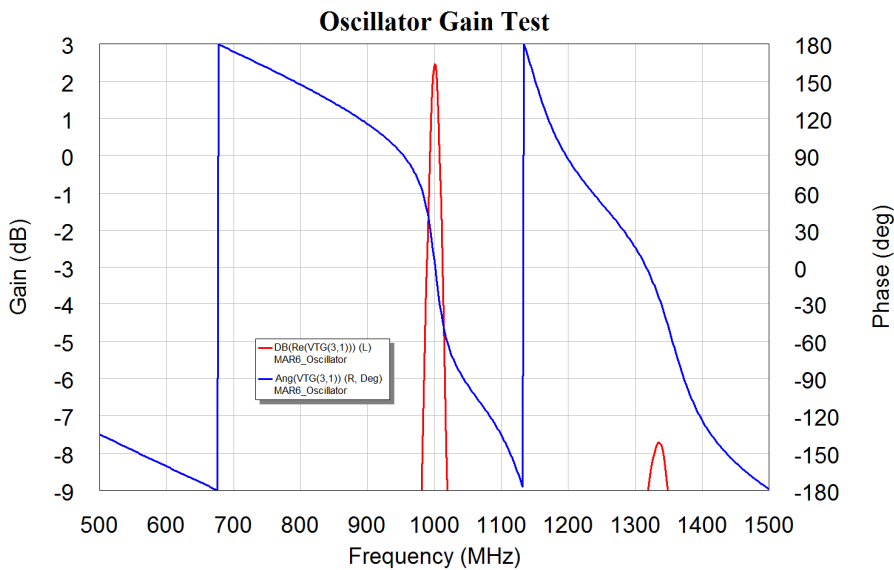


Figure 27. Complete Oscillator OSCTEST output.

The element Oscstest is used to check if the oscillator has the correct gain and phase in the feedback path. The phase shift around the loop should be exactly 0 degrees and the gain should be greater than one. An excess gain of 3 dB ensures that the loop gain is still greater than one, when different MAR 6 devices are used. The length of TL7 and TL8 are both adjusted in order to obtain the correct phase shift of 0 degrees at 1 GHz and the length of the resonator is adjusted to provide a maximum of gain at 1 GHz, to ensure that the oscillator does not oscillate at another frequency.

The resulting microstripline layout is shown in figure 28, with the oscillator output at the top, the supply voltage pad at the left and the largest element being the resonator. The resonator is shown slightly lighter, since that is a separate element in the layout.

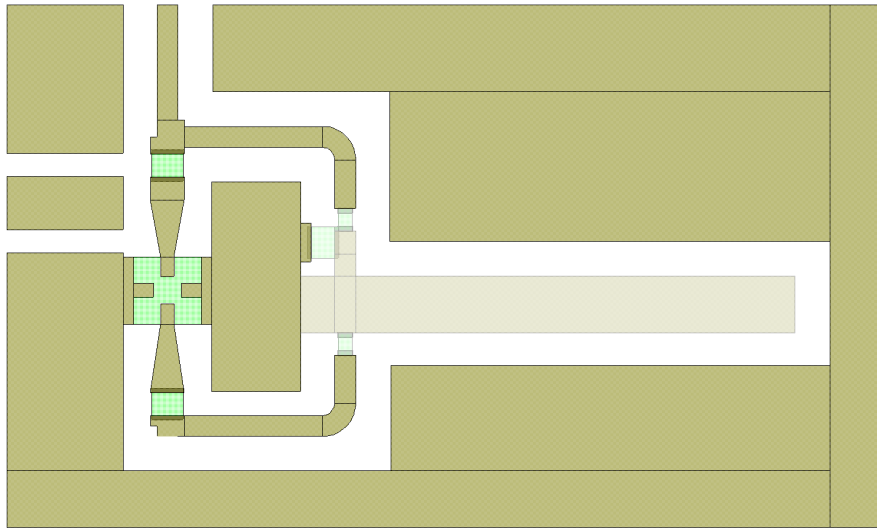


Figure 28. PCB layout for the 1GHz oscillator.

The only elements not shown on this layout are the power supply biasing and vias connecting the ground pins of the MAR to the ground-plane.

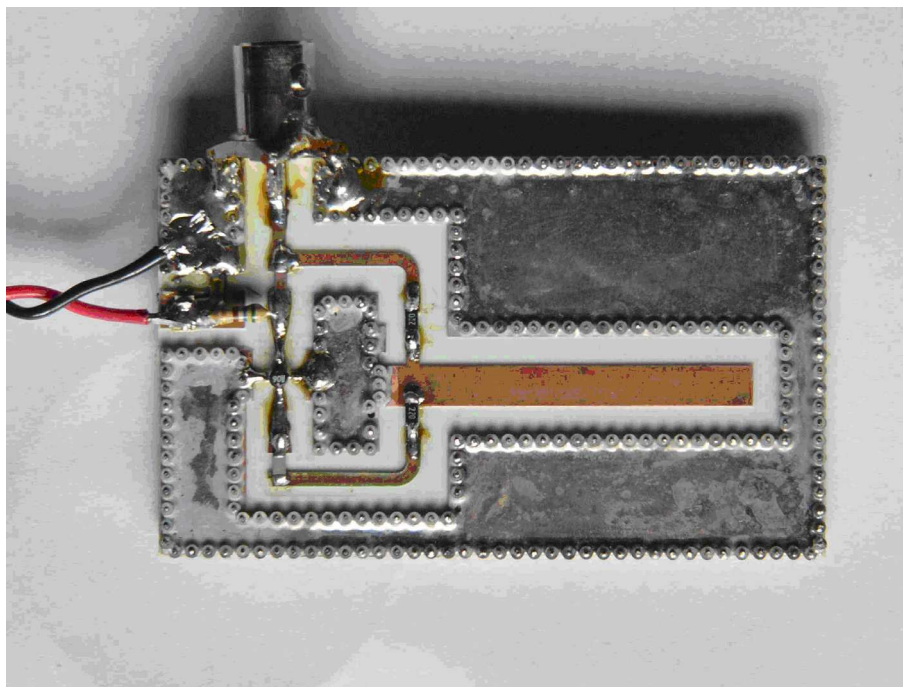


Figure 29. Photograph of the 1 GHz oscillator.

Figure 30 shows the spectrum obtained from the oscillator. The oscillator has a clean output signal and an acceptable phase noise performance. The output frequency is 990 MHz, which is within 1% of the design value. The output has a power of +5 dBm.

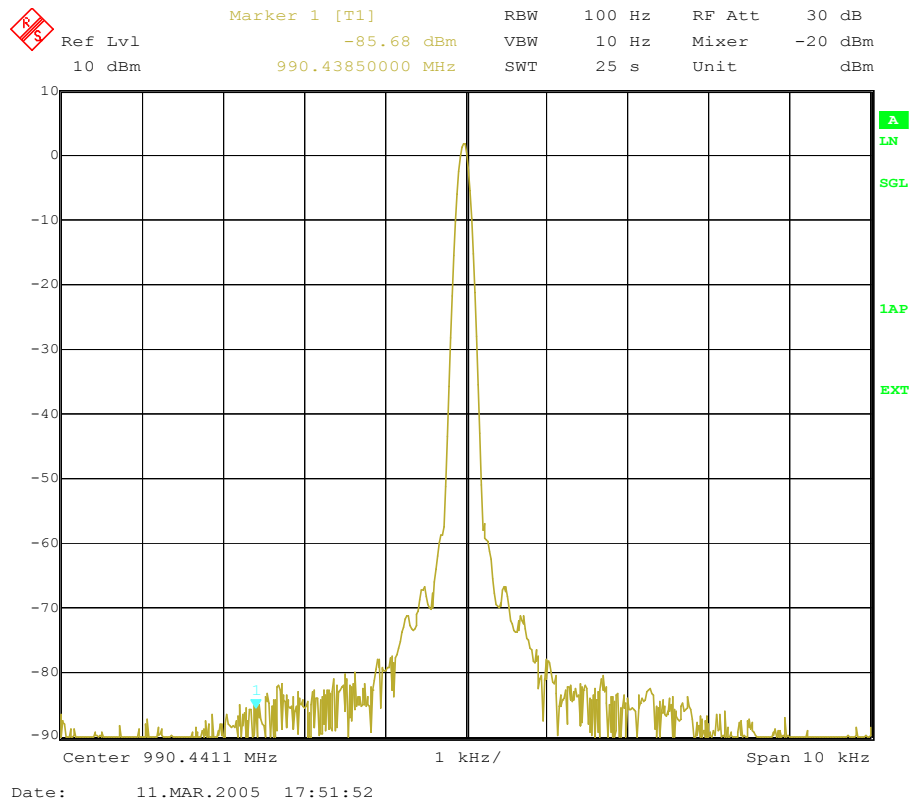


Figure 30. Measured output spectrum for the 1 GHz oscillator.

References

John Vig "Quartz Crystal Resonators and Oscillators for Frequency Control and Timing Applications - A Tutorial" John Vig, the 2009 IEEE president has graciously given permission for this PowerPoint presentation to be available under the "Resources" for this course.

Chapter 7

RF Filters

Introduction

Filters used for RF signals are nearly always Bandpass filters using coupled resonator design techniques. The basic properties of the most common types of filters are:

LC bandpass filters.

Typical unloaded Q values are 60-150, resulting in a large % Bandwidth filter with a high insertion loss. Frequency range 455 kHz to 2 GHz.

Helical Filters

Typical unloaded Q values > 1000 . The Q value can be increased, by increasing the size of the resonator cavity. Frequency range 30 MHz – 1 GHz.

Coaxial Filters

Typical unloaded Q value > 5000 . Frequency range 80 MHz – 2 GHz. Using a Ceramic dielectric results in a small size for mobile radio use. Air dielectric coaxial filters are used for high power diplexers in Radio and TV transmitters.

Microstrip and Stripline filters

Made using lines on PCB. Typical unloaded Q value 250. Wide % bandwidth.

Transmission Line Filters

Designs based on Short or open circuited stubs. Wide Bandwidth.

Interdigital Filters

High Q and $< 10\%$ bandwidth.

Acoustic filters:

Ceramic filters

Commonly used frequencies only. 455 kHz, 10.7 MHz IF filters, 800 MHz and 1.9 GHz diplexers for cellular phones.

Crystal Filters

Very High Q values and very low bandwidths. Typical 6 kHz Bandwidth at 10.7 MHz. Used for SSB filters. High cost compared to other filters.

SAW filters

Commercial Frequencies to 1 GHz. 10.7 MHz, 70 MHz. High insertion loss, can control amplitude response and group delay independently.

Several of the above filter types are discussed in detail in these notes.

Filter Design Revision

Most RF filter designs start with a normalised lowpass filter design and that filter has the required specifications in terms of filter order required, amplitude and group delay performance. This normalised lowpass filter is then transformed into the appropriate bandpass filter. There are two starting points:

- 1 Normalised LC filter tables or equations
- 2 K and Q filter tables.

These two are related and one can be derived from the other. For some filter types, like Butterworth filters, simple equations can be used for the normalised lowpass filter prototype. For RF designs K and Q tables are however better, since they include the effect of finite Q values in the resonators used. A good book for filter tables is A. I. Zverev, Handbook of Filter Synthesis, Wiley, 1967 and more recently from Artec House. This book is still in print.

Filter Tables

n	q0	I. L.	q 1	q n	k 12	k 23	k 34	k 45
	INF.	0.000	1.4142	1.4142	0.7071			
	14.142	0.915	1.4142	1.4142	0.7071			
	7.071	1.938	1.4142	1.4142	0.7071			
2	4.714	3.098	1.4142	1.4142	0.7071			
	3.536	4.437	1.4142	1.4142	0.7071			
	2.829	6.021	1.4142	1.4142	0.7071			
	2.357	7.959	1.4142	1.4142	0.7071			
	2.020	10.459	1.4142	1.4142	0.7071			
	INF.	0.000	1.0000	1.0000	0.7071	0.7071		
	20.000	0.958	0.8041	1.4156	0.7687	0.6582		
	10.000	2.052	0.8007	1.5359	0.7388	0.6716		
	6.667	3.300	0.9097	1.6301	0.7005	0.6879		
3	5.000	4.742	0.8226	1.7115	0.6567	0.7060		
	4.000	6.443	0.8406	1.7844	0.6077	0.7256		
	3.333	8.512	0.8625	1.8497	0.5524	0.7470		
	2.857	11.157	0.8884	1.9068	0.4883	0.7706		
	INF.	0.000	0.7654	0.7654	0.8409	0.5412	0.8409	
	26.131	1.002	0.5376	1.4782	1.0927	0.5668	0.6670	
	13.066	2.162	0.5355	1.6875	1.0745	0.5546	0.6805	
4	8.710	3.489	0.5417	1.8605	1.0411	0.5373	0.6992	
	6.533	5.020	0.5521	2.0170	1.0004	0.5161	0.7207	
	5.226	6.822	0.5656	2.1621	0.9547	0.4906	0.7444	
	4.355	9.003	0.5819	2.2961	0.9051	0.4592	0.7706	
	3.733	11.772	0.6012	2.4159	0.8518	0.4192	0.7998	

	INF.	0.000	0.6180	0.6180	1.0000	0.5559	0.5559	1.0000
	32.361	1.045	0.4001	1.5527	1.4542	0.6946	0.5285	0.6750
	32.361	1.045	0.5662	0.7261	1.0947	0.5636	0.5800	0.8106
	16.180	2.263	0.3990	1.8372	1.4414	0.6886	0.5200	0.6874
	16.180	2.263	0.5777	0.7577	1.0711	0.5408	0.6160	0.7452
	10.787	3.657	0.4036	2.0825	1.4088	0.6750	0.5080	0.7066
5	10.787	3.657	0.5927	0.7869	1.0408	0.5144	0.6520	0.6860
	8.090	5.265	0.4111	2.3118	1.3670	0.6576	0.4927	0.7290
	8.090	5.265	0.6100	0.8157	1.0075	0.4844	0.6887	0.6278
	6.472	7.151	0.4206	2.5307	1.3195	0.6374	0.4732	0.7542
	6.472	7.151	0.6293	0.8449	0.9722	0.4501	0.7267	0.5681
	5.393	9.425	0.4321	2.7375	1.2675	0.6149	0.4479	0.7821
	5.393	9.425	0.6508	0.8748	0.9355	0.4103	0.7663	0.5048

Table 1. Butterworth Response, K And Q Value filter table, From A. I. Zverev. "Handbook of Filter Synthesis", Wiley, pp 341.

Butterworth Filters

Butterworth filters have a maximally flat amplitude response. That means all the derivatives of the amplitude with frequency are zero at DC. The Butterworth response is a good compromise between attenuation characteristic and group delay.

For a Butterworth Lowpass filter of n^{th} order, with a cut off frequency of f_c and a source and load resistance of R , the filter component values are given by:

$$C_i = \frac{1}{\pi f_c R} \sin \frac{(2i-1)\pi}{2n} \quad i=1,3,5,\dots \quad \text{Eqn. 1}$$

$$L_i = \frac{R}{\pi f_c} \sin \frac{(2i-1)\pi}{2n} \quad i=2,4,6,\dots \quad \text{Eqn. 2}$$

The first component ($i=1$) is a shunt capacitor, the second ($i=2$) component is a series inductor etc. The normalised q values and coupling coefficients are related to the normalised lowpass impedances for a filter, using the following equations:

$$q_0 = Z_1 \quad q_n = Z_n \quad k_{ij} = \frac{1}{\sqrt{Z_i Z_j}} \quad \text{Eqn. 3}$$

Where Z_i is the normalised impedance as obtained from LC filter tables or from equations 1 and 2. Applying equation 3 to equations 1 and 2 gives:

$$q_0 = q_n = 2 \sin \frac{(2-1)\pi}{2n} = 2 \sin \frac{\pi}{2n} \quad \text{Eqn 4}$$

$$k_{ij} = \frac{1}{2 \sqrt{\sin \frac{(2i-1)\pi}{2n} \sin \frac{(2i+1)\pi}{2n}}} \quad i=1,3,5,\dots \quad \text{Eqn. 5}$$

These equations will then allow the k and q values for $IL = 0$ and $q_0 = \infty$ as shown in table 1 to be calculated.

Figure 1 shows the resulting circuit for a 7th order Lowpass filter with a 500 MHz cut-off frequency. The frequency response is shown in figure 2. The group delay of Butterworth filters is reasonably flat but has a rise near the cut off frequency. The step response of these filters exhibits some ringing, which degrades its use for data communications.

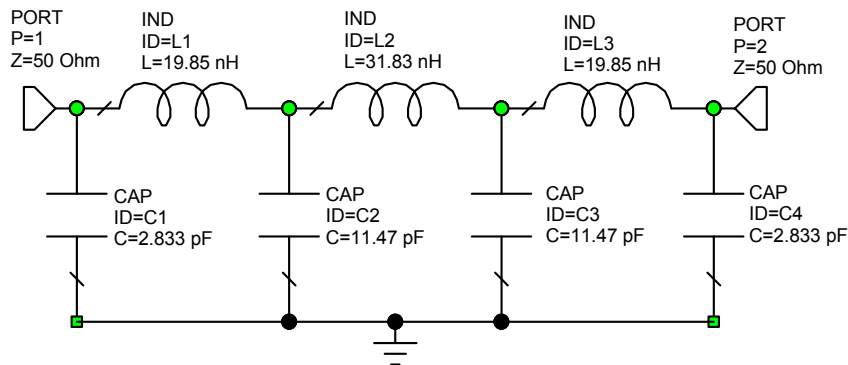


Figure 1. Butterworth Lowpass Filter.

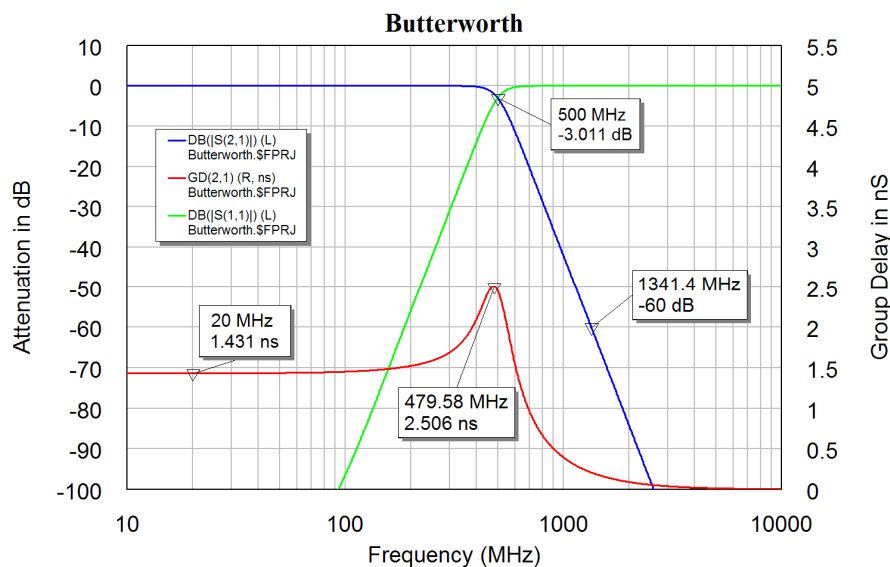


Figure 2. Butterworth Frequency Response.

Bessel filter

The Bessel filter has a maximally flat group delay and does not have any ringing or overshoot in its step response. As a result the Bessel filter type is very suitable for data communication systems.

Simple equations like equations 1 and 2 do not exist for Bessel filters. As a result the normalised filter element values have to be obtained from filter tables. Many filter tables for Bessel filters are normalised for a group delay of one second, rather than a 3 dB cut-off frequency. The Bessel filter in figure 3 has a cut-off frequency of 500 MHz so that accurate comparisons between the filter types can be made.

The Bessel filter has a less sharp roll-off of the attenuation characteristic, compared with the Butterworth filter, but has a flatter group delay as can be seen by comparing figure 2 and 4. For the Butterworth filter the 60 dB attenuation level occurs at 1.3 GHz while for the Bessel filter it occurs at 2.4 GHz. The group delay for the Bessel filter is less than that for the Butterworth filter, so that the signal appears sooner at the filter output.

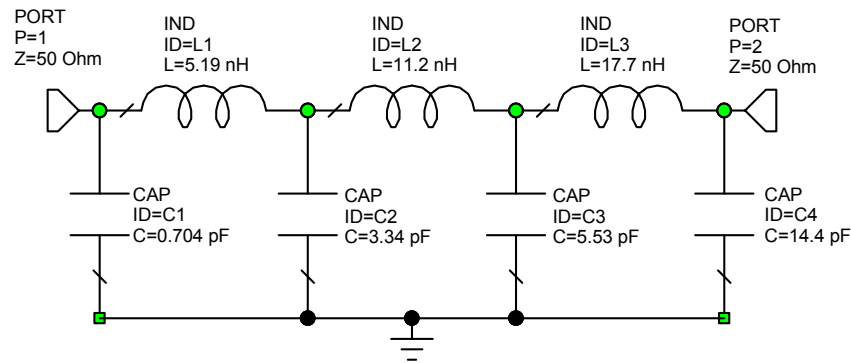


Figure 3. Bessel Lowpass Filter.

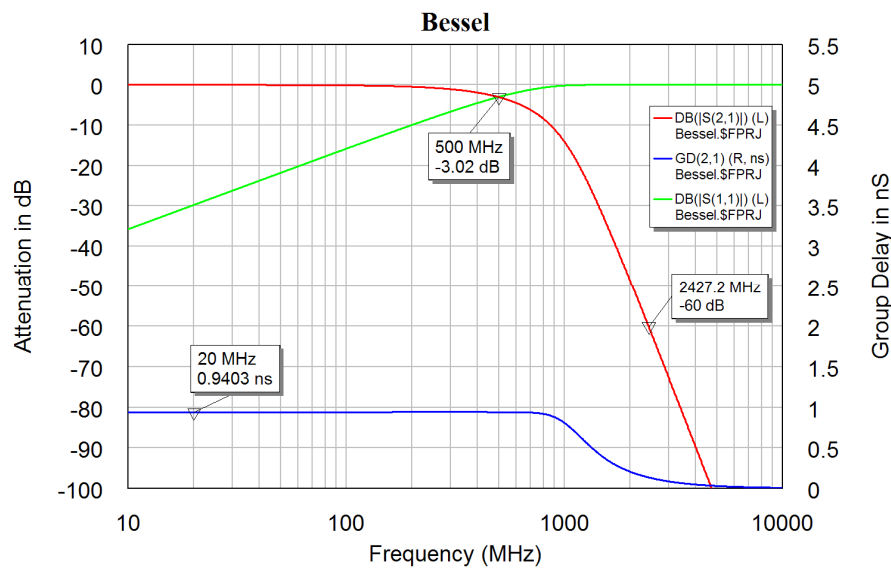


Figure 4. Bessel Lowpass Filter Frequency Response.

Chebyshev Filter

The pole positions for the Chebyshev filter lie on an ellipse, hence the Chebyshev filter is also called an elliptical filter. The Chebyshev filter has ripples in the passband and the value of the ripples is a parameter that is selected as part of the filter design. The filter of figure 5 has a 0.1 dB passband ripple as shown on figure 6. The inductors and capacitors for the Chebyshev filter are larger than those of the Bessel or Butterworth filters. The Chebyshev filter has a very sharp attenuation response in the stop band, with a -60 dB attenuation at 967 MHz, compared with 1.3 GHz for the same attenuation for the Butterworth filter. Increasing the passband ripple will increase the passband attenuation. The group delay for the Chebyshev filter is larger than that of the Bessel and Butterworth filters. As a result the Scale on figure 6 is different from figure 2 and 4.

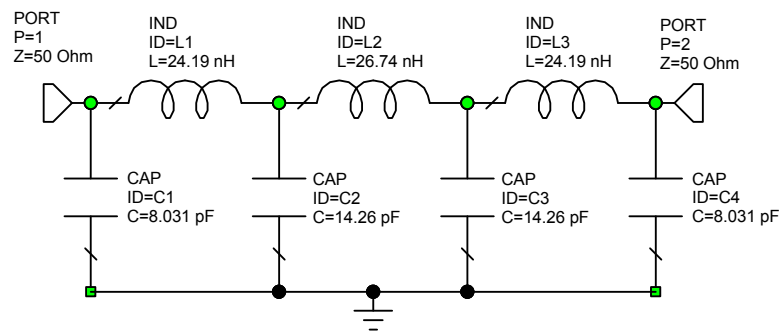


Figure 5. Chebyshev Lowpass Filter.

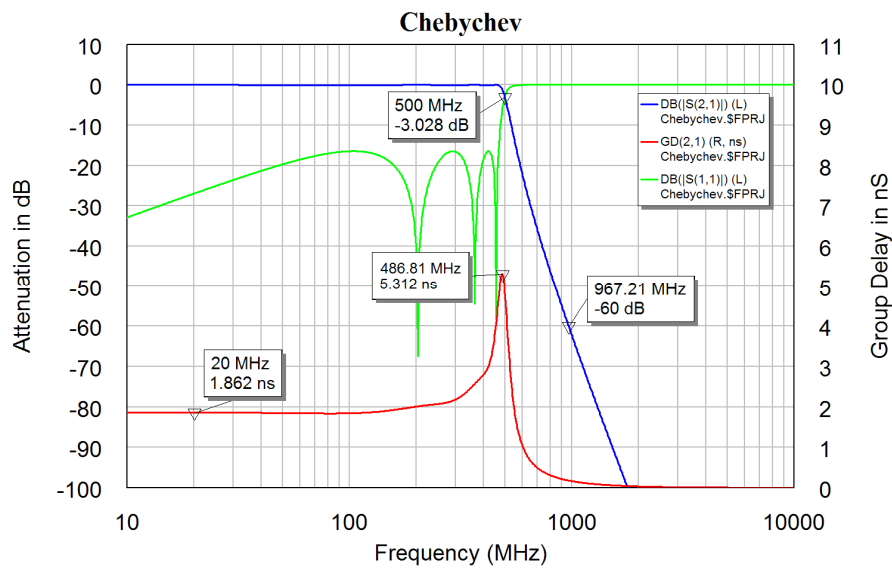


Figure 6. Chebyshev Lowpass Filter Frequency Response.

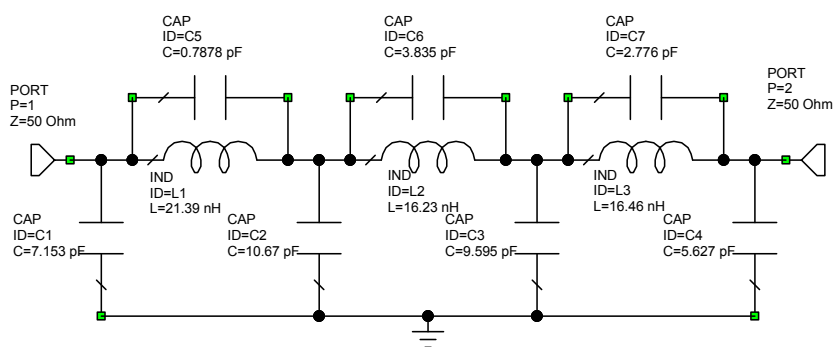


Figure 7. Cauer-Chebyshev Lowpass Filter.

A Cauer-Chebyshev filter has capacitors in parallel with the inductors to cause zeros in the stopband as shown in figure 7. The zeros are placed such that the minimum stopband attenuation values are the same as shown in figure 8. This gives an even higher stopband attenuation, with a 60 dB attenuation at 628 MHz compared with 1.3 GHz for the Butterworth filter. The Cauer-Chebyshev filter has an even bigger variation

in group delay than the Chebyshev filter and will thus have very poor transient response. The group delay of the Chebyshev and Cauer-Chebyshev filters are poor and these filters should not be used for data communications or applications where the group delay is important.

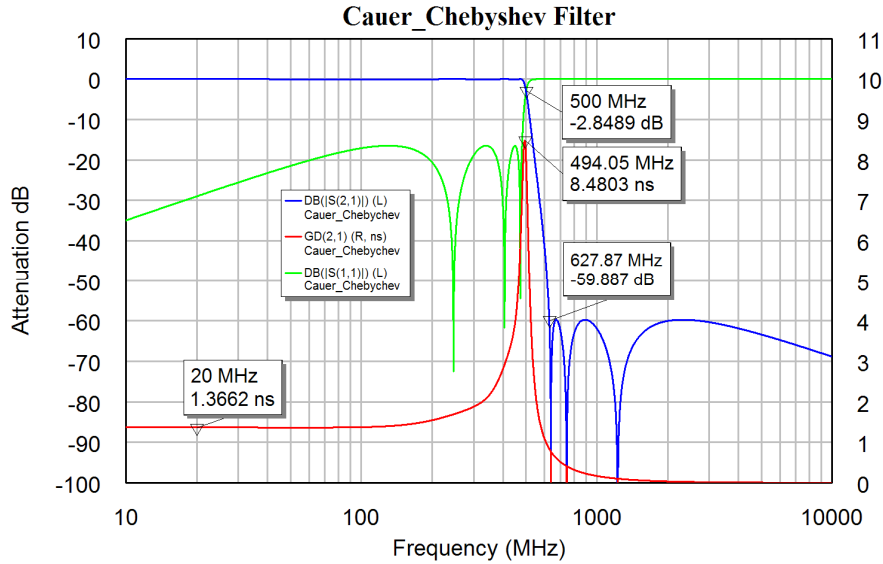


Figure 8. Cauer-Chebyshev Lowpass Filter Frequency Response.

Figure 9 shows the passband response of the four different filter types. The 0.1 dB passband ripple of the Cauer Chebyshev and Chebyshev filters can clearly be seen. The Bessel filter has a significant attenuation for frequencies above 100 MHz.

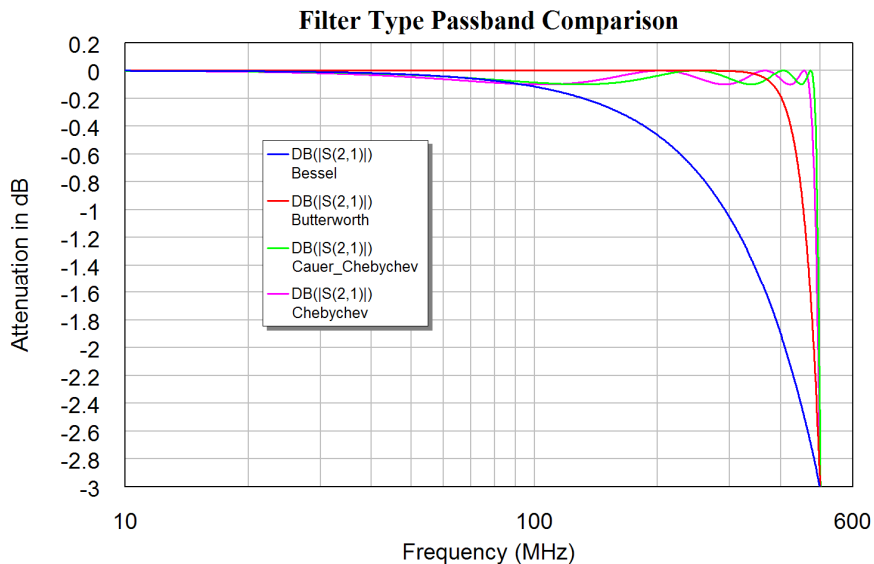


Figure 9. Passband Frequency Response of the filters of Figures 2, 4, 6 and 8.

Both the Chebyshev and Cauer-Chebyshev filters have poles on an ellipse and are elliptical filters. As a result it is better not to specify a filter as an elliptic filter since it does not fully specify the filter type.

From filter tables, which include losses due to the finite Q values of the filter elements, it can be determined that for a given Q value for the components, the Chebyshev filter has a higher passband insertion loss than a Butterworth filter and a Bessel filter has a lower insertion loss than a Butterworth filter. The same applies for Bandpass filters, so that for the same unloaded Q of the resonators used in coupled resonator RF filters, the Bessel filter will have the lowest insertion loss and the Chebyshev filter will have the highest insertion loss.

The selection of the correct filter type is critical to ensure that the filter used satisfies both the transient response requirements and the passband insertion loss and stopband attenuation requirements for the filter. In digital communication applications, the Bit Error Rate (BER) after demodulating is the critical parameter. To reject signals in an adjacent channel intuition suggests the use of a Chebyshev filter. However, computer simulations carried out at JCU for a 3rd Generation Mobile Radio system, have shown that the lowest demodulated BER when there is a large unwanted signal in an adjacent channel is obtained with a Bessel type filter response for the Channel filters.

RF Lowpass Filter design

Lowpass filters at RF and microwave frequencies can be designed and constructed using conventional LC filter design principles. Care should be taken to ensure that:

The impedance of the leads are kept as small as possible. In particular the impedance of the leads on capacitors connecting the capacitors to ground, or the length of any PCB layout track connecting the components to the ground-plane must be kept as small as possible, since it's inductance will effect the frequency response of the filter.

Components must be used that have self resonant frequencies well above the cut off frequency of the filter if a lowpass filter is used and well above any useable frequency if a high pass filter is used. Most commonly used capacitors have self resonant frequencies well below 1 GHz.

It is feasible to design conventional LC lowpass filters with cut off frequencies up to 1 GHz. When the frequency becomes too high for LC components to be used, inductors can be replaced with thin transmission lines of the length required to give the desired inductance and capacitors can be replaced by wide transmission lines.

As an example consider the design of a 7th order Butterworth lowpass filter with a cut off frequency of 2 GHz. From the equations 1 and 2 for Butterworth filters or from tables, by denormalising and using a cut off of 2 GHz and input impedance of 50 Ω , the component values shown in table 2 are obtained for the filter.

L C	Value	Line Length	Line Width
L1	1.771 nH	3.6 mm	0.5 mm
C2	1.985 pF	4.2 mm	10 mm
L3	7.170 nH	13.5 mm	0.5 mm
C4	3.183 pF	6.6 mm	10 mm
L5	7.170 nH	13.5 mm	0.5 mm
C6	1.985 pF	4.2 mm	10 mm
L7	1.771 nH	3.6 mm	0.5 mm

Table 2. LC filter values and corresponding microstrip line size.

For Rogers RO4003 substrate with $H = 0.83$ mm and $T=35$ microns, the width for a 50Ω transmission line is 1.9 mm. the thinnest line that is desirable is 0.5 mm and the thickest is 10 mm. That corresponds to impedances of 96.5Ω and 14.3Ω respectively. One needs to find out what length of transmission lines corresponds to the inductance required for the filter. In Microwave Office it is easy to compare the impedance of an inductor with one of a transmission line, as shown in figure 10.

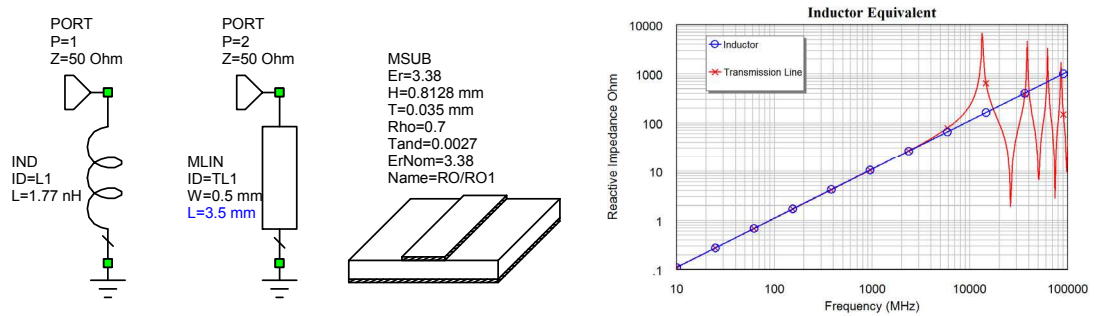


Figure 10. Replacement of Inductors using Microstrip Transmission lines

The length of the transmission line is tuned to ensure that at low frequency both have the same impedance. It can be seen that the short section of transmission line accurately represents the inductor for frequencies up to 10 GHz. This process is repeated for all the inductances. Note for larger inductances, at higher frequencies the transmission line will be a quarter wavelength resulting in an infinite impedance or half a wavelength, resulting in a very small impedance. For lowpass filters the length of the transmission line should be less than one quarter wavelength for all frequencies of interest.

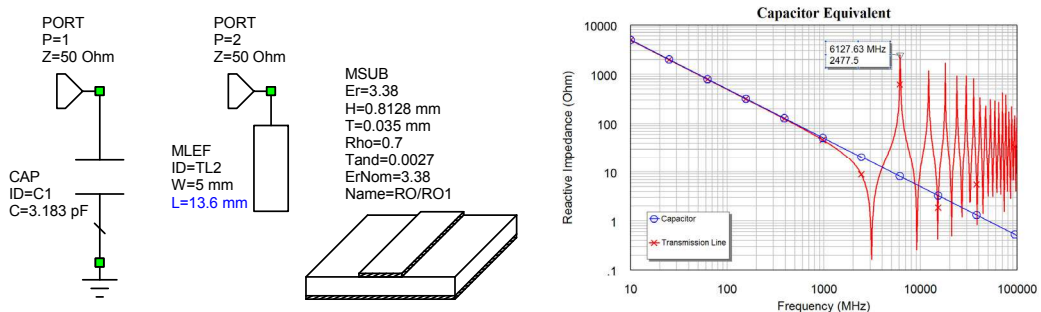


Figure 11. Replacement of capacitors using series Microstrip Transmission lines.

The Capacitors can be replaced with open circuited transmission lines as shown in figure 11. The resulting line sections have been placed in table 2 and it can be seen that some line sections are wider than they are long, which will cause some errors in the simulation as the actual fields will be different from what is assumed in the simulation of the transmission lines.

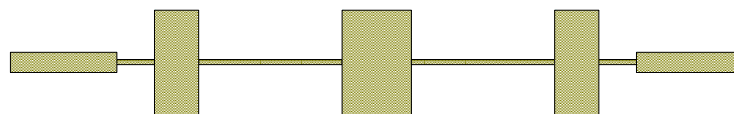


Figure 12. PCB Layout of the 2 GHz Lowpass filter.

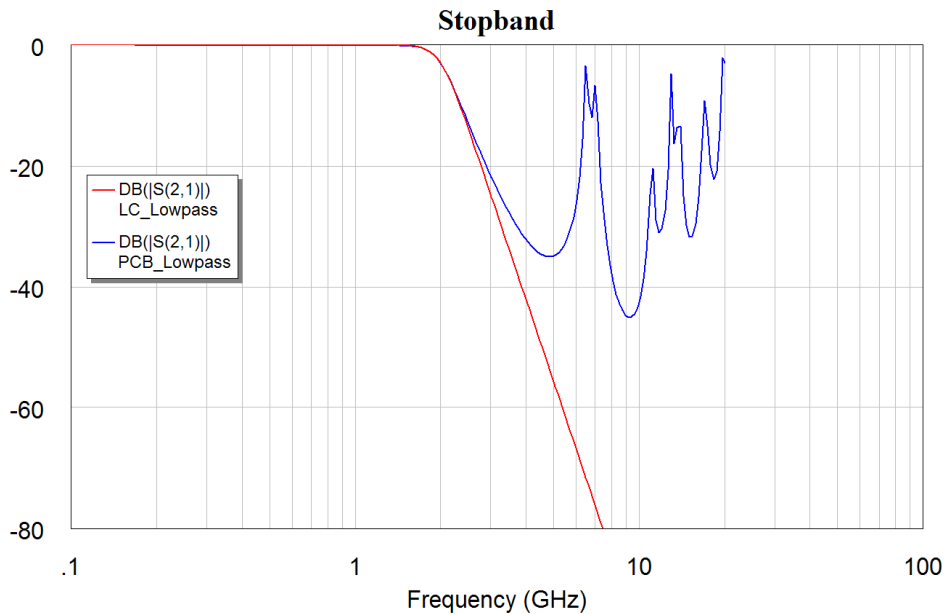


Figure 13. Frequency Response of the LC filter and the corresponding Microstrip design.

Figure 13 compares the frequency response of the ideal LC filter (red) with the PCB filter of figure 12 (blue) and it shows that the PCB filter behaves well in the passband, but that the stopband performance is not very good. That is due to the elements becoming comparable to a quarter or half wavelength long at certain frequencies. By replacing the capacitors with open circuited shunt transmission lines as shown in figure 14, it is possible to obtain a better stopband performance. In addition by making the lengths of the stubs connected at each cross-point slightly different the effect of the transmission lines being one quarter or one half wavelength is minimised. In figure 13, the transmission line has a high impedance of 2.48 kΩ at 2.48 GHz and in figure 14, by using stubs, the impedance is 1.82 kΩ at 9.2 GHz.

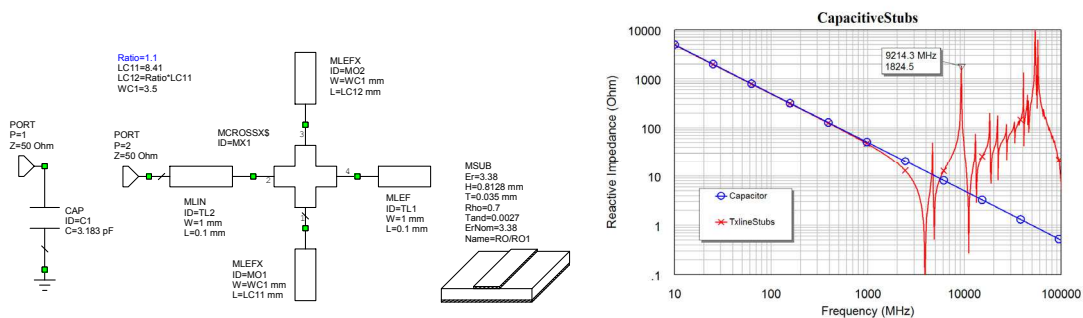


Figure 14. Replacement of capacitors using shunt Microstrip Transmission lines.

By using radial stubs as shown in figure 15, the resonance can be extended even further to give an peak impedance of 1.59 kΩ at a frequency of 12.5 GHz. The shape of the radial stub is shown in figure 15. The angle for that stub is set to 60 degrees. A wider angle stub will push the high impedance frequency even further. It is possible in a filter to vary the angles to ensure that the resonances do not coincide.

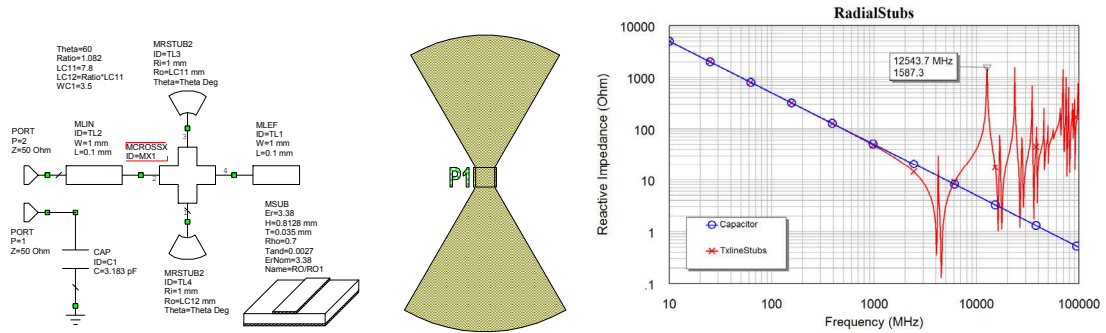


Figure 15. Replacement of capacitors using shunt Radial Stub Microstrip Transmission lines.

The transmission line replacement for all the elements in the desired lowpass filter can be calculated in a similar manner. Once the circuit schematic for the whole filter is complete, the lengths and width of the stubs and the lengths of the inductive sections are optimised to ensure the filter meets the passband and the stopband specifications. As part of this, the width to length ratio of the stubs can be changed to increase the attenuation at particular frequencies in the stopband. The resulting circuit diagram is shown in figure 16.

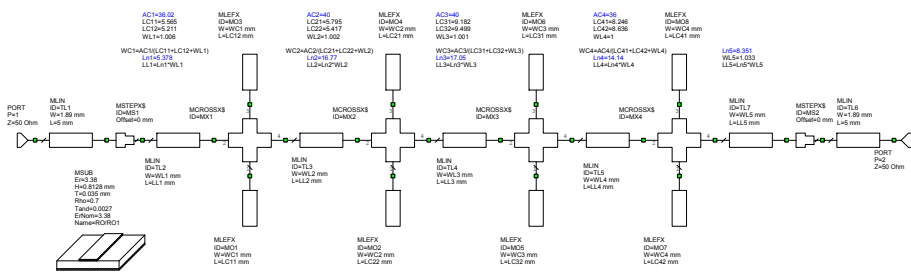


Figure 16. Circuit Schematic for the 2 GHz Lowpass Filter.

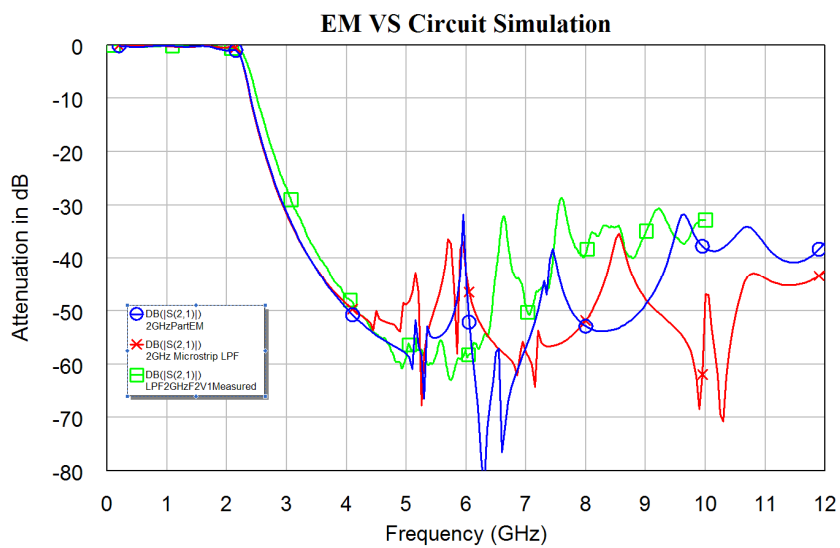


Figure 17. Frequency Response of the 2 GHz Lowpass Filter.

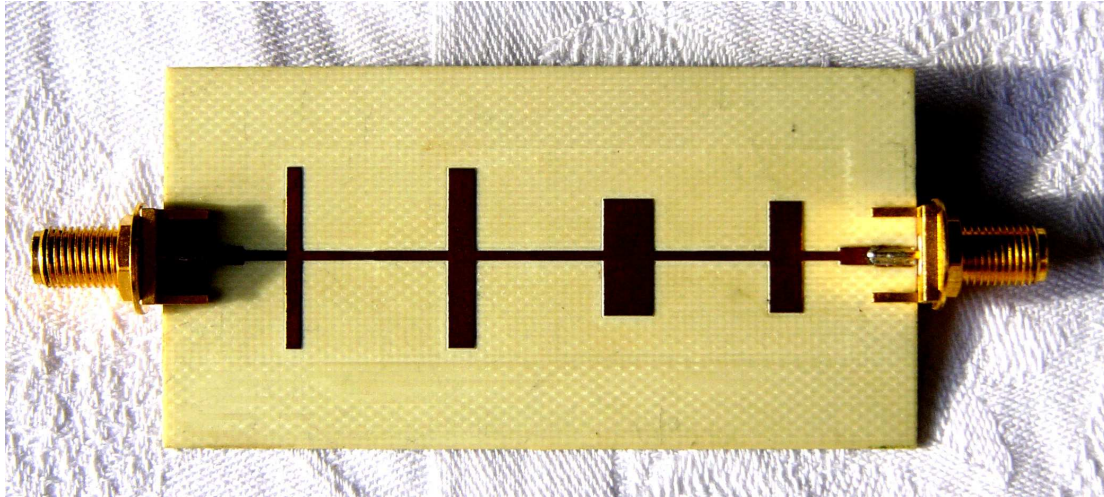


Figure 18. 2 GHz Lowpass filter hardware.

The behaviour of the resulting filter is also calculated using a full Electro-Magnetic simulation of the capacitive stub lines. Since the transmission lines replacing the inductors can be modelled accurately using a non-EM simulation, only a partial EM simulation, for modelling the capacitors, is required. The frequency response obtained from the circuit simulation, the partial EM simulation and the measured performance is shown in figure 17. It can be seen that there is a good agreement for frequencies below 4 GHz but that the stopband behaviour is still not adequate. The filter hardware realisation is shown in figure 18.

The attenuation in the stopband can be improved by adding open circuited stubs which create a transmission zero in the stopband at the frequencies where the filter without the stubs has an inadequate attenuation.

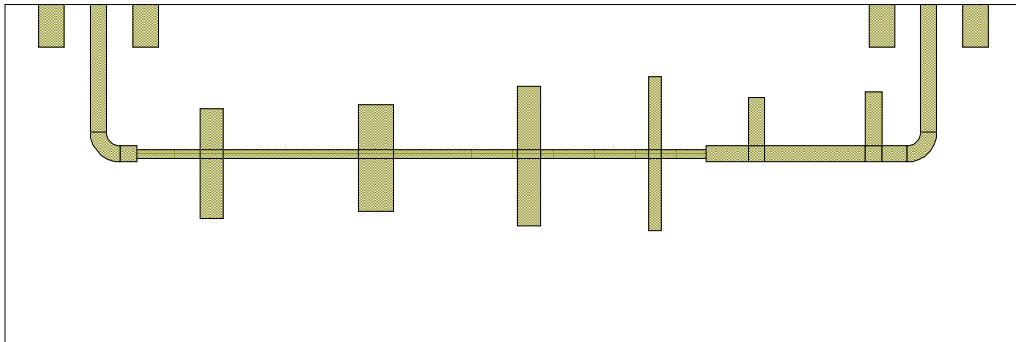


Figure 19. 2 GHz Lowpass Filter with Stubs Added.

In this application, a good stopband performance to 6 GHz was required. The stubs will affect the passband performance and the circuit elements need to be re-tuned and optimised to restore the passband performance to match that of figure 17. The resulting PCB layout is shown in figure 19.

Figure 20 shows the simulated and measured performance of the resulting filter. The simulated performance has a very good stopband performance. The measured performance has a significant amount of coupling between the input and output, which is due to electromagnetic coupling between the input and output tracks and leads

connecting the filter. The stopband performance was improved by enclosing the filter and placing microwave absorber on the ground-plane on the back of the filter and on the inside lid of the enclosure.

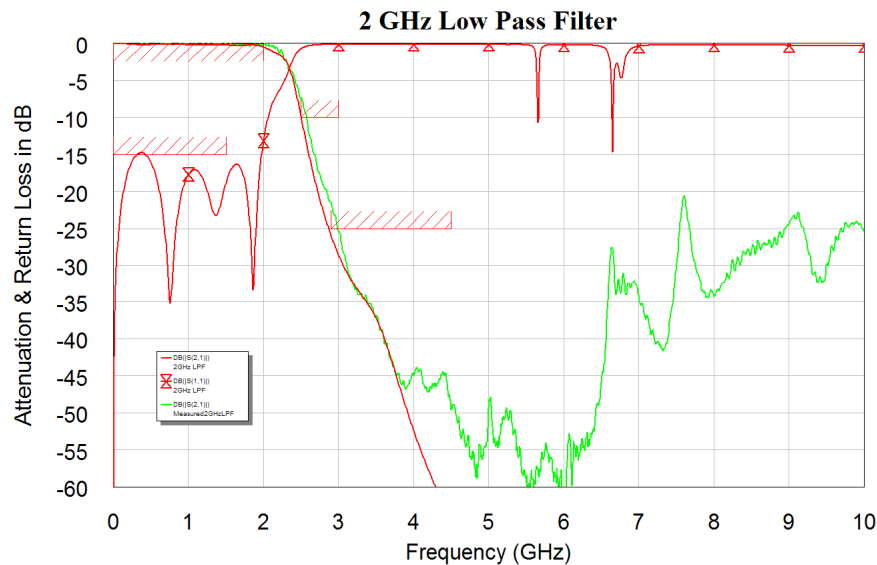


Figure 20. Simulated and Measured Performance of 2 GHz Lowpass Filter with Stubbs.

Bandpass Filter Design

LC Bandpass Filters

To illustrate the design principles, a filter with a centre frequency of 18.48 MHz and a bandwidth of 2 MHz is designed using different techniques. This particular filter was required for a weather satellite data receiver, designed at JCU, to filter the IF data signal prior to demodulation. Since the transmitted signal is a Binary Phase Shift Keyed (BPSK) modulated RF signal containing digital data, a Bessel filter results in the lowest BER after demodulation.

Low-Pass to Band-Pass Transformation

A simple way of designing bandpass LC filters is to use the low-pass to band-pass transformation, described in most filter books. The low-pass to band-pass transformation will often give impractical component values for the bandwidths required for most RF filters. As a result, the low-pass to band-pass transformation is not suitable for most bandpass filter designs.

More practical component values are obtained using coupled resonator designs. The filter resulting from the low-pass to band-pass transformation is shown in figure 21. A 2.0 mH and a 4.4 mH inductor is required. These are a very large inductors and will be difficult to make with acceptable Q values. Figure 22 shows the frequency response of this filter. The low-pass to band-pass transformation has transformed the amplitude response correctly, but the group delay is no longer flat.

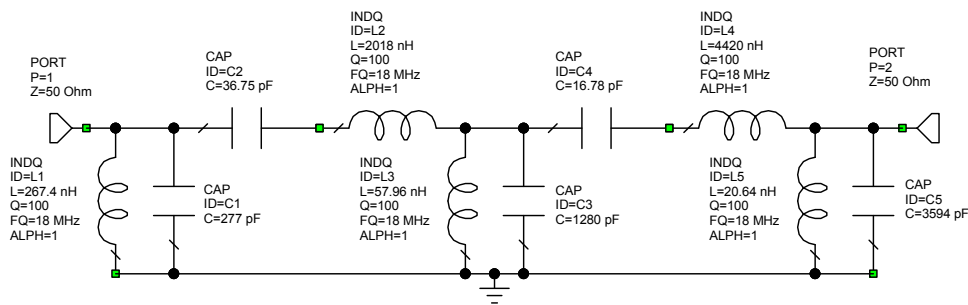


Figure 21. Filter from Lowpass to Bandpass Transformation.

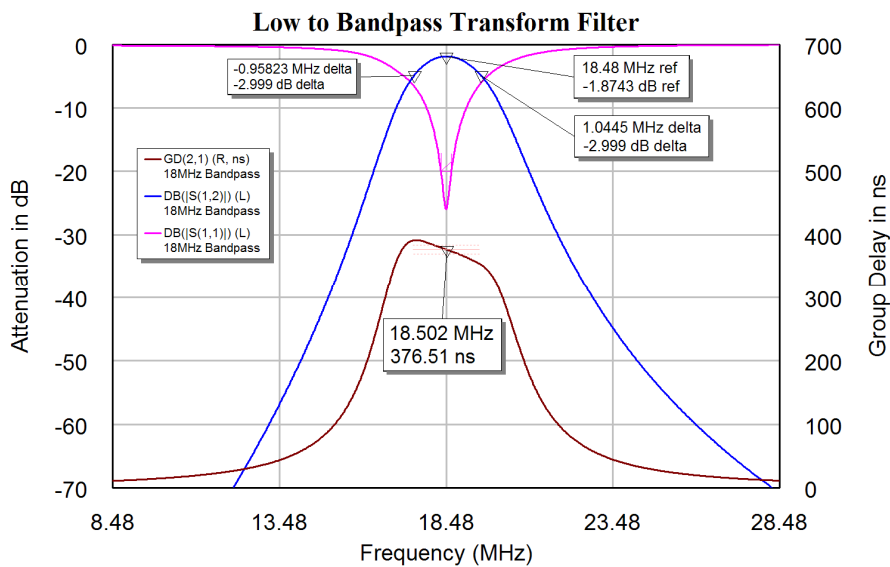


Figure 22. Frequency Response of Filter of Figure 19.

LC Coupled Resonator Filter

In coupled resonator filters, the filter consists of a series of resonators, which are coupled using impedances, coupling loops or apertures. The centre frequency of the filter is determined by the frequency of the resonator and the bandwidth of the filter is determined by the coupling between the resonators. The input impedance of the filter is determined by the coupling into the first resonator and output impedance is determined by the coupling out of the last resonator. For LC coupled resonator filters, the resonators consist of parallel LC circuits. The coupling between LC resonators can be done by connecting capacitors between the resonators, this is called capacitive coupling. The coupling can also be done by connecting inductors between the resonators, this is called inductive coupling. Capacitive coupling is the cheapest as standard capacitors can be used, while the inductors often need to be wound individually. Filter tables, equation 3 or for Butterworth filters, equations 5 give the required coupling factors (K) for the desired filter.

The loading required to achieve the desired first and last resonator Q values, can be obtained from the Q values of the filter tables, from equation 3 or for Butterworth filters, equation 4. In many cases, filters with 50 Ω input and output impedances are

required, while the desired loaded Q values of the resonators require very different impedances. A capacitive impedance transformer can be used to obtain the required impedance transformations.

Equations 3 and 4 only apply for lossless resonators. The K and Q filter tables in Zverev allow the filter to be designed to accommodate the finite Q values of the LC resonators, which result in the filter having an insertion loss. Table 1 shows the K and Q value table from Zverev for Butterworth filters. Denormalising the filter coefficients:

$$K_{ij} = k_{ij} \frac{BW}{F_c} \text{ and } Q_n = q_n \frac{F_c}{BW} \quad \text{Eqn. 6}$$

Zverev shows that the coupling capacitor is given by:

$$C_{ij} = K_{ij} \sqrt{C_i C_j} = k_{ij} \frac{BW}{F_c} \sqrt{C_i C_j} \quad \text{Eqn. 7}$$

where C_i and C_j are the resonator capacitors for the i th and j th resonator and K_{ij} is the denormalised coupling coefficient, k_{ij} is the normalised coupling coefficient from the tables, F_c is the centre frequency and BW is the filter bandwidth. Note the coupling capacitors are to be included in the total capacitance of the resonator so that for the resonator j the resonating capacitance is given by:

$$C_j = C_{res} - C_{ij} - C_{jk} \quad \text{Eqn. 8}$$

where C_{res} is the total resonating capacitance as determined from the resonant frequency and inductance for the resonator. Using coupling inductors results in:

$$L_{ij} = \frac{\sqrt{L_i L_j}}{K_{ij}} = \frac{F_c}{k_{ij} * BW} \sqrt{L_i L_j} \quad \text{Eqn. 9}$$

Where L_i and L_j are the resonator inductors. In a similar manner, the coupling inductors must be considered to be part of the inductance of the resonator, so that the total resonator inductance is made up the inductance of the resonator in parallel with the coupling inductors on either side.

$$\frac{1}{L_j} = \frac{1}{L_{res}} - \frac{1}{L_{ij}} - \frac{1}{L_{jk}} \quad \text{Eqn. 10}$$

where L_{res} is the total resonating inductance as determined from the resonant frequency and capacitance for the resonator. To facilitate the design of these filters, a visual studio .net program, shown in figure 23, has been developed for LC filters with capacitive coupling and is available for download from the AWR web site.

The design process is illustrated using the Bessel filter with a 18.48 MHz centre frequency and 2 MHz bandwidth filter, in the previous design. The filter design requires 4 resonators. Inductors with an inductance of 200 nH and an unloaded Q_0 of 100 are available. In LC resonators, the Q of the capacitors used is generally much higher than the Q of the inductors, so that by using equation 6, the resonator has a normalised q of:

$$q_0 = \frac{BW}{F_c} Q_0 = \frac{2}{18.48} 100 = 10.8. \text{ From the Bessel filter tables in Zverev, the nearest}$$

value corresponds to a q_0 of 10.048 and results in an insertion loss of 1.85 dB. Since the actual Q is slightly higher, one should obtain an actual insertion loss that is slightly less

as is evident from figures 25, 27 and 29. The corresponding K and Q values from this filter table for this value of q_0 are: $q_1 = 0.3891$, $q_4 = 0.5098$, $k_{12} = 1.7120$, $k_{23} = 0.6794$ and $k_{34} = 0.8512$. Entering those values in the LC Bandpass Filter design program gives the filter values as shown in figure 23. Entering those values in a Microwave Office schematic gives the filter shown in figure 24.

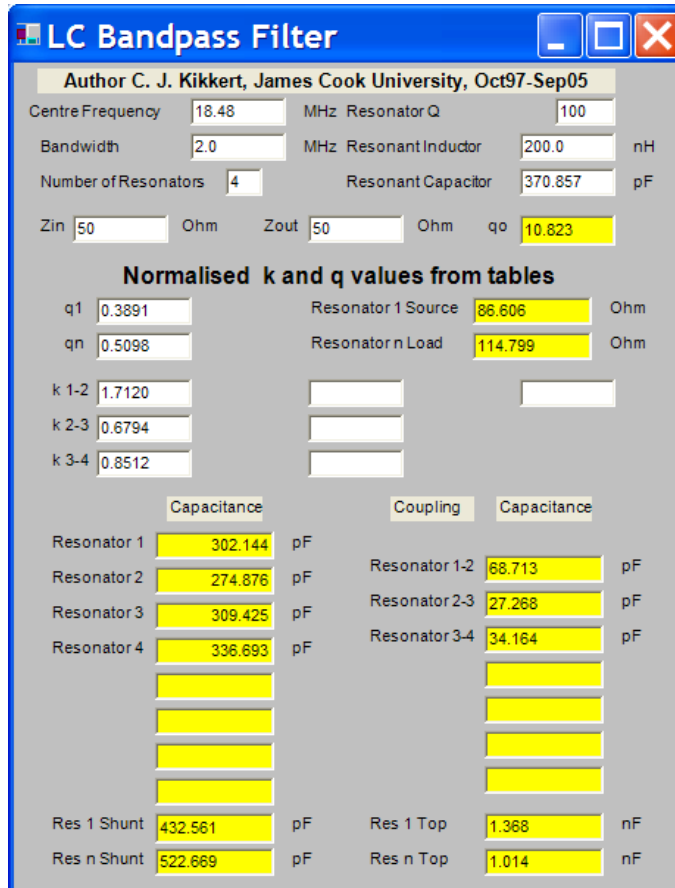


Figure 23. LC Bandpass Filter Design Program for a Bessel Filter.

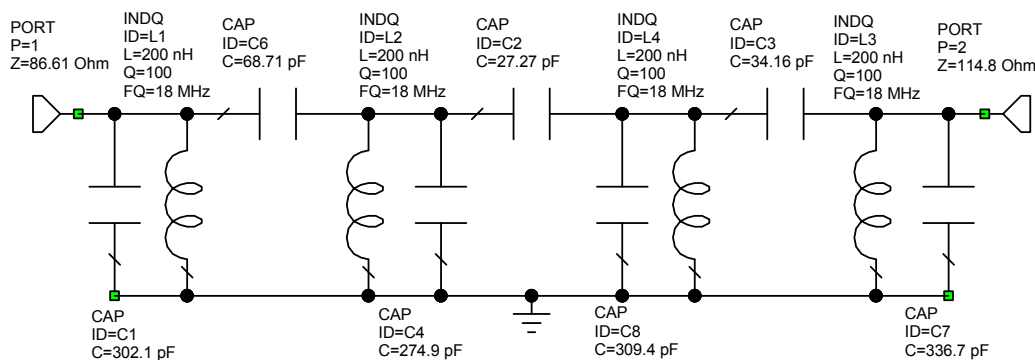


Figure 24. Capacitive Coupled Bessel LC Coupled Resonator Filter.

By comparing figure 22 and figure 25, it can be seen that capacitive coupling reduces the attenuation at high frequencies and increases the attenuation at low frequencies. In addition, the group delay is less flat than for the lowpass to bandpass transformation.

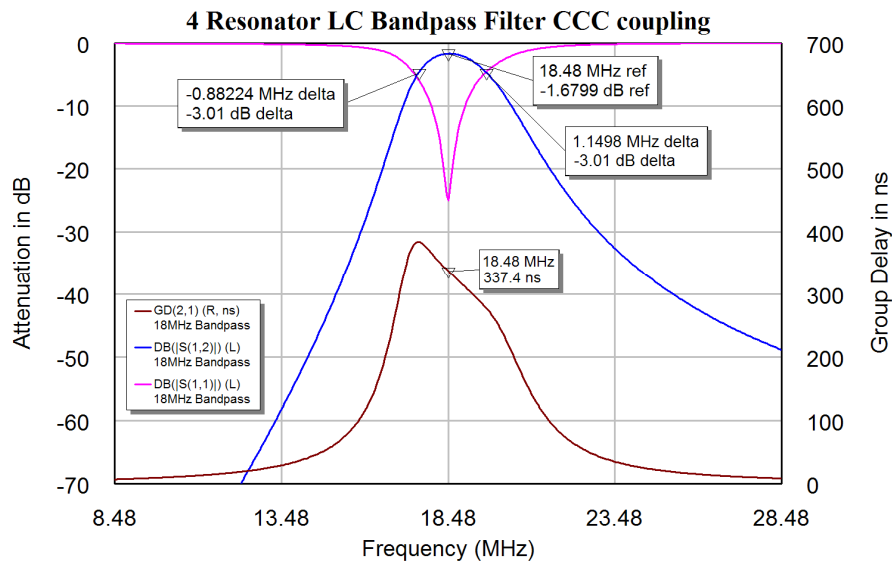


Figure 25. Frequency Response of the Filter of Figure 24.

Instead of using capacitive coupling, inductive coupling can be used. For capacitive coupling the total resonating capacitance is made up of the capacitor of a resonator plus the adjacent coupling capacitors according to equation 8, which is incorporated in the LC Bandpass filter design program of figure 23. For inductive coupling the capacitance of the resonators are simply the resonant capacitance (370.857 pF in the design example) and the inductance of the resonator is adjusted to account for the coupling inductors, resulting in the circuit of figure 26. Figure 27 shows the frequency response of the filter. The group delay for inductive coupling has an opposite slope to the one for capacitive coupling. By using a combination of capacitive and inductive coupling, as shown in figure 28, a flatter group delay is obtained, as shown in figure 29.

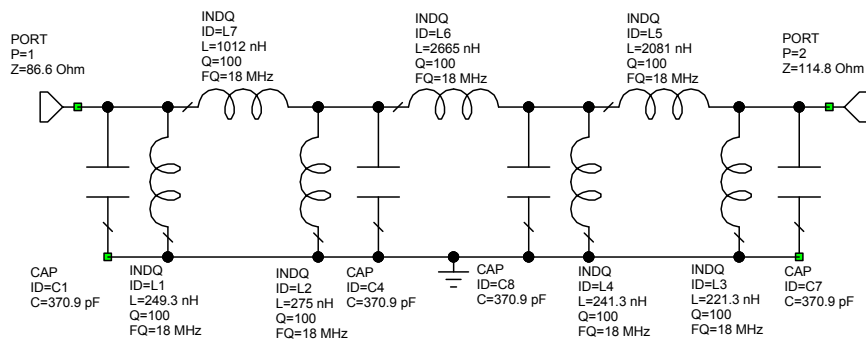


Figure 26. Inductively Coupled LC Resonator Filter

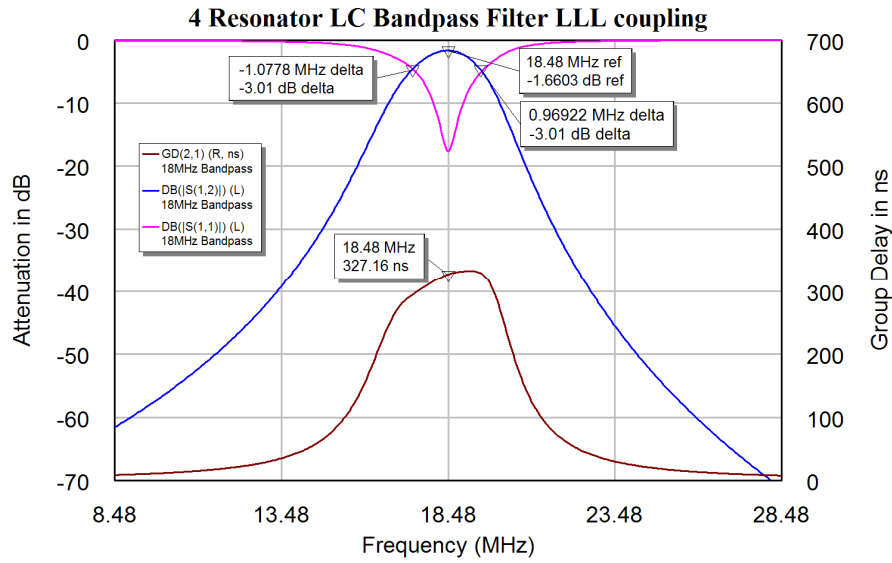


Figure 27. Frequency Response of the Filter of Figure 20.

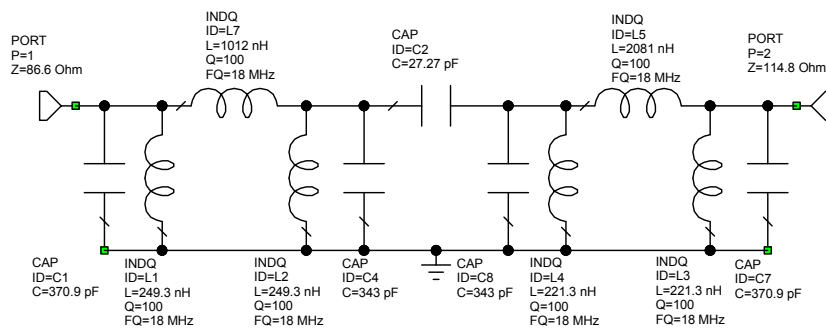


Figure 28. Filter with Both Capacitive and Inductive Coupling.

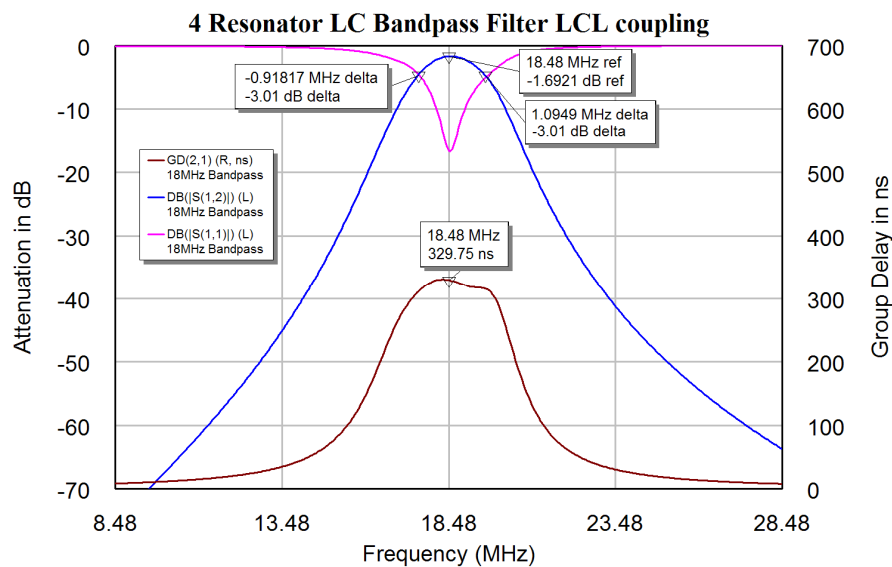


Figure 29. Frequency Response of the Filter of Figure 28.

The input and output impedances of the filter can be changed to 50Ω , by replacing $C1$ and $C7$ with capacitive transformers as shown in figure 30. This will slightly change the frequency response and the group delay. To achieve the best input and output match and a flat group delay, the filter is optimised to meet these specifications. To achieve the lowest insertion loss at the centre frequency. S_{11} and S_{22} are optimised to be better than -30 dB at 18.48 MHz. The group delay is optimised to be as close to 325 ns as possible. Having a constant group delay results in a Bessel type filter and the filter bandwidth is determined by the group delay. The 325 ns group delay results in a 2 MHz bandwidth. The component values after optimisation are shown in figure 30. Figure 31 shows the corresponding frequency response. The resulting filter has a very flat group delay.

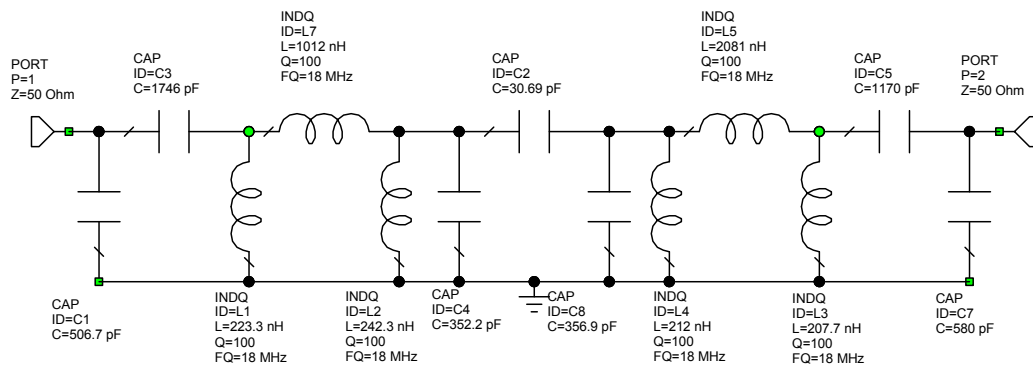


Figure 30. Optimised Coupled Resonator LC Filter.

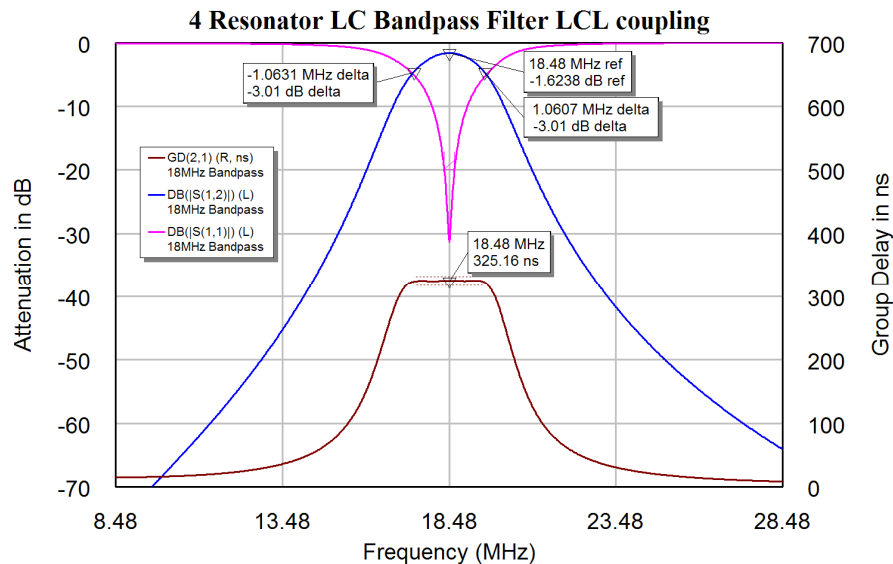


Figure 31. Frequency Response of the Filter of Figure 30.

HF Filters

At higher frequencies tuneable inductors become difficult to make and the inductors can be replaced by microstrip inductors as shown in figure 32. This is a Capacitive Coupled LC resonator filter with a 160 MHz centre frequency and a 27 MHz bandwidth. The vertical transmission lines form the inductors. The parallel plates at the end of the

transmission lines are pads for capacitors. Sufficient space is allowed to have 2 capacitors in parallel to permit the capacitors to be realised with a high precision. The first and last inductors are tapped transmission lines, to allow the input and output to be coupled to the filter at the correct impedances. Figure 33 shows the frequency response of the filter. This filter had to satisfy passband insertion loss constraints and as a result it corresponds to a Butterworth type frequency response and the group delay has peaks at the passband edges, similar to figure 2. Like the Bessel type filter of figure 25, the group delay is bigger at the lower corner frequency than the upper corner frequency. Like the other capacitive coupled filters, the attenuation at higher frequencies (220 MHz) is far less than the attenuation at lower frequencies (100 MHz). The measured frequency response of the filter is close to the calculated response shown in figure 33.

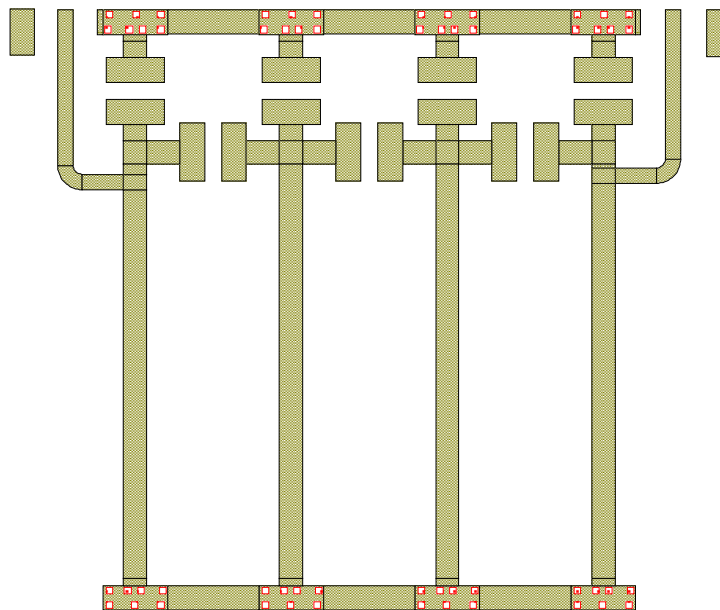


Figure 32. Coupled Resonator Filter using Microstrip Inductors.

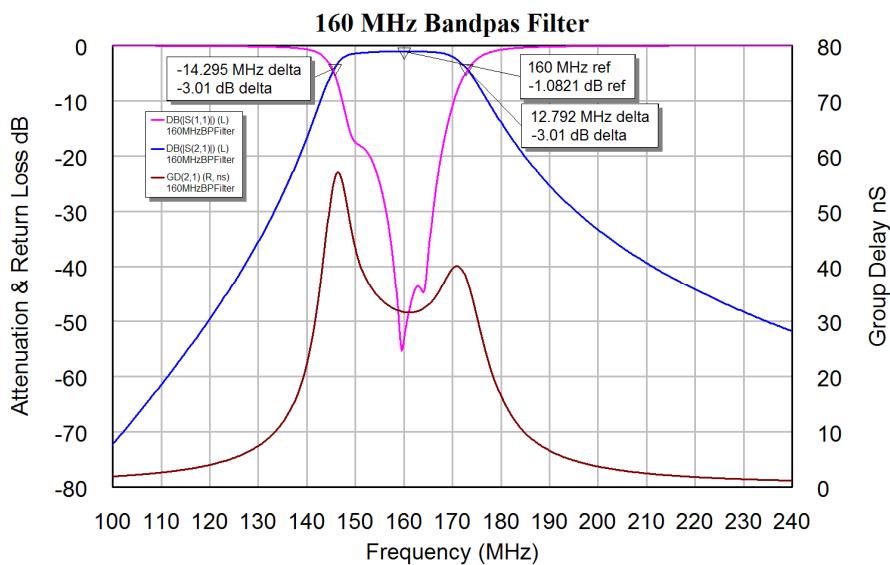


Figure 33. Frequency Response of the Filter of Figure 24.

Cauer-Chebyshev Bandpass filters

Cauer-Chebyshev filters have zeros in the stopband resulting in an equal ripples in the stopband as well as having ripples in the passband. It is more difficult to include zeros in the stopband of coupled resonator RF filters, as this requires coupling between adjacent resonators. It is however possible to include zeros of transmission by including open circuited stubs of one quarter wavelength at the appropriate frequency. Such stubs are normally used to suppress the unwanted passbands occurring at the second and third harmonic of the passband frequency. In other RF filters, transmission zeros are placed at frequencies that must be rejected, such as the transmission frequency in the receive input of a diplexer. In these cases an equal stopband ripple design as specified by the Cauer-Chebyshev filters is not implemented.

Parallel Coupled-Line Filter

This filter type is also known as a Stripline Filter. For this filter the design equations 11 to 14 can be used. However one can also use the generalised coupled resonator filter equations shown in equations 29 and 30 and applied to the interdigital filter design example on page 6.33.

The filter parameters $a(i)$ and the resulting even and odd mode Characteristic impedances are given as:

$$a(0) = \sqrt{\frac{\pi BW}{2q_1 F_c}} \quad \text{Eqn. 11}$$

$$a(i) = \frac{\pi BW}{2F_c} k_{i,i+1} \quad \text{Eqn. 12}$$

$$Z_{oo} = Z_{in} (1 - a(i) + a(i)^2) \quad \text{Eqn. 13}$$

$$Z_{oe} = Z_{in} (1 + a(i) + a(i)^2) \quad \text{Eqn. 14}$$

In these expressions BW is the Bandwidth of the filter, F_c is the centre frequency, q_1 , q_n are the normalised input and output loaded Q values and $k_{i,i+1}$ is the coupling coefficient between the I^{th} and the $(I+1)^{\text{th}}$ resonator as obtained from filter tables.

Example

Design a 4 resonator filter with a bandwidth of 70 MHz and a centre frequency of 1 GHz. The attenuation should be as low as possible in the passband. The input and output impedances should be 50 Ω . The filter is made using 0.82 mm thick RO4003 substrate with 35 micron copper.

A Butterworth filter type is selected for the initial design. Equations 4 and 5 can thus be used for obtaining the K and Q values, or they can be taken from table 1 to give:

Normalised	De-normalised
$q_1 = q_n = 0.7654$	$Q_1 = Q_n = 0.7654 * 1000 / 70 = 10.93$
$k_{12} = k_{34} = 0.8409$	$K_{12} = K_{34} = 0.8409 * 70 / 1000 = 0.05886$
$k_{23} = 0.5412$	$K_{23} = 0.5412 * 70 / 1000 = 0.03788$

Substituting this into equations 13 and 14 and substituting the resulting $a(0)$ and $a(i)$ into equations 11 and 12 gives the values for Z_{oe} and Z_{oo} shown below. Those values are then entered into the TxLine program (or Linecalc for ADS) as shown in figure 34.

Line	a	Z _{0e}	Z _{0o}	Width	Space	Length
0	0.3902	76.13	38.23	1.26 mm	0.12 mm	47.3 mm
1	0.09246	55.05	45.80	1.71 mm	1.08 mm	46.2 mm
2	0.05951	53.15	47.20	1.74 mm	1.57 mm	46.0 mm
3	0.09246	55.05	45.80	1.73 mm	1.2 mm	46.2 mm
4	0.3902	76.13	38.23	1.26 mm	0.12 mm	47.3 mm

Table 3 Parallel Coupled-Line Filter Parameters.

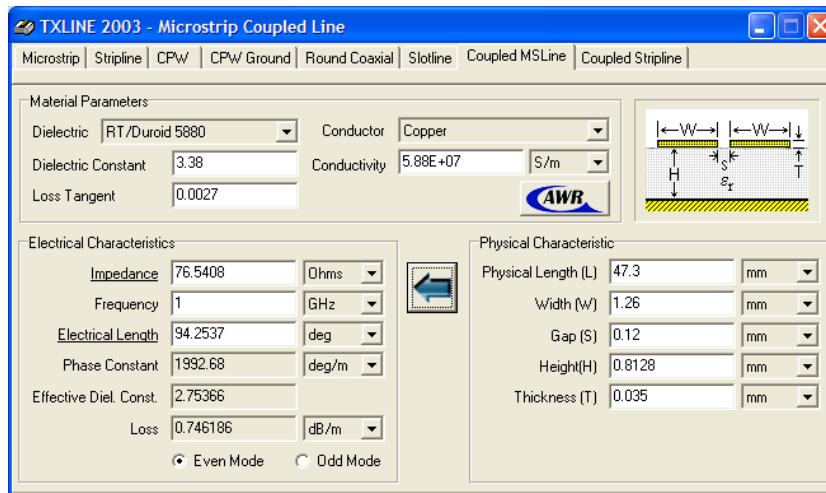


Figure 34. Calculating Line Widths and Coupling Gaps.

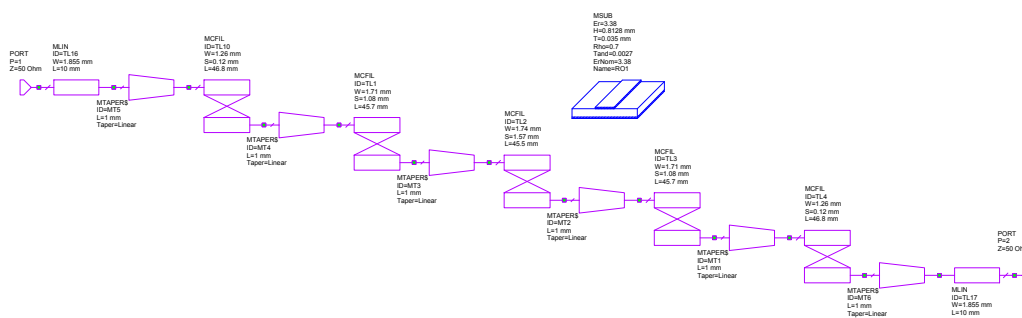


Figure 35. Microwave Office Schematic for the 1 GHz filter

Those line geometries are then entered in a circuit schematic to give the circuit shown in figure 35. End effects have been included by using the Microstrip filter element “MCFIL”. A 1 mm long taper has been added between each coupled section to ensure that the coupled lines do not produce a short circuit at the transition in width. As a result all resonators are shortened by 0.5mm to keep the total resonator length the same. The computer simulation software will produce a layout from the schematic as shown in figure 36. This layout can be plotted and produced as a PCB.

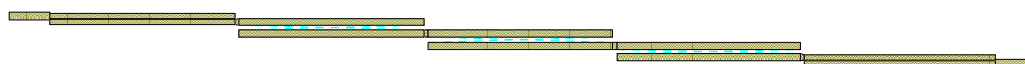


Figure 36. PCB layout for this filter produced by Microwave Office.

Figure 37 shows a close-up of the centre of the first resonator, and shows TL10, MT4 and TL1 of figure 35. It can be seen that without the tapered transition a short circuit would be produced. The filter from figure 35 as designed using the above procedure has a centre frequency of 981 MHz, and is 1.9% low. The bandwidth is 62 MHz and is 12 % low. The resonator lengths and coupling gaps are optimised, using the optimisation routines in MWO, to achieve the correct centre frequency and bandwidth. Since the design procedure gives a result very close to the specifications, the optimisation procedure is quick. The resulting frequency response is shown in figure 38. The insertion loss of the filter is 1.9 dB. The return loss can be improved if needed by setting optimisation goals on S_{11} and using the optimiser to automatically fine tune the elements.

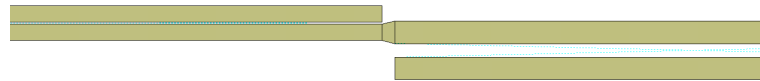


Figure 37. Close-up of part of figure 36, showing TL10, MT4 and TL1.

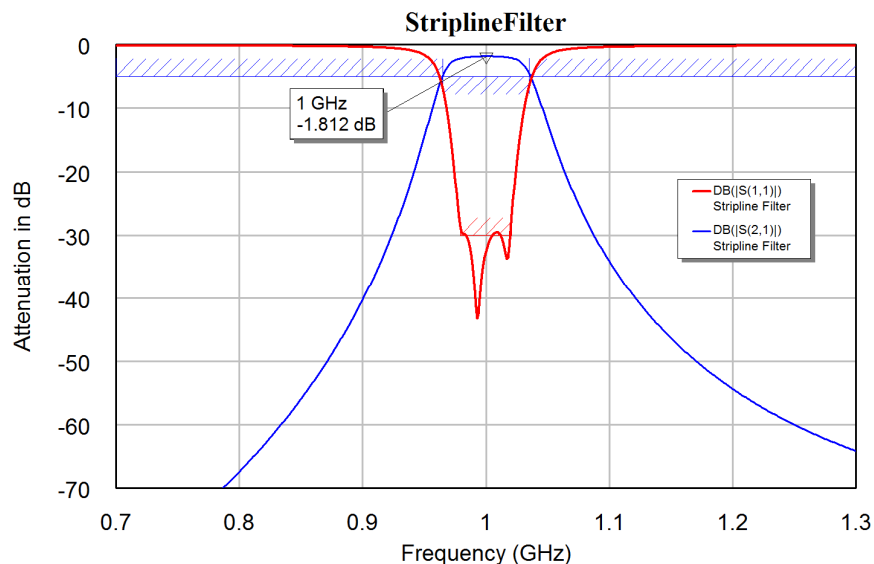


Figure 38. Frequency response of the filter from figure 35 after optimisation.

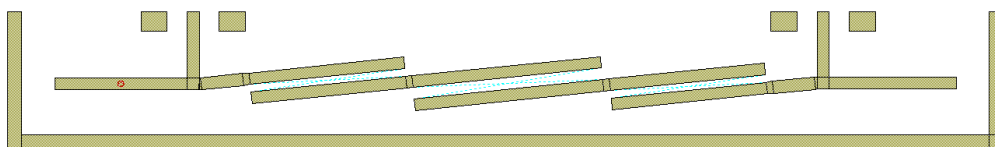


Figure 39. PCB layout for coupled line filter with tap coupling into and out of the filter.

For the filter in figure 35, 36 and 37, the input coupling gap is 0.14 mm. This gap is close to the limit of reliable manufacturing capability at JCU. To avoid this limitation, tap coupling is used to connect to the input and output resonators, as shown for the 100 MHz bandwidth at a 1.7 GHz centre frequency filter shown in figure 39. For wider bandwidth filters the input and output coupling gaps are very small and tap coupling is best. For very narrow bandwidth filters, the connection point for tap coupling becomes

too close to the effective ground point of the first resonator, so that line coupling as shown in figure 35 is more practical.

The actual filter, when produced, will have a centre frequency and bandwidth that will be slightly different from the simulated results. These differences are due to the computer simulation not being completely accurate, variations in PCB substrate materials, etching or milling errors in producing the PCB and so on. In many instances, the filter performance will be good enough. When the filter specifications are critical, a second iteration of the filter can be produced, where the simulation is biased to correct for the discrepancy between the measured and simulated results.

Hairpin Filter

The filters of figure 36 and 39 are long and skinny and are difficult to mount securely. To obtain a better form factor for the filter, the resonators can be folded as shown in figure 40. Coupled Resonator filters where the resonators are made up from quarter wavelength transmission lines will have additional passbands when the wavelength of the resonators are three quarter of a wavelength long, five quarter of a wavelength long and so on. These harmonic resonances are normally undesirable. To avoid these harmonic stubs can be added.

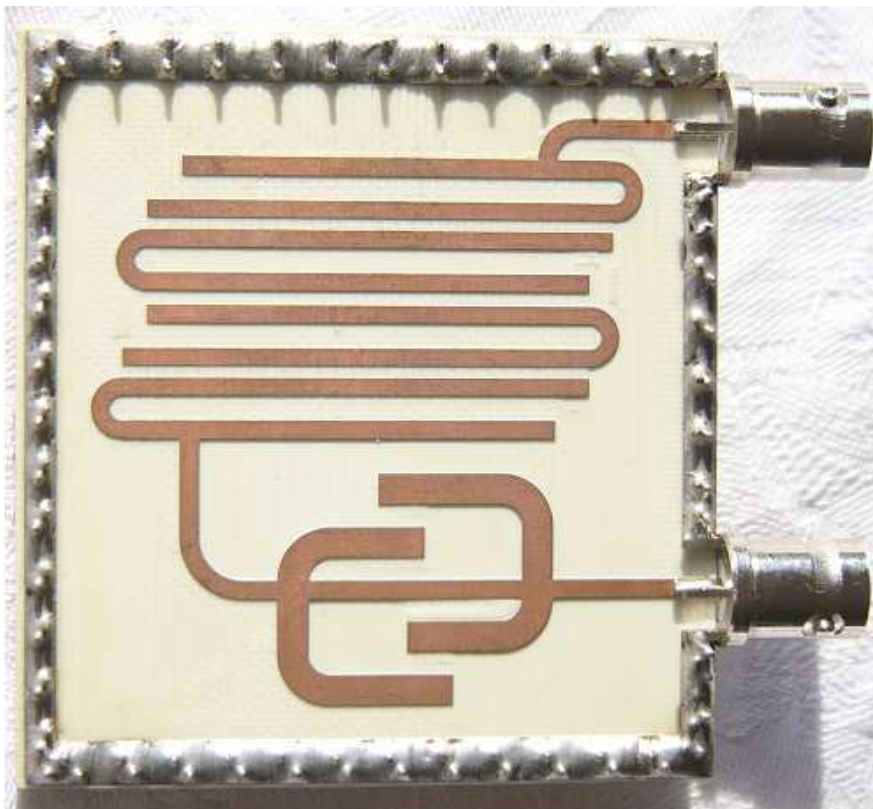


Figure 40. Hairpin filter.

The hairpin filter in figure 40 has two second and third harmonic suppression stubs incorporated as part of the design. The design procedure consists of firstly designing and optimising a basic hairpin filter as outlined in the previous example. Second and Third harmonic suppression stubs are then designed as a separate circuit, as shown in figure 41. The second harmonic stubs are one quarter wavelength long at the second harmonic and the third harmonic stubs are one quarter wavelength long at the third

harmonic. The spacing between the stubs is then adjusted such that the return loss of the circuit is large at the centre frequency of the filter, so that the harmonic stub circuit has the least effect on the filter performance. The stubs are folded to minimise the space used by the whole filter.

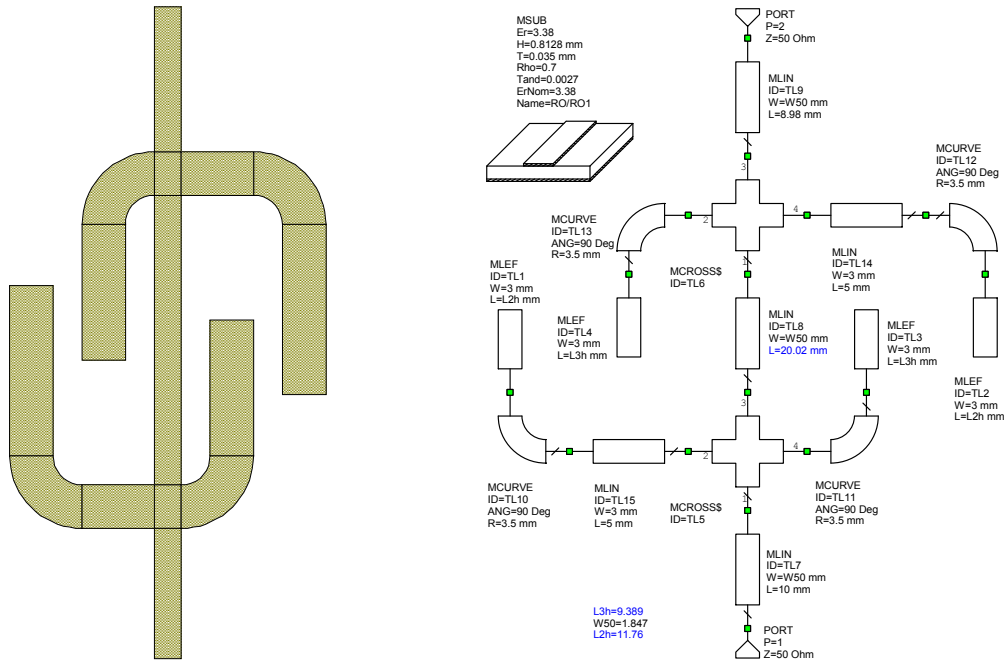


Figure 41. Folded Harmonic Stubs.

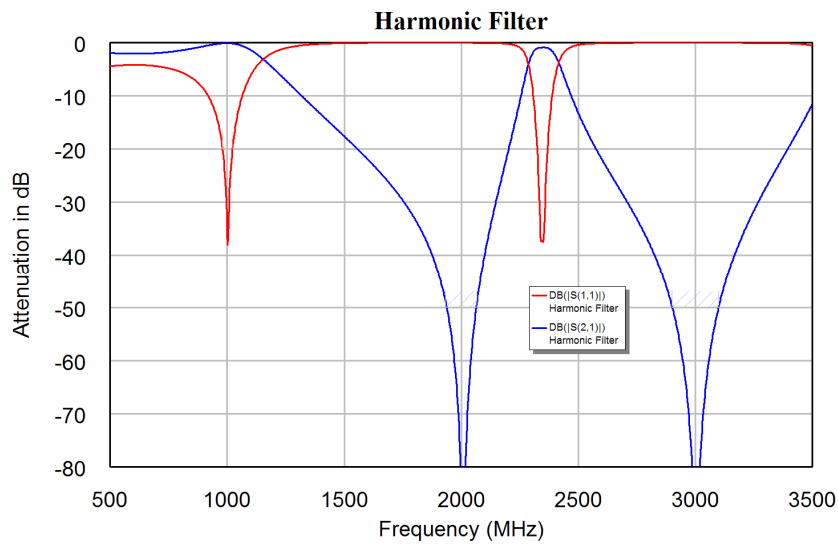


Figure 42. Frequency Response of Harmonic Stubs.

Figure 42 shows the frequency response of the harmonic stub circuit. It can be seen that there is some effect on the passband of the filter, so that further optimisation must be carried out in order to ensure that the combination of the hairpin filter and the harmonic stubs have the required passband response. Figure 43 shows the passband frequency response of the actual filter of figure 40 and compares it with the frequency response of the simulation. The filter was realised using the “MCFIL” elements used in figure 35

and using the coupled line element “MCLIN” with “MLEFX” or “MOPEN” elements compensating for the end effect of the open circuited ends of the coupled line elements. In addition an Electro Magnetic simulation is carried out on the coupled line sections. It can be seen that all the simulations give a good agreement with the measured results. The EM simulation in blue gives the poorest accuracy and requires the most computations.

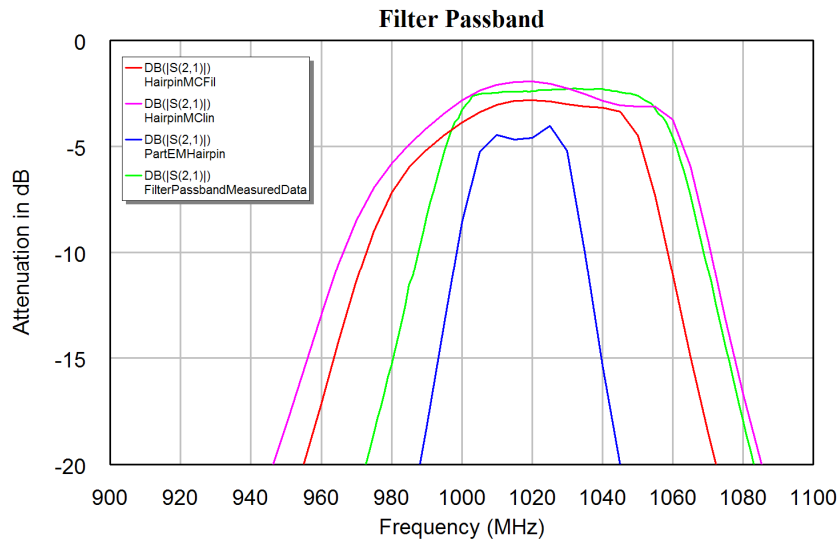


Figure 43. Frequency response of Hairpin filter.

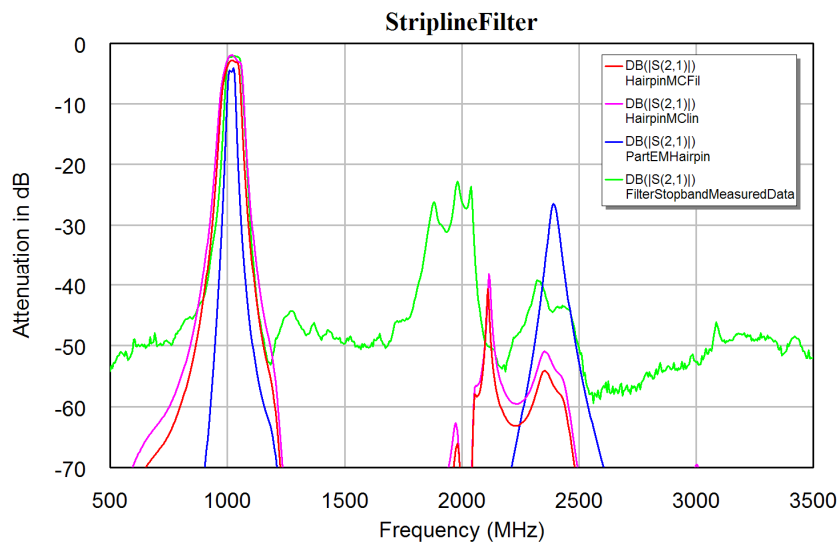


Figure 44. Frequency response of Hairpin filter of figure 40.

Figure 44 shows the stopband performance of the filter for both the measured performance and the computer simulation. The most significant difference is the reduction in attenuation in the stopband. This is due to Electro-Magnetic radiation between parts of the circuit and the input and output leads. The stopband attenuation can be optimised by mounting the filter in a conductive (aluminium) enclosure and applying microwave absorbing material in the appropriate places, to be determined experimentally. In many cases, applying the absorber to the back groundplane of the filter improves the stopband performance sufficiently.

Helical Filters

For high Q value resonators at UHF frequencies, a cylindrical rod of one-quarter wavelength long is placed inside a cavity. This cavity can be cylindrical but in many cases, the cavity is rectangular for ease of construction. Such filters are called coaxial filters, as the cross-section of the filter is a coaxial transmission line.

At VHF frequencies, the size of the coaxial filter becomes too large for many applications. To reduce the length of the resonator, the centre quarter wave resonator is wound as a helix. Often the helix is wound on a former. One has to ensure that the material for the former is not lossy at the operating frequency. Polyethylene is suitable for low loss formers.

The resonators have shields between them to confine the fields for the resonators. The resonators are coupled by having the appropriate shield height, so that some of the field of a resonator couples to the next resonator. The coupling is controlled by adjusting the difference between the height of the shield and the top of the helix as shown by dimension "h" in figure 45. Alternately, the coupling can be achieved by having a coupling hole in the centre of a full-height shield or by having a slot at the bottom of the shield. The choice of coupling aperture depends on the construction of the cavity.

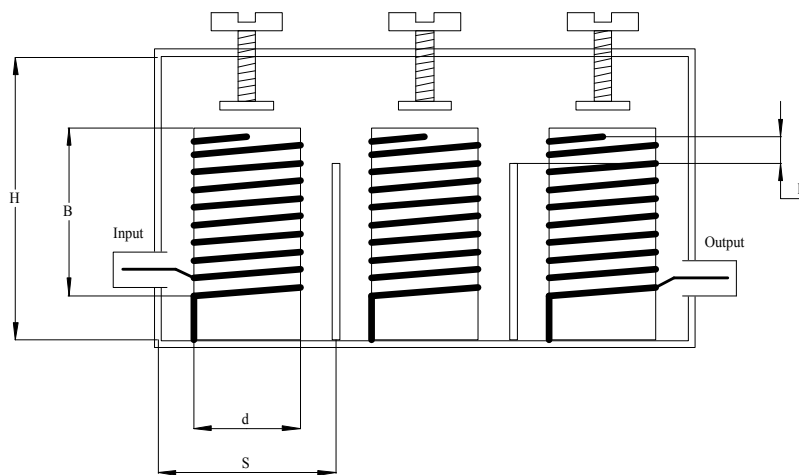


Figure 45. Drawing of a helical filter showing the sizes used in the formulae.

Formula for Helical Filters (from Zverev)

S is the width of the rectangular resonator cavity. (units m)

H is the height of the resonator cavity (units m)

B is the height of the helix (units m)

d is the diameter of the helix (units m)

N is the number of turns of the helix

Z_0 is the characteristic impedance of the helical transmission line in the cavity.

δ is the skin depth. The wire diameter should be > 5 times the skin depth.

Q_0 is the unloaded Q of the resonator cavity (f is in MHz).

If instead of a rectangular cavity, a cylindrical cavity is used, the diameter D of the cavity is $D = 1.2 S$.

For the cavity:

$$d=0.66S \quad \text{Eqn. 15}$$

$$B=S \quad \text{Eqn. 16}$$

$$H=1.6S \quad \text{Eqn. 17}$$

$$Q_0 = 2363 \times S \sqrt{f} \quad \text{Eqn. 18}$$

For the highest Q value, the wire diameter of the helix is chosen such that it is half the pitch of the helix. The gap between the wires is thus the same as the wire diameter.

For the helix:

$$N = \frac{40.6}{S \times f} \quad \text{Eqn. 19}$$

$$\delta = \frac{6.6 \times 10^{-5}}{\sqrt{f}} \quad \text{Eqn. 20}$$

$$Z_0 = \frac{2070}{S \times f} \quad \text{Eqn. 21}$$

$$\frac{R_b}{Z_0} = \frac{\pi}{4} \left(\frac{1}{Q_d} - \frac{1}{Q_0} \right) \quad \text{Eqn. 22}$$

The doubly loaded input Q_d is defined as $\frac{1}{2} Q_1$ for the input tapping point calculation and $\frac{1}{2} Q_n$ for the output tapping point calculation, and represents the total load seen by the resonator if there is a very small insertion loss as is normally the case. The electrical length θ from the bottom of the helix to the point where the input or output connects to the helix is given by:

$$\text{Sin}(\theta) = \sqrt{\frac{R_b R_{tap}}{2Z_0^2}} \quad \text{Eqn. 23}$$

The gap between the shield and the top of the helix is given by:

$$K = 0.071 \left(\frac{h}{d} \right)^{1.91} \quad \text{Eqn. 24}$$

It should be noted that when the bandwidth increases the gap between the top of the shield and the top of the coil increases. For wideband filters no shield is required, thus reducing the cost of construction. In that instance, it is also possible to vary the coupling by varying the spacing between the resonators.

Design Example:

Design a helical filter to have a 1 MHz bandwidth at 100 MHz. A diecast box of 112 mm width and 50 mm depth and 90 mm height is available. This can be split into two cavities 56 x 50 x 90 mm. The average side S is 53 mm. The H/S ratio is $90/53 = 1.7$, which is close enough to the $h = 1.6S$ value from equation 17

The K and Q values required can be obtained from table 1. Since for two resonators and Butterworth filters the K and Q values are independent of the insertion loss, equations 4 and 5 can be used to calculate the required K and Q values.

Equation 4 is $q_0 = q_n = 2\text{Sin} \frac{(2-1)\pi}{2n} = 2\text{Sin} \frac{\pi}{2n}$ and for a two-resonator filter $n = 2$, this gives $q = 2\text{Sin}(45 \text{ deg}) = 1.4142$

Equation 5 is $k_{ij} = \frac{1}{2\sqrt{\text{Sin} \frac{(2i-1)\pi}{2n} \text{Sin} \frac{(2i+1)\pi}{2n}}}$ and for a two-resonator filter this gives $k = 1/(2\text{Sin}(45 \text{ deg})) = 0.7071$

Applying equation 18 gives the unloaded Q of the cavity as: $Q_0 = 2363 * 0.053 * 10 = 1252$. The normalised unloaded Q is $1252 * 1/100 = 12.52$. From the filter table 1, the resulting filter will thus have close to 1 dB insertion loss.

Since $S = 53 \text{ mm}$, applying equation 15 gives the coil diameter as: $d = 35 \text{ mm}$. From equation 17, the coil height is 53 mm and equation 19 indicates it requires 7.6 turns. The optimum wire diameter is thus $53/(2*7.6) = 3.49 \text{ mm}$. A one-eighth of an inch copper tube is 3.2 mm and is used for winding the coil. The minimum wire diameter of five times the skin depth (equation 20) is 0.033 mm. For practical windings, the minimum skin depth requirement is normally satisfied.

From the filter tables $q_1 = q_n = 1.4142$ and $k_{12} = 0.7071$. Denormalising this gives $Q_1 = Q_n = 1.4142 * 100/1 = 141.42$ and $K_{12} = 0.7071 * 1/100 = 0.007071$. Q_1 and Q_n are the loaded Q values, which are due to the input and output load impedance being coupled into the resonators and thus appearing as a load to the resonators. The doubly loaded input Q is defined as $\frac{1}{2} Q_1$ and represents the total load seen by the resonator if there is a very small insertion loss as is the case here. The doubly loaded output Q is defined as $\frac{1}{2} Q_n$. Q_d is thus 70.71 for both the input and output. Putting this in the expression for R_b/Z_0 gives: $R_b/Z_0 = 0.0105$. Since we want the filter to be have 50Ω input and output impedance, $R_{\text{tap}} = 50 \Omega$ resulting in $\theta = 1.48$ degrees. Since the coil wire length is $7.6 * 35 * \pi = 842 \text{ mm}$ and corresponds to 90 electrical degrees, the tapping point should be $1.48 * 842 / 90 = 13.9 \text{ mm}$ from the bottom of the helix. In practice, the tapping point needs to be fine-tuned, to match the actual conditions after construction and include losses of the former used for winding the helix on.

For this Butterworth filter, the tapping points for the input and output are the same. For Chebychev or Bessel filters, or for lossy higher order Butterworth filters, the input and output tapping points will be different, and the above calculation needs to be performed for Q_1 and for Q_n .

The filter was constructed and performed exactly as expected. The measured bandwidth for the helical filter was 1 MHz and the insertion loss was 0.8 dB. A photograph of the filter is shown in figure 46 and the measured response is shown on figure 47.

The tuning procedure for adjusting the tapping point for the input and output, and for verifying and if needed adjusting the coupling, is described in Zverev on page 518 and Figure 9.23. This same procedure is used to determine the coupling factors for interdigital filters as shown in figures 51, 52, and equations 29 and 30 of these notes.

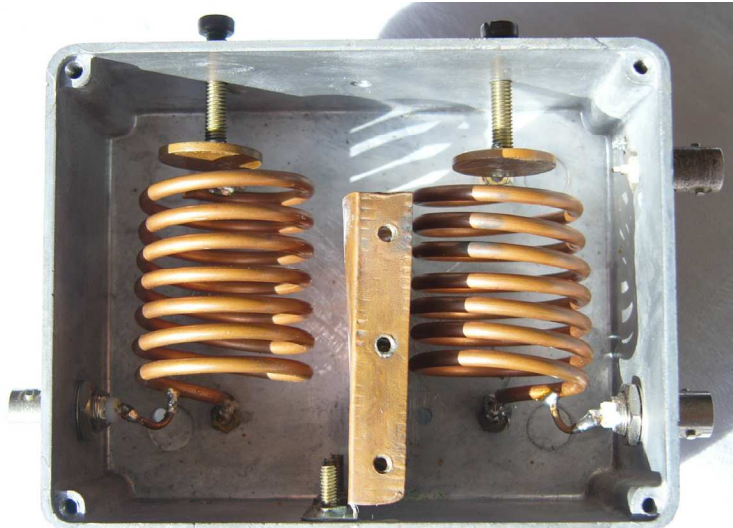


Figure 46. 101 MHz helical filter 1 MHz bandwidth

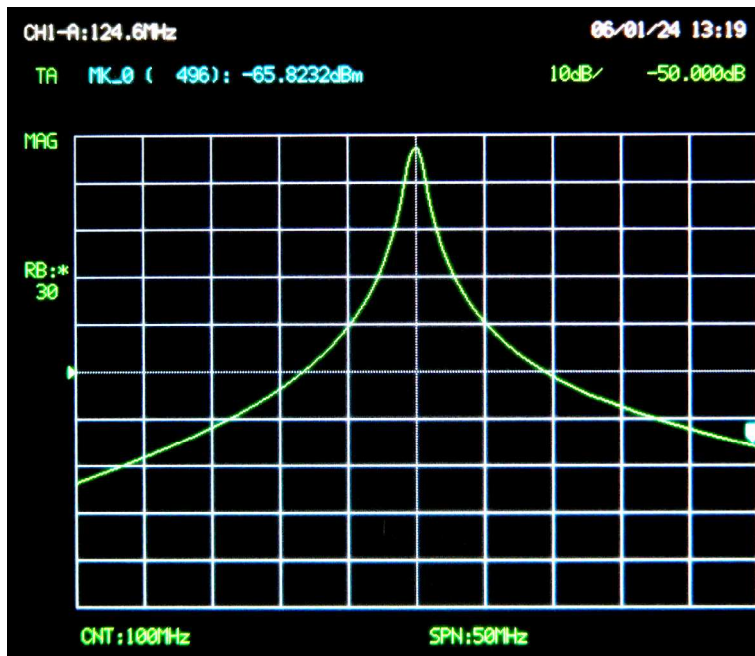


Figure 47. Frequency response of 101 MHz helical filter, vertical 10 dB/div.



Figure 48. Commercial Helical Filters. Temwell Left, Toko Right.

The left filter in figure 48 shows a 3-resonator 142 MHz helical filter with a bandwidth of 6 MHz from Temwell (www.temwell.com.tw). Each resonator is 8mm wide and 12mm high. Temwell make filters from 45 MHz to 2.6 GHz. The right filter is an older, 3-resonator, 137 MHz helical filter with a bandwidth of 2 MHz made by Toko (www.toko.co.jp). The resonators are 12mm wide and 18mm high. Toko now only make helical filters for 350 MHz to 1.5 GHz. The measured dimensions of these filters are the outside dimensions of the cavities. The ratio of the internal dimensions thus satisfies equation 17.

Interdigital Filters

With interdigital filters, the resonators are grounded at alternate ends. This reduces the coupling between the resonators and as a result, a compact filter can be constructed that has no walls between the individual resonators. A drawing of an interdigital filter is shown in figure 49a.

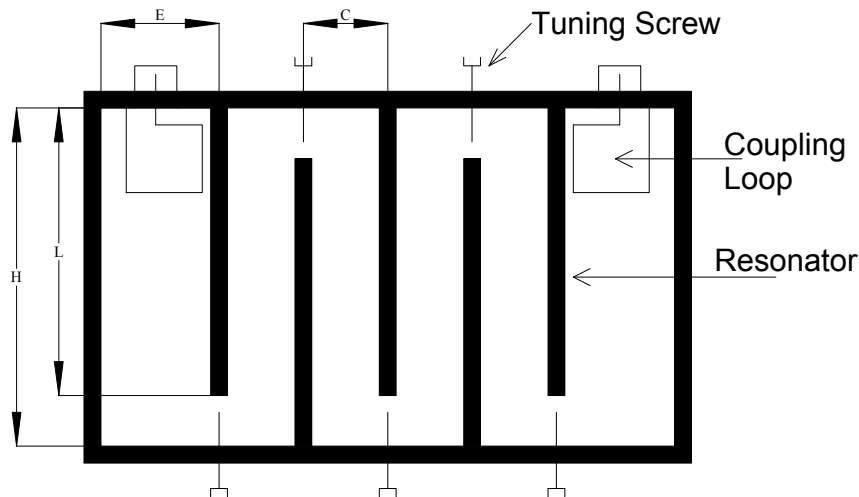


Figure 49a. Interdigital filter dimensions.

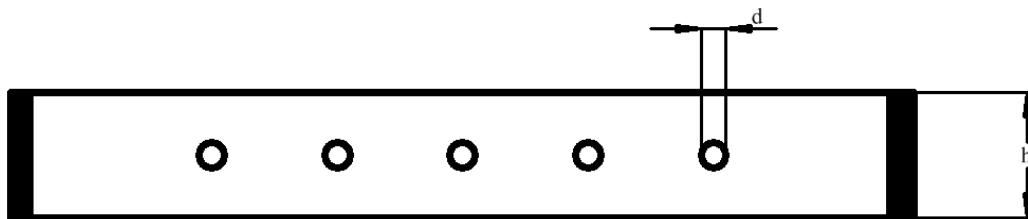


Figure 49b. Interdigital filter dimensions.

For a small bandwidth (<10%) M. Dishal in his paper, "A Simple Design Procedure for Small Percentage Bandwidth Round Rod Interdigital Filters" MTT, Vol 13, No5, Sep 1965, pp 696 – 698, provided the following equations for designing interdigital filters:

$$\frac{E}{h} = 0.6$$

Eqn. 25

$$\text{Log } K = \left[-1.37 \frac{C}{h} + 0.91 \frac{d}{h} - 0.048 \right] \quad \text{Eqn. 26}$$

Where h (figure 49b) is the spacing between the walls and d is the rod diameter. Knowing K from the filter tables and d and h from the design specifications, allows the spacing C between the resonators to be calculated.

In addition, the impedance of the resonator is given by:

$$Z_0 = 138 \text{Log} \left[\frac{4h}{\pi d} \right] \tanh \left(\frac{\pi E}{h} \right) \quad \text{Eqn. 27}$$

The singly loaded Q of the resonator is:

$$Q_1 = \frac{\pi R}{4Z_0} \frac{1}{\text{Sin}^2 \left(\frac{\pi \ell_1}{2L} \right)} \quad Q_n = \frac{\pi R}{4Z_0} \frac{1}{\text{Sin}^2 \left(\frac{\pi \ell_n}{2L} \right)} \quad \text{Eqn. 28}$$

Since Q_1 and Q_n can be obtained by de-normalising q_1 and q_n from filter tables, R is the desired termination impedance, (usually 50Ω) and Z_0 is the characteristic impedance of the resonator as obtained from equation 27, that the tapping points ℓ_1 and ℓ_n can be determined using equation 28. Interdigital filters can be constructed in two forms:

Round Rod Interdigital Filters

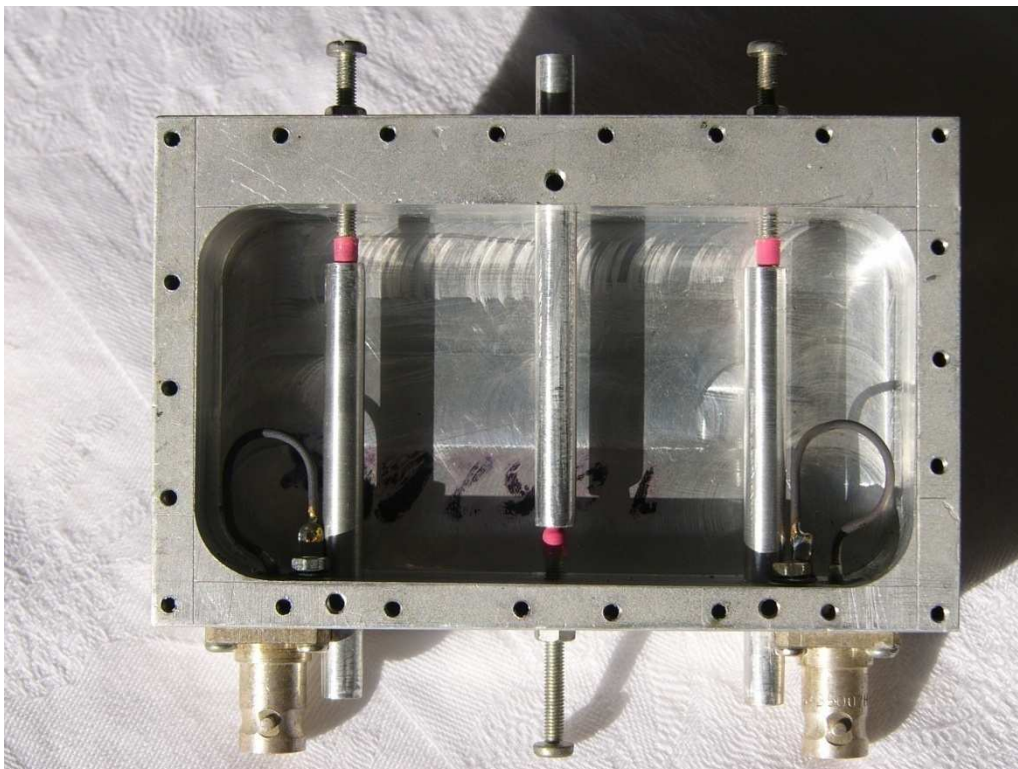


Figure 50. Interdigital filter for operation at 940 MHz, with top plate removed.

Similar to the Helical filter, the larger the filter cavity, the lower the insertion loss of the filter and the bigger the power handling capability of the filter. The Round Rod Interdigital filters are reasonably large and as a result have a low insertion loss and a

high power handling capability, permitting them to be used at the output of transmitters. These filters normally have bandwidths less than 10%. The filters become very large for frequencies below 300 MHz. The coupling into the filter can be achieved by coupling loops as shown in figure 50, or by direct tapping to the resonator rod. In most instances the resonator rods length can be adjusted. This provides a coarse tuning adjustment. In the figure 50, the Allan Key locking screws for the resonator rods can be seen at the base of each of the resonators allow the course adjustment to be performed. A small variable capacitor, in the form of an insulated screw that slides inside the hollow resonator rod, as shown in figure 50, result in filters that can easily be fine-tuned to the correct frequency.

The filter in figure 50 was designed using equations 25 to 28. Applying the course-tuning and fine-tuning and adjusting the coupling loops enabled a filter to be obtained, which satisfied the design specifications exactly.

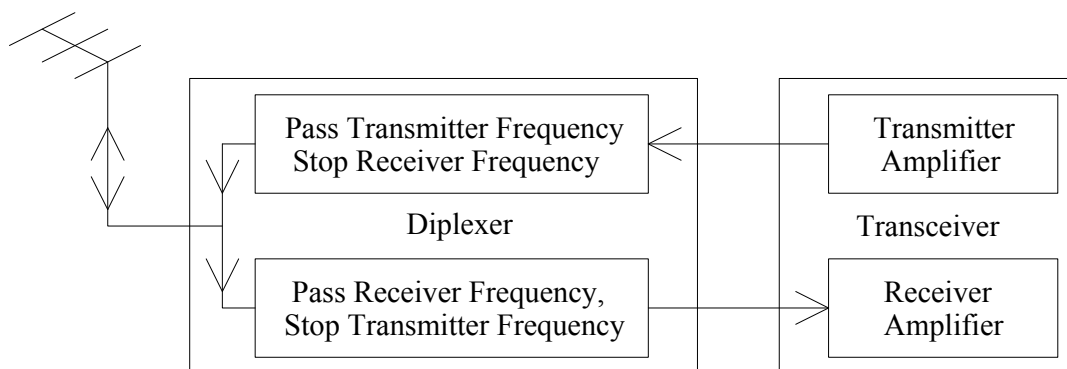


Figure 51. The use of a diplexer to provide full duplex operation.

Round rod interdigital filters are often used as a diplexer in mobile radio transceivers, as shown in figure 51. The filter connected to the receiver has a very high, typically greater than 60 dB, attenuation at the transmitter frequency. This ensures that the transmitter output, which is typically 25 Watt, does not damage the receiver input, which is typically designed to accurately demodulate signals of 1 nW. The use of the diplexer will thus permit full duplex operation, simultaneous transmission and reception, of the transceiver.

Mobile phones have similar diplexers, however to ensure a small size of the diplexer, the diplexer is made using a ceramic material with a typical dielectric constant of 30, allowing a $\sqrt{30}$ reduction in each dimension of the filter. The resulting filter will thus have 0.6% of the volume of the air-filled filter and also have a fraction of the weight.

PCB Interdigital filters

With circuit miniaturisation, and improved microstrip simulation tools, Interdigital filters are often designed using stripline or microstrip circuits for the resonating elements. The power handling capacity of these filters is small, so that they can only be used as filters in receivers or low power parts of communication equipment. The design procedure is illustrated with the following example.

Example:

Design a 5-resonator filter with a 70 MHz bandwidth centred at 1 GHz, using a RO4003 substrate for the PCB. The required k and q values can be obtained from table 1, the relevant part which is shown in table 4.

n	q0	I. L.	q 1	q n	k 12	k 23	k 34	k 45
	INF.	0.000	0.6180	0.6180	1.0000	0.5559	0.5559	1.0000
	32.361	1.045	0.4001	1.5527	1.4542	0.6946	0.5285	0.6750
	32.361	1.045	0.5662	0.7261	1.0947	0.5636	0.5800	0.8106
	16.180	2.263	0.3990	1.8372	1.4414	0.6886	0.5200	0.6874
	16.180	2.263	0.5777	0.7577	1.0711	0.5408	0.6160	0.7452
	10.787	3.657	0.4036	2.0825	1.4088	0.6750	0.5080	0.7066
5	10.787	3.657	0.5927	0.7869	1.0408	0.5144	0.6520	0.6860
	8.090	5.265	0.4111	2.3118	1.3670	0.6576	0.4927	0.7290
	8.090	5.265	0.6100	0.8157	1.0075	0.4844	0.6887	0.6278

Table 4. Butterworth response, K And Q value filter table, From A. I. Zverev. "Handbook of Filter Synthesis", Wiley, pp 341.

Notice that the k and q values vary depending on the losses. One could guess the losses to be about 2 dB and use the corresponding k and q values. Note that for each value of insertion loss, there are two sets of k and q values. Since the tap coupling is normally used and the tapping points only cover a limited range, it is desirable to select the table values where the difference between the q values is small.

Alternately, the design is done assuming no losses, so that equations 4 and 5 can be used. After the design is completed, any variations in k and q values required to accommodate the losses can be achieved by optimisation. That process is implemented here. The lossless q values are thus $q_1 = q_n = 0.6180$, resulting in $Q_1 = Q_n = 0.6180 \times 10^9 / 70 \times 10^6 = 8.828$.

The bandwidth of the first and last resonator, without loading due to adjacent resonators is given by equation 9.4.1 in Zverev as:

$$\text{Resonator 1 } \Delta_{3dB} = \frac{\text{Filter } BW_{3dB}}{q_1} \quad \text{Resonator } n \Delta_{3dB} = \frac{\text{Filter } BW_{3dB}}{q_n} \quad \text{Eqn. 29}$$

In our design the filter BW_{3dB} is 70 MHz, Δ_{3dB} is thus $70/0.618$ MHz = 113.2 MHz. For this filter, the input and output tapping points are the same. The tapping point in the circuit of figure 52 is thus adjusted to result in a 113.2 MHz bandwidth.

The tapping point can be determined using Microwave Office and the two-resonator circuit of figure 52. To prevent the second resonator from influencing the tuning of the tapping point, a very large coupling gap is used and the resonance of the coupled resonator is placed far away from the centre frequency by disabling all the possible elements as shown in figure 52. To measure the voltage of the input resonator, a high impedance (1 M Ω) port (port 2) is connected to the resonator. The signal at port 2 is then the voltage at the top of resonator and has the correct frequency response for determining the loading of the resonator, as shown in the graph of figure 52. After tuning the tapping point for the correct bandwidth, the correct q_1 and q_n for the filter has been determined.

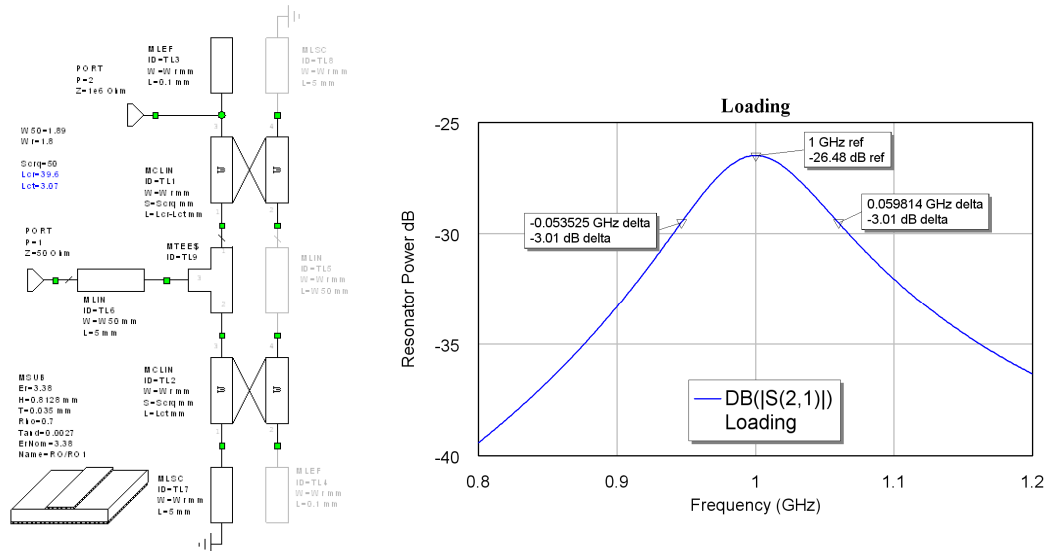


Figure 52. Left: Circuit for input tap and coupling determination, Right: Resonator loading

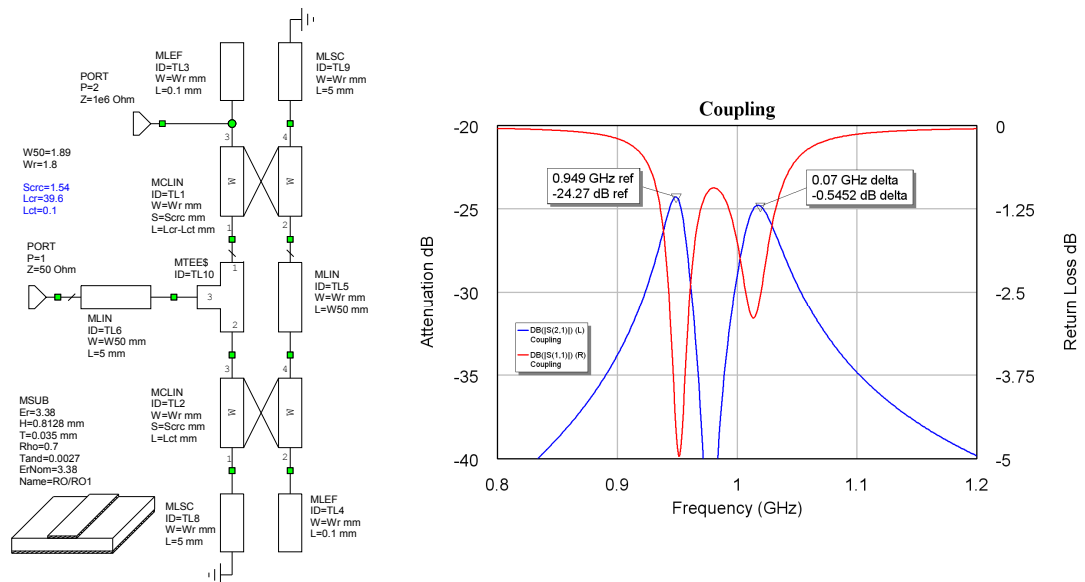


Figure 53. Interdigital filter coupling determination

The coupling gap is tuned to obtain the correct coupling between resonators. To reduce the effect of loading, the tapping length L_{ct} is made as small as possible, resulting in the test circuit shown in figure 53. When the second resonator is tuned and brought close to the first resonator, a double peak response will result as shown in figure 53. The frequency difference between the peaks is given by equation 9.4.3 in Zverev as:

$$\Delta_{fp} = k_{12} BW_{3dB} \tag{Eqn. 30}$$

For this filter $k_{12} = 1$, so that $\Delta_{fp} = 70$ MHz for the peaks in frequency response of the test circuit, coupling between the first and second resonator as shown in figure 53. This corresponds to a coupling gap of 1.54 mm. The same test circuit is now used to determine the coupling gaps for the other resonators. For the coupling between the second and the third resonator $\Delta_{fp} = 0.5559 * 70$ MHz = 38.9 MHz. The coupling gap is

now re-tuned to obtain a difference of 38.9 MHz between the peaks. This corresponds to a coupling gap of 2.5 mm. This procedure is then repeated for all the remaining coupling gaps for the filter using the respective coupling coefficients from tables or equations 4 and 5.

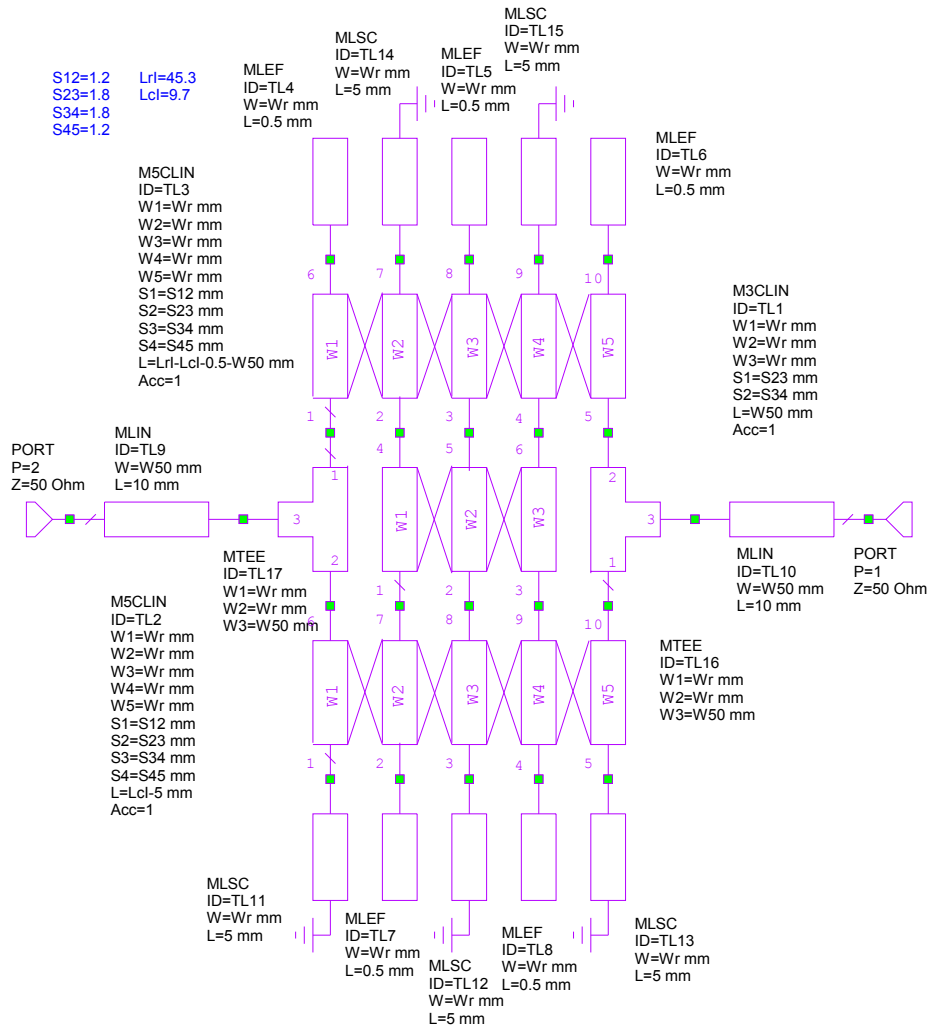


Figure 54. Circuit for the Interdigital Filter using Calculated Loading and Coupling values.

Simulating this circuit of figure 54 gives a filter with a response close to the desired value. As shown in figure 55. To obtain the desired specification precisely, the filter is optimised. For a lossless Butterworth filter, the coupling gaps are symmetrical, however for lossy filters or different filter types, asymmetrical coupling gaps result. For a practical Butterworth Bandpass filter, the design procedure can assume a lossless filter. Subsequent optimisation for the desired filter performance, accommodates the losses by allowing changes in values and asymmetry in coupling gaps, and thus changes in coupling coefficients, which are required for lossy filters compared to ideal filters as shown in table 4. Note that after optimisation, the resonators in this design are not of equal length and the filter is no longer symmetrical from the input and output. This asymmetry is expected from k and q filter tables corresponding to the 1.5 dB insertion loss of the filter.

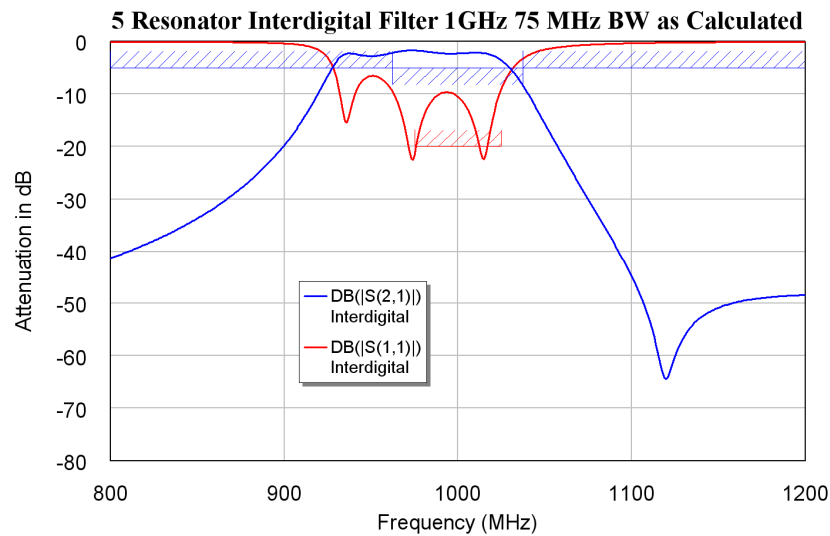


Figure 55. Frequency response of the filter of figure 54, as calculated.

Theoretically, all resonator lengths are the same. In practice it is however, better to allow the resonator lengths to vary slightly under optimisation in order to achieve the desired frequency response. The filter of figure 54 was optimised to give a 70 MHz bandwidth at a 1 GHz centre frequency, as shown in figure 56.

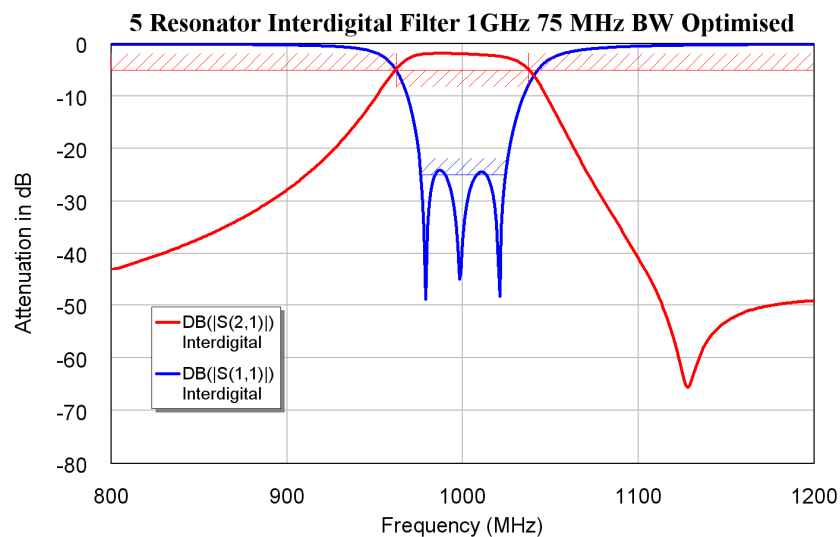


Figure 56. Frequency response of the filter of figure 54, after optimisation.

When the first prototype of the filter was produced, it was found to be 20 MHz (2%) low in centre frequency and have a passband amplitude response that is slightly sloping and a bandwidth that was too small. To compensate the centre frequency of the designed filter, was shifted to 1.02 GHz, the bandwidth was increased, and a slope was specified in the passband as shown in the red curve in figure 54. The measured performance of the second filter is shown in blue in figure 54 and it has a centre frequency of 984 MHz compared to the 1 GHz specification. The measured bandwidth is 92 MHz compared to the 70 MHz specification. This may be sufficiently close to satisfy the required specifications. If this performance is inadequate, then another filter needs to be designed.

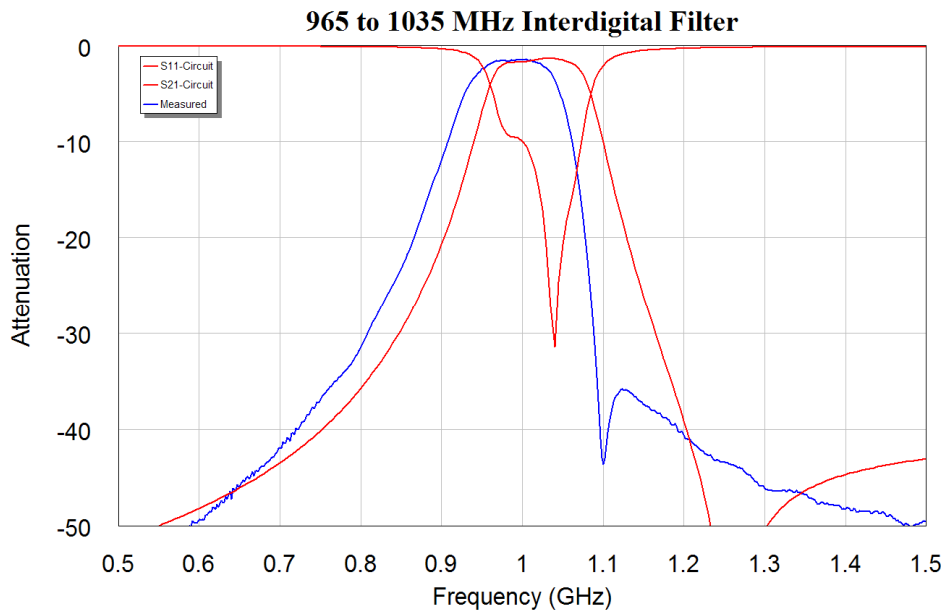


Figure 54. Frequency response of the 70 MHz bandwidth interdigital filter.

These values for tapping point and coupling gaps are then used for the design of the interdigital filter. The first prototype filter has a measured centre frequency, which is 2.2 % low. This difference could be due to a variety of factors, such as differences in PCB substrate, additional capacitance of the resonators to the ground-plane and a bigger end effect.

Figure 55 shows the resulting filter realisation. Interdigital filters are often used in commercial designs as can be seen in figure 56, which is part of a microwave layout produced by Codan in Adelaide, South Australia. Comparing figures 55 and 56, it can be seen that the procedure for earthing the grounded end of the resonator to the bottom layer ground-plane is slightly different. The positioning of the vias in figure 55 is the most likely cause of the centre frequency being 2% low.

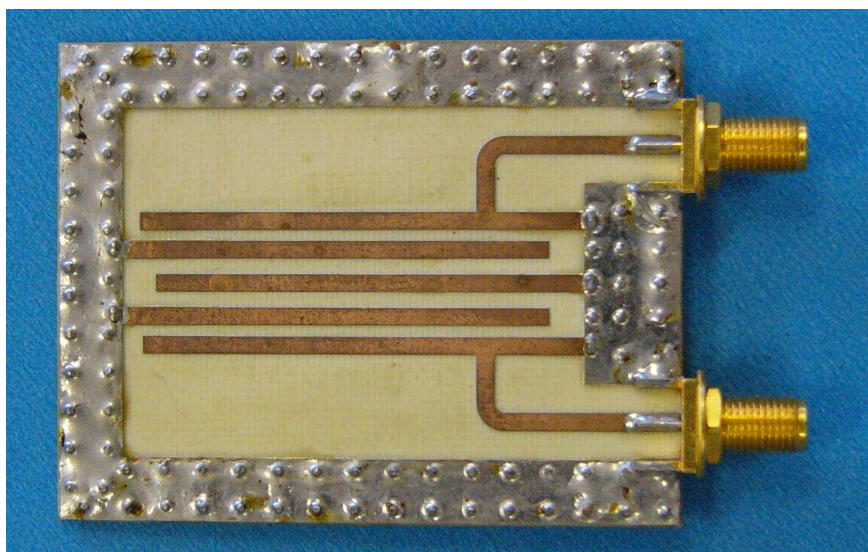


Figure 55. Microstrip interdigital filter 70 MHz bandwidth at 1 GHz

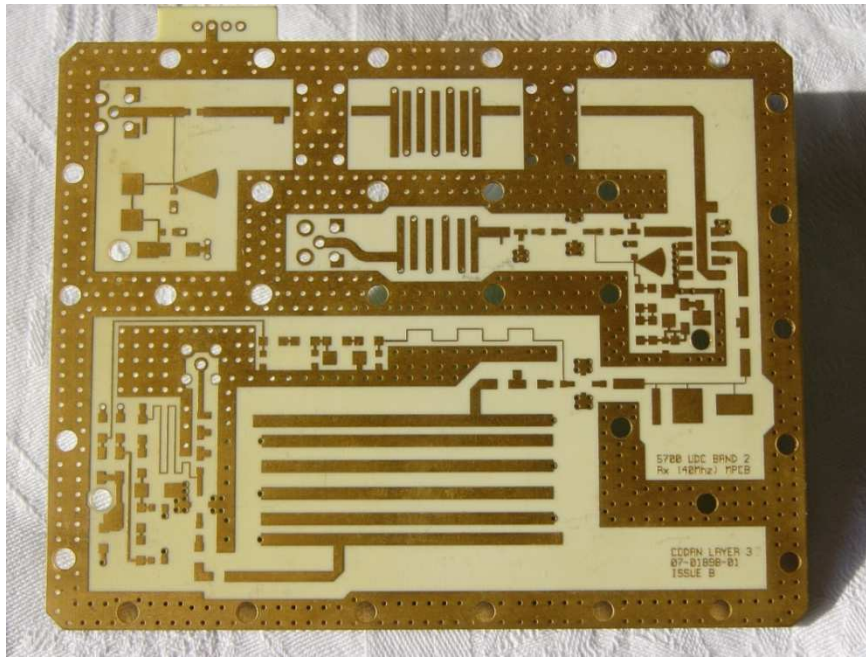


Figure 56. PCB showing three interdigital filters. (Courtesy Codan).

Direct Coupled Resonator Filters

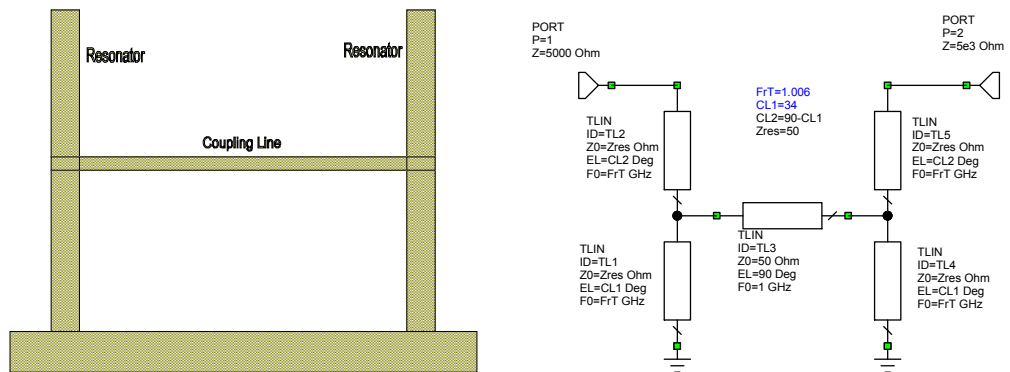


Figure 57. Transmission line coupled resonators.

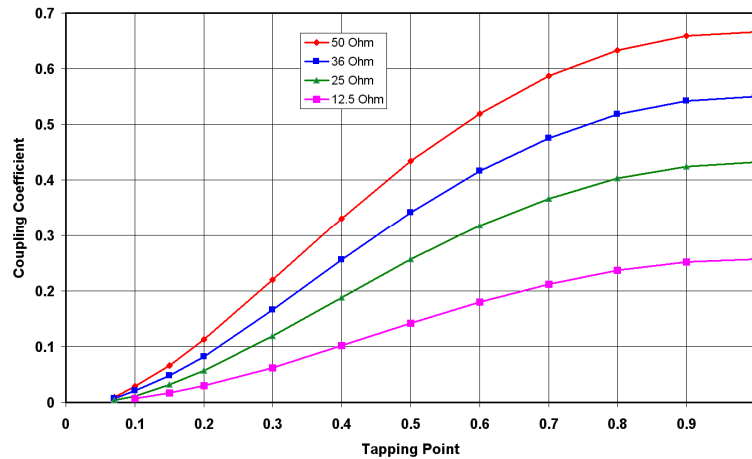


Figure 58. Coupling coefficient versus tapping point for different line impedances.

When the percentage bandwidth of the filter becomes greater than 20%, the coupling gaps for interdigital filters become too small to be produced using readily available technology. As a result, a different coupling technique is required. It is possible to couple two resonators using a quarter-wavelength long transmission line as shown in figure 57. The coupling can be varied by changing the tapping point. When this is done, graphs similar to figure 53 are produced by the circuit of figure 57 and from equation 30 the coupling coefficient can be determined as a function of tapping point as shown in figure 58, since the spacing between the peaks and the bandwidth are known..

Filter Design Example

The coupling coefficients shown in Figure 58 can now be applied to the design of a wideband filter. As an example, the design of a 5-resonator Butterworth bandpass filter with a lower 3 dB cut-off frequency of 750 MHz and an upper cut off frequency of 1250 MHz is chosen the filter will thus have a 50% bandwidth.

Equations 4 and 5 give the normalized Q values and coupling coefficients as:

Normalised	Denormalised for 50% Bandwidth
$q_1 = q_n = 0.618$	$Q_1 = Q_n = 1.236$
$k_{12} = k_{45} = 1$	$K_{12} = K_{45} = 0.5$
$k_{23} = k_{34} = 0.5559$	$K_{23} = K_{34} = 0.278$

Figure 58 shows that different transmission line impedances should be used for different coupling coefficients in order to obtain realistic tapping points. For the filter, 50 Ω transmission lines are used for the input and output resonators, which require the highest coupling coefficients of 0.5. For the other resonators, 36 Ω transmission lines, which have lower losses, are used. Interpolating the tapping points from figure. 58, results in the following normalised tapping points, Txline results in the following resonator line lengths:

Resonator 1	50 Ω	Tap = 0.487	Lr = 46.96 mm
Resonator 2	36 Ω	Tap = 0.614	Lr = 44.99 mm
Resonator 3	36 Ω	Tap = 0.426	Lr = 44.99 mm
Resonator 4	36 Ω	Tap = 0.614	Lr = 44.99 mm
Resonator 5	50 Ω	Tap = 0.487	Lr = 46.96 mm

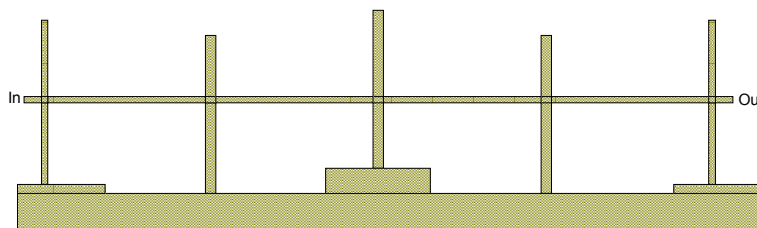


Figure 59. Filter layout for initial tap values.

Entering those values in the Microwave Office circuit schematic of the filter, results in the initial filter layout shown in Figure 59, with the corresponding frequency response shown in Figure 60. To highlight differences between the 750 MHz and 1250 MHz, corner frequency specifications and frequency-response obtained from the computer simulation, an optimisation mask is superimposed on Fig. 60. In addition, an optimisation mask for a -1 dB attenuation from 780 MHz to 1220 MHz is shown. It can

be seen that the design procedure results in a filter that has a bandwidth that closely matches the design specifications, but whose centre frequency is 3.5% low. This difference is due to the end effect of the open circuit resonators not being taken into account in the above calculations.

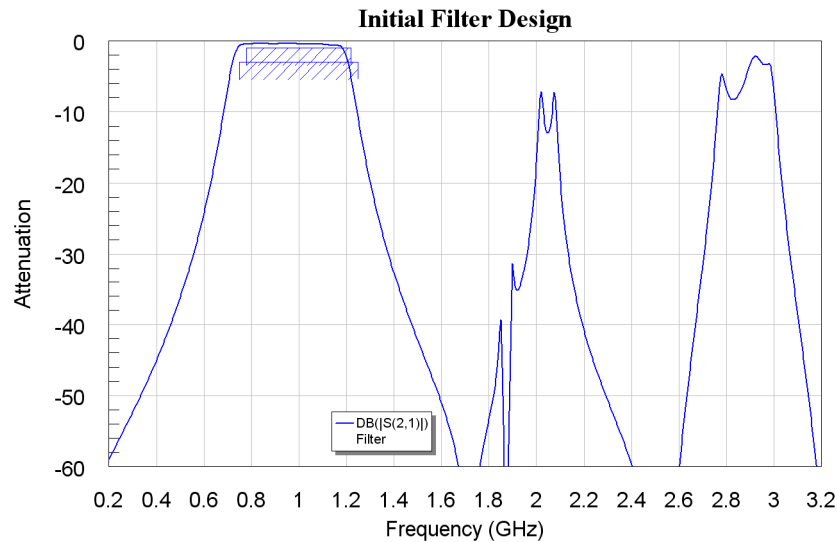


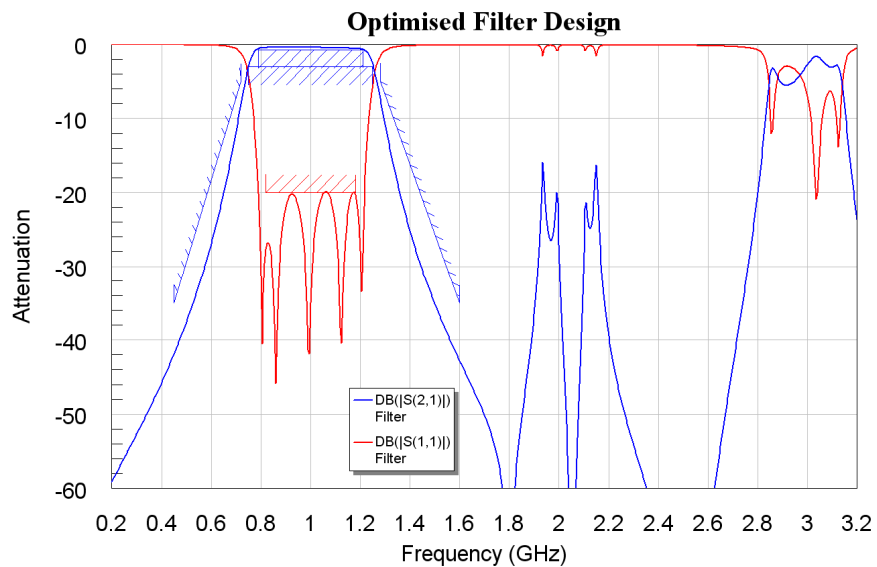
Figure 60. Frequency response for initial wideband filter.

Fine Tuning the Filter

To shift the centre frequency, the length of all the resonators is changed slightly using the 'tuning simulation' capability of Microwave Office. In addition, it is desirable to fine-tune the filter to obtain the lowest insertion loss. This is best achieved by ensuring that the filter has a low return loss. Setting the optimiser constraints on S_{11} to be less than -20 dB and carrying out the first stage of the optimisation process of the filter to meet this return loss as well as the passband specifications results in the following tapping points:

Resonator 1	50 Ω	Tap = 0.5147
Resonator 2	36 Ω	Tap = 0.5969
Resonator 3	36 Ω	Tap = 0.4304
Resonator 4	36 Ω	Tap = 0.5969
Resonator 5	50 Ω	Tap = 0.5147

Figure 61 shows the resulting frequency response of the filter after this first stage of optimisation. For a wideband filter implementation like this, the spurious response at the harmonics, particularly that at 2 GHz is unacceptable. To provide better attenuation at those frequencies, stubs need to be added to the filter. Those stubs will distort the frequency response of the filter. In order to minimise the effect of the stubs on the centre frequency of the filter, it is desirable to use two sets of stubs and vary the spacing between the two sets of stubs to provide a low return loss at the centre frequency of the filter. In addition, it is desirable to make the harmonic stubs slightly different lengths, to widen the bandwidth over which good harmonic attenuation is obtained.



The final step in the filter design is to change the layout from a simple design as shown in Figure 62, to a more compact and easier to manufacture design. To achieve this, the three tiered ground level shown in Figure 59 is made one level and the coupling transmission lines are folded and bent in order to take up as little space as possible, while connecting to the resonators at the correct tapping points. The harmonic stubs may be folded as shown in Figure 40 and 41. The final layout should also ensure that the input and output connectors are in the correct location for mounting the filter. Figure 62 is a photograph of the final filter.

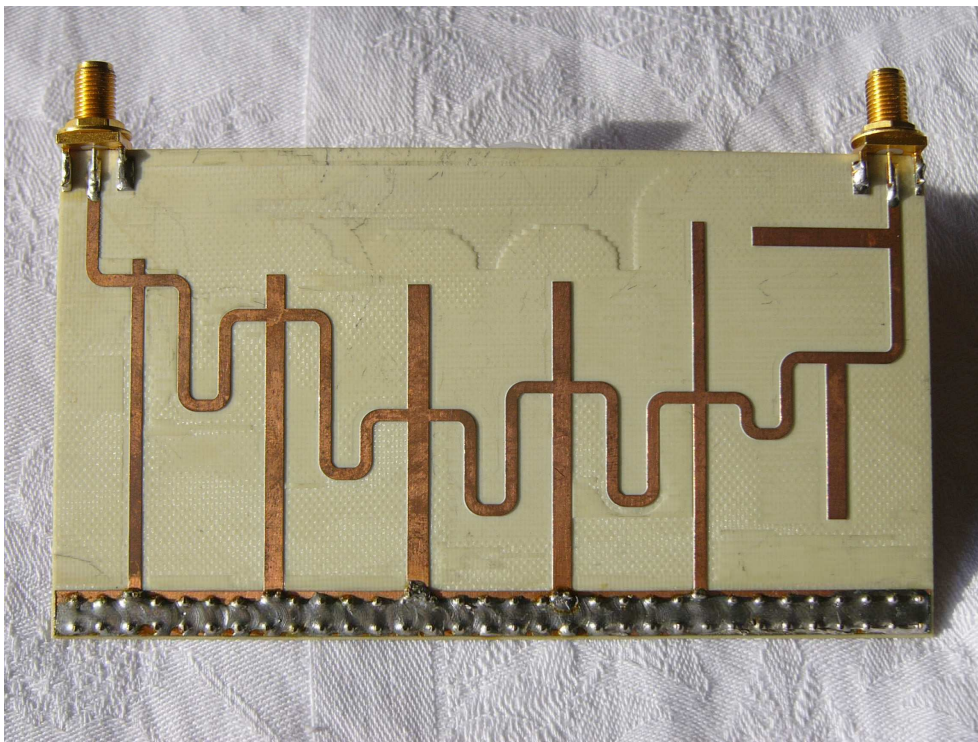


Figure 62. 750 MHz to 1250 MHz filter hardware.

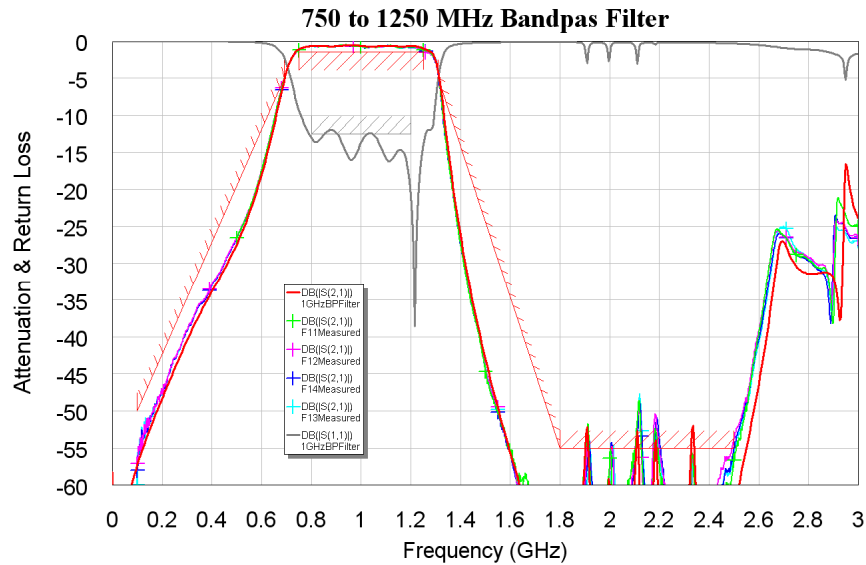


Figure 63. Frequency response of the filter of figure 61.

Fig. 63 shows the frequency response of the final filter after optimisation, it also shows the final optimisation limits used. To determine the reliability of the design technique, four filters were constructed. The measured frequency response of those filters is also shown in Figure 63. It can be seen that the design technique results in highly repeatable filters, whose measured performance agrees remarkably with the results from computer simulation. The agreement between the measured and simulated results for these filters is much better than those for the hairpin filter of Figure 40 or the interdigital filter of Figure 55. It should be noted that the right most resonator is significantly larger than the other resonators. This is required to compensate for the effects of the harmonic stubs on the passband response.

Microstrip Filter Comparison

When designing a Microstrip filter the four common filter types described in these notes can be used. For a fair comparison, a 5-resonator filter with a centre frequency of 1 GHz and a 70 MHz bandwidth was designed as an Interdigital filter, a Compline Filter, a Hairpin filter and a Direct-coupled resonator filter. The filters were optimised using the same optimisation limits. Each filter has 10 mm tracks connecting to the tapping point to allow a connector to be soldered to that track. The same RO4003 substrate was used and all resonators are 3 mm wide. For each of the filter types, a simple test circuit like those shown in figures 52, 53 or 57 is used. The tapping and coupling test circuit for the compline filter is shown in figure 64 and that for the hairpin filter is shown in figure 65.

The input tapping for all these four circuits is adjusted to obtain frequency responses like figures 52 and 53, but with the bandwidths as per equations 29 and 30 for the relevant filter. Since the centre frequency, bandwidth and the number of resonators for these filters is the same as those of figures 52 and 53, exactly the same responses should be obtained. The coupling tuning, can be done most accurately when the end resonator loading is reduced as done in figures 64 and 65.

Figure 66 shows the initial frequency response of the four, 5-resonator filters, when the tapping and coupling gaps are set to those calculated using the test circuits.

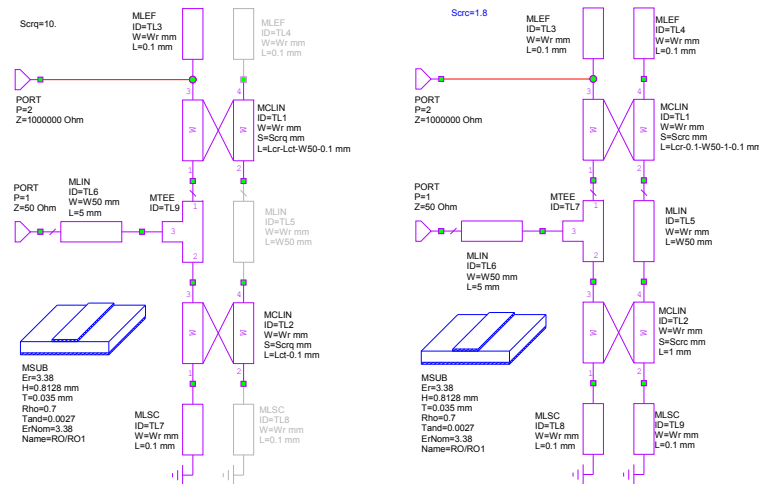


Figure 64. Resonator Loading and Coupling test circuit for Combine filters.

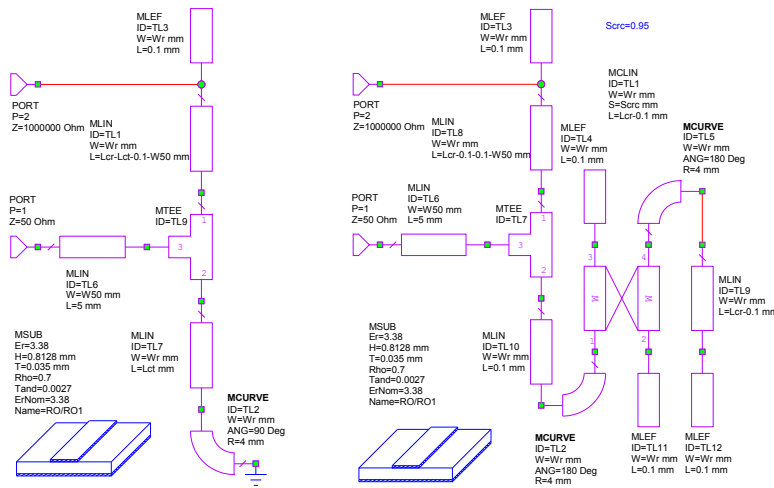


Figure 65. Resonator Loading and Coupling test circuit for Hairpin filters.

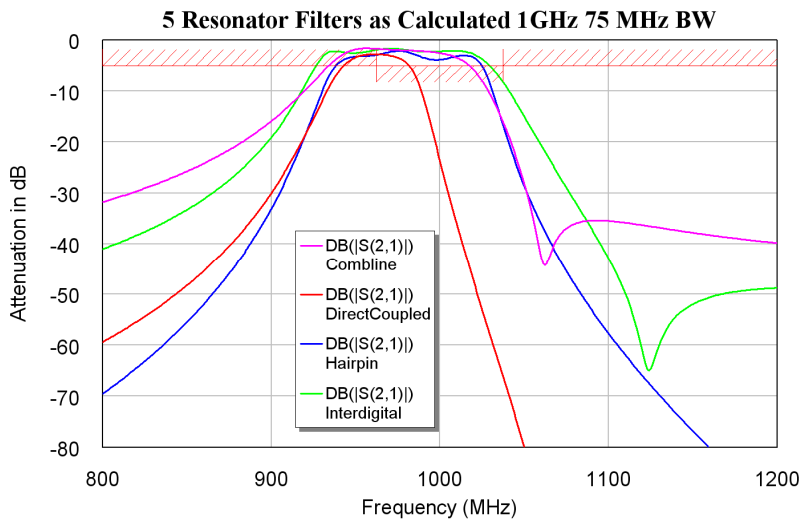


Figure 66. Filter performance with parameters as calculated.

The performance of all these filters is close enough that the specifications can be met using some simple optimisation. The tuning and optimisation is best done in three stages: Firstly adjust the resonator length using manual tuning, to give the correct centre frequency. The second step is to fine tune the coupling gaps and tapping points using optimisation, to get as close to the requirements as possible. The final step is to allow the individual resonator lengths to be optimised as well as further minor optimisation of the coupling gaps and resonators. Since there is a significant interaction between the parameters to be optimised, the local random optimisation is most likely to result in the best optimisation. If the optimisation gets stuck, changing the weight of the worst error may get the optimisation out of the local minima and thus result in lower error costs.

Figure 67 shows the final performance of the filters after optimisation. The Hairpin filter has a good symmetrical filter response and has good stopband attenuation. The Direct Coupled Resonator filter has a better higher frequency attenuation, but a poorer lower frequency attenuation. The interdigital filter has a poorer attenuation characteristic, compared with the other filters. In particular, the attenuation near 1 GHz is only 50 dB. The combline filter has the worst close-in stopband attenuation of these filters. Combline filters are used less often than interdigital filters.

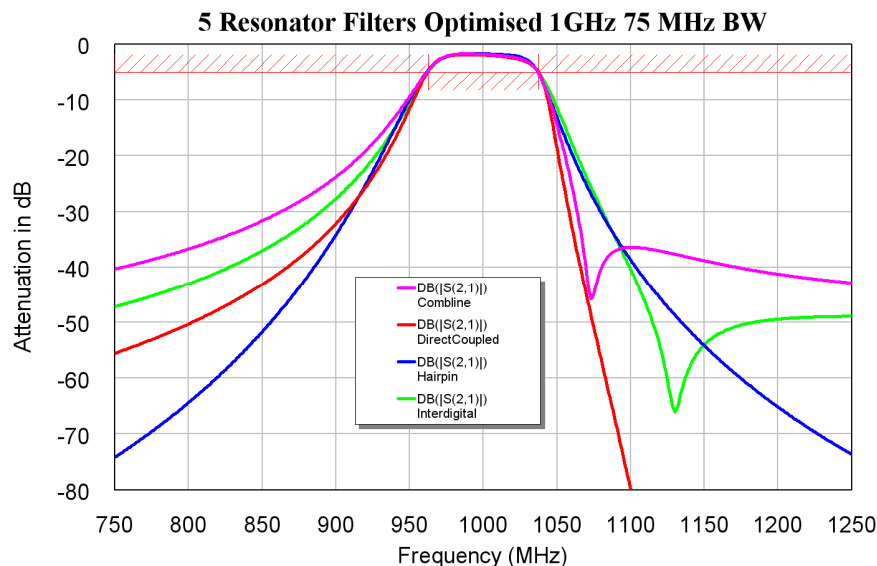


Figure 67. Frequency response of three 5-resonator filters.

Figure 68 shows the frequency response of the four filters at the harmonics of the 1 GHz passband. For the direct-coupled resonator filter the lengths of the coupling lines was 12.5% of a wavelength, which is half of the length of the coupling lines used for the filter in figure 62. This resulted in a lower harmonic attenuation. The direct coupled filter has the best close-in stopband attenuation, but the worst stopband attenuation above 2 times the centre frequency. The second harmonic response from the hairpin filter is significant, but can be removed using harmonic stubs. The interdigital filter does not have a significant harmonic response, but it does not have a very good stopband attenuation either. The stopband attenuation for interdigital filters does not significantly improve with filter order. The combline filter is the smallest, occupying 41x60 mm. The interdigital filter is slightly larger occupying 42x60 mm. The Direct Coupled Resonator filter, occupies 75 x 60 mm and the Hairpin filter is the largest, occupying 78 x 68 mm.

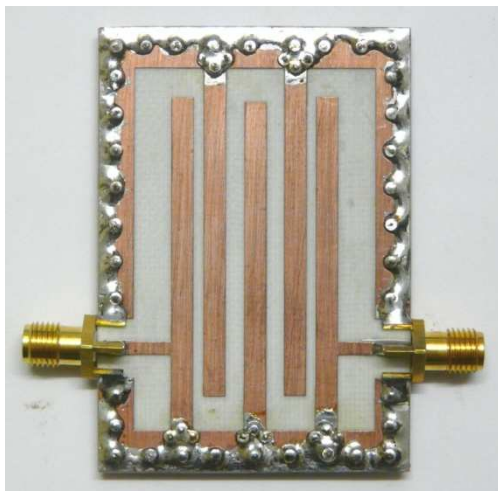
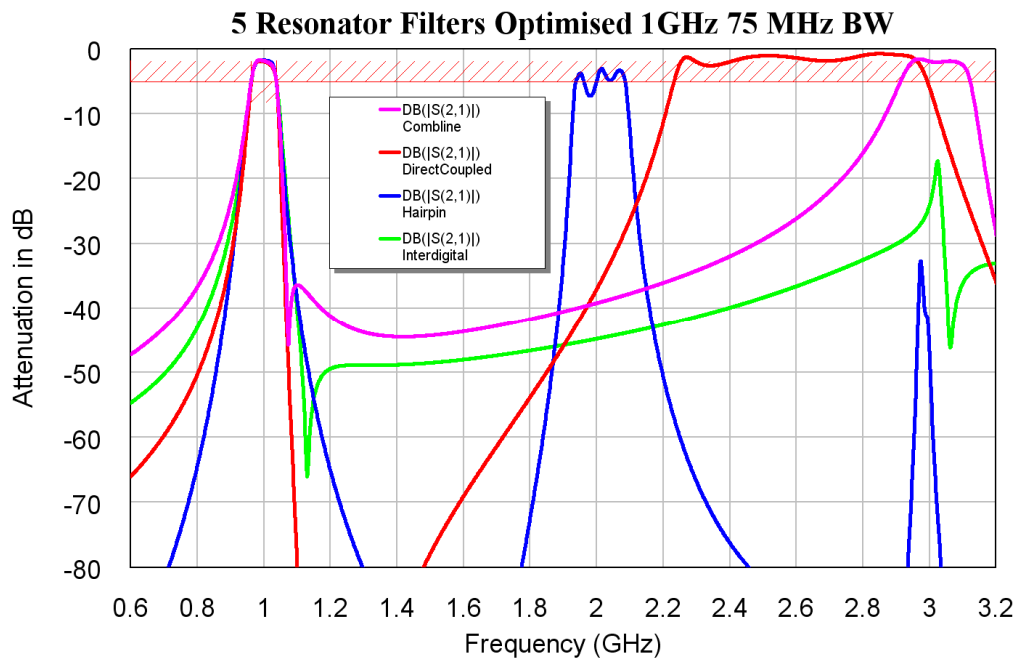


Figure 69. Interdigital filter hardware.
(42x60mm)



Figure 70. Comblin filter hardware.
(41x60mm)

Figures 69 to 72 show the hardware of the four filters, approximately to the same scale. The Comblin filter is slightly smaller than the interdigital filter, but in most instances, there is not enough space saving to warrant the worse stopband attenuation.

Figures 73 to 76 show the measured frequency responses of the filters. Comparing these with figures 67 and 68, shows the remarkable agreement between the calculated and measured results. The passband of the Interdigital, Comblin and Direct Coupled filters are a few percent lower than calculated. The difference matches the length of the pins used in connecting the grounded end of the resonators to the groundplane on the bottom of the PCB. This can be taken into consideration in the second iteration of the filter designs if needed.

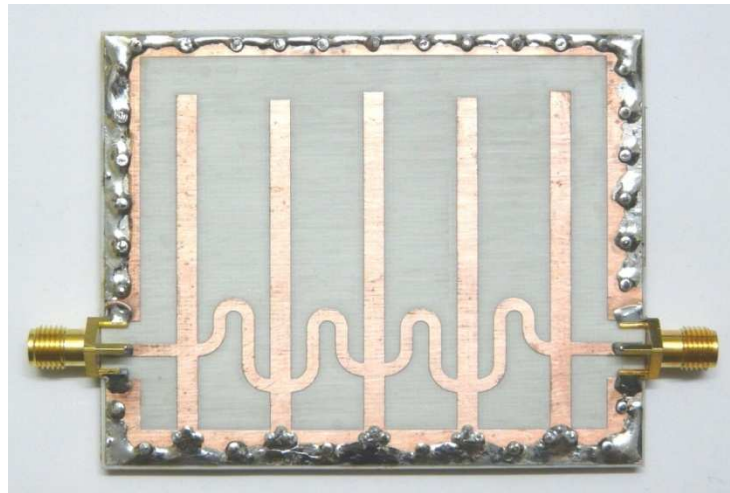


Figure 71. Direct Coupled filter hardware. (75x60mm)

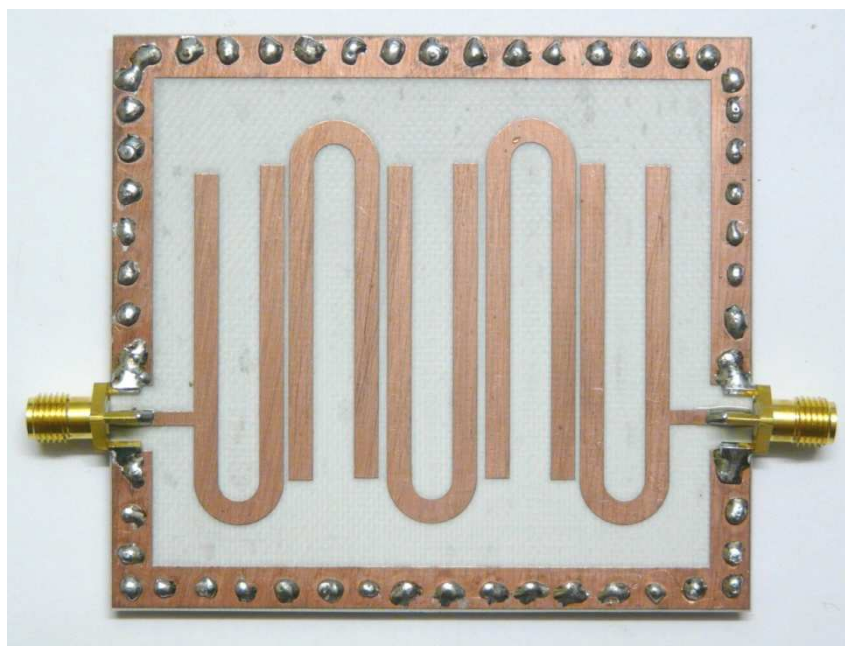


Figure 72. Hairpin filter hardware. (78x68mm)

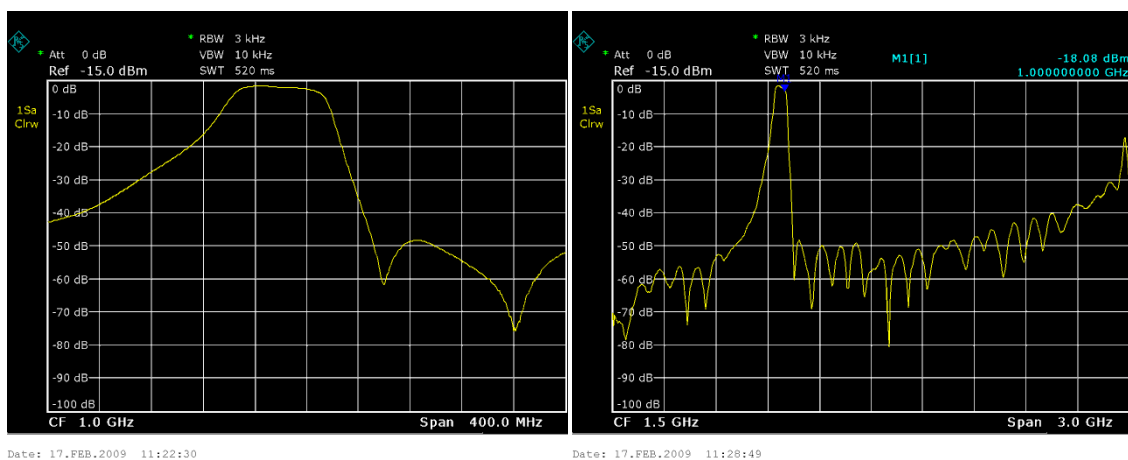


Figure 73. Measured frequency response of Interdigital filter.

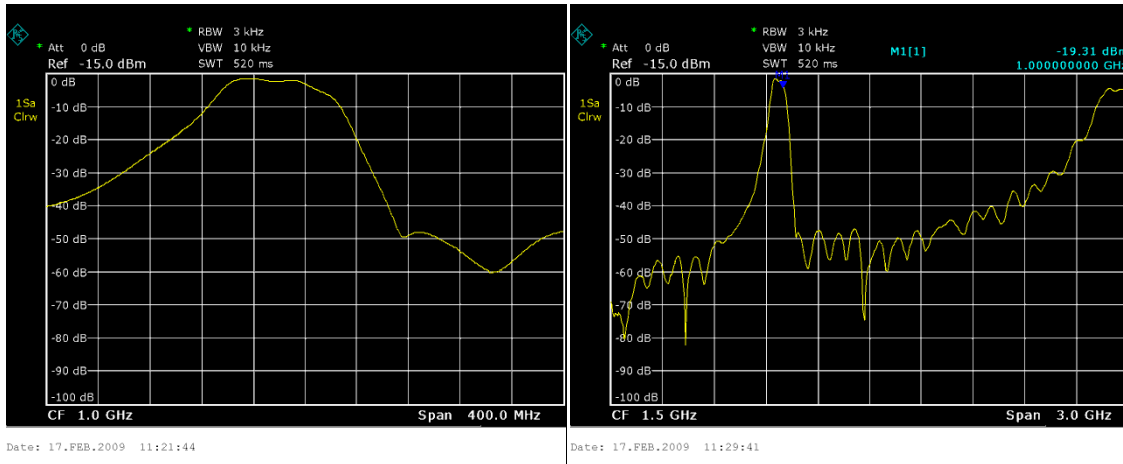


Figure 74. Measured frequency response of Combline filter.

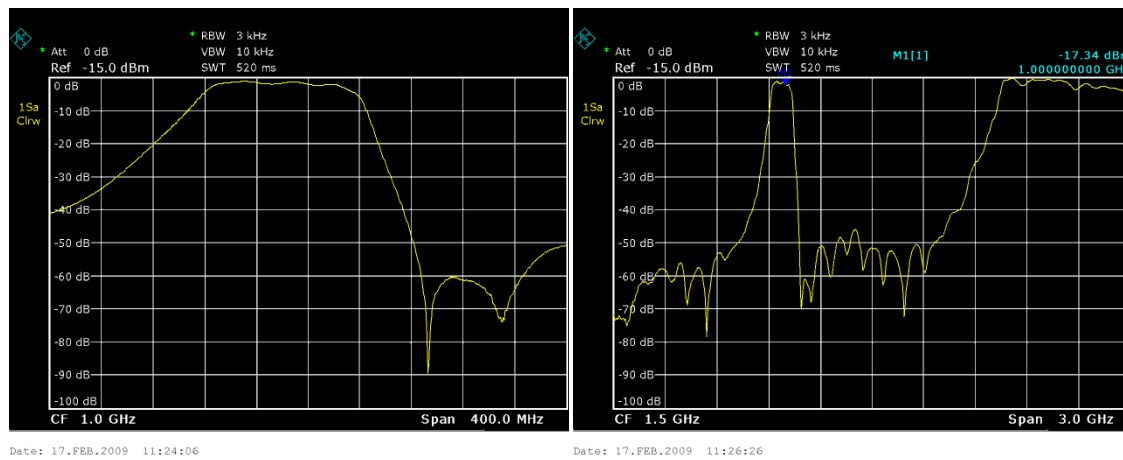


Figure 75. Measured frequency response of Direct Coupled filter.

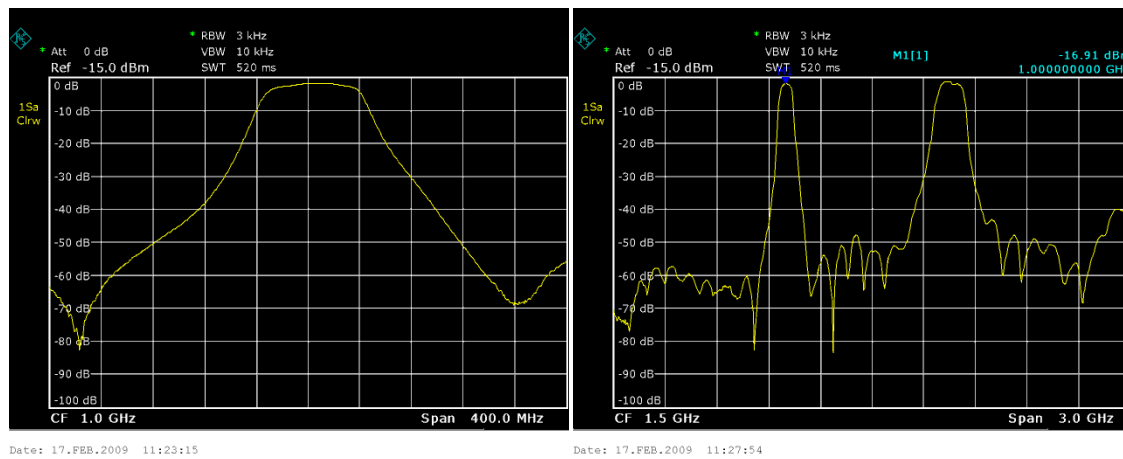


Figure 76. Measured frequency response of Hairpin filter.

The Hairpin filter has a measured centre frequency that is very close to the desired 1 GHz centre frequency. This is due to no ground connections being required, thus removing an uncertainty from the design. From the measured passband responses, Hairpin filters have a better close in stopband attenuation and a more accurate centre frequency are thus a good choice for one off designs, where the performance has to be correct first time.

Coaxial Filters

Coaxial filters are similar in principle to helical filters, except that the resonator is a straight rod, rather than a wound helix as shown in figure 77. The length of the centre rod is a quarter wavelength. For the highest Q values, the ratio of the centre rod diameter to the inner diameter of the cavity is such that the characteristic impedance of the coaxial line forming the resonator is 77Ω . The equation for the characteristic impedance of a coaxial transmission line is:

$$Z_c = \frac{1}{2\pi} \sqrt{\frac{\mu_0}{\epsilon_0}} \ln\left(\frac{B}{A}\right) = \frac{60}{\sqrt{\epsilon_r}} \ln\left(\frac{B}{A}\right) \quad \text{Eqn. 30}$$

So that the maximum Q is obtained when $B/A = 3.6$.

Typical Q values are in the range of 2000 to 10000. Because cavity filters have such a high Q, they are used in many applications requiring a low insertion loss. Air filled coaxial filters have a high power handling capability and are typically used for filters and combiners for radio and TV transmitters and in mobile radio and mobile phone base stations.

Figure 78 shows a typical coaxial filter used in a mobile radio talk-through repeater operating at 80 MHz. The total height of the filter is 1.2 m and the cavities are 200 mm in diameter. The cavities used in this filter have a Q of 5000. The round cylinders at the top of the cavities are isolators, which ensure that the input impedance to the filter is perfectly matched over the entire bandwidth of the transmitter.

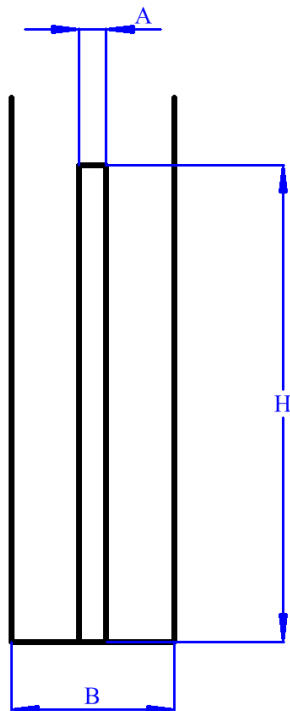


Figure 77. Coaxial cavity dimensions.



Figure 78. Coaxial cavity diplexer for 80 MHz.

Some coaxial cavities are much smaller. Most Mobile Phones have diplexers with ceramic filled coaxial resonators. Figure 79 shows a surface mount, ceramic 3-resonator coaxial filter for mobile phone applications. Using a high dielectric constant material for

the cavity gives a significant reduction in filter size. The centre frequency of this filter is 881 MHz. The filter is 14 mm long.

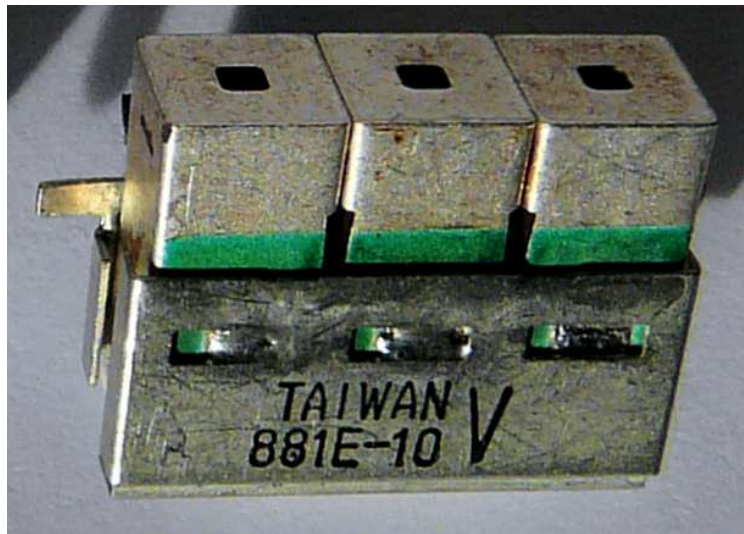


Figure 79. Coaxial cavity filter

For Mobile Radios, used by trucks or taxis to talk to their base, a coaxial diplexer is often used to provide isolation between the transmitter and the receiver in their Mobile Radio. Figure 80 shows a typical coaxial diplexer. The receive frequency is 450.625 MHz and the transmit frequency is 460.125 MHz. These radios typically have a transmission power level of 25 Watt (43.98 dBm). The receiver typically has signals of -60 dBm applied to it, so that the difference between the transmitted and received signal is more than 100 dB. Connecting the transmitter directly to the receiver, will result in severe damage to the input circuitry.



Figure 80. Cavity filter diplexer for mobile radio applications.

As shown in Figure 81, at the receiver frequency of 450.625 MHz, the diplexer of figure 80 causes a less than 1 dB loss between the antenna and the receiver ports and more than 60 dB isolation between the antenna and the transmitter ports, thus protecting the input from any spurious signals generated by the transmitter at the receiver frequency.

At the transmitter frequency of 460.125 MHz, the diplexer provides less than 1 dB loss between the transmitter port and the antenna port, so that virtually all the 25W output signal is transmitted. At this frequency, there is more than 60 dB isolation between the antenna and receiver ports, thus protecting the input from the high power levels generated by the transmitter.

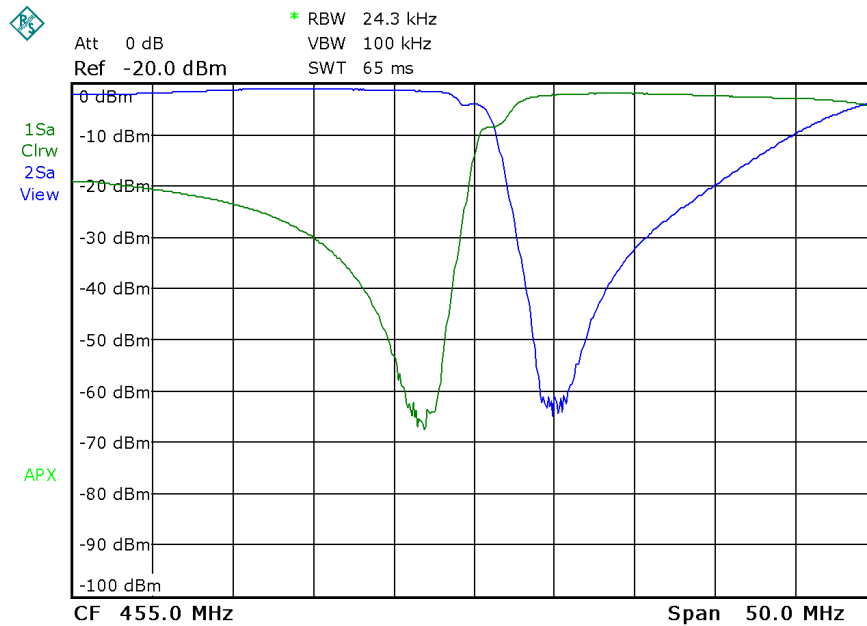


Figure 71. Frequency response of the diplexer of figure 70.

For low loss, high power microwave filters; it is often convenient to mill the whole filter out of a solid block of aluminium, as shown in figure 72. By including coupling between non-adjacent cavities, zeros of transmission can be included. In the filter of figure 72, non-adjacent cavity coupling has been applied to the first and last resonator.

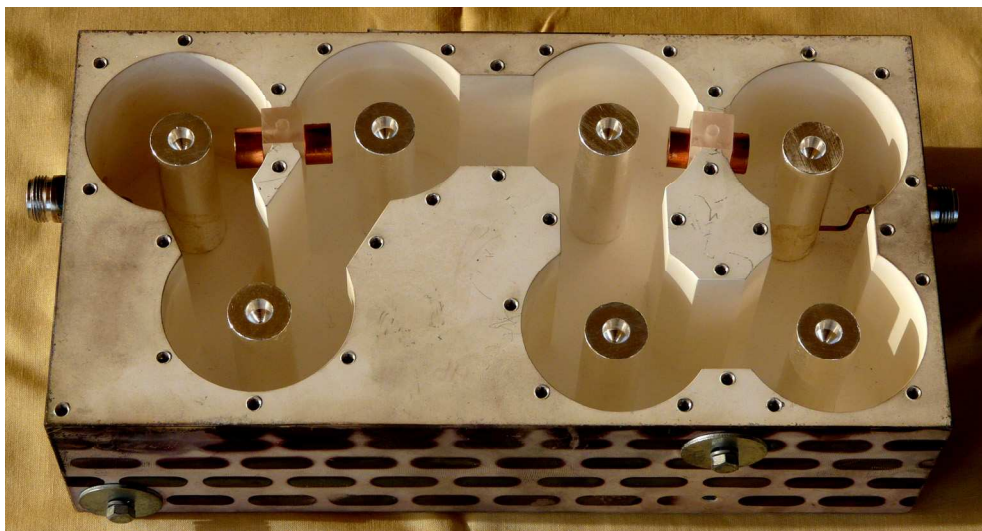


Figure 72. 1.8 GHz Coaxial Cavity Filter.

These filters are tuned by capacitive top loading on each resonator. Each of the resonators is thus a fraction shorter than a quarter wavelength, with the required top-loading capacitance making up this shortfall.

Ceramic Filters

For many consumer applications IF filters are required at only a few specific frequencies. For example, all FM radios have an IF of 10.7 MHz. All AM radios use a 455 kHz IF. As a result, commercial filter manufacturers like Murata have a wide variety of low cost filters available for those frequencies. To achieve small size, low cost and freedom from microphony, ceramic materials are used for the resonators. Typical 10.7 MHz ceramic IF filters are shown in figure 73. Many of the latest versions are surface mount instead of the through-hole filters shown in figure 73. The right hand filter contains two filters like the left hand one, inside the one casing and is used to provide more filtering of unwanted signals. Most of the FM IF filters are designed to provide a flat group delay over the passband. This minimised the distortion caused by the IF filter to the demodulated audio signals.



Figure 73. 10.7MHz ceramic IF filters.

In addition there are many filters available for specific IF applications, such as TV sound IF, 38.9 MHz for Digital Audio Broadcasting (DAB), 44 MHz for digital TV receivers etc.

Ceramic resonator filters are also used for RF filtering. The Murata Gigafil range for instance contains many different RF filters covering the 800 to 950 MHz mobile phone band and the 1.4 to 2.4 GHz mobile phone and WLAN bands.

Since these ceramic filters are mass-produced, their cost is very low and it may be worthwhile to modify one's design to be able to incorporate these filters.

SAW Filters

The resonators considered so far have electromagnetic or acoustic resonances with the resonator being a quarter wavelength. Voltages across an input transducer on the surface of a piezo-electric substrate causes an acoustic wave to travel along the surface of the substrate. These travelling waves then induce voltages on a second transducer, which is used as an output transducer. By correctly designing the shape of these transducers, filtering can be achieved, with independent control over both the amplitude and group delay. SAW filters are thus normally used for TV IF filters, IF filters for Radars and other applications where sharp filtering is required and where the group delay must be absolutely flat.

Since the input transducer generates a travelling wave in the direction of the output transducer as well as one in the opposite direction, which must be absorbed, SAW filters have a high insertion loss, typically 16 to 20 dB.

The design of SAW filters is outside the scope of these lectures.

References and Bibliography

A. I. Zverev, *Handbook of Filter Synthesis*, Wiley, 1967, Helical Filters pp 499-521, k and q Filter Tables, p 341, Eqn. 9.4.3 pp 517.

G. Matthaei, L. Young, and E. M. T. Jones, *Microwave Filters, Impedance-Matching Networks, and Coupling Structures*. Boston, MA: Artech House, 1980. pp.583-650.

M. Dishal, "A Simple Design Procedure for Small Percentage Bandwidth Round Rod Interdigital Filters" MTT, Vol 13, No5, Sep 1965, pp 696 – 698.

D. Pozar, *Microwave Engineering*, Third Edition, Wiley, 2005. pp. 416-438.

P. Martin, "Design Equations for Tapped Round Rod Combline and Interdigital Bandpass Filters", Nov 2002. Available: <http://www.rfshop.com.au/C&IDES.DOC>.

K&L Microwave, 9IR20-7500/X2000-O/O Wide Band Interdigital Filter, Available: <http://www.klmicrowave.com/bulletin2004/August/PDF/9IR20.pdf>.

Microwave Office, Product details available: <http://appwave.com/products/>.

Kikkert, C. J. "Designing Low Cost Wideband Microstrip Bandpass Filters", IEEE Tencon '05, Melbourne, Australia, 21-24 November 2005.

Kikkert, C. J. "A Design Technique for Microstrip Filters" ICECS 2008, St Julians, Malta, 31 Aug.-3 Sep. 2008,

Chapter 8

Amplifiers: Stability, Noise and Gain

IF amplifiers

A few years ago, if one had to use an RF or IF amplifier, one had to design that using individual transistors and associated passive components. Now for many commercial RF frequency bands there are low cost IC's available which perform as well or better than discrete transistor designs. For example the RF-Micro Devices RF2489 IC has a low noise amplifier covering the 869 to 894 MHz mobile radio bands with a noise figure of 1.1 dB, which is better than the transistor amplifier example used in these lectures. That IC also has a mixer, resulting in a low cost system. The IC's also have less stability problems. If a low noise amplifier, without a mixer is required, then the RF Micro Devices RF2361 amplifier can be used and that has a noise figure of 1.4 typically at 881 MHz and 1.3 at 1.95 GHz. Many other manufacturers have similar devices.

For IF amplifiers at HF frequencies it is now also possible to use high speed operational amplifiers, resulting in IF strips that have an excellent linearity and very low intermodulation distortion. For medium power amplification, VHF cable TV repeaters can be used. There are also many amplifier modules available with a very high linearity, particularly for frequency bands for mobile phones, wireless LAN, Bluetooth and other high volume consumer frequencies.

MMIC

Several IC manufacturers like Agilent, Minicircuits and Freescale (Motorola) produce general purpose Microwave Monolithic Integrated Circuits (MMIC): These can be used as general purpose amplifier blocks and can be used at frequencies from DC up to 10GHz. Several devices also have low noise figures, for example, the Minicircuits MAR6 amplifier has a bandwidth of DC to 2 GHz and a noise figure of 3 dB and the GALIS66 amplifier has a bandwidth of DC to 2 GHz and a noise figure of 2.7 dB. These devices have sufficient low noise figures to result in economical commercial solutions.

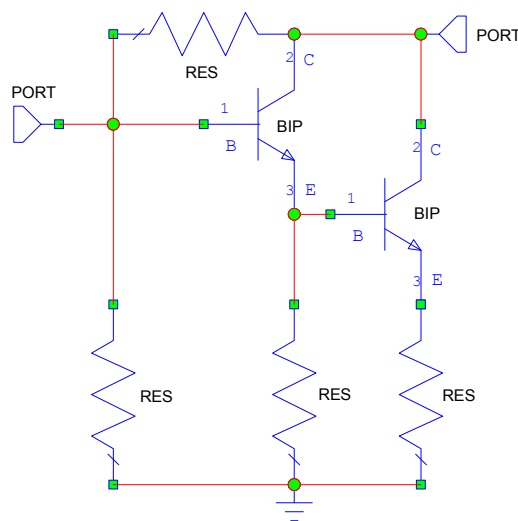


Figure 1. Typical Minicircuits MMIC circuit diagram.

There are basically two types of general purpose MMIC's: 1) Fixed voltage and 2) Constant current. The fixed voltage MMIC's are designed to operate at a supply voltage of typically 5 or 3.6 Volt.

Minicircuit's MAR, ERA, Gali and Lee series of amplifiers all require a constant current source and have a typical circuit diagram as shown in figure 1. Many of the MMIC's are made using InGaP HBTs (indium gallium phosphide heterojunction bipolar transistors). Others are made using gallium arsenide Enhancement Mode Pseudomorphic High Electron Mobility Transistor (PHEMT).

A suitable constant current supply is achieved by using a resistor to set the current supplied to the MMIS. The RF loading of that resistor is minimised by having a large inductor in series with the resistor. Since the resistor is typically $600\ \Omega$ for a 12 Volt supply voltage, in many applications a slightly reduced gain can be tolerated and the inductor can be removed. This series resistor, together with the DC feedback resistor, between the collector and base of the transistor in figure 1, result in a stable quiescent current as the temperature changes.

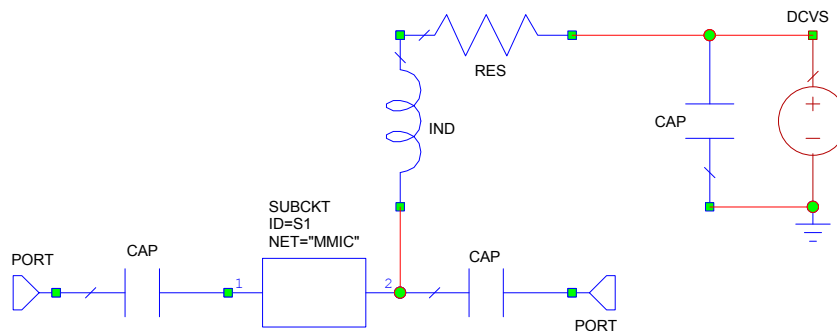


Fig.2 Typical connection requirement for the MMIC.

Most of the devices are unconditionally stable. However since these devices have very wide bandwidths, microwave layout techniques must be used to ensure that the devices remain stable. As a typical example it is essential that the inductance of the earth pin connections of the MMIC is kept as low as possible. This is achieved by ensuring that earth pins of the MMIC are soldered to a large ground plane and that very close to the earth pin of the MMIC that ground-plane has a via connecting the top ground-plane to the bottom ground-plane of the microstrip PCB layout.

These amplifier modules and MMIC's can now be used for the majority of RF and microwave designs. There are however some applications, such as very low noise amplifiers of very high frequency applications and high power amplifiers, where amplifier modules and MMIC's can not be used. For such designs a knowledge of stability, noise and gain circles of the amplifier is essential.

Stability

For power amplifier design single power transistors are used to provide the required amplification at the required frequency, with the required linearity. The amplifier should be stable and not oscillate at any frequency under normal operating conditions. Amplifier stability and ensuring that the transistor is matched, so that the highest power output is obtained are the most critical parameters in a power amplifier design.

Smith Chart Revision

A good reference for this material is D. M. Pozar: “Microwave Engineering” 3rd Edition, Wiley, Chapter 11

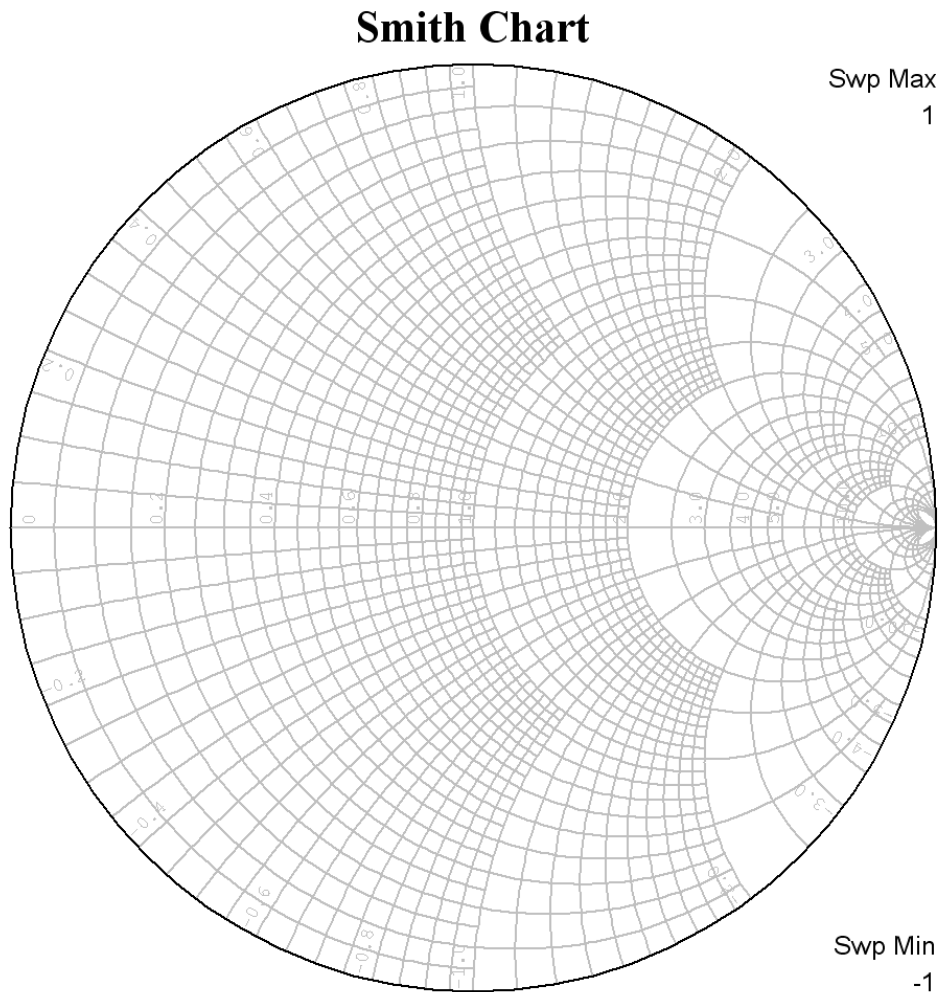


Figure 3. Smith Chart

Figure 3 shows a Smith Chart, which is a plot of the normalised reflection coefficient Γ .

$$\Gamma = \frac{Z_L - 1}{Z_L + 1} = |\Gamma| \angle e^{j\theta} = \Gamma_r + j\Gamma_i$$

Hence the Smith chart also represents Z_L and we can plot contours of $Z_L = R_L + jX_L$. Solving for R_L and X_L gives:

$$R_L = \frac{1 - \Gamma_r^2 - \Gamma_i^2}{(1 - \Gamma_r)^2 + \Gamma_i^2} \quad \text{and} \quad X_L = \frac{2\Gamma_i}{(1 - \Gamma_r)^2 + \Gamma_i^2}$$

R_L and X_L form a family of circles.

The Smith chart is a very useful tool for showing impedance values versus frequency.

Scattering Parameters Revision

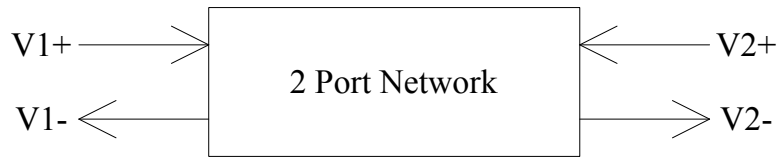


Figure 4. S parameter definitions

$$\begin{bmatrix} V_1^- \\ V_2^- \end{bmatrix} = \begin{bmatrix} S_{11} & S_{12} \\ S_{21} & S_{22} \end{bmatrix} \begin{bmatrix} V_1^+ \\ V_2^+ \end{bmatrix}$$

$$S_{11} = \left. \frac{V_1^-}{V_1^+} \right|_{V_2^+ = 0} \quad \text{i.e. reflection coefficient at port 1 with an ideal match at port 2}$$

$$S_{22} = \left. \frac{V_2^-}{V_2^+} \right|_{V_1^+ = 0} \quad \text{i.e. reflection coefficient at port 2 with an ideal match at port 1}$$

$$S_{21} = \left. \frac{V_2^-}{V_1^+} \right|_{V_2^+ = 0} \quad \text{i.e. forward gain}$$

$$S_{12} = \left. \frac{V_1^-}{V_2^+} \right|_{V_1^+ = 0} \quad \text{i.e. reverse gain, i.e. effect of output on input.}$$

An amplifier is unilateral if $S_{12} = 0$ i.e. the reverse gain is zero. That applies to many amplifiers, particularly operational amplifiers and other IC's where the output is well separated from the input.

The input reflection coefficient is:

$$\Gamma_{in} = S_{11} + \frac{S_{12}S_{21}\Gamma_{Load}}{1 - S_{22}\Gamma_{Load}} \quad \text{For a unilateral amplifier } \Gamma_{in} = S_{11}$$

$$\Gamma_{out} = S_{22} + \frac{S_{21}S_{12}\Gamma_{Source}}{1 - S_{11}\Gamma_{Source}} \quad \text{For a unilateral amplifier } \Gamma_{out} = S_{22}$$

The available power gain of an amplifier is:

$$G_A = \frac{\text{Power available from network}}{\text{Power available from source}} = \frac{|S_{21}|^2(1 - |\Gamma_S|^2)}{|1 - S_{11}\Gamma_S|^2(1 - |\Gamma_{out}|^2)} \quad (\text{Poazar 3}^{\text{rd}} \text{ ed. Eqn. 11.12})$$

The Available Power Gain is a useful measure of how well the amplifier is matched.

$$G_T = \frac{\text{Power delivered to the load}}{\text{Power available from source}} = \frac{|S_{21}|^2(1 - |\Gamma_S|^2)(1 - |\Gamma_L|^2)}{|1 - \Gamma_S\Gamma_{in}|^2|1 - S_{22}\Gamma_L|^2} \quad (\text{Poazar 3}^{\text{rd}} \text{ ed. Eqn. 11.13})$$

The Transducer Power Gain is a useful measure of the gain of the amplifier. There are measurement functions for available power gain and transducer gain in Microwave Office.

Under ideal conditions, $\Gamma_s = 0$ and $\Gamma_L = 0$ so that $G_A = G_T = |S_{21}|^2$

An amplifier includes input and output matching circuits as shown

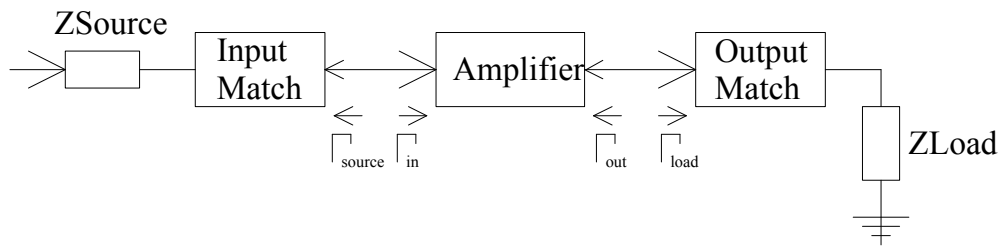


Figure 5. Amplifier Block Diagram

The input match provides maximum power when $\Gamma_{in} = \Gamma_{source}^*$ so that the gain of the input matching network is $G_S = 1$. Similar when the output has a conjugate match so that $\Gamma_{out} = \Gamma_{load}^*$, then $G_L = 1$. In general:

$$G_S = \frac{1 - |\Gamma_S|^2}{1 - \Gamma_{in} \Gamma_S} \quad (\text{Pozar 3}^{rd} \text{ ed. Eqn. 11.17a})$$

$$G_0 = |S_{21}|^2 \quad (\text{Pozar 3}^{rd} \text{ ed. Eqn. 11.17b})$$

$$G_L = \frac{1 - |\Gamma_L|^2}{1 - \Gamma_{out} \Gamma_L} \quad (\text{Pozar 3}^{rd} \text{ ed. Eqn. 11.17c})$$

The gain of the whole amplifier is:

$$G_T = G_S * G_0 * G_L$$

Under ideally matched conditions $G_S = 1$ and $G_L = 1$ so that the gain is thus:

$$G_T = |S_{21}|^2, \text{ as was obtained before.}$$

Stability Requirements

Oscillations will occur if $G_S \rightarrow \infty$ or $G_L \rightarrow \infty$

For oscillations due to the input, $\Gamma_{in} * \Gamma_S = 1$. If $\Gamma_S = 1$ then for oscillations $\Gamma_{in} = 1$.

$$\Gamma_{in} = S_{11} + \frac{S_{12} S_{21} \Gamma_{Load}}{1 - S_{22} \Gamma_{Load}}$$

This is a circle on the Smith Chart called Input Stability Circle. Oscillators often are designed by deliberately making $\Gamma_{in} * \Gamma_S = 1$ and having the source impedance a frequency selective network, such that this condition for oscillation is only satisfied at one frequency. The amplifier is stable for input conditions if $\Gamma_{in} < 1$.

For oscillations due to the output $\Gamma_{out} * \Gamma_L = 1$. If $\Gamma_L = 1$ then for oscillations $\Gamma_{out} = 1$.

$$\Gamma_{out} = S_{22} + \frac{S_{21} S_{12} \Gamma_{Source}}{1 - S_{11} \Gamma_{Source}}$$

This is a circle on the Smith Chart called Output Stability Circle. The amplifier is stable for output conditions if $\Gamma_{Out} < 1$. Microwave Office allows Stability Circles to be plotted at different operating conditions. To see these circles the region outside the normal Smith Chart may need to be viewed.

For unilateral amplifiers $S_{12} = 0$, so that $\Gamma_{in} = S_{11}$. and $\Gamma_{out} = S_{22}$. This makes it relatively easy to ensure that the amplifier is stable.

Unconditional Stability

An amplifier is unconditionally stable if $|\Gamma_{In}| < 1$ and $|\Gamma_{Out}| < 1$ for all passive load and source impedances. As an example, the first version of the MAR6 amplifier is unconditionally stable. For this to occur, both the input and output stability circles lie outside the normal Smith Chart. The second version, the MAR6A amplifier is conditionally stable.

Conditional Stability

An amplifier is conditionally stable if $|\Gamma_{In}| < 1$ and $|\Gamma_{Out}| < 1$ only for certain load and source impedances. As an example the early version of the MAR8 amplifier was only conditionally stable and both input and output reflection coefficients had to be less than 0.5. For conditional stability, either or both the input and output stability circles partially lie inside the normal Smith Chart.

Stability Factors: Measures of Stability

The Rollet's stability factor, K is defined as:

$$K = \frac{1 - |S_{11}|^2 - |S_{22}|^2 - |\Delta|^2}{2|S_{12}S_{21}|} \quad \text{Where } |\Delta| = |S_{11}S_{22} - S_{12}S_{21}|$$

In addition the auxiliary stability factor is defined as:

$$B = 1 + |S_{11}|^2 - |S_{22}|^2 - |\Delta|^2$$

For unconditional stability $K > 1$ and $B > 0$.

The Geometric Stability Factor, μ is defined as:

$$\mu = \frac{1 - |S_{22}|^2}{|S_{22} - \Delta S_{11}^*| + |S_{12}S_{21}|}$$

This stability factor measures the distance from the centre of the Smith Chart to the nearest unstable region. For unconditional stability $\mu > 1$. In addition, the larger the value of μ , the more stable the amplifier.

The Rollet's stability factors K and B and the Geometric Stability Factors for both the input and output of an amplifier are available as measurements in Microwave Office, so that an amplifier's stability can easily be determined at any frequency. It is important that the stability of an amplifier is determined at all possible frequencies, since if the device is unstable it will likely oscillate. If the designer only measures the performance of the amplifier in the operating band and oscillating frequency is far removed from this

frequency, the designer will be at a loss to explain the very poor amplifier performance until a spectrum analyser is used to check for oscillations over a wide frequency range.

If the amplifier is not unconditionally stable then the source and load must be carefully controlled to ensure that the amplifier is stable under normal operating conditions.

Design for Maximum Gain

To design an amplifier for maximum gain, the input matching network and the output matching network are both designed to provide a conjugate impedance match at the operating frequencies, thus making $G_S = 1$ and $G_L = 1$, as outlined above. Since the power gain depends on the impedance match at the input, one can plot constant gain circles on the Smith Chart, to show how the gain varies with the matching impedance. Designing an amplifier for maximum power gain may result in unstable operation.

Amplifier Noise Figure

In many instances an amplifier must be designed for a low noise figure. The input matching conditions for the lowest noise figure are different from those for a high power gain, so that a reduced gain is obtained from the amplifier. In addition the match for best noise may make the amplifier only conditionally stable.

The interaction between stability factors, noise factors and gain are shown using the following example:

Design a low noise amplifier for the region of 950 to 1000 MHz using a 2SC3357 low noise transistor. The specifications of that transistor are: NF = 1.1 dB TYP., Ga = 7.5 dB TYP. @ VCE = 10 V, IC = 7 mA, f = 1 GHz.

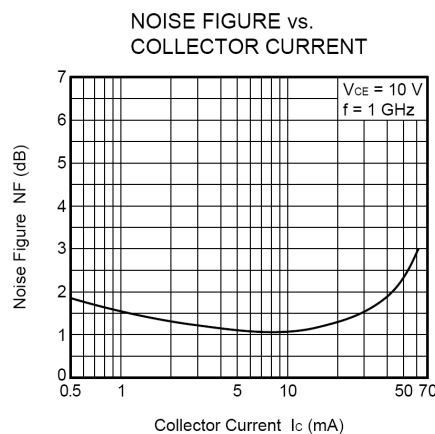


Figure 6. Noise figure versus Collector Current (2 2SC3357 data sheet from NEC)

The noise figure will vary with frequency. At < 1 MHz the noise rises due to $1/f$ noise at a rate of 20 dB per decade. This $1/f$ noise is not normally included in the model for the transistor, since external components such as coupling capacitors are likely to dominate the noise figure at those frequencies. At high frequencies the noise rises because of changes in the transistor parameters. The noise figure in these the regions rises at 40 dB per decade. In addition the noise voltage changes with collector current and voltage across the transistor. The variation of noise figure for the transistor is shown in figure 6.

To start the design use a basic amplifier as shown in figure 7. The biasing resistors are chosen to cause a 7 mA collector current, corresponding to the minimum noise figure.

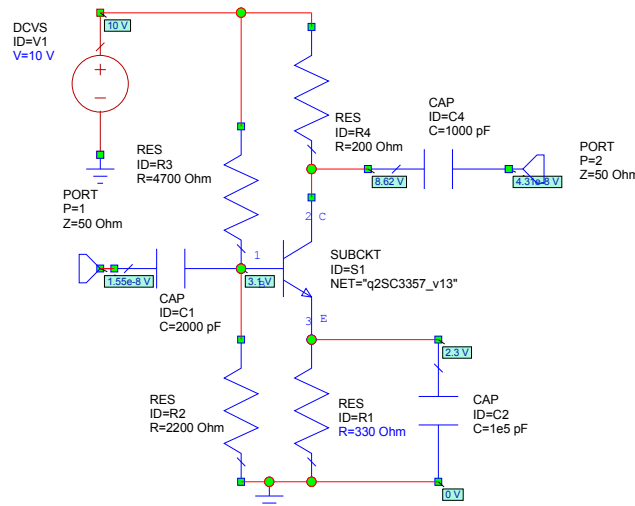


Figure 7. Basic Low Noise Amplifier

The Noise figure and gain can now be calculated using computer simulation and are shown in figure 8. The rise in noise figure at low frequency is due to the input coupling capacitor causing an impedance mismatch at low frequency. The rise in noise figure at high frequency is due to changes in transistor parameters and corresponds to a drop in gain. The Supply voltage, emitter resistor and bias resistor values are tuned, to obtain the best noise figure. The values shown in figure 7 correspond to the lowest noise figure consistent with a high power gain.

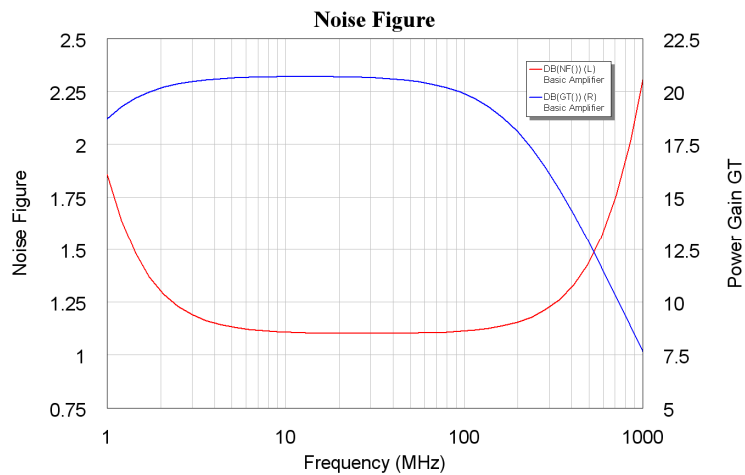


Figure 8. Noise figure and Gain of the Basic Amplifier

Figure 9 shows a plot of K , B and Input μ and Output μ stability factors. It can be seen that in the region of 25 MHz to 300 MHz, the amplifier is only conditionally stable. The amplifier is stable with a 50 Ω source and load impedance as shown in the gain plot of figure 8. Figure 10 shows the input and output stability circles plotted at 100 MHz, confirming that the amplifier is only conditionally stable. The input stability circle is shown in pink and the output stability circle is shown in blue. It can be seen that the output stability circle causes the biggest problem. Figure 11 shows the input and output stability circles over a 50 to 1500 MHz sweep. For an unconditionally stable amplifier, the entire Smith Chart can be seen.

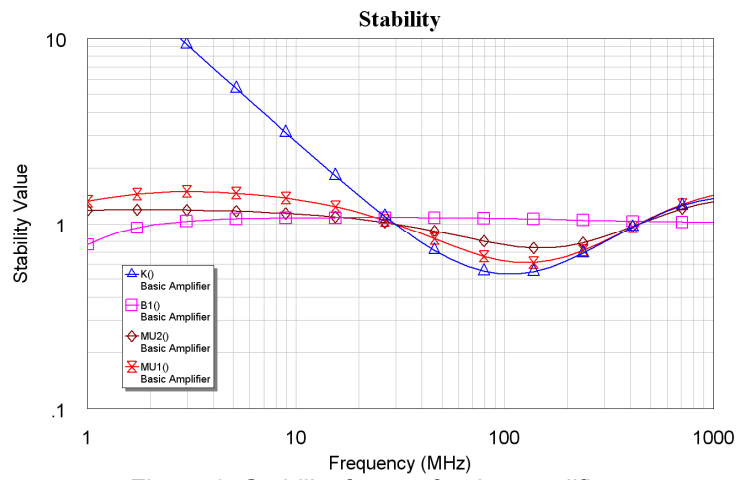


Figure 9. Stability factors for the amplifier.

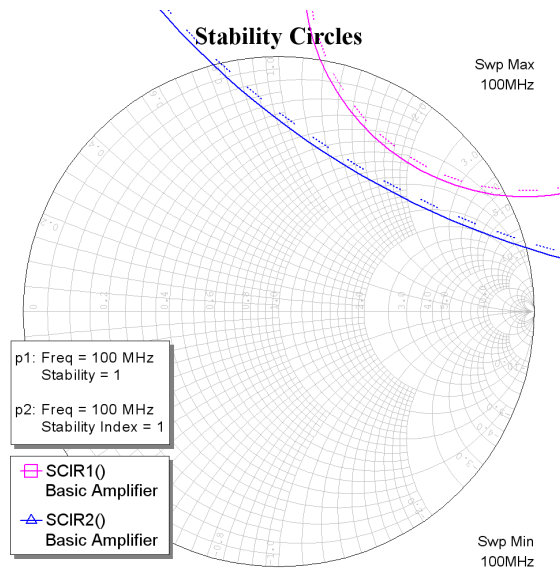


Figure 10. Stability Input and Output Circles at 100MHz.

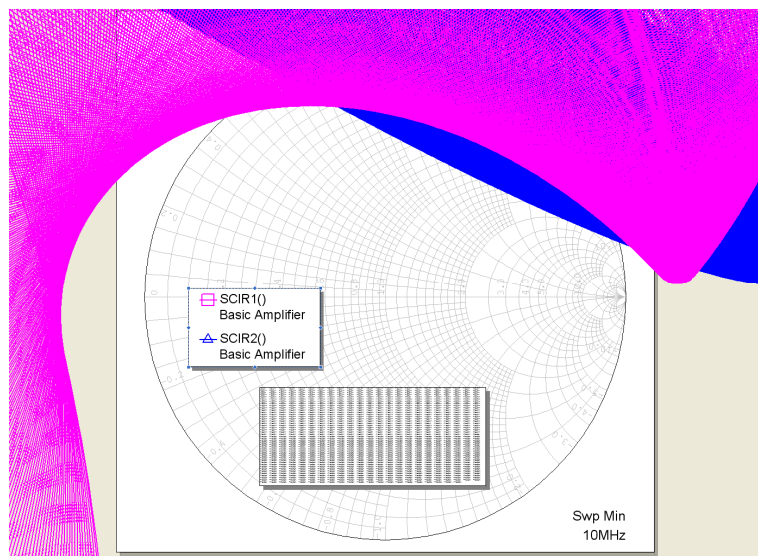


Figure 11. Stability Input and Output Circles over 50-1500MHz.

Figure 12 shows the constant Noise figure circles and the constant gain circles at 100 MHz. Note that the centre of the constant noise circles lie close the origin of the Smith Chart, so that the existing 50 Ω match is good for the best noise figure. The centres for the circles for available power are nowhere near the centre of the Smith Chart, so that a match for noise figure will not result in the highest power gain. Normally the first stage of a low noise amplifier is matched for the lowers noise figure and the second stage is matched for the highest power gain.

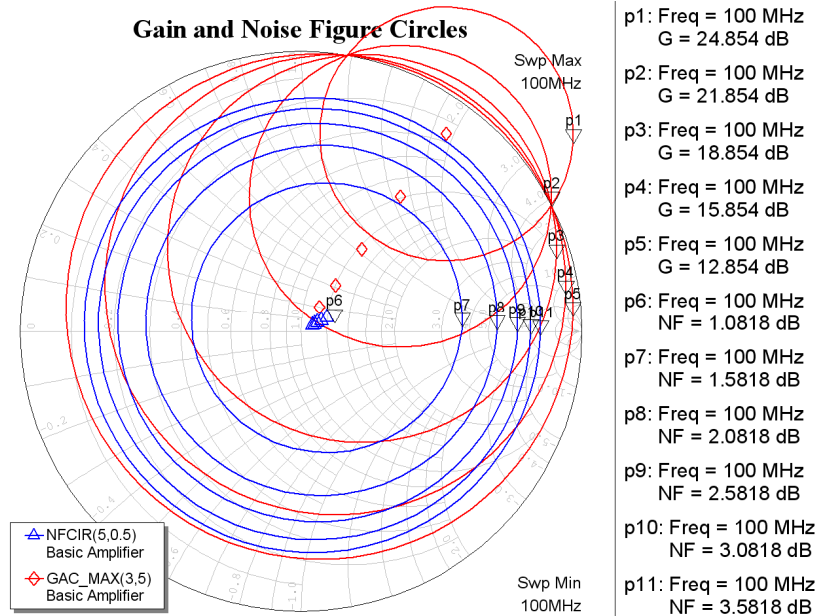


Figure 12. Constant Gain and Noise Figure Circles at 100 MHz.

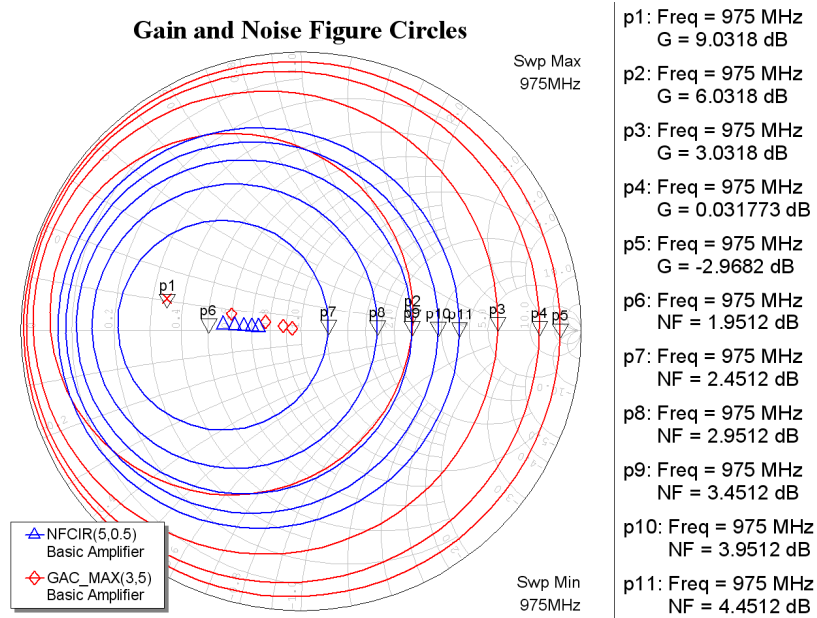


Figure 13. Constant Gain and Noise Figure Circles at 975 MHz.

In the region of 950 to 1000 MHz the constant gain and noise circles are very different, as shown in figure 13, so that the input matching needs to be changed to obtain the best noise figure. Again, the centres of constant noise figure and those of constant available power, do not coincide, so that one must either match for the best noise figure or the best power

maximum useable frequency for the transistor and it is much better to use a higher frequency transistor, so that the noise figure and gain are flatter at the operating frequency. Such transistors are however likely to be more expensive.

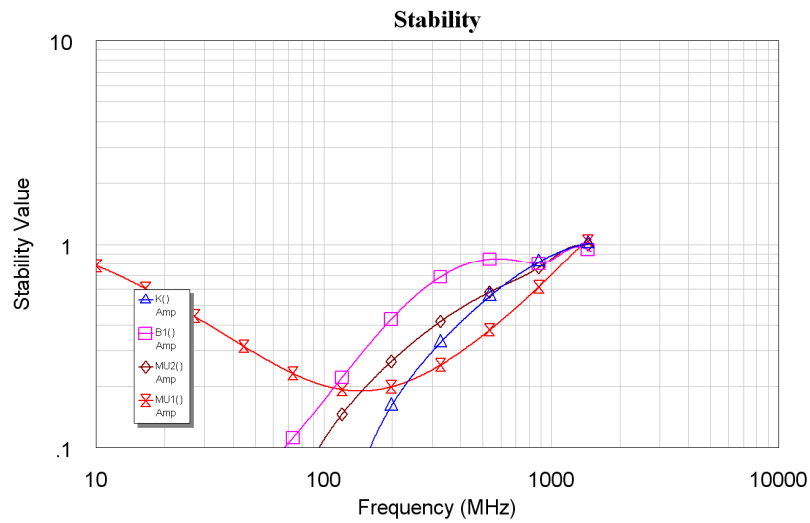


Figure 16. Stability Factors for the 950-1000 MHz amplifier.

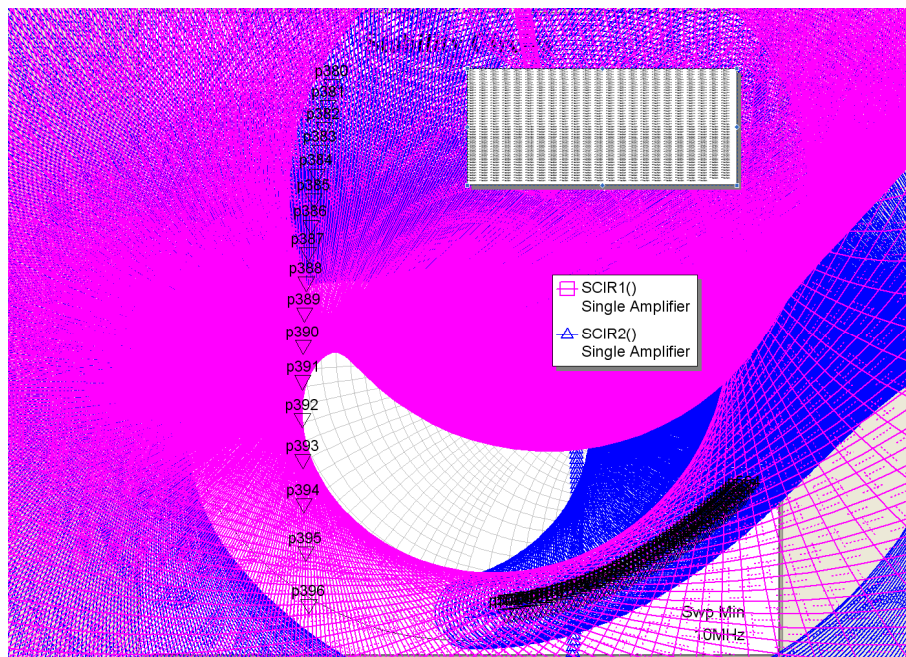


Figure 17. Stability Input and Output Circles of the amplifier of fig 11. over 50-1500MHz frequency range.

Comparing figures 16 and 17 with figures 9 and 11, it can be seen that the amplifier is far less stable than the basic amplifier. The amplifier is unconditionally stable in the 950 - 1000 MHz frequency region, however it is close to instability in the 30 to 300 MHz frequency region.

Figure 18 shows the gain and noise figure circles of the amplifier at 975 MHz. Note that the centre of the noise figure circles has been shifted to the origin due to the input tuning. The output tuning has little effect on the noise figure. The best noise figure that can be

obtained is 1.68 dB. The output matching is adjusted to increase the output power at 975 MHz as much as possible.

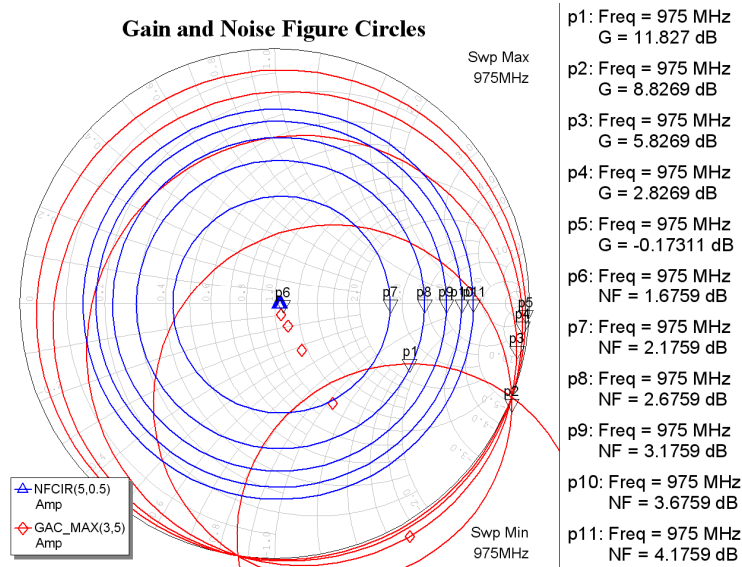


Figure 18. Gain and Noise Figure Circles for the 950-1000 MHz amplifier.

In many practical situations, particularly with power amplifiers, the transistors used will have a falling gain at 20 dB per decade over the operating range. As shown in the above example, that can lead to instability at frequencies far removed from the operating region. Any simulation for a practical design must include a stability analysis over a very wide frequency range.

It is not possible to improve the stability by say changing the output L3, of figure 14, to a tuned network and thus reducing the bandwidth of the amplifier, since that results in impedances close to the edge of the Smith Chart for some frequencies, thus worsening the stability. It is in general very difficult to ensure unconditional stability and a low noise figure. In some instances the exact source impedance, from say an Antenna, and load impedance, from following amplifiers is known and the amplifier can be kept stable. In other instances the source and load impedances are not well known, or well controlled and the amplifier design must then ensure that the amplifier is unconditionally stable.

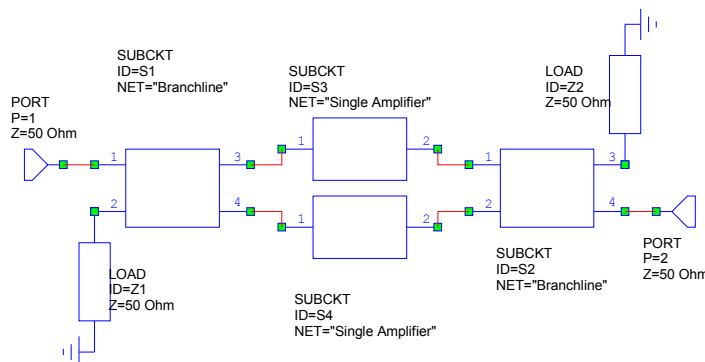


Figure 19. Dual Low Noise Amplifier.

If the amplifier is conditionally stable in the required operating frequency region, then the stability may be improved by using a branch line coupler or other 90 degree hybrid and

have two identical low noise amplifiers connected to them, as shown in figure 19. The use of 90 degree hybrids causes each of the amplifiers to see a VSWR of better than 2:1 in all instances and any reflections from the inputs of the amplifiers will end up in the load resistor connected to the port. That will improve the stability close to the operating frequency but may make the stability away from the operating frequency worse. In the circuit of figure 14, the amplifier is unconditionally stable in the 950 to 1000 MHz region, so this technique will not have any effect. The bandwidth of this amplifier is too wide for Branchline couplers to be used to improve the stability, as these are narrowband devices, however other 90 degree hybrids, like the Backward Coupled Transmission Line Hybrid can be used effectively.

Chapter 9

Impedance Matching of Power Amplifiers

Introduction

In order to obtain the most power from a bipolar or field effect transistor, the input and output impedances of the device must be matched to that of the circuit in which it is placed. Similarly if an antenna is to be driven effectively, the antenna needs to be matched. For the maximum power transfer, the source impedance and the load impedance must be a conjugate match, that is the resistive parts must be the same and the imaginary parts must be the same magnitude but opposite polarity.

There are three basic types of matching:

Transformer matching: RF Transformers can be used to produce very wideband impedance matching. The main limitations are the restricted range of available impedances (due to the turns-ratios being limited) and the frequency limitations on transformers.

LC matching: where inductors and capacitors are used to effect the impedance transformation. LC matching results in a relatively narrow bandwidth match. LC matching is very practical at frequencies from 30 MHz to 300 MHz. LC matching permits easy tuning of the match to allow for device variations.

Transmission line matching: By using a transmission line of a required length and Characteristic Impedance, the required composite match can be obtained. Such a match tends to be of a broader frequency range than LC matching and can be applied at frequencies above about 150 MHz. It is difficult to tune the length and characteristic impedance of a transmission line once constructed.

For each application, each of the above matching techniques must be evaluated against the design criteria and the most appropriate technique selected.

Choice of Components and Q value

It is very important that the value of capacitors and inductors used be measured at the operating frequency. Many capacitors are not suitable for RF applications, as their self resonance frequency is below the required operating frequency. For power applications, inductors with ferrite cores may not be suitable as their losses may be too high.

For a simple parallel tuned network, like the Pi network, the circulating current in a resonator is approximately Q times the external load current. For a 50 Watt amplifier, driving a 50 Ω load a Q of 10 the current circulating in the Pi network is thus of the order of 10 Amps. This can cause significant heating and failure of the components. For some networks like both the T networks and the Bandpass L network, very high voltages can be experienced at some nodes and this can lead to voltage breakdown of components. The higher the Q the higher the stress on the components. A high Q value can also cause the matching network to drift out of match if the components change due to temperature. In general a Q value as low as possible is desirable, as this will give the widest bandwidth match and the lowest component stress. If the network is to be used as an output matching network of an amplifier and harmonics are to be filtered as well,

a higher Q value should be considered, since the higher the Q, the higher the attenuation at the amplifier harmonics. Since the current and voltage limits in the output matching networks are very important, a trade-off between the Q value and Number for filter sections required to achieve the required harmonic attenuation may need to be considered.

Large Signal Parameters: The large signal input and output impedances and the large signal S parameters are very different from the small signal impedances and small signal S parameters. The large signal parameters should be used in the design.

LC Matching

In LC Matching Inductors and Capacitors are used to obtain the required conjugate impedance match. The equations for calculating the components required are contained in Motorola Application note 267. LC matching is very practical for power amplifiers from 30 to 300 MHz. A good indication of the suitability of LC matching for a transistor is by noting the test circuits used by the manufacturers for the proposed device.

Because it is easy to tune the matching network using variable capacitors, these LC matching networks are normally used by the manufacturers to determine the input and output impedance of the devices. The device is placed in a test jig and the matching network is adjusted to obtain the required output power at a good efficiency and with a low input return loss. The values of the resulting LC matching components are then used to determine the input and output impedance of the device.

AN267 describes 4 matching networks. In all the equations, the device impedance is $R_d + jX_d$ and the load impedance is R_L . This notation is different from AN267, to avoid confusion between R_1 and R_L , particularly is a capital L is used. In the equations it is not assumed that the device is capacitive, so that X_d is used for the reactive part of the device impedance, instead of $-X_{\text{out}}$. Also in AN267 for the Bandpass T and the Lowpass T networks, different expressions for A and B are used. In these notes consistent expression for A and B are used.

Pi Network

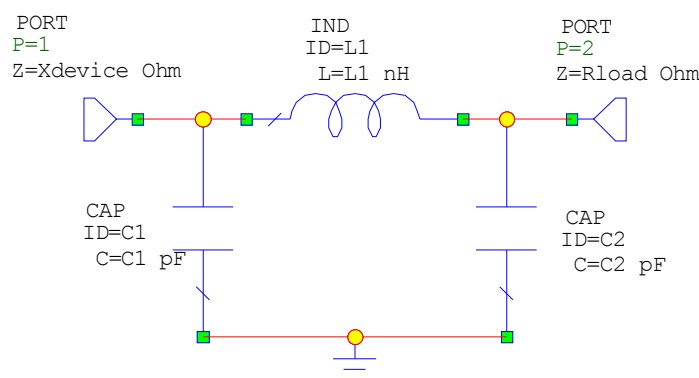


Figure 1. Pi Matching Network.

The Pi matching network is very useful for matching high impedance sources to 50 Ω loads. Pi matching is normally used in valve amplifiers. For high power solid-state devices, the impedance values become impractical with very large capacitors and very small inductors being required. Figure 1 shows the Pi network used for matching.

To obtain the component values, firstly decide on a Q value for the matching network. The Q value will effect the bandwidth, harmonic attenuation and component stress. For the Pi network, the input impedance needs to be a parallel network, so that a series to parallel transformation may need to be applied before the network evaluation as shown in equation 1, which transforms the device impedance of $R_D + jX_D$ into R_P in parallel with X_P . The equations for the Pi network in AN267 assume that the device is resistive and that any reactive impedances are compensated for after the Pi network is designed. This also applies for the Visual Basic program included with these notes. The equations in the included MWO files handle reactive parts correctly. The complete equations for the Pi matching network are as follows:

$$R_p = \frac{R_D^2 + X_D^2}{R_D} \quad X_p = \frac{R_D^2 + X_D^2}{X_D} \quad \text{Eqn. 1}$$

$$Y_{C1} = \frac{1}{X_{C1}} = \frac{Q}{R_p} + \frac{1}{X_p} \quad \text{Eqn. 2}$$

$$X_{C2} = R_L \sqrt{\frac{\frac{R_p}{R_L}}{(Q^2 + 1) - \frac{R_p}{R_L}}} \quad \text{Eqn. 3}$$

$$X_L = \frac{QR_p + (\frac{R_p R_L}{X_{C2}})}{Q^2 + 1} \quad \text{Eqn. 4}$$

Note that $Q^2 + 1$ must be larger than R_p/R_L for X_{C2} to be valid.

Low Pass T Network

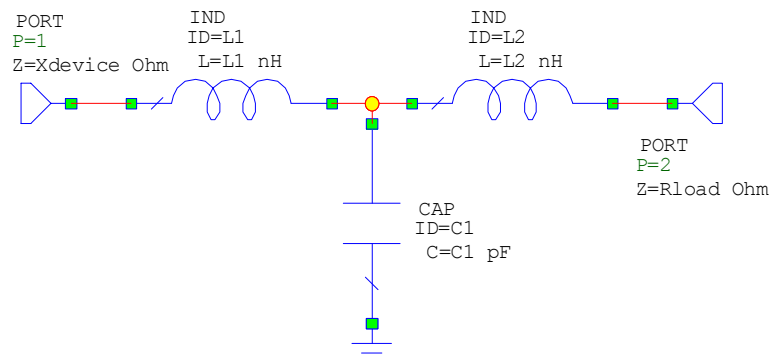


Figure 2. T Matching Network.

The Low pass T network is very good for use as an output matching network for a power amplifier stage, where the amplifier is to be connected to an antenna. Having a

series inductor (L1) as the element connected to the device results in an open circuit to the second harmonic currents, resulting in a reduced current flow through the transistor and resulting in a higher efficiency. However since the output voltage is more distorted a higher inter-modulation distortion may result. For more severe filtering of harmonics, a cascaded set of low pass matching networks is desirable.

The equations for the low pass T network are as follows:

$$X_{L1} = QR_D - X_D \quad \text{where } R_D + jX_D \text{ is the device impedance} \quad \text{Eqn. 5}$$

$$X_{L2} = R_L A \quad \text{Eqn. 6}$$

$$X_{C1} = \frac{B}{Q + A} \quad \text{Eqn. 7}$$

where

$$A = \sqrt{\left[\frac{R_D(1+Q^2)}{R_L} \right]} - 1 = \sqrt{\left[\frac{B}{R_L} \right]} - 1 \quad \text{Eqn. 8}$$

$$B = R_D(1+Q^2) \quad \text{Eqn. 9}$$

Note this network clearly shows that the Q used in the matching network relates to the impedance transformation ratio. The minimum Q occurs when $A_1=0$, so that

$$Q_{\min} = \sqrt{\frac{R_L}{R_D} - 1} \quad \text{Eqn. 10}$$

Bandpass L network

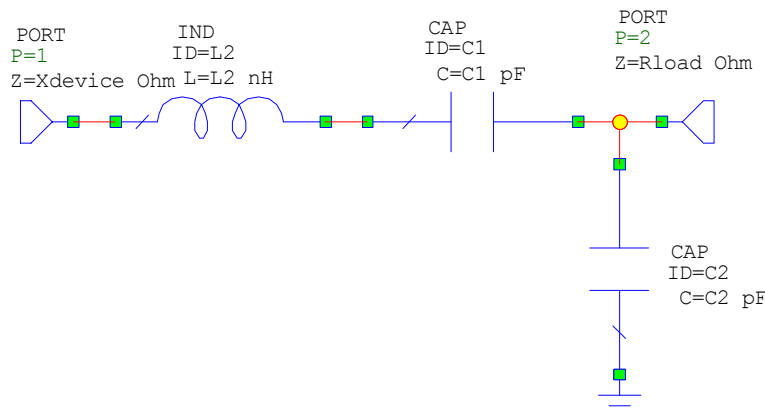


Figure 3. Bandpass L Matching Network.

The bandpass L network is often used as test circuit by semiconductor manufacturers. It has a DC block, to allow biasing to be set up for the input of transistors and to prevent any DC supply from appearing on the output of an amplifier stage. Normally C1 and C2 are adjustable, making it very easy to tune the amplifier for either a peak of output for an output matching network or for the best input match for an input matching network.

The equations for the band pass L network are as follows:

$$X_{C1} = QR_D \quad \text{where } R_D + jX_D \text{ is the device impedance} \quad \text{Eqn. 11}$$

$$X_{C2} = R_L \sqrt{\frac{R_d}{R_L - R_d}} \quad \text{Eqn. 12}$$

$$X_{L2} = X_{C1} + \left(\frac{R_D R_L}{X_{C2}} \right) \quad \text{Eqn. 13}$$

The device Reactance X_D is incorporated in either C_2 for capacitive device impedances or into L_2 for inductive device impedances. This will ensure the lowest Q of the network and thus the widest bandwidth. This network can only be used if $R_D < R_L$, since the parts under the square root sign

Bandpass T network

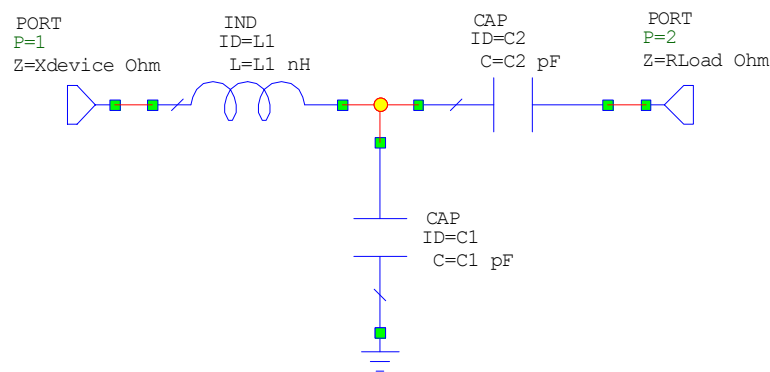


Figure 4. Bandpass T Matching Network.

The equations for the band pass T network are as follows:

$$X_{L1} = QR_D - X_D \quad \text{where } R_D + jX_D \text{ is the device impedance} \quad \text{Eqn. 14}$$

$$X_{C2} = A R_L \quad \text{Eqn. 15}$$

$$X_{C1} = \frac{B}{Q - A} \quad \text{Eqn. 16}$$

Where A and B and the minimum Q are as before:

$$B = R_D(1 + Q^2) \quad A = \sqrt{\left[\frac{R_D(1 + Q^2)}{R_L} \right] - 1} = \sqrt{\left[\frac{B}{R_L} \right] - 1} \quad \text{Eqn. 17}$$

This network can only be used if $R_D < R_L$, since otherwise negative values for C_1 result.

Important notes:

- 1 Some of the equations for the Pi network are different since the reactive parts of the device are handled in the equations presented here, while they are not in AN267 or the Visual Basic program included under the "Resources" for this course.
- 2 In these notes A and B are kept the same in these notes, while A and B are swapped and changed in AN267.
- 3 In AN267 the term A for the Bandpass T is wrong. AN267 uses:

$$A_{267} = \sqrt{\left[\frac{R_D(1+Q^2)}{R_L} \right] - 1} = \sqrt{\left[\frac{B}{R_L} \right] - 1} \quad \text{Eqn. 18}$$

That will not give a correct match, as can be verified by using Microwave Office. The square root should be extended to cover the -1 term as in the expression for A in equation 17.

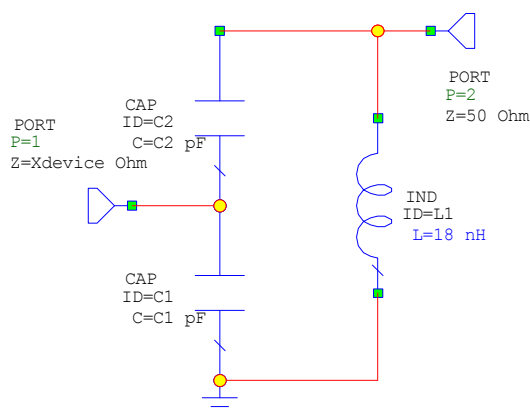
Capacitive Impedance Transformer

Figure 5. Capacitive Impedance Transformer Matching Network.

The capacitive transformer is not included in AN267, but this network can be quite useful and give very realisable components in inter-stage matching networks. The network is thus used to match the output impedance of one transistor to the input impedance of another transistor. The circuit is related to the Lowpass Pi network, except the ground and the input port are changed. For this network the output impedance at port 2 is always larger than that at port 1.

For a non-reactive device, the equations for the component values are the same as those for the Pi network, with the input impedance being the same (at port 1), but the reference impedance 50Ω now being the same as $(R_1 - R_{\text{device}})$ used in the Pi network. So instead of R_1 , the value $R_1 - R_{\text{device}}$ is used in the equations. The values can also easily be obtained using computer optimisation, as was done in the example below. The calculations for the Capacitive Transformer in the included MWO file, handles the reactive part by using the equations for a resistive device and then tuning C2 and L1 to obtain a correct match.

Example

The above equations will now be applied to an MRF1535, 35 Watt LDMOS FET in order to obtain a suitable match. This FET is suitable for operation from 135 MHz to 520 MHz and can thus be used for mobile radio applications. An amplifier at 150 MHz is required.

To calculate the components, equations 1 to 18 must be evaluated. The author wrote a Visual Basic program, which is included under the "Resources" section of these notes. For a Pi network, AN267 did not include the device reactance as part of C1. The Visual Basic program follows this practice as it is easy to manually include any device capacitance as part of C1 and produce the lowers Q in the process. With the current MWO software, it is easier to include the equations 1 to 18 as part of the "Global Variables" and this has been done for the production of figures 9 to 18. The resulting MWO file is included as part of these lectures.

Using the manufacturers data, the input impedance at the required frequency is determined. It should be noted that these values do depend on individual device and the quiescent current, so that in practice the actual values may be slightly different. For this device the input impedance is the same at 137 MHz and 155 MHz, and is $5 + j0.9 \Omega$. The $j0.9 \Omega$ reactance corresponds to a 955 pH inductor at 150 MHz.

The Q value to be selected for the matching network is a compromise. For a wide bandwidth a low Q is required. However the desired matching may not be possible at low Q values. For this FET only the bandpass L and Pi network are possible for matching with Q values below $Q = 3$. This is shown in figure 7 for a Q value of 2.5. The Pi network requires a 8.17 nH inductor, which is a fraction small to make reliably.

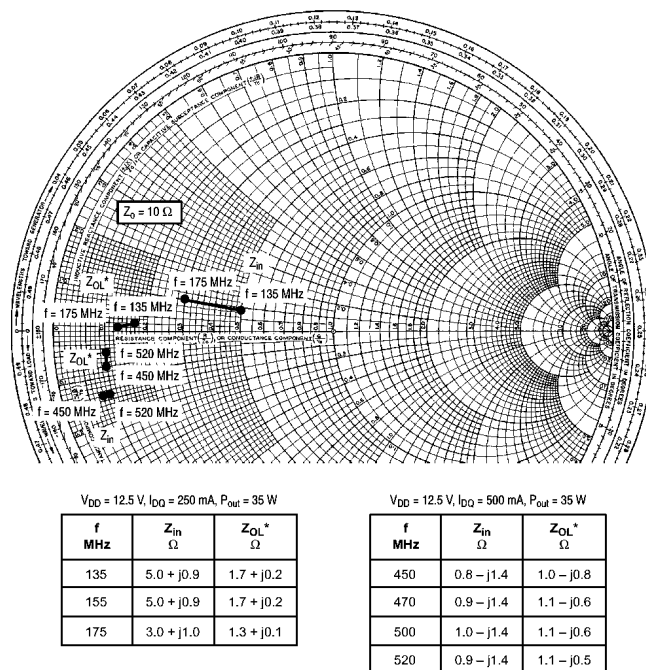


Figure 6. Part of Datasheet showing large signal Input and Output impedances.

For matching into a 50 Ω load, the minimum Q for both T networks is 3. The designs below use a Q of 3.5, which is sufficiently high to be able to have all matching networks, so that they can be compared and is sufficiently low to have as wide a bandwidth as possible. Figures 8 to 18 show that the bandwidth over which a good

match is obtained is relatively small compared with transformer matching and transmission line matching.

A Visual Basic program incorporating the matching equations for the different networks is included in the "Resources" for this course and can be used to perform the calculations as shown below. This allows Q values to be varied easily to ensure the network uses practical components. As mentioned before, figure 8 does not fully compensate for the reactive part of the source impedance for the Pi network. For this example with $Z_d=5+j0.9$ and $Q=3.5$, figure 8 evaluates C_1 as 755.25 pF while the correct value as calculated by the equations in the included MWO file is 756.41 pF.

Matching Networks

Author C. J. Kikkert, James Cook University, Dec 96 - Jul 05
Based on Motorola Application Note 267

Device Resistance	5	Frequency (MHz)	150
Device Reactance	0.9	Network Q	2.5
Termination Resistance	50	Qmin	3.0

Bandpass T Network (A)		Lowpass Pi Network (B)	
Device End Series L		Device End Shunt C	549.7 pF
Shunt C		Series L	8.1741 nH
Term. End Series C		Term. End Shunt C	176.56 pF

Bandpass L Network (C2)		Lowpass T Network (D)	
Device End Series C	84.883 pF	Device End Series L	
Device End Series L	28.223 nH	Shunt C	
Term. End Shunt C	63.662 pF	Term. End Series L	

Figure 7. Input Matching component values for a MRF1532 FET, $Q=2.5$.

Matching Networks

Author C. J. Kikkert, James Cook University, Dec 96 - Jul 05
Based on Motorola Application Note 267

Device Resistance	5	Frequency (MHz)	150
Device Reactance	0.9	Network Q	3.5
Termination Resistance	50	Qmin	3.0

Bandpass T Network (A)		Lowpass Pi Network (B)	
Device End Series L	17.613 nH	Device End Shunt C	755.25 pF
Shunt C	48.924 pF	Series L	8.1114 nH
Term. End Series C	37.223 pF	Term. End Shunt C	239.47 pF

Bandpass L Network (C2)		Lowpass T Network (D)	
Device End Series C	60.83 pF	Device End Series L	17.613 nH
Device End Series L	33.529 nH	Shunt C	65.185 pF
Term. End Shunt C	63.662 pF	Term. End Series L	30.244 nH

Figure 8. Input Matching component values for a MRF1532 FET, $Q=3.5$

The matching components are incorporated in a computer simulation package, like Microwave Office, as shown below. In order to have a source impedance of $5 + j0.9 \Omega$, a voltage controlled voltage source with a zero output impedance is used. This is then followed by a network representing the input impedance of the FET. It is however possible make the impedance of port 1 to be the resistive part of the device impedance. The transfer function then will always have an insertion loss rather than the gain as indicated in the following figures. A passive network cannot have a power gain. The power gain is provided here by the voltage dependent source. For figures 9 to 18, impedance matching with a $Q = 3.5$ as indicated in figure 8 is used.

Pi network

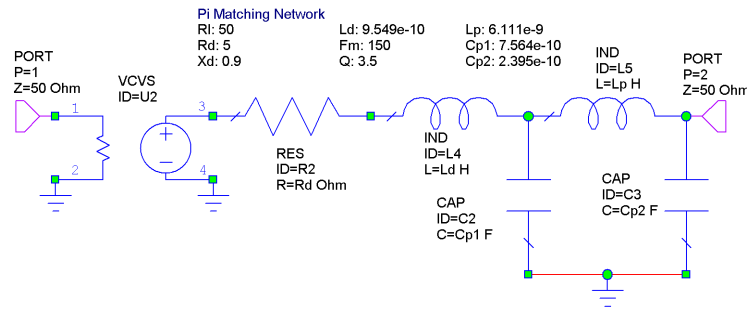


Figure 9. Circuit representation of the input impedance and the matching network.

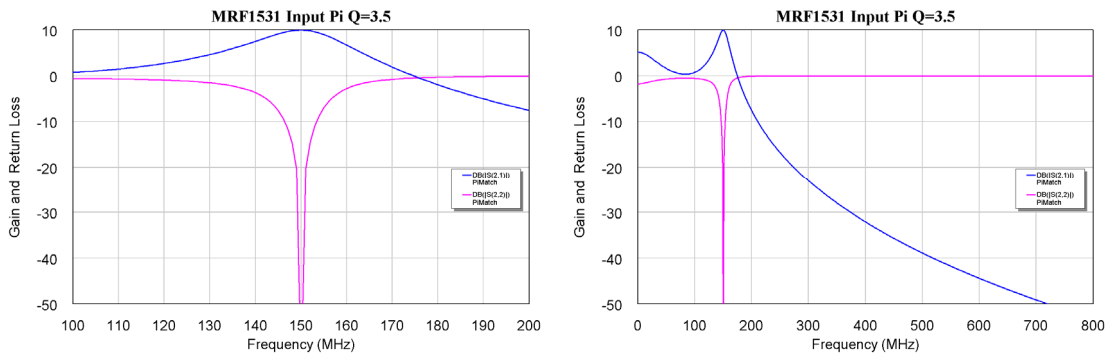


Figure 10. Frequency Response of the Pi Matching Network

Lowpass T network

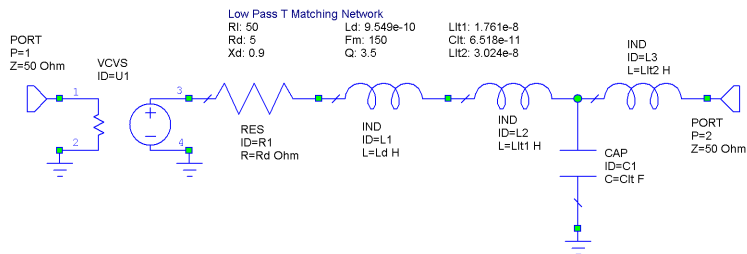


Figure 11. Circuit representation of the input impedance and the matching network.

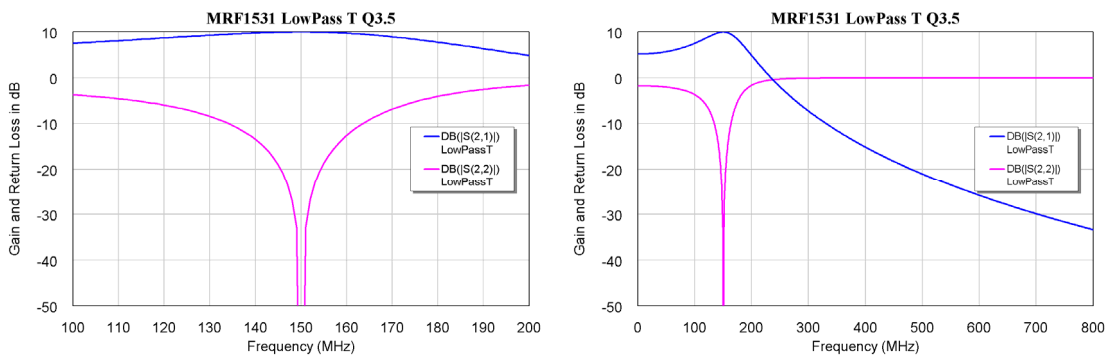


Figure 12. Frequency Response of the Lowpass T Matching Network

Bandpass T network

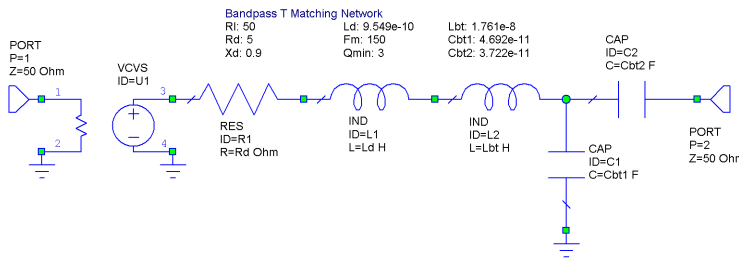


Figure 13. Circuit representation of the input impedance and the matching network.

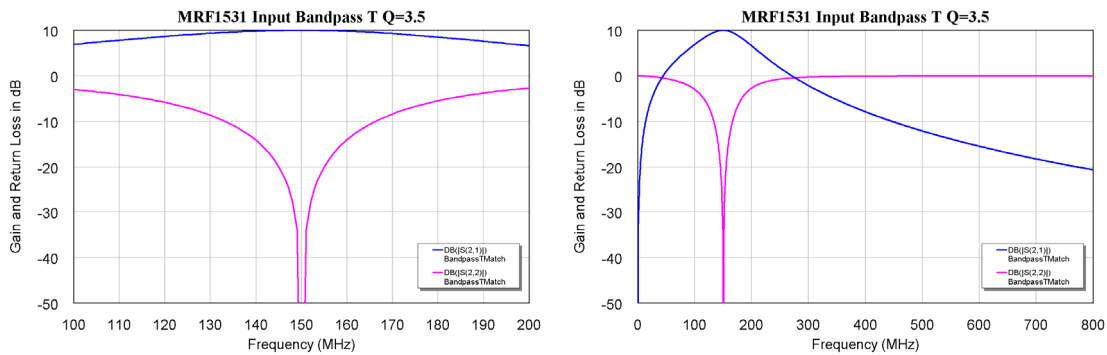


Figure 14. Frequency Response of the Bandpass T Matching Network (Harmonic View)

BandPass L Network

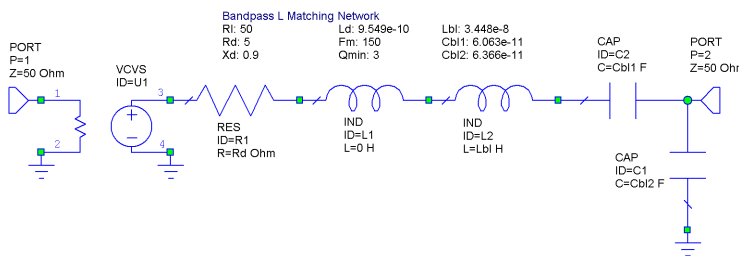


Figure 15. Circuit representation of the input impedance and the matching network.

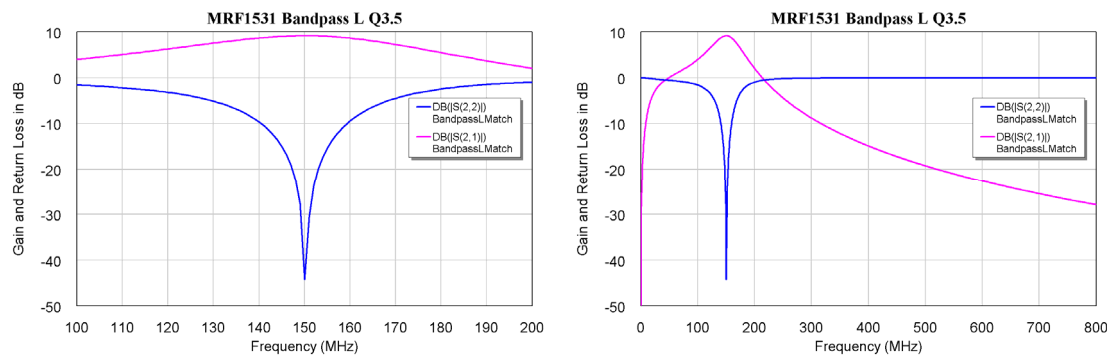


Figure 16. Frequency Response of the Bandpass L Matching Network

Capacitive Transformer Resonator

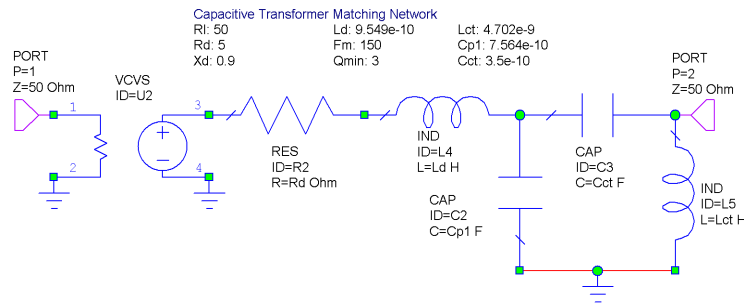


Figure 17. Circuit representation of the input impedance and the matching network.

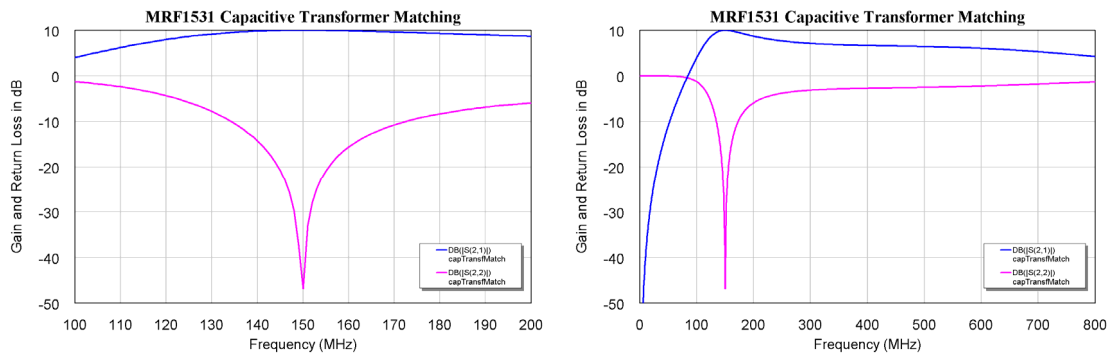


Figure 18. Frequency Response of the Bandpass L Matching Network.

Comparing figures 9 to 18, shows that for the equations 1 to 18, the Pi matching network has the lowest bandwidth, but its Q can be adjusted to make the bandwidth comparable to the other networks.

Transformer matching

In transformer matching, an RF transformer, as described in Chapter 3 of these notes is used to provide the impedance transformation required. Since the number of turns used must be an integer and the impedance transformation is the turns ratio squared, the impedance transformation ratios are limited to the square of simple fractions. For the matching of the FET in this example, a $5 + j0.9 \Omega$ impedance is required. This can best be approximated by a 3:1 turns ratio transformer, giving a 9:1 impedance transformation, so that a 50Ω source is transformed into a 5.55Ω impedance, which is sufficiently close to $5 + j0.9 \Omega$ for most of the power to be transferred effectively. If needed, the reactive part can be resonated out, using a $-j0.9 \Omega$ reactive impedance in series.

Transformer matching provides a very wideband match, of typically three decades (1000:1 frequency range) if the impedance of the device to be matched does not change. In practice the device impedance changes significantly over such a frequency range, thus limiting the effective frequency range for the matching. FET amplifiers that are well matched up to 100 MHz can easily be designed, as is evident from many power FET manufacturers application notes.

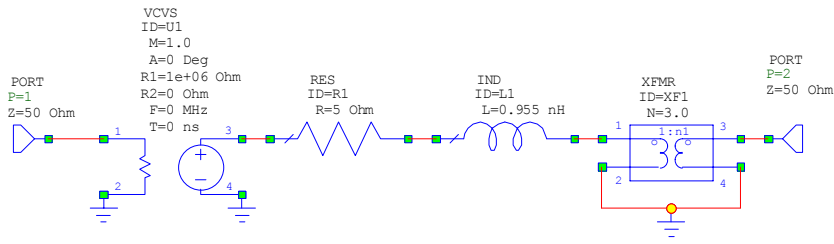


Figure 19. Circuit representation of the input impedance and the matching network.

By adding a 23.7 pF capacitance across pin 1 and 2 of the transformer, the match can be extended as shown in the right graph of figure 20. The value of the capacitance required is best determined experimentally.

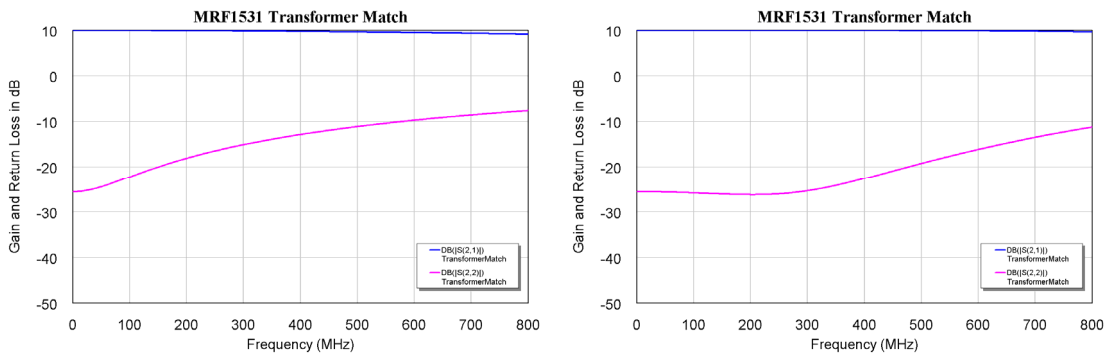
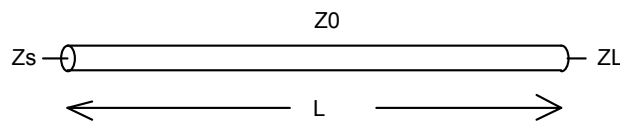


Figure 20. Frequency Response of Transformer Match (Left) and the Optimised Transformer Match (Right).

Transmission Line Matching

For a transmission line of characteristic impedance Z_0 and length L , the



The impedance looking into a transmission line that is terminated in a load Z_L is:

$$Z_s = Z_0 \frac{Z_L + jZ_0 \tan(\beta l)}{Z_0 + jZ_L \tan(\beta l)} \tag{Eqn. 19}$$

By substituting $Z_s=R_s+jX_s$ and $Z_L=R_L+jX_L$ and then solving for Z_0 and the transmission line length θ as an electrical length, one obtains the following equations:

$$Z_0 = \sqrt{\frac{R_s |Z_L|^2 - R_L |Z_s|^2}{R_L - R_s}} \tag{Eqn. 20}$$

$$\theta = \text{Arc tan} \left(\frac{Z_0 (R_s - R_L)}{R_s X_L + R_L X_s} \right) \tag{Eqn. 21}$$

This assumes that Z_0 is real and $\tan(\beta l)$ is real. These equations do not always give a match, but if no match is possible, shifting the impedance by using a short length of transmission line will always result in a match. A simple visual basic program TlineMatch, can be used to evaluate the equations above. This program is included with the resources for this course. This program gives $Z_0 = 15.78\Omega$ and $\theta = 86.37$ degrees.

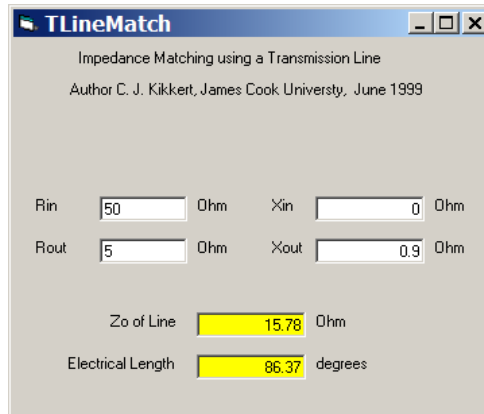


Figure 21. Tline Match Panel

Those line parameters can now be used in Microwave Office to simulate the matching performance.

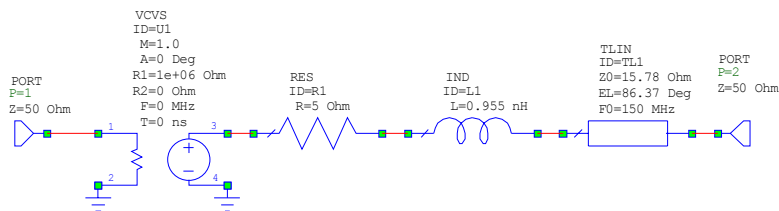


Figure 22. Circuit representation of the input impedance and the matching network.

From figure 23, it can be seen that transmission line matching gives a very broad band impedance match. The only limitation is that the line lengths can physically become too large. This is why this technique is predominantly used above 100 MHz. Transmission lines can also replace the inductors used in the LC matching, for networks like the T network, and such networks are commonly used above 100 MHz.

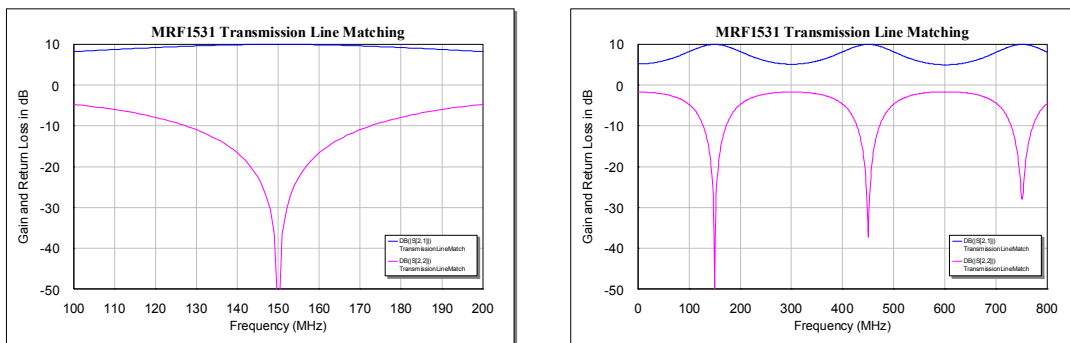


Figure 23. Frequency Response of the Transformer Match.

Broadband Matching

Sometimes a wideband match is required. This can either be a wideband match into an active device, or a simple impedance transformation. If a wideband match into an active device is required, then the either the device impedance must be able to be accurately represented by a simple circuit, ie resistor and capacitor or inductor or one must use the large signal S parameter data as a data table in Microwave office. The matching network is then designed. The design can use broadband matching equations published by Motorola in as a succession of simple matching networks. As an example consider an impedance transformation from 50 ohm to 1.85 ohm. The impedance transformation ratio is 27 to one and this is achieved by cascading three pi networks with impedance transformations of 3 to one. The impedance levels are thus 50Ω, 16.67 Ω, 5.55Ω and 1.85Ω. The match is required for the 250MHz to 500MHz range. The individual impedance match calculations are done at a centre frequency of 353 MHz, the geometric mean of 250MHz and 500MHz.

To get the broadest match, a low Q is used. A Q of 0.4 will give realisable components for the pi network.

The screenshot shows a software window titled "Matching Networks" with a blue header. Below the header, it states "Author C. J. Kikkert, James Cook University, Dec 96 - Jul 05" and "Based on Motorola Application Note 267". The interface contains several input fields and calculated values for four different network types:

Parameter	Value
Device Resistance	5
Device Reactance	0.9
Termination Resistance	50
Frequency (MHz)	150
Network Q	3.5
Qmin	3.0

Bandpass T Network (A)		Lowpass Pi Network (B)	
Device End Series L	17.613 nH	Device End Shunt C	755.25 pF
Shunt C	46.924 pF	Series L	6.1114 nH
Term. End Series C	37.223 pF	Term. End Shunt C	239.47 pF

Bandpass L Network (C2)		Lowpass T Network (D)	
Device End Series C	60.63 pF	Device End Series L	17.613 nH
Device End Series L	33.529 nH	Shunt C	65.185 pF
Term. End Shunt C	63.662 pF	Term. End Series L	30.244 nH

Figure 24. Component calculation for the first element.

Repeating the component calculation using the same Q and centre frequency for the other elements results in the circuit diagram below. All the elements are made optimisable and the network is entered into computer simulation software like Microwave Office. If the calculations are done correctly, a good starting match results as shown in figures 24 and 25.

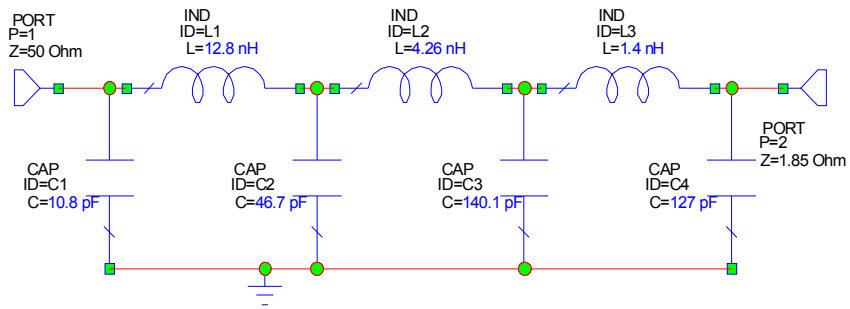


Figure 25. Starting Broadband Match Schematic

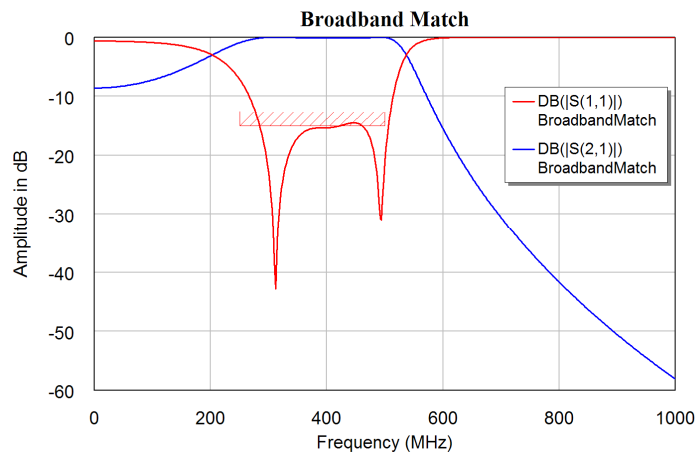


Figure 26. Starting Broadband Match Input Impedance.

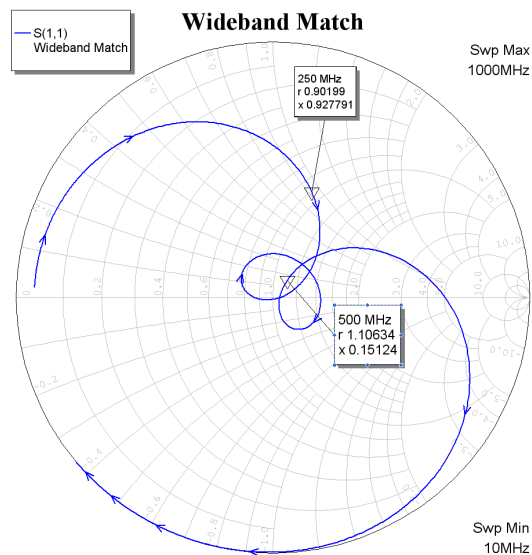


Figure 27. Starting Broadband Match Input Impedance.

The impedance match does not quite meet the required 250 MHz to 500 MHz bandwidth, so the network is optimised to meet the specification of having S_{11} to be less than -15 dB.

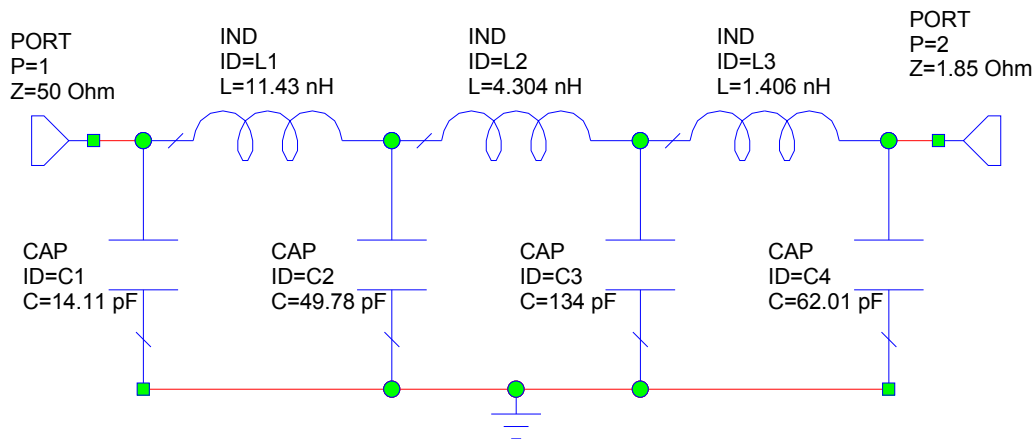


Figure 28. Final Broadband Match Schematic

The optimisation produces the matching network shown in figure 28. The biggest change in component value is that of the device end (port2) where the 127 pf starting capacitance has become 62 pf. The frequency response is shown in figure 29. It can be seen that S_{11} is now less than -15 dB for the entire 250 – 500 MHz frequency range. Figure 30 shows the Smith chart of the network after optimisation. It can be seen that a good match is obtained.

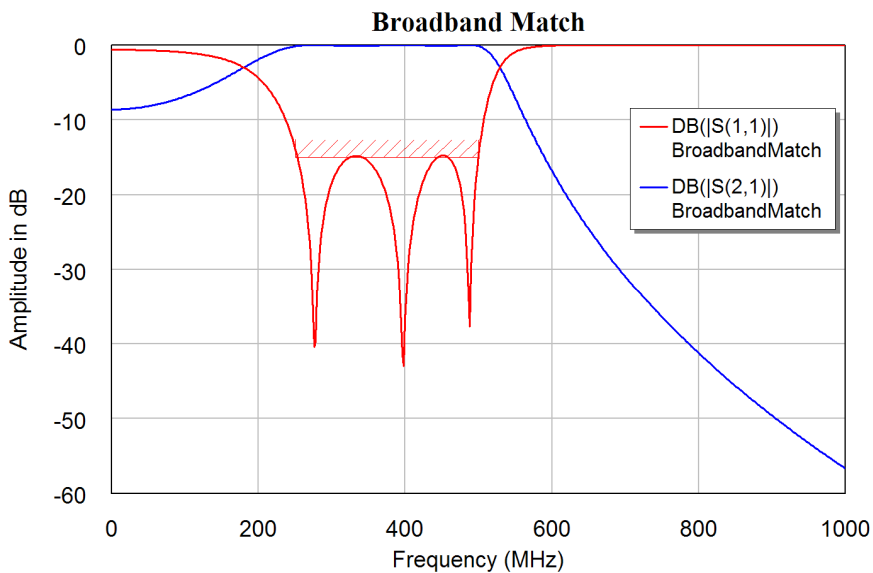


Figure 29. Final Broadband Match Input Impedance.

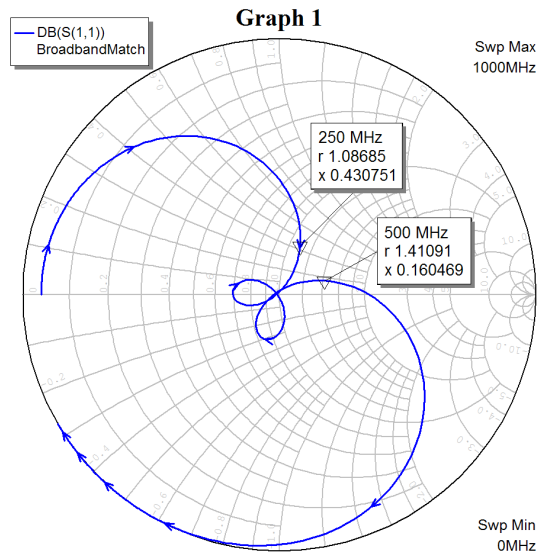


Figure 30. Final Broadband Match Input Impedance.

Broadband Amplifier

Applying broadband matching to a transistor or FET results in additional problems in that since the device is not normally unilateral, there is an interaction between the input and output matching. As an example consider the MRF 1535 transistor that we used before for the impedance matching. From the manufacturer’s data sheet, the S parameters at a drain current of 2 Amp is as follows:

```
!MRF 1535, 12.5V 35W transistor
# MHZ S MA R 50
!F      S11      Ang      S21      Ang      S12      Ang      S22      Ang
!MHz   |S11|     Ang    |S21|     Ang    |S12|     Ang    |S22|     Ang
50     0.94    -176    9.42     88     0.005    -72     0.89    -177
100    0.94    -178    4.56     82     0.005     4       0.89    -177
150    0.94    -178    2.99     78     0.003     7       0.89    -177
200    0.94    -178    2.14     74     0.005    17       0.90    -176
250    0.95    -178    1.67     71     0.004    40       0.90    -175
300    0.95    -178    1.32     67     0.007    35       0.91    -175
350    0.95    -178    1.08     67     0.005    57       0.92    -174
400    0.96    -178    0.93     63     0.003    50       0.93    -173
450    0.96    -178    0.78     62     0.007    68       0.93    -173
500    0.96    -177    0.68     61     0.004    99       0.94    -173
550    0.97    -177    0.59     58     0.008    78       0.93    -175
600    0.97    -178    0.51     57     0.009    92       0.92    -174
```

The lines beginning with ! are comments and have been added for clarity. The line

MHZ S MA R 50

indicates that the frequency in the following file is in MHz, it is an S parameter file and the values are magnitude (rather than dB) and the reference impedance is 50 ohm.

This can now be used as a sub-circuit in Microwave Office. For this example a match from 250MHz to 500MHz is required. An input matching network of the form shown in figure 1 is required. The initial component values are calculated at the centre of the desired frequency range, using a cascaded section of bandpass T and lowpass T

sections, with a progressive impedance transformation. Similarly an output matching network consisting of lowpass T and Pi sections is produced. These networks are then connected to the large signal S parameter model of the transistor. The resulting network is optimised for a good input and output match over the 250 to 500 MHz range. The circuit after optimisation is shown in figure 31

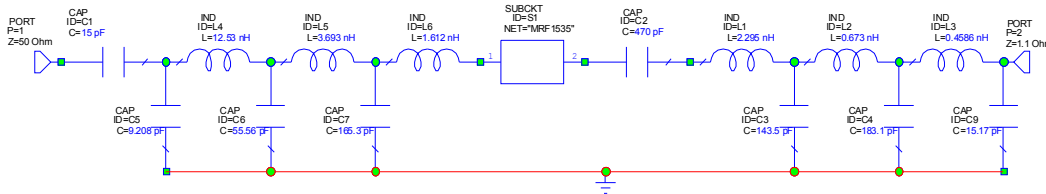


Figure 31. Optimised Broadband Amplifier Matching Network

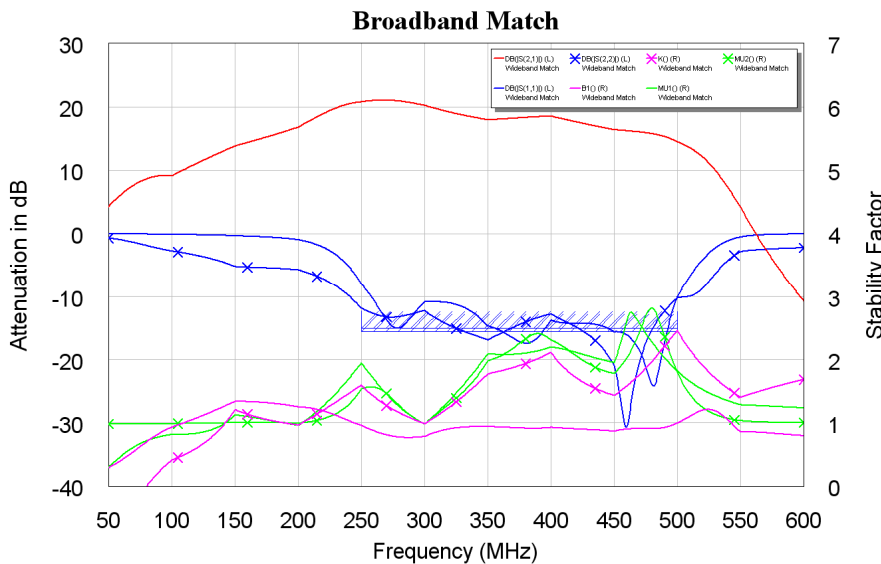


Figure 32. Performance of Broadband Amplifier

Figure 32 shows the performance of the optimised amplifier, it can be seen that a good input and output match is obtained and that this results in a close to 20 dB gain over the entire 250 to 500MHz band. There are however some problems. For unconditional stability, K must be greater than one and B1 must be greater than zero or the input and output μ coefficients must be greater than one. This is the case in the 250 to 500 MHz frequency band, but is no the case outside this region, particularly in the 50 to 100MHz frequency range.

Figure 33 shows the Smith chart indicating the input and output impedances of the whole amplifier as well as the input and output impedances of the FET. Note from the diagram how the parameters change at 50 MHz intervals. That is related to the 50 MHz measuring interval of the S parameters.

In a commercial design, further optimisation and circuit modification may be required to provide a flatter gain characteristic by providing a slight impedance mismatch and changing the optimisation parameters in accordance. In addition steps need to be taken to ensure that the amplifier does not oscillate in the 50 to 100 MHz frequency range.

Stabilisation may be obtained by using resistors, which are only effective at low frequencies, by decoupling them using series inductors. As can be seen here since the FET has a very high gain at low frequency, the amplifier will tend to oscillate at low frequencies.

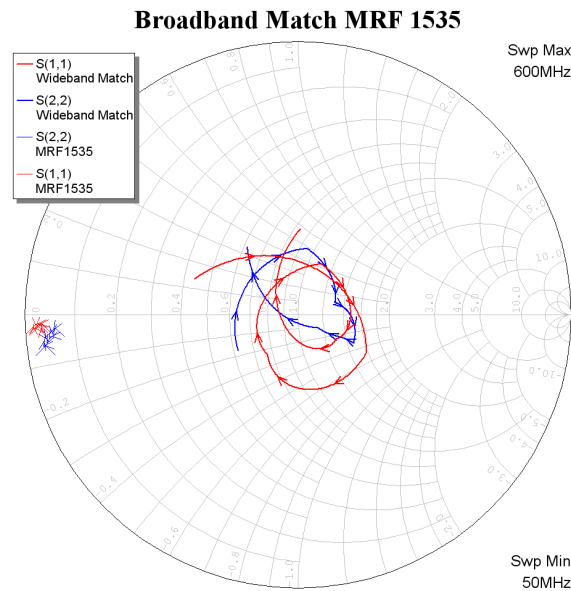


Figure 33. Impedance Match of Broadband Amplifier

In many cases the matching networks are more complex than what has been described here. As an example figure 34 shows the circuit for an MRF 9060 amplifier 60 Watt amplifier operating in the 900 to 1000 MHz frequency region. This is one of the examples from Microwave Office and is similar to sample designs done by Motorola. FET's are more linear than transistors and are thus preferred for applications requiring a low intermodulation distortion, as is required in mobile radio base-station amplifiers. FET's have very high gains at low frequencies and are thus more susceptible to instability. During the last few years, the number of available RF devices has reduced significantly, particularly devices operating below 800 MHz.

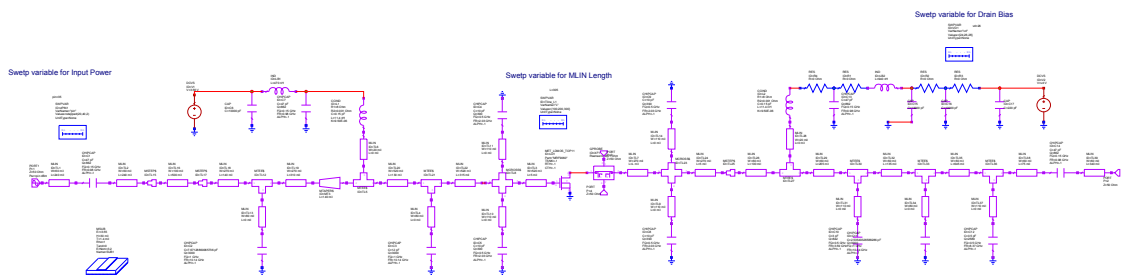


Figure 34. 60 Watt 900 MHz FET amplifier.

Figure 35 shows the layout of this amplifier. The impedance required for the transmission lines for the input matching is very low, since the input impedance is very low. High quality RF capacitors must be used to ensure that the losses in the capacitors

are not excessive. The frequency characteristic of those capacitors, taking the self resonance into account, is included in the analysis. For further details see the MWO, “Motorola LDMOS swept variables” example in the amplifier section of the MWO examples. When doing a power amplifier design it is essential to look at the sample designs produced by the manufacturer for the transistor to be used.

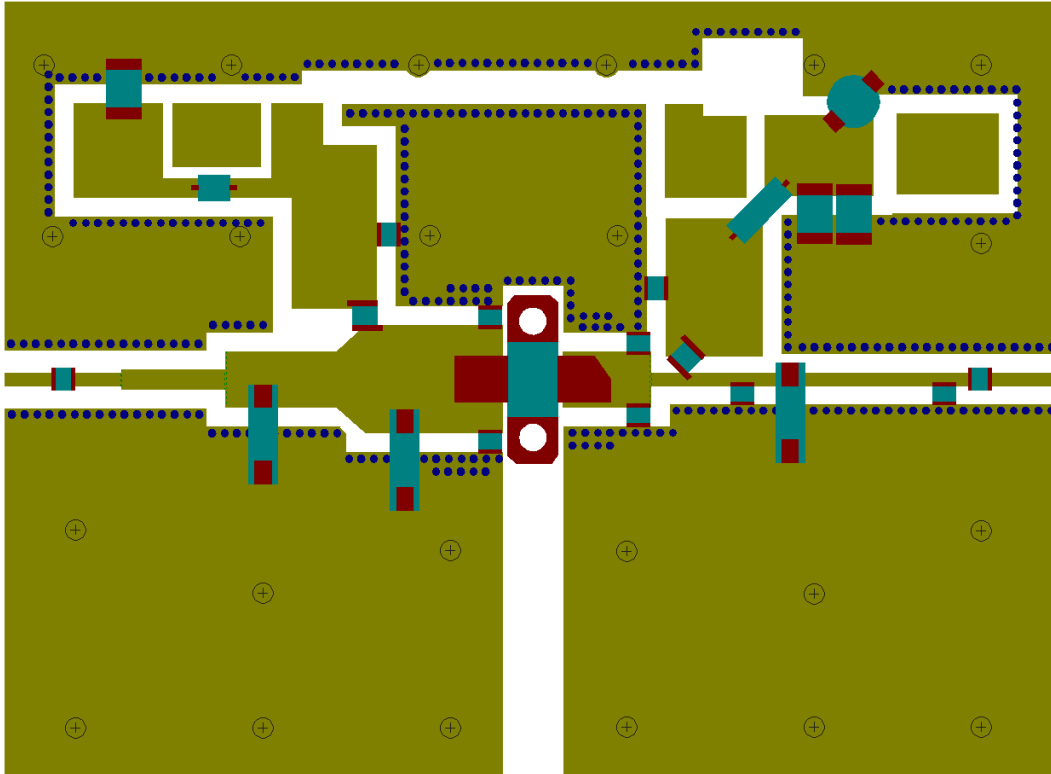


Figure 35. 60 Watt 900 MHz FET amplifier layout.

Chapter 10

Circuit Manufacture

Introduction

Printed Circuits Boards consist of an insulating material forming the PCB substrate onto which conductive tracks are placed. Components forming the circuit are connected to those tracks.

There are two basic ways of producing printed circuit boards:

Conductive Layer Removal

A conductive layer, like copper, covers one or both side of the PCB substrate and the conductive layer is removed where there are to be no tracks. The metal can be removed using Chemical Etching, Milling or Laser Ablation.

For conventional Printed Circuit Board manufacture, chemical etching of copper clad printed circuit boards is the most common PCB manufacturing technique.

Depositing Tracks and Vias

In this method, the conductive tracks are deposited onto the substrate. For the production of plated through holes, this process is always required. The areas of the PCB where tracks are to be placed are processed through a series of chemical baths to chemically deposit a thin copper coating of approx 1.5 μm . Electroplating is then used to build up the thickness of the tracks or vias.

For Thick and LTCC circuits, the tracks are screen printed on a bare substrate material and then fired to make them permanent.

Printed Circuit Board Materials

Most Printed Circuit Board substrates are made by having thin copper sheets glued to an insulating material. The copper thickness depends on the applications. Typical thicknesses are 2, 1, $\frac{1}{2}$ and $\frac{1}{4}$ oz copper per square foot, which corresponds to a copper thickness of 70 μm , 35 μm , 18 μm or 9 μm respectively. The copper thickness together with the track width must satisfy the current carrying capability and attenuation requirement of the transmission lines. For printed circuit boards the copper that is not wanted is removed, by etching or milling.

Conventional PCB substrates

FR3

This is a substrate consisting of a mixture of paper pulp and epoxy. It is mainly used in low cost consumer products, and is not normally used for multilayer boards. FR3 has a Dielectric Constant of approximately 2.3 but this is not controlled and the loss tangent is not specified. FR3 is less tolerant to scorching heat than FR4.

An advantage of FR3 and similar paper based laminated are that holes and slots can be punched. This laminate is not recommended for RF designs. At JCU we have been

using FR3 for PCB's since the fibreglass used in FR4 is carcinogenic. Very special precautions need to be made to ensure that the particles produced by the PCB milling process are not inhaled. FR3 is safer in that respect. FR3 is normally light brown with a smooth texture.

Figure 1 shows a typical low cost AM/FM radio manufactures using FR3 circuit board. The advantage of being able to punch out a particular shape can be seen..

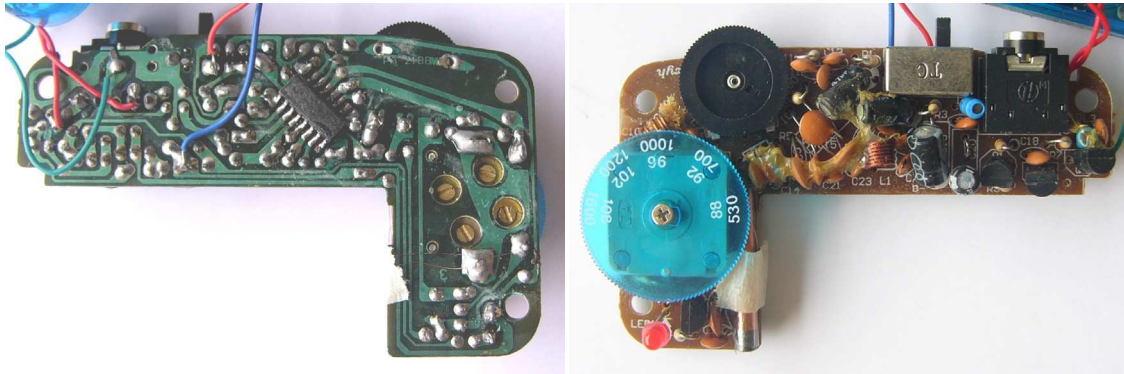


Figure 1 FR3 Printed Circuit Board for a low cost AM / FM radio.

FR4

This is a substrate consisting of a mixture of fibreglass and epoxy. It is suitable for professional quality PCB's and has the following properties:

Dielectric Constant	4.7 at DC decreasing to 4.4 at 10 GHz.
Dissipation factor (Tan(δ))	0.014
Q at 50 MHz	95
Max Temperature	130 °C

Table 1. FR4 Properties.

FR4 PCB's can be made with many layers. Typical PCB's have 4 layers, with one layer being earth, one layer being the supply voltage and the outer layers containing the tracks that are connected to the IC's and passive components. FR4 is normally pale green and semi-translucent, often this can be seen at the left edge of the board as in figure 2. The large component at the left edge of the board is a ceramic diplexer.

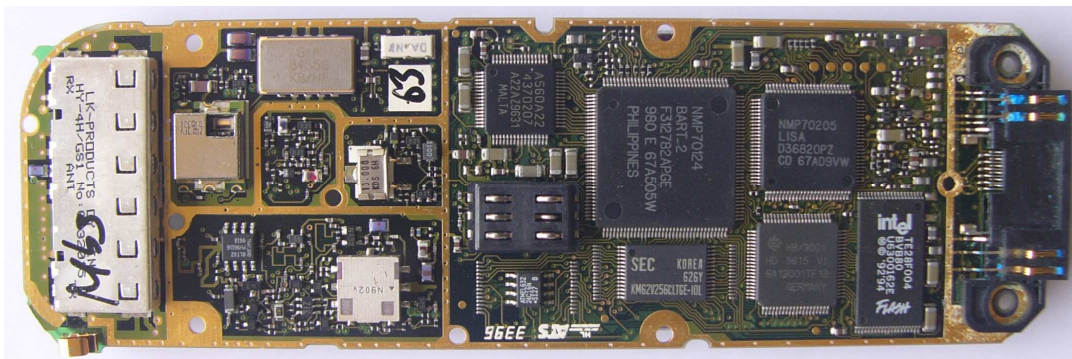


Figure 2. FR4 Multilayer Printed Circuit Board. (Nokia Mobile Phone).

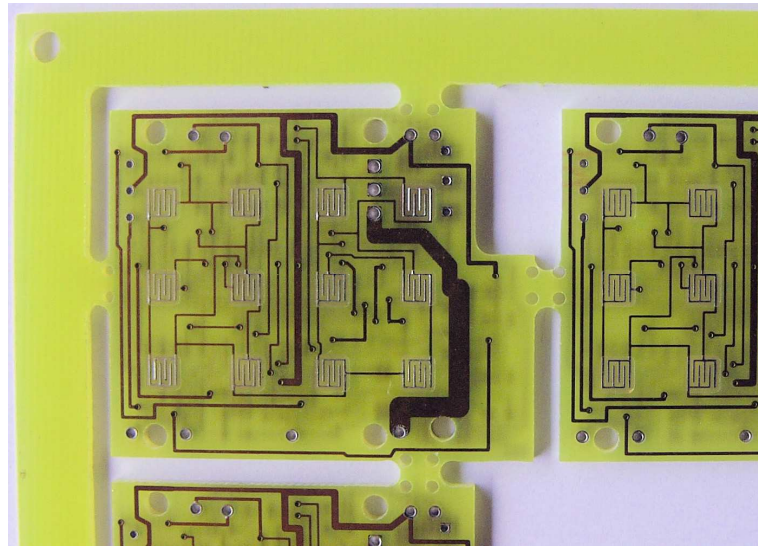


Figure 3. FR4 Printed Circuit Board, showing cut-outs. (JCU Layouts).

Normally many printed circuits are etched together on one sheet as shown in figure 3. Cut-outs are provided to enable the individual circuits to be removed easily.

Microwave and RF printed Circuit Board Materials.

FR3 and FR4 can be used for PCB's to 1 GHz, however above these frequencies the losses become significant. To avoid reflections, at microwave frequencies many of the connections are made using transmission lines of a specified impedance. For FR3 and FR4, the dielectric constant and thickness varies from one batch to the next, so that the characteristic impedance of transmission lines on the PCB also varies. This is not suitable for many RF designs. Rogers Corporation (<http://www.rogerscorporation.com>), are a large RF PCB substrate material manufacturer and make the following laminates:

RT/duroid 58X0

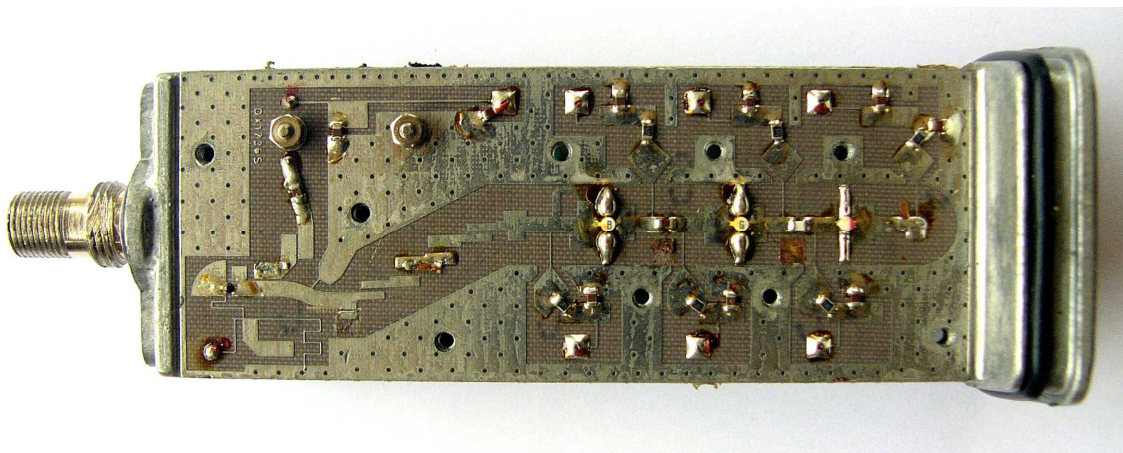


Figure 4. Ku band (12 GHz) Low Noise Converter (LNC) using RF/duroid (Norsat).

RT/Duroid 58X0 is a Glass microfiber reinforced PTFE (Teflon) composite. The two products in this family are RT/duroid 5870 ($\epsilon_r = 2.33$) and 5880 ($\epsilon_r = 2.2$) materials.

These are the oldest Rogers products and were developed in the 1960's. The low dielectric constant and the low dielectric loss of typically 0.0005 make these materials best suited for high frequency/ broad band applications where dispersion and losses need to be minimized. A high dielectric constant reduces the size of the circuit. For frequencies above 20 GHz circuits with a high dielectric constant become too small. Because of their low water absorption characteristics, RT/duroid 58X0 is good for applications in high moisture environments. The LNC of figure 4 is located at the focal point of antenna, which is sometimes very hot, sometimes cold and sometimes very wet. RT/duroid is thus a good choice for the PCB material. RT/duroid is flexible and for thin laminates requires care in mounting them securely. RT/duroid is normally brown and the woven glass mat can clearly be seen.

RT/duroid 6000 (PTFE/Ceramic Laminates)

There are three laminates in this family RT/duroid 6002 ($\epsilon_r = 2.94$), RT/duroid 6006 ($\epsilon_r = 6.15$) and 6010LM ($\epsilon_r = 10.2$). The thermal coefficient of the laminate matches that of copper. The laminates are more rigid and thus easier to mount. This product is ideal for applications in thermal changing environments (space). Multilayer boards are possible with this laminate. RT/duroid 6000 is a military specified substrate and thus very expensive.

RO3000 and RO3200 (PTFE/Ceramic Laminates)

The RO3000® materials family consists of four grades, RO3003™ ($\epsilon_r = 3.0$), RO3035 ($\epsilon_r = 3.50$), RO3006 ($\epsilon_r = 6.15$) and RO3010 ($\epsilon_r = 10.2$). These laminates are aimed at a commercial market and are a lot cheaper than the corresponding RT/duroid 6000 laminates. The temperature coefficient of expansion matches that of copper and FR4 in the X-Y plane. Multilayer RO3000/FR4 boards can easily be made.

RO4000

The RO4000 series is a woven glass/ ceramic loaded thermoset plastic resin Laminate and were developed as a low cost commercial laminate, that is specially suited for multilayer boards using RO4000 and FR4. The boards have a glass transition temperature (T_g) $>280^\circ\text{C}$ and can thus be used with conventional PCB processing techniques, such as wave soldering and surface mount techniques. Unlike PTFE based microwave materials, no special through-hole treatments or handling procedures are required. Therefore, RO4000 material circuit processing and assembly costs are comparable to epoxy/glass laminates. RO4003C has an ϵ_r of 3.38 and RO4350B has an ϵ_r of 3.48.

Multilayer Boards

There are many applications that require RO4003 material to be bonded. One example is a stripline RF circuit one other is a RO4003/FR4 multilayer board for both RF and digital signal processing. Several types of adhesives can be used depending on the laminates to be bonded. Figure 5 shows a typical construction requiring an RO4003 stripline circuit bonded to an FR4 multilayer construction.

For constructing a stripline circuit by using two RO4003 laminates, a high frequency bond-film like the RO4400 “prepreg” sheet from Rogers is required. The bond-film should have a dielectric constant similar to the laminates to be bonded and the loss tangent of the bond-film should match that of the laminates.

For bonding of an RF substrate to an FR4 substrate, a higher loss bond-film can be used. In addition the dielectric constant is not critical. A good low cost option is to use the standard bond films used for FR4 for making multilayer PCBs.

For bonding the laminates are located precisely using locating pins and the boards are clamped at a pressure of 2.8 MPa and a temperature of 225°C for more than one hour. Since air has an $\epsilon_r = 1$, it is important to prevent air bubbles, particularly when high dielectric substrates are used.

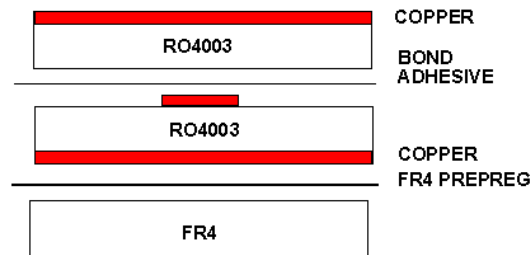


Figure 5. Bonding laminates to form a multilayer board (Courtesy Rogers Corporation).

Non-Clad Substrates

Companies like Morgan Electro Ceramics, (<http://www.morganelectroceramics.com>) and Coors Ceramics (<http://www.coorsceramics.com/>) produce dielectric materials that can be used for RF substrates. The dominant substrate material is Alumina, but other materials with higher dielectric constants are also used.

These non-clad substrates are used for precision microwave circuits using Thin film techniques and for low cost thick film circuits at both RF and low frequencies.

Companies like UltraSource Inc. (<http://www.ultra-source.com/company.html>) specialise in the design and production of thin film circuits, predominantly for space and military applications.

Companies like Hybrid Electronics, (<http://www.hybrid-electronics.com/index.htm>) specialise in the design and production of thick film circuits.

As an indication of the types of materials available and their RF applications, the following is a list of some of the RF and Microwave materials from Morgan Electro Ceramics.

D6

This is a low permittivity material that is used predominantly for supports for dielectric resonators however it can be used effectively for substrate applications and also for GPS patch antenna applications. The dielectric constant is 6.

Alumina Substrates

Alumina is the dominant substrate material for Thick and Thin film applications. The dielectric constant is close to 10, with both the dielectric constant and cost increasing with the purity of the substrate. For lower cost applications, Thick film substrate materials with 85% to 95% purity are used. In many cases these substrates are used “as fired” for low frequency applications or ground flat for low cost microwave applications. For precision, low loss microwave applications 99.5% to 99.8% purity substrates are used and these may be ground and polished in order to remove any

surface irregularities and ensure a constant thickness of the entire substrate. Alumina is ideal for demanding low loss applications, such as substrates for thin film circuits.

D30

Morgan Electro Ceramics D30 dielectric composition has a dielectric constant of 30 and a Q_0 typically 50,000 at 2 GHz and 15,000 at 10 GHz. The material is specifically designed for telecommunications filter applications where a high Q is an absolute requirement. This ceramic is predominantly used for resonators.

D43

Morgan Electro Ceramics D43 material has a high $\epsilon_r = 43$, with a Q_0 typically 30,000 at 0.9 GHz and 22,000 at 2.0 GHz. This material is very good for resonators and filters for mobile radio applications.

D88

Morgan Electro Ceramics D88 material offers a high dielectric constant of $\epsilon_r = 88$. The material offers maximum miniaturisation whilst still offering a temperature coefficient that is tuneable through zero.

Manufacturing

RF printed circuit boards can be designed in a similar way to conventional PCBs, so that programs like Protel, (Altium) can be used to produce the circuit board layout. For circuits like stripline filters, and other RF circuits, where the characteristics and lengths of transmission lines are critical, then Software like Microwave Office or ADS is required. All of these programs can produce Gerber Plot files, which are used by either commercial PCB manufacturers, or by the milling machines used to produce prototype RF boards. The Gerber Plot files can also be imported into Protel to produce a combined RF and conventional PCB. Such technology is required for the Multilayer boards shown in figure 5.

Normal PCBs are protected using a soldermask. Unless the thickness and the dielectric constant of the soldermask is taken into account in designing the RF circuit, it should not be used. To prevent corrosion, Gold plating can be used on the RF circuits.

Manufacturing using PCB milling machine

At JCU we use a milling machine to produce PCB's. The ceramic filler used in the RO4003 substrates are much more abrasive than the epoxy, paper and fibreglass used in the FR3 and FR4 type substrates. As a result the cost of milling bits is a major cost in the production of those boards. For milling RT/Duroid, the substrate needs to be thick enough to be able to be held flat as part of the milling process, so that the more rigid RO4003 substrates are the best to use in PCB milling machines.

Layout Hints

Many PCB manufacturers can etch to an accuracy, such that the thinnest tracks can be 0.2 mm wide and have a minimum spacing of 0.2 mm between tracks. Many of the modern ICs have 0.5 mm pitch of the leads on the IC. The 0.5 mm track pitch is close to the maximum resolution of present day PCB manufacture.

The minimum drill size that should be used is 0.5 mm diameter. The minimum pad size for vias or leaded components is the drill size plus 0.5 mm, however small pads will lift off easily when components are soldered to them. For through-hole components use a

drill size that is approximately 0.1 mm larger than the lead size and use a pad that is approximately 1 mm larger than the drill size. The recommended hole size for a standard leaded resistor or capacitor is 0.9 mm with a pad size of 2 mm. To ensure that that the circuit can be changed if needed, for prototyping boards a bigger pad size is advisable

For milling of PCBs, the tolerances are slightly different. A minimum recommended track size is 0.5 mm, with a 0.2 mm minimum spacing. (0.2 mm wide milling bits are the smallest milling commonly used). Having a 0.25 mm spacing ensures that 2 milling cuts are made, thus reducing the chance of short circuits. For short track lengths, track widths of 0.2 mm are possible, however such thin tracks should be avoided for long tracks since the milling machine positioning accuracy is 0.1 mm. When milling circuit boards, as much groundplane as possible should be left on the board, to minimise the amount of milling that has to be done and minimise the milling time and cost.

Thin Film

Thin film circuits are normally produced by firstly applying a very thin (1 to 2 micron) seed-layer of gold to an alumina substrate. A photographic mask is then applied to the places where no track is required and the tracks are then electroplated to the correct thickness of several tens of microns. The photo-resist is then removed and a quick etch removes the seed-layer, where no tracks should be, but does not completely remove the tracks. Solder-pads are then added where required, together with dielectric dams to prevent the lead from solder leaching into the gold. The polished Alumina used for the Thin film substrates has a very low dielectric loss. Thin film circuits can be made to better accuracies and smaller sizes than etched PCB's

Thin film techniques are expensive compared with other techniques and are thus used for circuits where the other techniques cannot be used. Examples are the 20 Watt Class C 800-900 MHz amplifier hybrid, shown in figure 6. The whole circuit including heat-sink is 56 mm long. The bond-wires for the large output transistor on the right can clearly be seen.

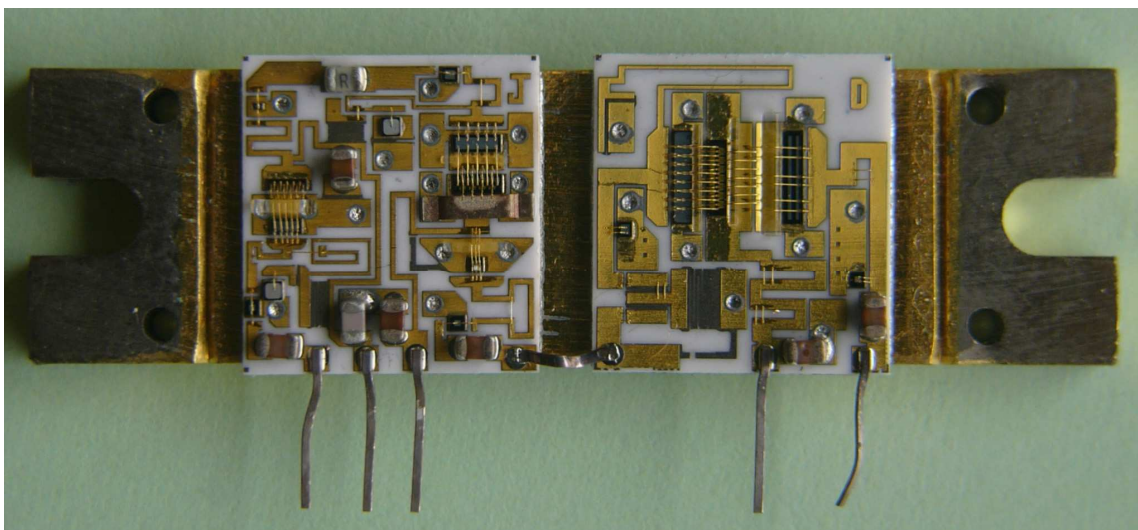


Figure 6. 20 Watt Class C Amplifier Hybrid MHW820 (Motorola).

Thick Film

Thick film techniques have a slightly higher circuit set up cost as several screen masks need to be made, but they have a lower increment cost as no etching or milling of the PCB's are required. In thick film techniques, a substrate, which normally is an alumina substrate, has conductive, resistive or insulating inks applied to them using precision screen printing technology. The substrate is then fired at typically 850 °C to harden the tracks and thus provide the correct circuit connections. Dielectric layers can be made, so that tracks can cross each other. For a multilayer track circuit, several separate firings may need to be made. Similarly capacitors can be made by firstly using a conductive ink to form the one electrode and firing that. Then a dielectric layer is applied and fired, followed by another conductive layer for the other electrode. Resistors can be made using resistive inks and inductors can be made by printing conductive spirals. This results in a high-density circuit board of low cost. The low thermal coefficient of expansion (TCE) of ceramic materials guarantees mechanical stability and is closely matched to that of ICs for bare chip assembly.

The screen has a photographically produced mask applied to it, with the screen being open where the tracks need to go and being blocked everywhere else. The screen is placed in contact with the substrate and the ink pastes are applied with a squeegee to the screen. The inks can also be applied using other techniques, such as spraying, dipping using the appropriate screening techniques to ensure that the inks are only deposited where they are supposed to be.

Figure 7 shows some typical thick film circuits. The circuit on the left shows that thick film circuits can have a high component density. After the circuit is tested, the whole circuit is protected with a protective coating as shown on the right of figure 7. This makes thick film circuits very suitable for hazardous or wet environmental conditions.

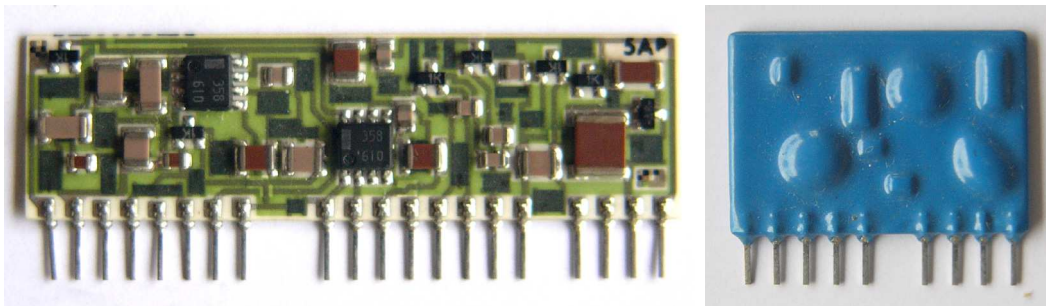


Figure 7. Thick film circuits before and after a protective coating has been applied.

Screens

The ink is normally applied using a squeegee. When the ink is applied, the thickness of the ink is close to the thickness of the screen. By varying the thickness of the screen the thickness of the tracks can be varied.

The screens used for the printing can be made from stainless steel, with a typical fibre diameter between 30 and 100 microns, a 50 to 224 micron mesh aperture and 65 to 220 micron mesh thickness with an aperture of 39 to 47%. Stainless steel screens are used for large production runs.

Screens can also be made from polyester. Polyester screens have a shorter life but are cheaper, and are thus used for smaller production runs. The screens have a typical fibre

diameter between 35 and 110 microns, a 43 to 185 micron mesh aperture and 60 to 160 micron mesh thickness with an aperture of 30 to 40%.

Pastes (Inks)

Conductivity: The conductivity of the pastes is given in terms of milliohm/square. The resistance of a printed conductor of 10 mm x 10 mm, is the same as the resistance of a conductor of 100 mm x 100 mm, as long as the thickness is the same.

Thick film inks contain precious metals, glass, and/or ceramic powders dispersed in an organic medium. Specialized compositions create conductors, resistors, and dielectrics for a variety of applications and operating environments. Table 2 shows the conductivity of various conductive inks. Copper inks are difficult to use since they require an oxygen free atmosphere in the ovens, to prevent oxidation. The palladium inks are used for solder pads.

Conductor Material	Sheet resistance (mΩ/square)
Copper	1.5
Silver platinum	2.0
Gold	3.0
Silver palladium	30
Gold palladium	30

Table 2. Comparison of sheet resistance of conductive pastes.

RF applications of Thick Film Circuits

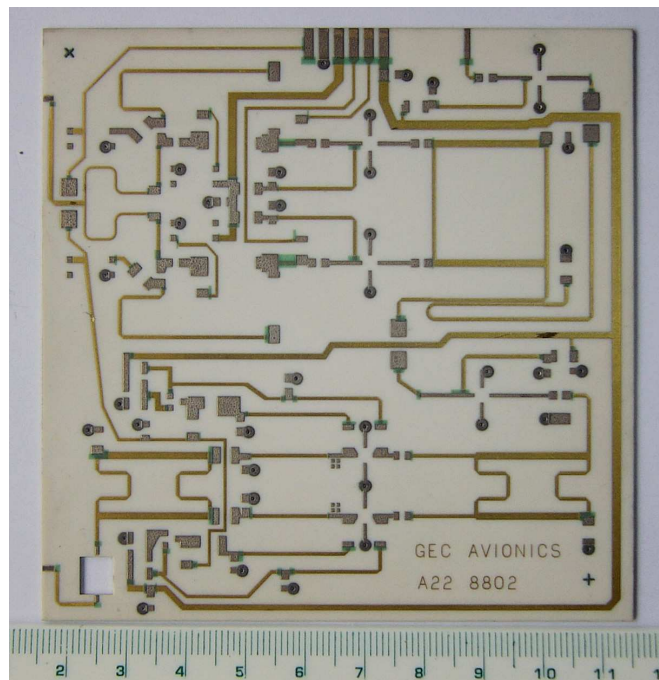


Figure 8. Thick film RF circuit on alumina. (GEC Avionics, designer Kikkert).

The alumina substrate has a very low loss, and that is why it is used for thin film circuits. The application of the required tracks using thick film techniques is a lot

cheaper than doing the same using thin film techniques. For accurate transmission line widths, fine screens need to be used and the spreading of the inks needs to be allowed for. Figure 7 shows a circuit for a low noise amplifier and I-Q gain control circuit for a receiver beam steering application at 1.6 GHz. The circuit is 100 mm x 100 mm in size.

Thick film techniques are also used to produce patch antennae for mobile radio systems. In many cases the antenna needs to be shaped to conform to the contours of the mobile phone. Thick film techniques are also used to coat the ceramic block of the dielectric filter used as a diplexer shown on the left of figure 2.

Low Temperature Cofired Ceramic (LTCC)

The Low Temperature Cofired Ceramic (LTCC) technology is a means of producing multilayer circuits at a low cost. The technique is similar to thick film techniques, except many layers of ceramic are used, each of which has conductive, dielectric and / or resistive pastes applied to them. The ceramic sheet is called a green sheet, since the ceramic still has not been fired. This normally is supplied on a tape. The printed sheets are then laminated together and fired in one process. By means of vias, connections can be made from one layer to another, as shown in figure 9.

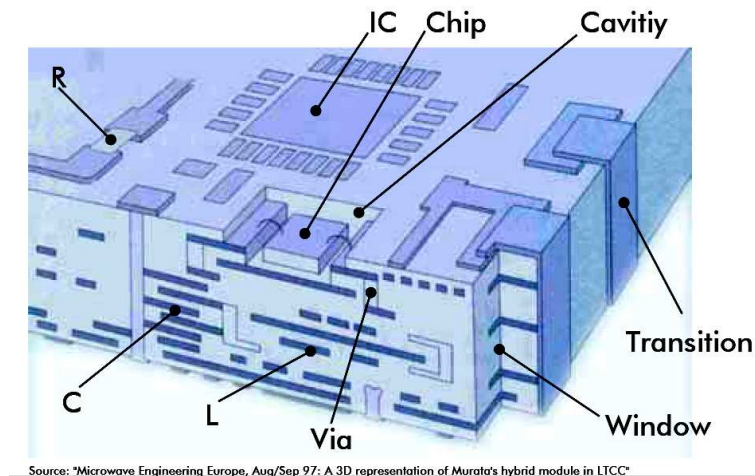


Figure 9. Typical LTCC circuit.

The low firing temperature for the ceramic green sheets allow low resistivity conductors like silver, gold, copper and alloys with palladium and platinum to be used.

The pastes are printed on the greensheet with the help of a conventional thick film techniques. Special thick-film pastes must be used since the ceramic shrinks 10 to 15 percent in x/y-axis and about 10 to 45 percent in z-axis.

It is also possible to integrate passive elements like resistors, capacitors and inductors into the substrate. Resistors are processed with the help of special pastes, which have to be printed on the tape just like conductor lines and are cofired. Capacitors and inductors can be made by forming the conductive lines into plates or coils respectively. LTCC technology permits the construction of stripline as opposed to microstrip circuits, thus reducing radiation and permitting the construction of couplers with a high amount of coupling. Combining that with the ability to include active devices on the same small circuit opens up great possibilities.

For further information see: <http://www.ltcc.de/>.

Operational Amplifiers

High Speed Operational Amplifiers

Operational amplifiers with 3 dB bandwidths of up to 1.5 GHz are now available, such operational amplifiers are used in consumer applications like hard disk drives and computer monitors, industrial and medical applications, such as CAT scanners. In addition one can use these operational amplifiers for IF amplifiers in many communication receiver applications.

These high speed amplifiers fall into three categories:

Voltage Feedback Amplifiers

Current Feedback Amplifiers

Dual Feedback Amplifiers

The Voltage Feedback amplifiers have the same properties as the LF356 or 741 operational amplifiers, used at low frequencies.

The Voltage feedback amplifiers have lower noise, better dc performance and more freedom in feedback configuration. The Current Feedback amplifiers have faster slew rates, lower distortion but restrictions on feedback configurations.

If an operational amplifier has input voltages V_1 and V_2 at the input terminals, then for a voltage feedback amplifier the output voltage is:

$$V_{out} = A(s) (V_1 - V_2),$$

where $A(s)$ is the open loop gain, which is frequency dependent. Consider the noninverting amplifier configuration:

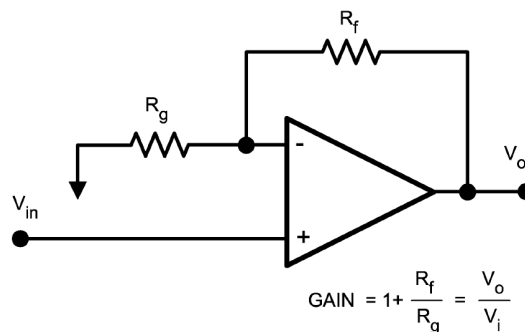


Figure 1. Noninverting Amplifier (National Semiconductor Appl Note OA-30)

$$\text{If one makes: } G = \frac{R_f + R_g}{R_g} \text{ then } V_o = V_{in} \left[\frac{G}{1 + \frac{G}{A(s)}} \right]$$

Since $G(s)$ decreases with frequency as shown in figure 2, the bandwidth of the amplifier will depend on the gain as is also shown in figure 2.

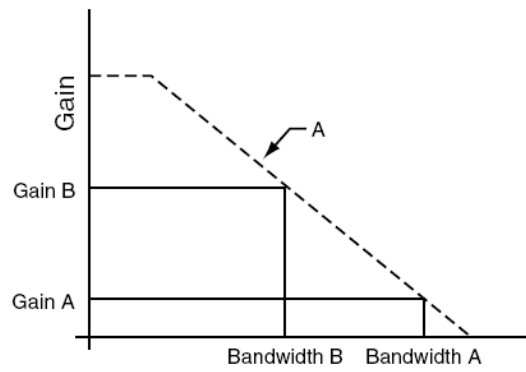


Figure 2. Open loop and Closed loop gain of Voltage Feedback Amplifier (National Semiconductor Appl Note OA-30)

The Current feedback amplifier

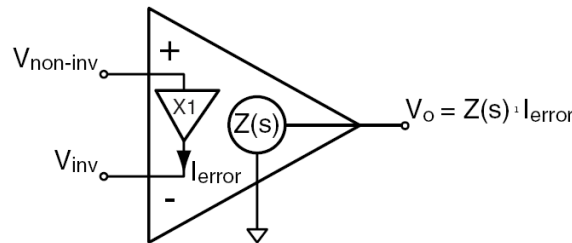


Figure 3 Current Feedback amplifier configuration (National Semiconductor Appl Note OA-30)

For the inverting amplifier configuration, the equations for the amplifier are:

$$i_{error} = \frac{V_{in} - V_o}{R_f} + \frac{V_{in}}{R_g}$$

Since $V_o = Z(s)I_{error}$, substituting for lerror in the above equation after manipulation leads to:

$$V_o = \frac{R_g}{Z(s) + R_f} V_{in}$$

The current feedback amplifier will thus have a transfer function of:

$$V_o = V_{in} \left[\frac{G}{1 + \frac{R_f}{Z(s)}} \right] \text{ compared with a transfer function of :}$$

$$V_o = V_{in} \left[\frac{G}{1 + \frac{G}{A(s)}} \right] \text{ for the voltage feedback amplifier.}$$

Where $G = \frac{R_f + R_g}{R_g}$ is the ideal amplifier gain, which is the same for both amplifiers.

The difference is thus in the way $G/A(s)$ and $R_f/Z(s)$ behave with frequency. Halving both R_f and R_g will double the bandwidth and keep the gain the same for the current feedback amplifier, but not change the gain for the voltage feedback amplifier. Doubling the gain by halving R_g will halve the bandwidth of the Voltage feedback amplifier but will not change the bandwidth of the current feedback amplifier. The use of low impedances will allow current amplifiers with high bandwidths to be obtained. Current feedback amplifiers have higher input currents and that makes them less suitable for integrators.

There is basically no slew rate limit for the current feedback amplifier, so that much higher slew rates can be obtained. Current feedback amplifiers generally result in have a lower distortion than Voltage Feedback amplifiers, as can be seen in the table 1.

Current and Voltage Feedback Amplifier Comparison

	Current Feedback	Voltage Feedback
Device	LMH 6702	LMH6624
3dB Bandwidth	720 MHz	1.5 GHz
Slew rate	3100 V/ μ s	350 V/ μ s
Noise Voltage	1.83 nV/ $\sqrt{\text{Hz}}$	0.92 nV/ $\sqrt{\text{Hz}}$
Noise Current	3.0 pA/ $\sqrt{\text{Hz}}$	2.3 pA/ $\sqrt{\text{Hz}}$
Distortion (HD2)	-79 dBc (20 MHz, 2Vpp)	-63 dBc (10 MHz, 1Vpp)
Distortion (HD3)	-88 dBc (20 MHz, 2Vpp)	-80 dBc (10 MHz, 1Vpp)
Input Offset Voltage	1 mV	0.1 mV
Input Offset Current	13 μ A	0.1 μ A
Load Resistor test circ	100 Ω	100 Ω
Feedback Resistor test circ	237 Ω	500 Ω
Feedback Resistor range	Narrow	Very wide
Supply Voltage	$\pm 5\text{V}$ to $\pm 6\text{V}$	$\pm 2.5\text{V}$ to $\pm 6\text{V}$
Supply Current	12.5 mA	12 mA
Cost (US\$/1000)	\$1.49	\$1.67

Table 1. Current and Voltage Feedback performance comparison

Low Noise designs using Operational Amplifiers:

The noise associated with a resistor is

$$E_{NR} = \sqrt{4kTBR}$$

Where:

- K = Boltzman's constant 1.38E-23 Joules/°Kelvin
- T = Absolute temperature Kelvin
- B = Bandwidth in Hz
- R = Resistance in Ω

In a circuit each resistor is then associated with its own noise source which has a random noise voltage of E_{NR} .

In addition the operational amplifier produces noise which can most accurately be represented as voltage (e_{ni}) and current noise sources (i_{ni+} and i_{ni-}) at the inputs, as shown in figure 4.

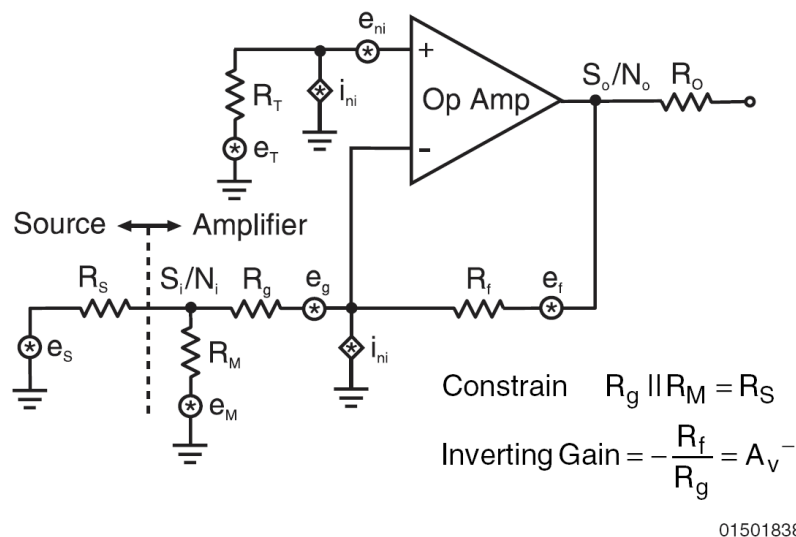


Figure 4 Noise sources in an operational amplifier configuration (National Semiconductor Appl Note OA-11)

The values for e_{ni} and for i_{ni+} and i_{ni-} are normally obtained from manufacturers data sheets. The table 2 shows the noise performance of some low noise amplifiers from different manufacturers. The noise of operational amplifiers will rise at low frequency, as shown in figures 5 to 8, and is inversely proportional to frequency at low frequencies, due to flicker noise or 1/f noise. The corner frequency of that 1/f noise may be important in a design. For example is a microphone amplifier is required, the noise performance at less than 1 kHz is important and the LMH6622 has a better noise performance at those frequencies than the LMH6624, which has a better noise performance at higher frequencies only.

Manufacturer	Part	nV/sqrtHz	1/f Hz	GBWP MHz	VinOffset mV
Texas Instruments	TLE2037	2.5		50	0.1
Texas Instruments	OPA2300	3		150	5
Analog Devices	AD8028	4.3	300Hz	190	0.9
Analog Devices	AD8099	0.85		500	0.2
Analog Devices	AD797	0.9	100 Hz	110	0.025
National Instruments	LMH6624	1	10kHz	1500	0.5
National Instruments	LMH6622	2	1kHz	160	1.2
National Instruments	LF356	12	100Hz	5	3

Table 2. Low Noise Operational Amplifiers.

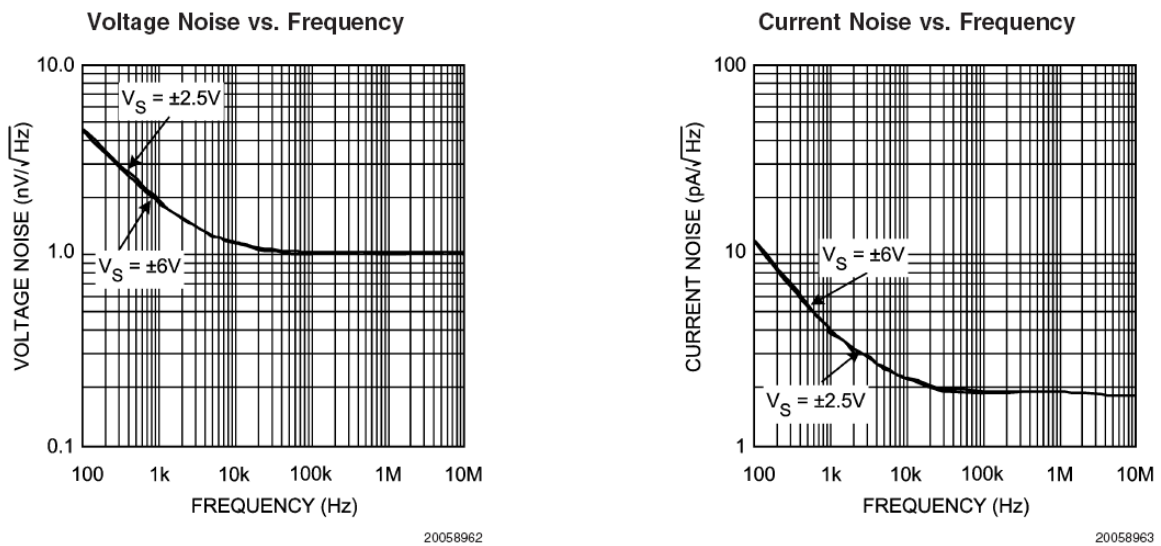


Figure 5. Noise of LMH6624L versus frequency

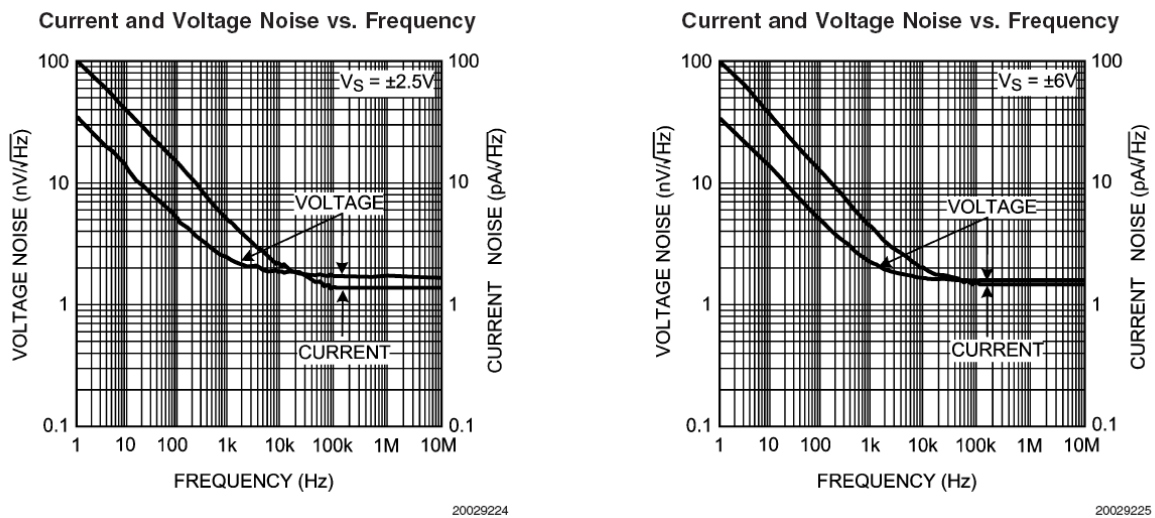


Figure 6. Noise of LMH6622 versus frequency

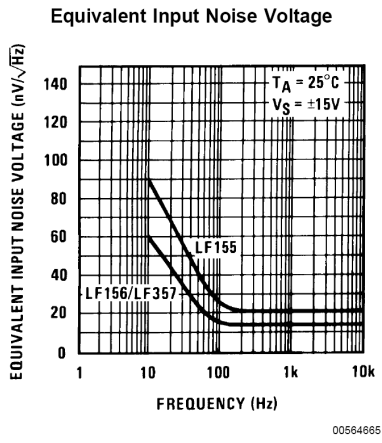


Figure 7. Noise of LF356 and AD8027/AD8028 versus frequency

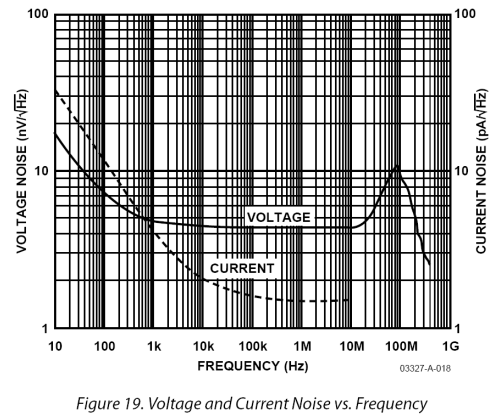


Figure 19. Voltage and Current Noise vs. Frequency

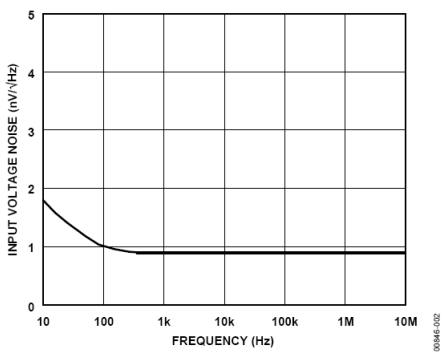


Figure 2. AD797 Voltage Noise Spectral Density

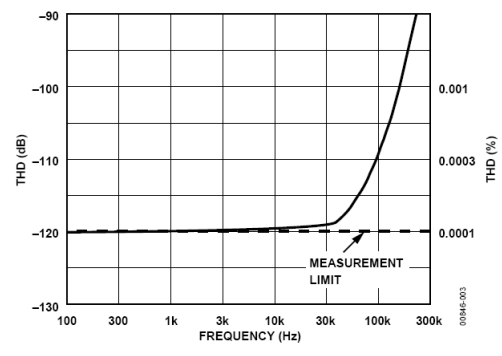


Figure 3. THD vs. Frequency

Figure 8. Noise and Distortion of AD797

Note the lower 1/f point of the AD8027/8028, but the higher noise voltage of the AD8027.

Example

A microphone has a 100 Ω source impedance and requires a load resistance larger than 1 kΩ for the microphone to operate correctly. The output from the microphone is 3mV. An amplifier with a voltage gain of 1000 is required.

The noise obtained from an operational amplifier circuit for a microphone amplifier using an inverting and noninverting amplifier configuration is shown in table 3.

Operational amplifier Noise calculation

4kT 1.60E-20

Microphone, 10mV out, RI 1k,

Bandwidth (Hz) 20000

Op Amp LMH6624
L

Rs Source resistance

Rg Input resistance series with inverting input

Rf Feedback resistor

	Non Inverting Op Amp			Inverting Amp		
	Value	Noise Power/Hz	Output Noise Power/Hz	Value	Noise Power/Hz	Output Noise Power/Hz
en V	1.00E-09	1.00E-18	1.00E-12	1.00E-09	1.00E-18	1.00E-12
in+ A	2.3E-12	1.90E-18	1.91E-12	2.3E-12	0.00E+00	0.00E+00
in- A	2.3E-12	5.28E-22	5.29E-16	2.3E-12	6.84E-17	6.86E-11
Rs	600	9.60E-18	9.62E-12	0	0.00E+00	0.00E+00
Rg	10	1.60E-19	1.60E-13	3600	5.76E-17	5.76E-11
Rf	10000	1.60E-16	1.60E-16	360000	5.76E-14	5.76E-14
Gain	1001			1001		
				1000		
Total Power/Hz			1.27E-11			1.27E-10
Total Noise Power			2.54E-07			2.54E-06
Noise Voltage mV		5.04E-01			1.60E+00	

Mic Output mV 2.5 2502.5 2500

SNR 73.92 63.90

Noise figure 1.20 6.45

Table 3. Noise for inverting and noninverting amplifier configurations.

References:

Noise: National data sheet: "LMH6624/LMH6626 Single/Dual Ultra Low Noise Wideband Operational Amplifier"

"Current vs. Voltage Feedback Amplifiers" National Semiconductor Application Note OA-30